BEYOND PICTURES

Brain imaging and neurobiological correlates in developmental disorders

UMC Utrecht Brain Center

Sara Ambrosino

BEYOND PICTURES

Brain imaging and neurobiological correlates in developmental disorders

Sara Ambrosino

The studies described in this thesis were performed at the Brain Center, Department of Psychiatry, University Medical Center Utrecht, Utrecht, the Netherlands. Research was supported by the Hersenstichting Nederland grant F2009(1)-17, the Netherlands Organisation for Scientific Research (NWO) VIDI 91776384 and VICI 453-10-005 grants to Prof. dr. S. Durston, and the Innovative Medicines Initiative 2 Joint Undertaking under grant agreement No 777394 for the project AIMS-2-TRIALS.

Publication of this thesis was financially supported by the Brain Center.
ISBN: 978-90-393-7584-6

Cover: Vincenzo Ambrosino | info@vincenzoambrosino.it
Layout: Tara Schollema | www.persoonlijkproefschrift.nl
Print: Ridderprint | www.ridderprint.nl

BEYOND PICTURES

Brain imaging and neurobiological correlates
in developmental disorders

VERDER DAN HET OOG REIKT

Verbanden tussen hersenscans en neurobiologie
binnen ontwikkelingsstoornissen

(met een samenvatting in het Nederlands)

Proefschrift

ter verkrijging van de graad van doctor aan de Universiteit Utrecht op gezag van
de rector magnificus, prof.dr. H.R.B.M. Kummeling, ingevolge het besluit
van het college voor promoties in het openbaar te verdedigen op
dinsdag 31 oktober 2023 des middags te 12.15 uur

door

Sara Ambrosino di Bruttopilo

geboren op 2 oktober 1978
te Ravenna, Italië

Promotor:

Prof. Dr. S. Durston

Copromotor:

Dr. B. Oranje

Beoordelingscommissie:

Prof. Dr. K.P.J. Braun
Prof. Dr. W. Cahn
Prof. Dr. N. van Haren
Prof. Dr. H.E. Hulshoff Pol
Dr. M.H. Lequin

CONTENTS

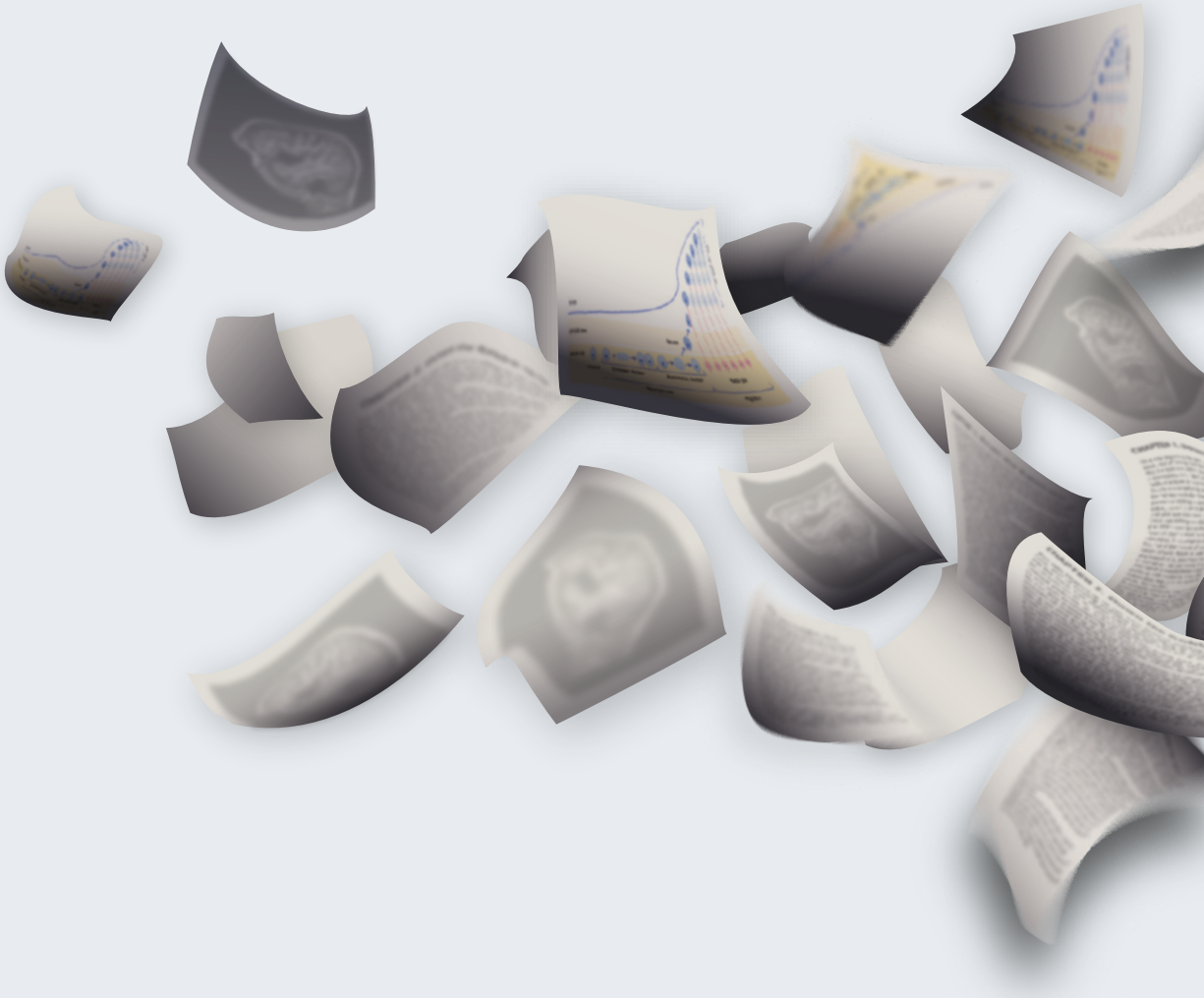

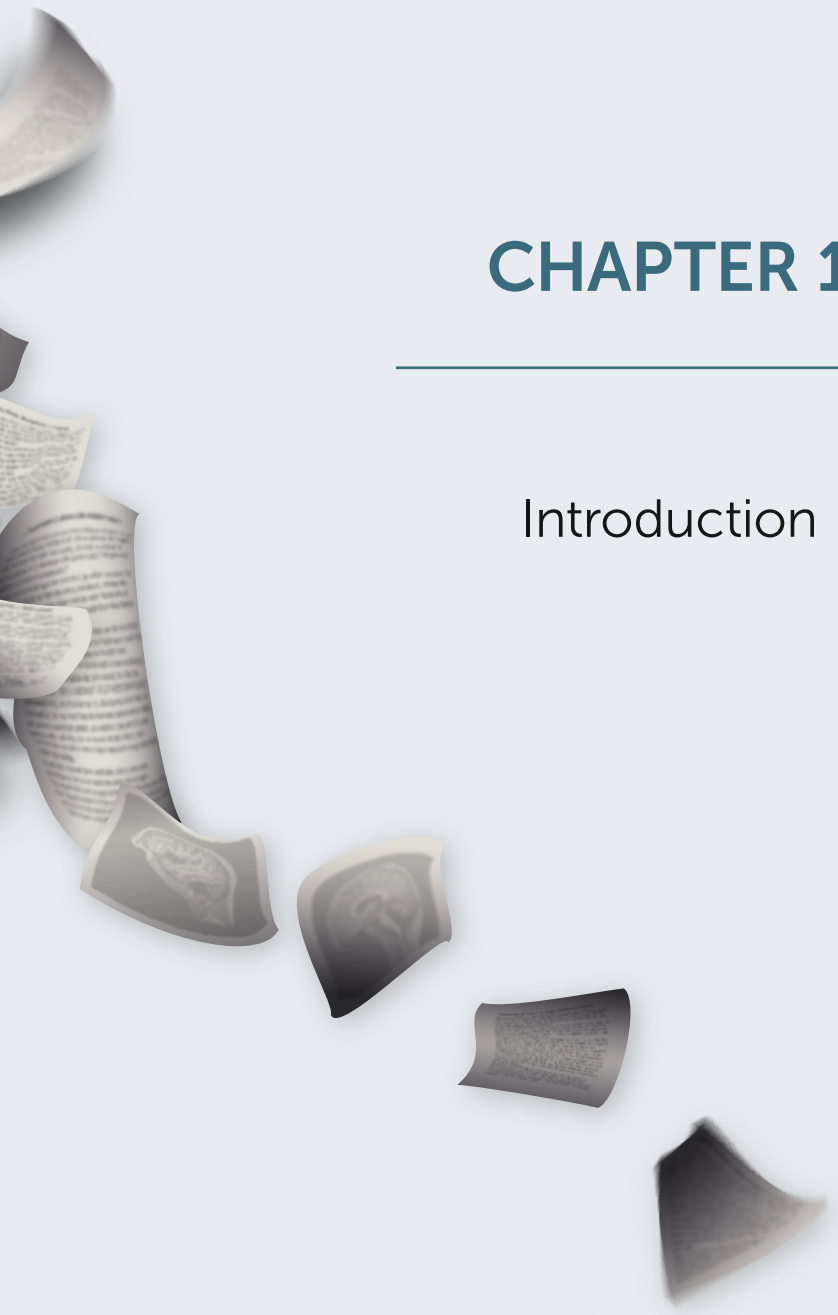

CHAPTER 1

Introduction

Brain Magnetic Resonance Imaging (MRI) is a powerful diagnostic tool in neurology. It provides highly detailed information on human brain structure, function, and metabolism, in a non-invasive way. The multiplanar capability and excellent soft tissue contrast of structural MRI remains unmatched by any other current imaging technique in studying brain morphology. As such, brain MRI scans are widely implemented in clinical practice to investigate different structures of the central nervous system, permitting the identification of a wide variety of pathologic changes with precision.

However, the correct interpretation of MRI images strongly depends on the integration of imaging features and clinical information (Radue et al. 2016). Imaging findings may be so subtle that they can be detected radiologically only with the "guidance" of a specific clinical question. Vice versa, in case of a suspected lesion, a combination of several imaging parameters is of crucial importance to narrow the differential diagnosis (Radue et al. 2016).

Yet, brain MRI sensitivity is generally assumed to be much higher than its specificity, so the relationship between features of an MRI image and the clinical picture is not a one-to-one matter. Brain MRI findings are generally not pathognomonic of a specific condition, but may be -highly, probably, or possibly- correlated with neurological signs and symptoms. As such, they may facilitate the diagnostic process toward more targeted etiopathological investigations (Boddaert et al. 2009). Notably, lesions may have consequences for brain organization and connectivity even at remote distance from their original site (Goldam and Galkin 1978), making the topographical correspondence between imaging findings and clinical symptoms less direct.

Arguably, such correspondence may be even more complicated for disorders that are heterogenous, both at causal and phenotypic levels, like most psychiatric conditions (Wardenaar and de Jonge 2013). This heterogeneity particularly applies to neurodevelopmental disorders, which encompass a broad range of conditions with onset in the developmental period (American Psychiatric Association 2022). Autism Spectrum Disorder (ASD) and Attention-Deficit/Hyperactivity Disorder (ADHD) are currently the two most frequently diagnosed developmental conditions (Elsabbagh et al. 2012; Polanczyk et al. 2014). Clinically, both present variably as a function of multiple factors (including age, gender, developmental level, and environmental factors), and both are highly comorbid not only with each other, but also with several other disorders (Simonoff et al. 2008; Gnanavel et al. 2019). This renders the phenomenology of autism and ADHD extremely heterogeneous, which makes it inherently difficult to link neuroimaging findings to behaviour.

Furthermore, the clinical characteristics vary between individuals, as well as within individuals over time, and, as such, are not permanent features of ASD and ADHD. They may vary significantly across different stages of development, waxing and

waning, and as such, they emphasize the developmental nature of these conditions. Furthermore, because of this complexity, the relationship between clinical outcome and neuroimaging findings may be age-dependent. Moreover, ASD and ADHD typically manifest during childhood, when the brain still shows greater structural and functional plasticity in response to maladaptive processes (Johnson 1997). Plastic changes of the brain are equally age-dependent, as the brain responds in qualitatively different ways to the same event at different ages (Kolb and Gibb 2011).

Therefore, it is not surprising that it is a challenge to identify brain MRI changes associated with behavioural changes in neurodevelopmental disorders. Despite the enormous neuroscientific efforts to search for neurobiological substrates of autism and ADHD, no imaging (or other biological) marker has proven to correlate sufficiently reliably, sensitively, or consistently, with the symptoms or the putative neurodevelopmental pathways involved. None can be used for identifying or clinically profiling of children with suspected neurodevelopmental disorders: as a result, diagnosing ADHD or ASD relies solely on clinical evaluation.

With all these complexities in mind, one may question whether there is any reason for optimism about using neuroimaging research to investigate neurodevelopmental disorders. The answer, in our view, is that there is.

Multifactorial aetiologies and clinical heterogeneity are increasingly recognized, improvements in clinical phenotyping, putative stratification and improved brain imaging approaches all contribute substantially to shaping a more cohesive view of developmental disorders, including ASD and ADHD. The multifaceted complexity of neurodevelopmental disorders needs to be carefully assessed, and then placed in the framework of typical brain development (morphometry and biology). These are prerequisites for allowing more precise inferences about associated neurobiology, and will therefore be explored further in the next paragraphs.

NEURODEVELOPMENTAL DISORDERS

ASD is a group of life-long neurodevelopmental conditions typically diagnosed in early childhood using semi-structured behavioural assessments and clinical interviews (Lord et al. 1994, 2000). These instruments evaluate the presence of deficits in social communication abilities, restrictive and repetitive patterns of behaviour and interests, and atypical sensory responses, as defined by the Diagnostic and Statistical Manual of Mental Disorders (5th edition Text Revision, DSM-5-TR, American Psychiatric Association 2022) (see Text box 1). However, there is a wide heterogeneity in clinical presentation, both in terms of symptom profiles and severity, hence the term "spectrum" (Lai et al. 2013). Furthermore, 70% of individuals with ASD have one or more psychiatric comorbidities (Simonoff et al. 2008), making the phenomenology of this disorder highly variable between individuals. The most common comorbidity in children with ASD is ADHD (Kaat et al. 2013; Joshi et al. 2017).

ADHD is primarily characterized by impairing levels of inattention, disorganization, and/or hyperactivity-impulsivity, present before the age of 12 years. While symptoms tend to cluster together, some individuals can be classified as predominantly inattentive, and others as predominantly hyperactive and impulsive. Individuals with both sets of core behavioural symptoms meet criteria for the combined type. Text box 2 lists the diagnostic criteria as defined by the DSM-5-TR (American Psychiatric Association 2022). Similarly to ASD, individuals with ADHD may often meet criteria for other psychopathologies, especially Oppositional Defiant Disorder (co-occurring in about 35% of children with ADHD), a significant portion of whom develop Conduct Disorder at a later age (Connor et al. 2010).

Epidemiologically, ASD and ADHD are relatively common conditions, with an estimated worldwide prevalence of approximately 1-2.8% and 5-7%, respectively (Baird et al. 2006; Faraone et al. 2015; Thomas et al. 2015; Xu et al.2019). Both conditions are also more prevalent in males, with an average male to female ratio of 4:1 for ASD (Fombonne 2005), and 2.45:1 for ADHD (Polanczyk et al. 2007).

Prognostically, ADHD often persists into adulthood, with related impairments in social, academic, and occupational performance. ASD may be extremely disabling, with significant impairments in adaptive functioning throughout the life span. However, there is a wide heterogeneity in the level of adaptive outcome in ASD, which is only explained in part by the overall level of cognitive abilities (Tillmann et al. 2019).

Given their high prevalence, frequent chronic morbidity, and related functional disability, ASD and ADHD are important public health concerns. This in itself justifies the

considerable efforts to search for neurobiological correlates. Potentially, such correlates could be used as biological targets for new treatments and intervention strategies, under the assumption that they relate to the aetiology of the observed symptoms. This is particularly urgent for ASD treatment, since no pharmacological intervention is currently available to cure or even improve core symptoms.

The established clinical heterogeneity of the autism spectrum is also reflected in the tremendous biological heterogeneity among individuals. Hundreds of common and rare risk genes (most of which are key regulators of synaptic plasticity), as well as environmental risk factors have been identified. Yet none are shared by all individuals with ASD (Bourgeron 2015). Likewise, a complex polygenetic and multifactorial aetiology, where multiple genes of small and different effect contribute synergistically with environmental risk factors, have been implicated in ADHD (Sharp et al. 2009). Thus, investigating the neurobiological substrates of ASD and ADHD is inherently complex.

However, multiple risk factors may converge on a smaller number of neurobiological cascades to lead to specific clinical characteristic(s). Therefore, a viable strategy to identify neurobiological markers in such heterogenous populations may be to parse the groups into more homogenous clinical, and potentially biologically distinct, subtypes. We take this "subtyping" approach in chapter 4 of this thesis, where we investigate developmental trajectories of brain structures in ASD subgroups based on co-occurring symptoms of ADHD (ASD+ and ASD-), in comparison with individuals with a primary ADHD diagnosis. In chapter 5, we investigate neuroradiological findings in individuals with mild intellectual disability (ID) with and without ASD (ID-ASD and ID-controls). Hypothetically, there may be shared brain changes between the ASD+ and ADHD groups, as well as between the ID-ASD and ID-controls groups. This would help dissect the complex ASD phenotype by using these (neurobiologically) informative characteristics. Ultimately, this subtyping may prove useful for treatment: symptoms mediated by similar mechanisms may be treated by the same (or similar) treatment, while disorder-specific biological pathways may benefit from different interventions.

Text box 1. DSM-5-TR Diagnostic criteria for **Autism Spectrum Disorder**

A. **Persistent deficits in social communication and social interaction across multiple contexts, as manifested by all of the following, currently or by history (examples are illustrative, not exhaustive; see text):**

1. Deficits in social-emotional reciprocity, ranging, for example, from abnormal social approach and failure of normal back-and-forth conversation; to reduced sharing of interests, emotions, or affect; to failure to initiate or respond to social interactions.
2. Deficits in nonverbal communicative behaviors used for social interaction, ranging, for example, from poorly integrated verbal and nonverbal communication; to abnormalities in eye contact and body language or deficits in understanding and use of gestures; to a total lack of facial expressions and nonverbal communication.
3. Deficits in developing, maintaining, and understanding relationships, ranging, for example, from difficulties adjusting behavior to suit various social contexts; to difficulties in sharing imaginative play or in making friends; to absence of interest in peers.

B. **Restricted, repetitive patterns of behavior, interests, or activities, as manifested by at least two of the following, currently or by history (examples are illustrative, not exhaustive; see text):**

1. Stereotyped or repetitive motor movements, use of objects, or speech (e.g., simple motor stereotypies, lining up toys or flipping objects, echolalia, idiosyncratic phrases).
2. Insistence on sameness, inflexible adherence to routines, or ritualized patterns of verbal or nonverbal behavior (e.g., extreme distress at small changes, difficulties with transitions, rigid thinking patterns, greeting rituals, need to take same route or eat same food every day).
3. Highly restricted, fixated interests that are abnormal in intensity or focus (e.g., strong attachment to or preoccupation with unusual objects, excessively circumscribed or perseverative interests).
4. Hyper- or hyporeactivity to sensory input or unusual interest in sensory aspects of the environment (e.g., apparent indifference to pain/temperature, adverse response to specific sounds or textures, excessive smelling or touching of objects, visual fascination with lights or movement).

C. Symptoms must be present in the early developmental period (but may not become fully manifest until social demands exceed limited capacities, or may be masked by learned strategies in later life).

D. Symptoms cause clinically significant impairment in social, occupational, or other important areas of current functioning.

E. These disturbances are not better explained by intellectual developmental disorder (intellectual disability) or global developmental delay. Intellectual developmental disorder and autism spectrum disorder frequently co-occur; to make comorbid diagnoses of autism spectrum disorder and intellectual developmental disorder, social communication should be below that expected for general developmental level.

Note: Individuals with a well-established DSM-IV diagnosis of autistic disorder, Asperger's disorder, or pervasive developmental disorder not otherwise specified should be given the diagnosis of autism spectrum disorder. Individuals who have marked deficits in social communication, but whose symptoms do not otherwise meet criteria for autism spectrum disorder, should be evaluated for social (pragmatic) communication disorder.

Specify current severity based on social communication impairments and restricted, repetitive patterns of behavior:

- Requiring very substantial support
- Requiring substantial support
- Requiring support

Specify if:

- With or without accompanying intellectual impairment
- With or without accompanying language impairment
- Associated with a known genetic or other medical condition or environmental factor
- Associated with a neurodevelopmental, mental, or behavioral problem
- With catatonia

Text box 2. DSM-5-TR Diagnostic criteria for **Attention-Deficit/Hyperactivity Disorder**

A. A persistent pattern of inattention and/or hyperactivity-impulsivity that interferes with functioning or development, as characterized by (1) and/or (2):

1. **Inattention: Six (or more) of the following symptoms have persisted for at least 6 months to a degree that is inconsistent with developmental level and that negatively impacts directly on social and academic/occupational activities:**

- Note: The symptoms are not solely a manifestation of oppositional behavior, defiance, hostility, or failure to understand tasks or instructions. For older adolescents and adults (age 17 and older), at least five symptoms are required.

a. Often fails to give close attention to details or makes careless mistakes in schoolwork, at work, or during other activities (e.g., overlooks or misses details, work is inaccurate).
b. Often has difficulty sustaining attention in tasks or play activities (e.g., has difficulty remaining focused during lectures, conversations, or lengthy reading).
c. Often does not seem to listen when spoken to directly (e.g., mind seems elsewhere, even in the absence of any obvious distraction).
d. Often does not follow through on instructions and fails to finish schoolwork, chores, or duties in the workplace (e.g., starts tasks but quickly loses focus and is easily sidetracked).
e. Often has difficulty organizing tasks and activities (e.g., difficulty managing sequential tasks; difficulty keeping materials and belongings in order; messy, disorganized work; has poor time management; fails to meet deadlines).
f. Often avoids, dislikes, or is reluctant to engage in tasks that require sustained mental effort (e.g., schoolwork or homework; for older adolescents and adults, preparing reports, completing forms, reviewing lengthy papers).
g. Often loses things necessary for tasks or activities (e.g., school materials, pencils, books, tools, wallets, keys, paperwork, eyeglasses, mobile telephones).
h. Is often easily distracted by extraneous stimuli (for older adolescents and adults, may include unrelated thoughts).
i. Is often forgetful in daily activities (e.g., doing chores, running errands; for older adolescents and adults, returning calls, paying bills, keeping appointments).

2. **Hyperactivity and impulsivity: Six (or more) of the following symptoms have persisted for at least 6 months to a degree that is inconsistent with developmental level and that negatively impacts directly on social and academic/occupational activities:**

- Note: The symptoms are not solely a manifestation of oppositional behavior, defiance, hostility, or a failure to understand tasks or instructions. For older adolescents and adults (age 17 and older), at least five symptoms are required.

a. Often fidgets with or taps hands or feet or squirms in seat.
b. Often leaves seat in situations when remaining seated is expected (e.g., leaves his or her place in the classroom, in the office or other workplace, or in other situations that require remaining in place).
c. Often runs about or climbs in situations where it is inappropriate. (Note: In adolescents or adults, may be limited to feeling restless.)
d. Often unable to play or engage in leisure activities quietly.
e. Is often "on the go," acting as if "driven by a motor" (e.g., is unable to be or uncomfortable being still for extended time, as in restaurants, meetings; may be experienced by others as being restless or difficult to keep up with).
f. Often talks excessively.
g. Often blurts out an answer before a question has been completed (e.g., completes people's sentences; cannot wait for turn in conversation).
h. Often has difficulty waiting his or her turn (e.g., while waiting in line).
i. Often interrupts or intrudes on others (e.g., butts into conversations, games, or activities; may start using other people's things without asking or receiving permission; for adolescents and adults, may intrude into or take over what others are doing).

>>

>> B. Several inattentive or hyperactive-impulsive symptoms were present prior to age 12 years.

C. Several inattentive or hyperactive-impulsive symptoms are present in two or more settings (e.g., at home, school, or work; with friends or relatives; in other activities).

D. There is clear evidence that the symptoms interfere with, or reduce the quality of, social, academic, or occupational functioning.

E. The symptoms do not occur exclusively during the course of schizophrenia or another psychotic disorder and are not better explained by another mental disorder (e.g., mood disorder, anxiety disorder, dissociative disorder, personality disorder, substance intoxication or withdrawal).

Specify whether:
- (F90.2) Combined presentation: If both Criterion A1 (inattention) and Criterion A2 (hyperactivity-impulsivity) are met for the past 6 months.
- (F90.0) Predominantly inattentive presentation: If Criterion A1 (inattention) is met but Criterion A2 (hyperactivity-impulsivity) is not met for the past 6 months.
- (F90.1) Predominantly hyperactive/impulsive presentation: If Criterion A2 (hyperactivity-impulsivity) is met and Criterion A1 (inattention) is not met for the past 6 months.

Specify if:
- In partial remission: When full criteria were previously met, fewer than the full criteria have been met for the past 6 months, and the symptoms still result in impairment in social, academic, or occupational functioning.

Specify current severity:
- Mild: Few, if any, symptoms in excess of those required to make the diagnosis are present, and symptoms result in no more than minor impairments in social or occupational functioning.
- Moderate: Symptoms or functional impairment between "mild" and "severe" are present.
- Severe: Many symptoms in excess of those required to make the diagnosis, or several symptoms that are particularly severe, are present, or the symptoms result in marked impairment in social or occupational functioning.

BRAIN DEVELOPMENT: MORPHOMETRY AND BIOLOGY

The human brain is a highly complex structure, which goes through extensive maturational changes across the lifespan. An important reason for investigating structural properties of the brain over time is that these properties may inform us on the developmental processes involved. A fascinating example of such a possible brain morphology - biology correspondence is the cerebral cortex, arguably the most complex structure of the human brain.

The cortical structure is topologically equivalent to a highly folded three-dimensional sheet, whose volume can be considered the product of cortical thickness and cortical surface area. These features are expressions of different cytoarchitectonic properties of the cortex, which is organized in columns that run perpendicular to the surface. According to the radial unit hypothesis of cortical development (Rakic 1995), the cells within a column share a common origin during proliferation in the germinal matrix, and they differentiate and migrate radially to their definitive location within the cortex during the second trimester of gestation. The surface area of the cortex is closely

associated with the number of the radial units formed by symmetric and asymmetric cell division during early phases of proliferation, whereas its thickness is influenced by the number of cells migrated within a column (Rakic 1995, figure 1). Therefore, perturbations during the phases of symmetric and asymmetric cell division may influence both the surface area and the thickness of the cortex, by impairing the number of precursors and/or of postmitotic nerve cells (White et al. 2010). However, changes affecting the symmetric phase of progenitor cell division will have a dramatic impact on cortical surface area (Rakic 1995). This developmental principle has been called "late equals large", as neurons migrating into late-developing brain structures undergo a longer period of symmetrical division, resulting in a larger volume of these structures (White et al. 2010). Conversely, pathogenic events during the later phase of neurogenesis may disturb the cortical surface development in a less severe way. These are beautiful, and certainly not exhaustive, examples illustrating how different morphometric features of the brain may be indicative of the neurodevelopmental processes underlying them; especially, when the different features are investigated *simultaneously*. On the one hand, distinct cortical dimensions should be assessed independently since they are regulated through different neurodevelopmental mechanisms (Panizzon et al. 2009), on the other, they are not entirely independent of each other and cannot vary freely. Therefore, studying either cortical thickness or cortical surface area in isolation may lead to misinterpretations if accompanying morphological features are not accounted for (Wang et al. 2021). Instead, assessing the multidimensional nature of brain structures in one methodological design is a more comprehensive way to capture the complexity of the underlying neurobiology.

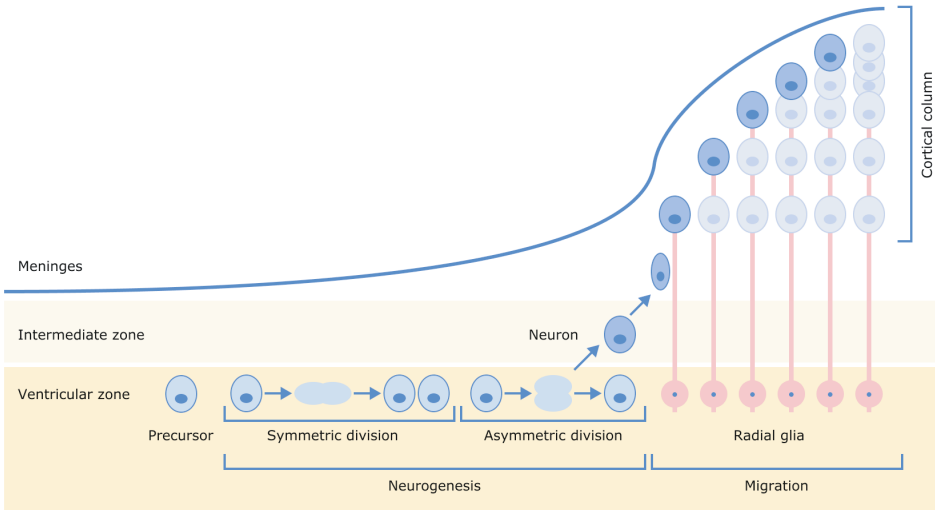

Figure 1. Cortical development: neurogenesis and neuronal migration.

For some -arguably more complex- features, such inferences may be less straightforward. For example, the cortex is notably extensively convoluted. This is necessary for the large cortical surface area to fit within a restricted cranial volume (the cortical surface area is about three times as large as the inner surface of the skull). Another fundamental feature of cortical morphology is therefore the folding (or gyrification), and is particularly complex in the human brain (Van Essen and Drury 1997). Cortical gyrification is a complex developmental process, which starts after the initial phases of neurogenesis and plateaus at birth/early infancy. This results in a dramatic increase in cortical surface area relative to brain volume, by folding "inwards or outwards" in sulci and gyri, respectively. Several embryogenetic processes have been hypothesized to drive this process, including proliferation/apoptosis, differential expansion of superior and inferior cortical layers, differential growth of the progyral versus prosulcal regions, variation in the pattern of connections. However, the precise mechanisms underlying folding complexity remain unresolved (White et al. 2010; Mangin et al. 2010).

Nonetheless, delineation of distinct morphometric properties of brain structure may powerfully inform neurobiological models of typical and atypical brain development. To this aim, recent advances in computational methods for structural MRI allow measurement of subcortical volumes and complete assessment of the cortical structure, by estimation of surface area, thickness and gyrification separately and along the entire cortical mantle, with accuracy comparable to post-mortem studies (Fischl et al. 2002; Fischl & Dale 2000). Neuroimaging pipelines enable relatively rapid computation of hundreds of parameters in virtually unlimited datasets; as such they have enormously enhanced our understanding of typical brain development and related changes in neuropsychiatric conditions (summarized in text box 3).

Text box 3. Structural neuroimaging findings in ASD and in ADHD

Structural MRI studies consistently report a larger brain volume in children with ASD aged 2-4 years, compared to typically developing children (Courchesne et al. 2001; Courchesne 2002). This early brain enlargement, accompanied by increased head size (Lainhart et al. 1997), persists until the age of 5-6 years, and it is unresolved whether it continues later in life or not (Courchesne et al. 2001; Aylward et al. 2002). This suggests that developmental trajectories of brain maturation may be atypical in ASD, with a period of early overgrowth followed by arrested and possibly decreasing brain volume at older ages (Courchesne et al. 2011). This overgrowth seems to be related to increased white matter volume (Carper et al. 2002; Hazlett et al. 2005; Schumann et al. 2010), and expansion of cortical surface area, but not thickness, in ASD (Hazlett et al.2011). Whitin the cerebral cortex, frontal and temporal lobes exhibit the greatest volumetric increase (Chen et al.2011). Differences have also been reported in several subcortical volumes in ASD (Li et al. 2021), but with less consistency across studies.

Conversely, most structural neuroimaging studies in ADHD have reported reductions in volume of subcortical structures, particularly in (parts of) the striatum, for affected individuals compared to controls (Nakao et al. 2011; Frodl and Skokauskas 2012; Hoogman et al. 2017). Studies on cortical development suggested a delay of brain maturation in ADHD, with cortical thickness and surface area attaining their maturational pick a few years later than typically developing controls, particularly in prefrontal regions (Shaw et al. 2007, 2012).

In this thesis, we offer a contribution to current knowledge of structural neuroimaging in ASD and ADHD by assessing developmental trajectories of cortical and subcortical brain structures in two large independent cohorts of individuals with ADHD (chapter 3), and with ASD and/or ADHD (chapter 4), compared to typically developing controls. Notably, we employed a longitudinal design in both studies. This is important, as brain structures vary substantially in size and shape, and develop differently across the life span from one individual to another. Longitudinal study designs are therefore more suited to capturing developmental trajectories within individuals over time than cross-sectional studies that compare brain structures between individuals of certain age groups. Hence, longitudinal neuroimaging studies are particularly important in ASD and ADHD research, given the developmental nature of these conditions.

One limitation of quantitative neuroimaging studies is that they have an inherently limited ability to discriminate between the possible different natures of the morphological changes observed. For instance, a reduction in the volume of the cerebellum may be isolated, or associated to pons hypoplasia, or related to compression or distortion by a posterior fossa cyst: pathogenetically, these are very different conditions.

Furthermore, computational neuroimaging pipelines may miss the presence of unpredictable anomalies, such as neuronal heterotopias within white matter, or even be unable to process images in case of major deviations from typical brain geometry. So, paradoxically, a major limitation of computational neuroimaging is that it disregards the possible presence of gross abnormalities, which may generate 'biased' findings towards typical brain anatomy. This may significantly hamper the identification of neuroimaging markers in *any* brain condition, because it underestimates the intrinsic complexity of neuroimaging data.

Instead, qualitative anomalies represent a valuable source of inter-individual variability in brain morphology, as they may point to specific developmental mechanisms. As such, they should be investigated explicitly and in great detail with the use of suitable methodologies. In chapter 5, we systematically characterize qualitative brain MRI findings in one of the largest cohorts of individuals with ASD in the world using a comprehensive scoring system.

Structural morphometric data complement and may assist in interpreting functional neuroimaging studies using functional MRI (fMRI), and vice versa. fMRI makes use of the blood-oxygenation-level-dependent (BOLD) response, a marker of blood physiological changes in response to neural activity. These physiological changes cause a change in the MR signal from any region activated by its use of oxygen, and, as such, permits indirect quantification of brain activity. Typically, the BOLD response is measured during the performance of various cognitive tasks or in rest (resting-state fMRI). Furthermore, innovative analyses-approaches for fMRI permit the investigation of network properties

of the brain: no brain region works alone. Specifically, correlations between fluctuations in the BOLD signal are used to assess the degree to which different brain regions operate in concert with one another (functional connectivity). In the second chapter of this thesis, we investigate functional connectivity in children with ASD. Similar to more comprehensive assessments of structural MRI, investigating the integrated nature of brain functioning may elucidate neural correlates of brain disorders in a more comprehensive way than investigating regions in isolation.

In sum, the complex characteristics of brain structure and function, as well as of clinical phenotypes in neurodevelopmental disorders, are of more than just academic interest. Rather, they may permit us to deconstruct these complexities into features with more direct embryological or other neurodevelopmental interpretations. This is of particular relevance in ASD and ADHD research, given the neurodevelopmental nature of these disorders. Together, different neuroimaging features may contribute to constructing a more analytical and interpretative model of brain development in these conditions. Ultimately, this scientific endeavour may have relevance for both diagnostic and therapeutic purposes.

OUTLINE OF THIS THESIS

In the present thesis, we attempt to go **beyond pictures** in MRI research in ASD and ADHD: we explore both functional and structural MRI substrates and raise possible neurobiological implications.

In **chapter 2**, we investigate functional connectivity networks in children with ASD during performance of a cognitive control task using a multivariate data-driven approach.

Next, we focus on the quantitative and qualitative aspects of brain structure in ASD and ADHD. In **chapter 3** we assess developmental trajectories of subcortical volumes and multiple cortical dimensions in a large longitudinal sample of individuals with ADHD. These trajectories are further investigated in **chapter 4**, by comparing individuals with ADHD with individuals within the autism spectrum. Qualitative studies of brain morphology provide complementary information to quantitative studies: in **chapter 5**, we comprehensively and systematically characterize qualitative findings of brain morphology in one of the worldwide largest cohorts of individuals with ASD. We provide a general discussion of our findings in **chapter 6**.

REFERENCES

American Psychiatric Association. 2022. Diagnostic and statistical manual of mental disorders: DSM-5-TR (Fifth edition, text revision). American Psychiatric Association Publishing.

Aylward EH, Minshew NJ, Field K, Sparks BF, & Singh N. 2002. Effects of age on brain volume and head circumference in autism. Neurology. 59(2), 175–183. https://doi.org/10.1212/wnl.59.2.175

Baird G, Simonoff E, Pickles A, Chandler S, Loucas T, Meldrum D, Charman T. 2006. Prevalence of disorders of the autism spectrum in a population cohort of children in South Thames: the Special Needs and Autism Project (SNAP). Lancet. Jul 15;368(9531):210-5. doi: 10.1016/S0140-6736(06)69041-7. PMID: 16844490.

Boddaert N, Zilbovicius M, Philipe A, Robel L, Bourgeois M, Barthélemy C, Seidenwurm D, Meresse I, Laurier L, Desguerre I, Bahi-Buisson N, Brunelle F, Munnich A, Samson Y, Mouren MC, Chabane N. 2009. MRI findings in 77 children with non-syndromic autistic disorder. PLoS One 4(2):e4415. doi: 10.1371/journal.pone.0004415.

Bourgeron T. 2015. From the genetic architecture to synaptic plasticity in autism spectrum disorder. Nat Rev Neurosci. Sep;16(9):551-63. doi: 10.1038/nrn3992. PMID: 26289574.

Carper RA, Moses P, Tigue ZD, Courchesne E. 2002. Cerebral lobes in autism: early hyperplasia and abnormal age effects. Neuroimage. Aug;16(4):1038-51. doi: 10.1006/nimg.2002.1099. PMID: 12202091.

Chen R, Jiao Y, Herskovits EH. 2011. Structural MRI in autism spectrum disorder. Pediatr. Res. 69 (5Pt 2), 63R–8R. https://doi.org/10.1203/PDR.0b013e318212c2b3

Connor DF, Steeber J, McBurnett K. 2010. A review of attention-deficit/hyperactivity disorder complicated by symptoms of oppositional defiant disorder or conduct disorder. Journal of Developmental & Behavioral Pediatrics, 31(5), 427-40.

Courchesne E. 2002. Abnormal early brain development in autism. Mol. Psychiatry, 7 Suppl 2, S21–S23. https://doi.org/10.1038/sj.mp.4001169

Courchesne E, Campbell K, & Solso S. 2011. Brain growth across the life span in autism: age-specific changes in anatomical pathology. Brain Res. J. 1380, 138–145. https://doi.org/10.1016/j.brainres.2010.09.10

Courchesne E, Karns CM, Davis HR, Ziccardi R, Carper RA, Tigue ZD, Chisum HJ, Moses P, Pierce K, Lord C, Lincoln AJ, Pizzo S, Schreibman L, Haas RH, Akshoomoff NA & Courchesne RY. 2001. Unusual brain growth patterns in early life in patients with autistic disorder: an MRI study. Neurology, 57(2), 245–254. https://doi.org/10.1212/wnl.57.2.245

Elsabbagh M, Divan G, Koh YJ, Kim YS, Kauchali S, Marcín C, Montiel-Nava C, Patel V, Paula CS, Wang C, Yasamy MT, Fombonne E. Global prevalence of autism and other pervasive developmental disorders. Autism Res. 2012 Jun;5(3):160-79. doi: 10.1002/aur.239. Epub 2012 Apr 11. PMID: 22495912; PMCID: PMC3763210.

Faraone SV, Asherson P, Banaschewski T, Biederman J, Buitelaar JK, Ramos-Quiroga JA, Rohde LA, Sonuga-Barke EJ, Tannock R, Franke B. 2015. Attention-deficit/hyperactivity disorder. Nat Rev Dis Primers. Aug 6;1:15020. doi: 10.1038/nrdp.2015.20. PMID: 27189265.

Fischl B, Dale AM, 2000. Measuring the Thickness of the Human Cerebral Cortex from Magnetic Resonance Images. Proceedings of the National Academy of Sciences, 97, 11044-11049.

Fischl B, Salat D. H., Busa, E., Albert, M., Dieterich, M., Haselgrove, C., van der Kouwe, A., Killiany, R., Kennedy, D., Klaveness, S., Montillo, A., Makris, N., Rosen, B., Dale, A. M. (2002). Whole brain segmentation: automated labeling of neuroanatomical structures in the human brain. Neuron. 33(3), 341-55.

Fombonne E. 2005. Epidemiology of autistic disorder and other pervasive developmental disorders. J Clin Psychiatry. 66 Suppl 10:3-8. PMID: 16401144.

Frodl T, Skokauskas N. 2012. Meta-analysis of structural MRI studies in children and adults with attention deficit hyperactivity disorder indicates treatment effects. Acta Psych Scand. 125:114–126.

Gnanavel S, Sharma P, Kaushal P, Hussain S. Attention deficit hyperactivity disorder and comorbidity: A review of literature. 2019. World J Clin Cases. Sep 6;7(17):2420-2426. doi: 10.12998/wjcc.v7.i17.2420. PMID: 31559278; PMCID: PMC6745333.

Goldman PS, Galkin TW. 1978. Prenatal removal of frontal association cortex in the fetal rhesus monkey: anatomical and functional consequences in postnatal life. Brain Res. Sep 8;152(3):451-85. doi: 10.1016/0006-8993(78)91103-4. PMID: 99206.

Hazlett HC, Poe M, Gerig G, Smith RG, Provenzale J, Ross A, Gilmore J, Piven J. 2005. Magnetic resonance imaging and head circumference study of brain size in autism: birth through age 2 years. Arch Gen Psychiatry. Dec;62(12):1366-76. doi: 10.1001/archpsyc.62.12.1366. PMID: 16330725.

Hazlett HC, Poe MD, Gerig G, Styner M, Chappell C, Smith RG, Vachet C, Piven J. 2011. Early brain overgrowth in autism associated with an increase in cortical surface area before age 2 years. Arch Gen Psychiatry. May;68(5):467-76. doi: 10.1001/archgenpsychiatry.2011.39. PMID: 21536976; PMCID: PMC3315057.

Hoogman M, Bralten J, Hibar DP, Mennes M, Zwiers MP, Schweren LS, et al. 2017. Subcortical brain volume differences in participants with attention deficit hyperactivitydisorder in children and adults: a cross-sectional mega-analysis. Lancet Psychiatry. 4(4):310–319.

Johnson MH. 1997. Developmental cognitive neuroscience. Cambridge, MA: Blackwell Publishers.

Joshi G, Faraone SV, Wozniak J, Tarko L, Fried R, Galdo M, Furtak SL, Biederman J. 2017. Symptom Profile of ADHD in Youth With High-Functioning Autism Spectrum Disorder: A Comparative Study in Psychiatrically Referred Populations. J Atten Disord. Aug;21(10):846-855. doi: 10.1177/1087054714543368. Epub 2014 Aug 1. PMID: 25085653; PMCID: PMC4312732.

Kaat AJ, Gadow KD, Lecavalier L. 2013. Psychiatric symptom impairment in children with autism spectrum disorders. J Abnorm Child Psychol. Aug;41(6):959-69. doi: 10.1007/s10802-013-9739-7. PMID: 23605958.

Kolb B, Gibb R. 2011. Brain plasticity and behaviour in the developing brain. J Can Acad Child Adolesc Psychiatry. Nov;20(4):265-76. PMID: 22114608; PMCID: PMC3222570.

Lai MC, Lombardo MV, Chakrabarti B, Baron-Cohen S. 2013. Subgrouping the autism "spectrum": reflections on DSM-5. PLoS Biol.;11(4):e1001544. doi: 10.1371/journal.pbio.1001544. Epub 2013 Apr 23. PMID: 23630456; PMCID: PMC3635864.

Lainhart JE, Piven J, Wzorek M, Landa R, Santangelo SL, Coon H, & Folstein SE. 1997. Macrocephaly in children and adults with autism. J Am Acad Child Adolesc Psychiatry. 36(2), 282–290. https://doi.org/10.1097/00004583-199702000-00019

Li X, Zhang K, He X, Zhou J, Jin C, Shen L, Gao Y, Tian M, & Zhang H. 2021. Structural, Functional, and Molecular Imaging of Autism Spectrum Disorder. Neurosci Bull. 37(7), 1051–1071. https://doi.org/10.1007/s12264-021-00673-0

Lord C, Risi S, Lambrecht L, Cook EH Jr, Leventhal BL, DiLavore PC, Pickles A, Rutter M. 2000. The autism diagnostic observation schedule-generic: a standard measure of social and communication deficits associated with the spectrum of autism. J Autism Dev Disord. Jun;30(3):205-23. PMID: 11055457.

Lord C, Rutter M, Le Couteur A. 1994. Autism Diagnostic Interview-Revised: a revised version of a diagnostic interview for caregivers of individuals with possible pervasive developmental disorders. J Autism Dev Disord. Oct;24(5):659-85. doi: 10.1007/BF02172145. PMID: 7814313.

Mangin JF, Jouvent E, Cachia A. 2010. In-vivo measurement of cortical morphology: means and meanings. Current Opinion in Neurology, 23(4), 359-6c7.

Nakao T, Radua J, Rubia K, Mataix-Cols D. 2011. Gray matter volume abnormalities in ADHD: voxel-based meta-analysis exploring the effects of age and stimulant medication. Am J Psychiatry. 168(11):1154–1163.

Panizzon M S, Fennema-Notestine C, Eyler, LT, Jernigan TL, Prom-Wormley E, Neale M, Jacobson K, Lyons MJ, Grant MD, Franz CE, Xian H, Tsuang M, Fischl B, Seidman L, Dale A, Kremen WS. 2009. Distinct genetic influences on cortical surface area and cortical thickness. Cerebral Cortex, 19(11), 2728-35.

Polanczyk G, de Lima MS, Horta BL, Biederman J, Rohde LA. 2007. The worldwide prevalence of ADHD: a systematic review and metaregression analysis. American Journal of Psychiatry, 164(6), 942-948.

Polanczyk GV, Willcutt EG, Salum GA, Kieling C, Rohde LA. 2014. ADHD prevalence estimates across three decades: an updated systematic review and meta-regression analysis. Int J Epidemiol. Apr;43(2):434-42. doi: 10.1093/ije/dyt261. Epub 2014 Jan 24. PMID: 24464188; PMCID: PMC4817588.

Radue EW, Weigel M, Wiest R, Urbach H. 2016. Introduction to Magnetic Resonance Imaging for Neurologists. Continuum (Minneap Minn). Oct;22(5, Neuroimaging):1379-1398. doi: 10.1212/CON.0000000000000391. PMID: 27740981.

Rakic P. 1995. A small step for the cell, a giant leap for mankind: a hypothesis of neocortical expansion during evolution. Trends Neurosci. Sep;18(9):383-8. doi: 10.1016/0166-2236(95)93934-p. PMID: 7482803.

Sharp SI, McQuillin A, Gurling HM. 2009. Genetics of attention-deficit hyperactivity disorder (ADHD). Neuropharmacology, 57, 590-600.

Shaw P, Eckstrand K, Sharp W, Blumenthal J, Lerch JP, Greenstein D, Clasen L, Evans A, Giedd J, Rapoport JL. 2007. Attention-deficit/hyperactivity disorder is characterized by a delay in cortical maturation. Proc Natl Acad Sci U S A. Dec 4;104(49):19649-54. doi: 10.1073/pnas.0707741104. Epub 2007 Nov 16. PMID: 18024590; PMCID: PMC2148343.

Shaw P, Malek M, Watson B, Sharp W, Evans A, Greenstein D. 2012. Development of cortical surface area and gyrification in attention-deficit/hyperactivity disorder. Biol Psychiatry. Aug 1;72(3):191-7. doi: 10.1016/j.biopsych.2012.01.031. Epub 2012 Mar 13. PMID: 22418014.

Schumann CM, Bloss CS, Barnes CC, Wideman GM, Carper RA, Akshoomoff N, Pierce K, Hagler D, Schork N, Lord C, Courchesne E. 2010. Longitudinal magnetic resonance imaging study of cortical development through early childhood in autism. J Neurosci. Mar 24;30(12):4419-27. doi: 10.1523/JNEUROSCI.5714-09.2010. PMID: 20335478; PMCID: PMC2859218.

Simonoff E, Pickles A, Charman T, Chandler S, Loucas T, Baird G. 2008. Psychiatric disorders in children with autism spectrum disorders: prevalence, comorbidity, and associated factors in a population-derived sample. J Am Acad Child Adolesc Psychiatry. Aug;47(8):921-9. doi: 10.1097/CHI.0b013e318179964f. PMID: 18645422.

Thomas R, Sanders S, Doust J, Beller E, Glasziou P. 2015. Prevalence of attention-deficit/hyperactivity disorder: a systematic review and meta-analysis. Pediatrics. Apr;135(4):e994-1001. doi: 10.1542/peds.2014-3482. Epub 2015 Mar 2. PMID: 25733754.

Tillmann J, San José Cáceres A, Chatham CH, Crawley D, Holt R, Oakley B, Banaschewski T, Baron-Cohen S, Bölte S, Buitelaar JK, Durston S, Ham L, Loth E, Simonoff E, Spooren W, Murphy DG, Charman T; EU-AIMS LEAP group. 2019. Investigating the factors underlying adaptive functioning in autism in the EU-AIMS Longitudinal European Autism Project. Autism Res. Apr;12(4):645-657. doi: 10.1002/aur.2081. Epub 2019 Feb 11. PMID: 30741482; PMCID: PMC6519242.

Van Essen DC, Drury HA. Structural and functional analyses of human cerebral cortex using a surface-based atlas. 1997. J Neurosci. Sep 15;17(18):7079-102. doi: 10.1523/JNEUROSCI.17-18-07079.1997. PMID: 9278543; PMCID: PMC6573261.

Xu G, Strathearn L, Liu B, O'Brien M, Kopelman TG, Zhu J, Snetselaar LG, Bao W. 2019. Prevalence and Treatment Patterns of Autism Spectrum Disorder in the United States, 2016. JAMA Pediatr. Feb 1;173(2):153-159. doi: 10.1001/jamapediatrics.2018.4208. PMID: 30508021; PMCID: PMC6439607.

Wang Y, Leiberg K, Ludwig T, Little B, Necus JH, Winston G, Vos SB, Tisi J, Duncan JS, Taylor PN, Mota B. 2021. Independent components of human brain morphology. Neuroimage. Feb 1;226:117546. doi: 10.1016/j.neuroimage.2020.117546. Epub 2020 Nov 10. PMID: 33186714; PMCID: PMC7836233.

Wardenaar KJ, de Jonge P. 2013. Diagnostic heterogeneity in psychiatry: towards an empirical solution. BMC Med. Sep 12;11:201. doi: 10.1186/1741-7015-11-201. PMID: 24228940; PMCID: PMC3846412.

White T, Su S, Schmidt M, Kao CY, Sapiro G. 2010. The development of gyrification in childhood and adolescence. Brain & Cognition, 72(1), 36-45.

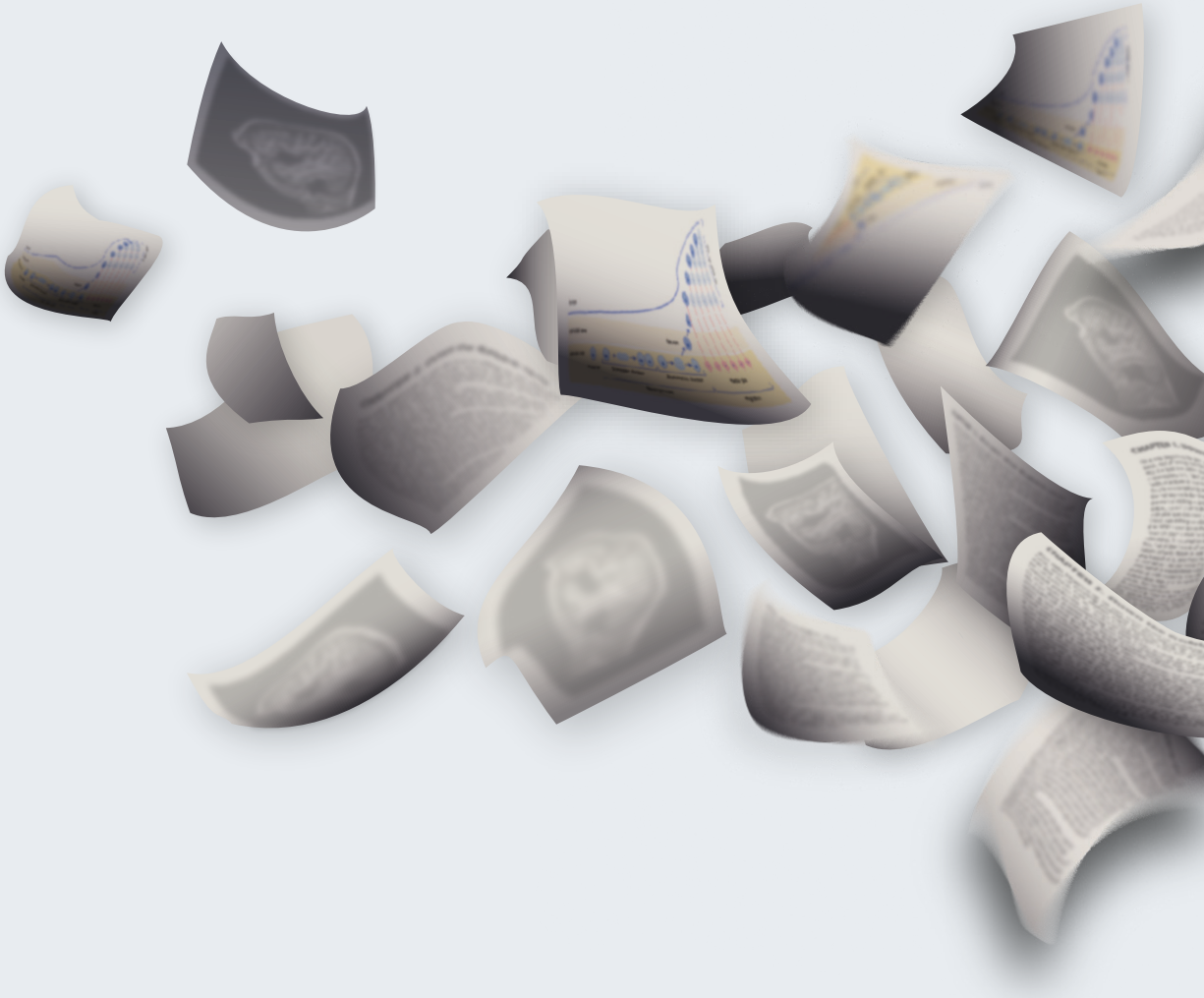

CHAPTER 2

Functional connectivity during cognitive control in children with autism spectrum disorder: an independent component analysis

Sara Ambrosino & Dienke Bos, Tamar van Raalten,
Nieke Kobussen, Janna van Belle, Bob Oranje, Sarah Durston

Journal of Neural Transmission. 2014. 121:1145–1155

ABSTRACT

Restrictive and repetitive behavior in autism may be related to deficits in cognitive control. Here, we aimed to assess functional connectivity during a cognitive control task and compare brain network activity and connectivity in children with autism spectrum disorder and typically developing children using a multivariate data-driven approach.

19 high-functioning boys with autism spectrum disorder and 19 age-matched typically developing boys were included in this study. Functional magnetic resonance imaging was performed at 3T during the performance of a cognitive control task (go/no-go paradigm). Functional networks were identified using Independent Component Analysis (ICA). Network activity and connectivity was compared between groups and correlated with clinical measures of rigid behavior using multivariate analysis of covariance.

We found no differences between the groups in task performance or in network activity. Power analysis indicated that, if this were a real difference, it would require nearly 800 subjects to show group differences in network activity using this paradigm. Neither were there correlations between network activity and rigid behavior.

Our data do not provide support for the presence of deficits in cognitive control in children with autism spectrum disorder, or the functional networks supporting this ability.

INTRODUCTION

Autism Spectrum Disorders (ASD) are characterized by three defining symptoms clusters: impairments in social interaction, communication difficulties, and restrictive, repetitive and stereotyped patterns of behaviors (American Psychiatric Association 2000). It has been suggested that different aetiological processes contribute to these disorders, and one useful way to study more homogeneous subgroups may be to focus on core areas of symptoms (Langen et al. 2011a, b). The cluster of rigid behavior may in part reflect problems in cognitive control (Hill 2004; Solomon et al. 2008). Cognitive control comprises a wide range of abilities that help maintain an appropriate cognitive set in working memory to achieve a later goal, such as planning, mental flexibility, sustained attention, interference inhibition, response suppression (or inhibitory control), outcome monitoring and the ability to deal with novelty (Chan et al. 2008). Some behavioral manifestations of rigidity in ASD seem particularly related to motor-response inhibition (Mosconi et al. 2009). Rigid behavior could then reflect the inability to inhibit pre-potent or ongoing motor behaviors when they are no longer appropriate, resulting in an inability to favor the expression of other, more adaptive responses.

Functional Magnetic Resonance Imaging (fMRI) studies have shown activation of a network of brain regions during the execution of cognitive control tasks, including prefrontal cortex, anterior cingulate cortex, striatum and posterior parietal cortex. This network of functionally connected regions has been termed the cognitive control network (Durston and Casey 2006; Cole and Schneider 2007). However, effective cognitive control is also related to the concurrent modulation of other networks, i.e. coactivation of the salience network (Menon and Uddin 2010) and deactivation of the default mode network (Buckner et al. 2008; Raichle et al. 2001) during cognitive control tasks.

Several fMRI studies of cognitive control have reported atypical activation in task-related areas in individuals with ASD compared to controls, particularly in the frontostriatal circuitry (for review, see Dichter 2012). Only few studies of functional connectivity during cognitive control have been conducted and most of them report reduced connectivity in the cognitive control network and related brain regions in ASD (Just et al. 2007; Kana et al. 2007; Solomon et al. 2009; Agam et al. 2010). This could be taken to suggest immature functional integration or segregation of networks in ASD. Furthermore, it suggests that symptoms of ASD, such as rigid behavior, may be related to underconnectivity of functional networks rather than to changes in the discrete regions of the cognitive control network. This would support the developmental disconnection hypothesis as an explanatory model for deficits in executive functioning in ASD (Geschwind and Levitt 2007).

In the current study we aimed to investigate connectivity both within and between functional networks involved in cognitive control in a group of high-functioning boys with ASD and age-matched typically developing boys. We used Independent Component

Analysis (ICA) to identify cognitive control networks and investigate their activity and connectivity. ICA is a data-driven method that decomposes fMRI data into spatially independent, but temporally coherent networks (Calhoun et al. 2001; Calhoun et al. 2002a; Calhoun et al. 2009; Calhoun and Adali 2006). Decomposition into networks in this manner greatly reduces the number of comparisons made compared to standard GLM analyses. As such, ICA is more sensitive to between group differences than a traditional GLM-analysis (Congdon et al. 2010; McKeown and Sejnowski 1998). In addition, ICA allows one specific voxel to contribute to more than one temporally coherent network, and as such it may be involved in more than one pattern of response. Therefore, ICA may even detect differences that are obscured in traditional GLM analyses (Beldzik et al. 2013; Xu et al. 2013a). Based on the developmental disconnectivity hypothesis of ASD, we hypothesized 1) reduced connectivity between cognitive control and other task-related networks in ASD, and 2) that reduced connectivity of the cognitive control network would be related to severity of rigid behavior in ASD.

METHODS

Participants and clinical data

A total of 38 boys, 19 with a diagnosis of ASD (aged 9-14 years) and 19 age-matched typically developing boys, were included in the study. In addition to age, participants were matched at the group level for hand preference and IQ. The study and its procedures were approved by the Institutional Review Board of the University Medical Centre Utrecht, the Netherlands. Written informed consent was obtained from the parents of all subjects after full disclosure of the study purpose and procedure. Children provided written and/or verbal informed assent.

For participants with ASD, a qualified researcher from the lab confirmed the clinical diagnosis by means of the Autism Diagnostic Interview – Revised (ADI-R) (Lord et al. 1994). The Diagnostic Interview Schedule for Children (DISC, version 2.3 or IV), parent version (Shaffer et al. 2000), was administered to parents of the typically developing children in order to confirm the absence of any psychiatric diagnosis in the participant. In addition, controls were excluded in case of first-degree relatives with a history of psychiatric problems. In both groups, additional exclusion criteria were IQ below 70, any major physical or neurological illnesses, or the presence of metal in the body that precluded the MRI session.

The Repetitive Behavior Scale Revised (RBS-R) was administered to provide a quantitative measure of the full spectrum of repetitive behaviors in ASD participants (Bodfish et al. 1999, 2000); the scale includes measures of stereotyped-, self-injurious-, compulsive-, and ritualistic behavior, insistence on sameness and restricted interests.

Full scale IQ was assessed with the Wechsler Intelligence scale for children WISC-III (Wechsler 2005). Table 1 lists the demographic and clinical characteristics of the sample; the appropriate parametric, non-parametric, chi-squared or Fisher exact tests were performed to test for between-group differences on these variables.

Table 1. Demographics and clinical characteristics

		ASD (N=19)	Controls (N=19)	Group differences (p-values)
Age	M (SD) Range	11.5 (1.2) 9.0 - 12.8	11.1 (1.6) 9.1 - 14.2	.367
Total IQ[a]	M (SD) Range	112.2 (15.3) 80 - 150	120.2 (15.8) 88 - 152	.134
Handedness	N Right/Ambidextrous/Left	19/0/0	17/2/0	.486
SES[b]	Education Father (years) M (SD)	14.5 (0.5)	13.9 (2.6)	.500
ADI-R Social	M (SD)	20.6 (4.3)	.	.
ADI-R Communication	M (SD)	15.2 (4.3)	.	.
ADI-R Repetitive	M (SD)	6.0 (2.6)	.	.
Total RBS-R[c]	M (SD)	24.9 (15.5)	.	.
Medication	N Medicated/Unmedicated	7[d]/12	0/19	.008

[a]unavailable for two subjects with ASD; [b]unavailable for ten controls and thirteen subjects with ASD; [c]unavailable for one subject with ASD; [d]five children on methylphenidate, three children on risperidone. Abbreviations: ASD, Autism Spectrum Disorder; N, number; M, mean; SD, standard deviation; IQ, intelligence quotient; SES, Socio-Economic Status; ADI-R, Autism Diagnostic Interview Revised; RBS-R, Repetitive Behavior Scale Revised.

Seven children with ASD were on psychoactive medication at the time of study. The five children with ASD that were on methylphenidate were instructed not to take their medication for at least 24 hours prior to the scanning session. As this is not possible for risperidone due to a longer washout period, the use of risperidone was permitted for three subjects with ASD. All other participants were medication-naïve. Prior to the MRI scanning, children under 13 years of age were acclimated to the MRI procedure in a practice session using a mock scanner as described by Durston et al. (2009); subjects aged 13 years or over were also offered the opportunity to do a practice session. Participants were scanned only in case of a successful practice session.

Task design

All subjects participated in an fMRI-session, during which they performed a go/no-go task, as described previously (Durston et al. 2002a, b, 2003, 2006), in short: participants were instructed to focus on a centrally presented fixation point, and to respond as fast as possible to visually presented go stimuli with a button press, and to withhold responding

when a rare non-target was presented (no-go). In order to make the task interesting for children, Pokémon characters were used as stimuli. The task consisted of four sessions of equal length (3 min 56 s). Each run contained a total of 57 trials, with 25% no-go trials. No-go trials were preceded by 1, 3 or 5 go trials in pseudo-randomized order. Each stimulus was displayed for 500 ms, followed by an interval of 3500 ms. Stimuli were projected using a through-projection screen and slide projector. Behavioral responses were collected using a magnet compatible air pressure button device.

Statistical analysis of task performance

SPSS Statistics version 20.0.0 for Mac OS X (SPSS Inc., Chicago, Illinois) was used for the analyses of the behavioral measures from the task. Accuracy on go-trials and accuracy on no-go trials (mean accuracy and following 1, 3 or 5 preceding go-trials) were calculated. Mean reaction time on successful go-trials was measured.

Developmental effects were investigated by calculating Pearson's correlations (*r*) between age and behavioral measures. In the ASD group only, *r* coefficients were calculated to investigate the correlation between symptoms of rigidity (RBS-R total score) and performance parameters. Group differences in task performance were investigated using a univariate general linear model, with age at scan and age-by-diagnosis interaction entered as covariates. An uncorrected alpha level of .05 was used for these analyses.

fMRI acquisition

Data were acquired using a 3.0T Philips Allegra MRI scanner (Philips Medical Systems, Best, the Netherlands). Task-related functional images were collected in 4 runs of 119 frames with a 2D-EPI SENSE sequence (TR/TE= 2000/35 ms, flip angle = 70°, matrix 68x66, FOV= 24 cm, voxel size 3x3x3.5 mm^3). A high-resolution T1-weighted image was acquired for spatial normalization and visualization purposes (TR/TE=10/4.6 ms, flip angle = 8°, matrix 304x299, FOV = 24 cm, voxel size 0.75x0.75x0.8 mm^3). Independent clinical neuroradiologists evaluated all T1 scans and no gross morphological or signal abnormalities were reported for any of the participants.

fMRI pre-processing

fMRI data were preprocessed using the Statistical Parametric Mapping 8 (SPM8) software (Wellcome Dept. of Cognitive Neurology, www.fil.ion.ucl.ac.uk) running under the MATLAB R2012a programming and run-time environment (The Mathworks, Sherborn, MA, USA). First, functional images were realigned using rigid body transformations, followed by unwarping to remove residual distortions induced by movement and field inhomogeneity. None of the sessions contained images with a total linear displacement more than 3 mm in any direction. Average translation head motion was 1.05 mm, did not correlate with age (r = .047, p = .781) and was not significantly different between

groups (p = .153). In addition, we calculated mean framewise displacement (FD) and the Root Mean Square (RMS) of motion as reported by Power and colleagues (2012) and Van Dijk and colleagues (2012) respectively. Both were within acceptable limits (FD Power et al. = .210 (SD = .097); RMS Van Dijk et al. = .048 (SD = .022)) and did not differ between diagnostic groups (p = .210 and p = .241 respectively).

Next, slice-timing correction was performed to compensate for slice acquisition delays by temporally aligning all slices to the same reference time point (middle slice); given the interaction between timing shifts and motion, we chose performing realignment first to minimize the effect of inter-slice movement (Sladky et al. 2011). This step was followed by co-registration of the functional and structural images. T1-weighted images were segmented into grey and white matter. Then, functional and anatomical images were normalized to Montreal Neurological Institute (MNI) template (Friston et al. 1995). Finally, images were spatially smoothed with a Gaussian kernel of 6 mm at full width at half maximum.

fMRI Independent Component Analysis

Preprocessed time series were analyzed using the Group ICA of fMRI Toolbox (GIFT, http://icatb.sourcefourge.net, version 2.e) to identify spatially independent and temporally coherent networks (Calhoun et al. 2001, 2009). To minimize the impact of artifacts, we first ran ICA on each subject individually. After inspecting all images on the individual subject level, cleaned images of all 38 subjects were included in a Group ICA. The method is detailed in the following sections.

Single subject analysis

Independent component (IC) estimation was performed using the Infomax algorithm (Bell and Sejnowski 1995), which was repeated 20 times in ICASSO in order to maximize the stability of the derived components (Himberg et al. 2004). The dimensionality of the data (number of networks) was estimated per subject using minimum description length (MDL) criteria tool built into GIFT. Images were back reconstructed using GICA3, (Erhardt et al. 2011), which is a back-reconstruction method in which individual subject maps are reconstructed from the raw data using the ICA mixing matrix. Timeseries were then converted for visualization to reflect percent signal change. After single subject ICA, both the spatial pattern and the frequency spectrum of each component were inspected for the presence of possible image artifacts. Components containing obvious artifacts (e.g. edges, ventricles) were discarded.

Group analysis

The cleaned data of all 38 subjects were carried forward to the group analysis. Group ICA was performed using the Infomax algorithm, which was repeated 20 times with ICASSO. All components showed high stability as indicated by the cluster quality index,

Iq > .9. The number of components estimated through MDL was 44. Individual subject component maps were back-reconstructed using GICA3, and finally timecourses and spatial maps were normalized into z-scores (Beckmann et al. 2005).

Selection of networks

We selected those components out of the initial 44 that reflected neuronal networks, based on the level of statistical significance and visual inspection for artifacts (McKeown et al. 1998; Calhoun et al. 2002b; Calhoun et al. 2004a, b; Kim et al. 2009; Meda et al. 2009a; Zhang and Li 2012). Five components were discarded as they showed a high spatial correlation with the probabilistic map of white matter or cerebrospinal fluid ($r^2 > .025$) provided in SPM8 while also showing low correlations with the cerebral grey matter map ($r^2 < .05$). Identification of the remaining components was performed through spatial multiple linear regression with established templates (Allen et al. 2011; Segall et al. 2012). Components with a spatial correlation greater than $r^2 > .05$ with template networks were carried forward to the final selection. Visual inspection of the eleven discarded components suggested that they represented eye movements, head motion or cardiac-induced pulsatile artifacts at the base of the brain.

To compute the degree of task-relatedness of the remaining 28 components, we regressed the corresponding timecourses against the design matrix (go and no-go stimuli together, along with their first temporal derivative) using the temporal multiple linear regression implemented in GIFT. The resulting beta weights (β) reflect the degree to which a component was modulated by the task events of interest. Beta-weights of each IC for each task condition across the four runs were averaged per subject, and the group means of averaged β for each task condition were tested against zero using one-sample t-tests (Zhang and Li 2012; Xu et al. 2013b). Eleven components were selected for the final analyses, with correlations significant at $p < .001$ with either go or no-go events. They were named according to the template they were spatially correlated with or based on visual inspection of the corresponding spatial map.

Group differences in functional connectivity

Group-differences in functional connectivity within the eleven selected components (intra-network connectivity) and among them (inter-network connectivity) were tested using the Mancovan toolbox (Allen et al. 2011) implemented in GIFT. We examined three connectivity measures: component spatial maps, component time course spectra, and between component functional network connectivity (Jafri et al. 2008). The voxel intensity in spatial map dictates the correspondence between a voxel time course and an IC time course (Balsters et al. 2013a); therefore, provides a measure of co-activation/synchronization (strength of connectivity) in a region within a given network. The spectra of time course reflect the degree of fluctuation in amplitude of the intrinsic activity

captured by fMRI data within the network (Calhoun et al. 2012). Although ICs generated by ICA are maximally independent of each other (Calhoun and Adali 2006), their timecourses can still exhibit temporal dependencies (Arbabshirani et al. 2013): functional network connectivity evaluates the extent to which temporal coherence between networks is related to the variables of interest. A multivariate selection strategy was first performed in order to identify potential significant relationships between components measures and variables of interest: the initial design matrix included diagnosis and age as covariate, as well as an age by diagnosis interaction. In addition we included a head movement estimate as nuisance regressor (Allen et al. 2011; Balsters et al. 2013a, b), defined as the average of translation parameters, log-transformed for data normalization. Univariate analyses were performed within the reduced model to test for specific relationships between covariates of interest and connectivity properties. An alpha level of .05 was used for all analyses. Results were corrected for multiple comparisons using false discovery rate (FDR) (Genovese et al. 2002). Cohen's *d* standardized effect sizes were calculated from corrected *p* values.

Functional connectivity and clinical data correlations

In the sample of subjects with ASD, we analyzed the relationship between behavioral rigidity as measured by the RBS-R and functional connectivity measures (spatial maps, time course spectra, and functional network connectivity) of the eleven networks of interest selected for the group analysis. For this purpose, we ran a separate MANCOVA model with RBS-R total score and age as covariates, $p = .05$ FDR corrected for univariate testing.

RESULTS

Task performance

All participants were able to successfully perform the task: mean accuracy on go trials was 99% for both subjects with ASD and controls, and did not significantly differ between groups. Mean accuracy on no-go trials was 76% (SD = .15) for participants with ASD and 82% (SD = .12) for controls, did not differ between groups (t = 1.46, p = .153) and did not correlate with age. In line with findings from earlier studies using the same paradigm (Van Belle et al. submitted; Durston et al. 2002a), no-go accuracy decreased with the number of preceding go-trials (1, 3 or 5) for both children with ASD (83%, 74%, 72%) and controls (87%, 81%, 78%). Mean accuracy on no-go trials after 1, 3 or 5 go trials did not correlate with age and did not differ between ASD subjects and controls. Mean reaction time decreased with age (r = -.374, p = .022) and did not differ between groups (ASD 633 $\pm$ 104 ms, controls 620 $\pm$ 51 ms; mean $\pm$ SD). In the ASD group, RBS-R total score was not correlated with age or with any of the measures of task performance.

Networks

From the twenty-eight IC containing neural networks (Fig. 1), eleven correlated with the task and were therefore identified as of interest for further analysis. These networks included frontal/attentional networks (IC 30, 33, 34), default mode networks (ICs 12 and 28), visual networks (ICs 9, 15, 26), a hippocampus network (IC 41), an auditory network (IC 44) and a temporal network (IC 29) (Fig. 2).

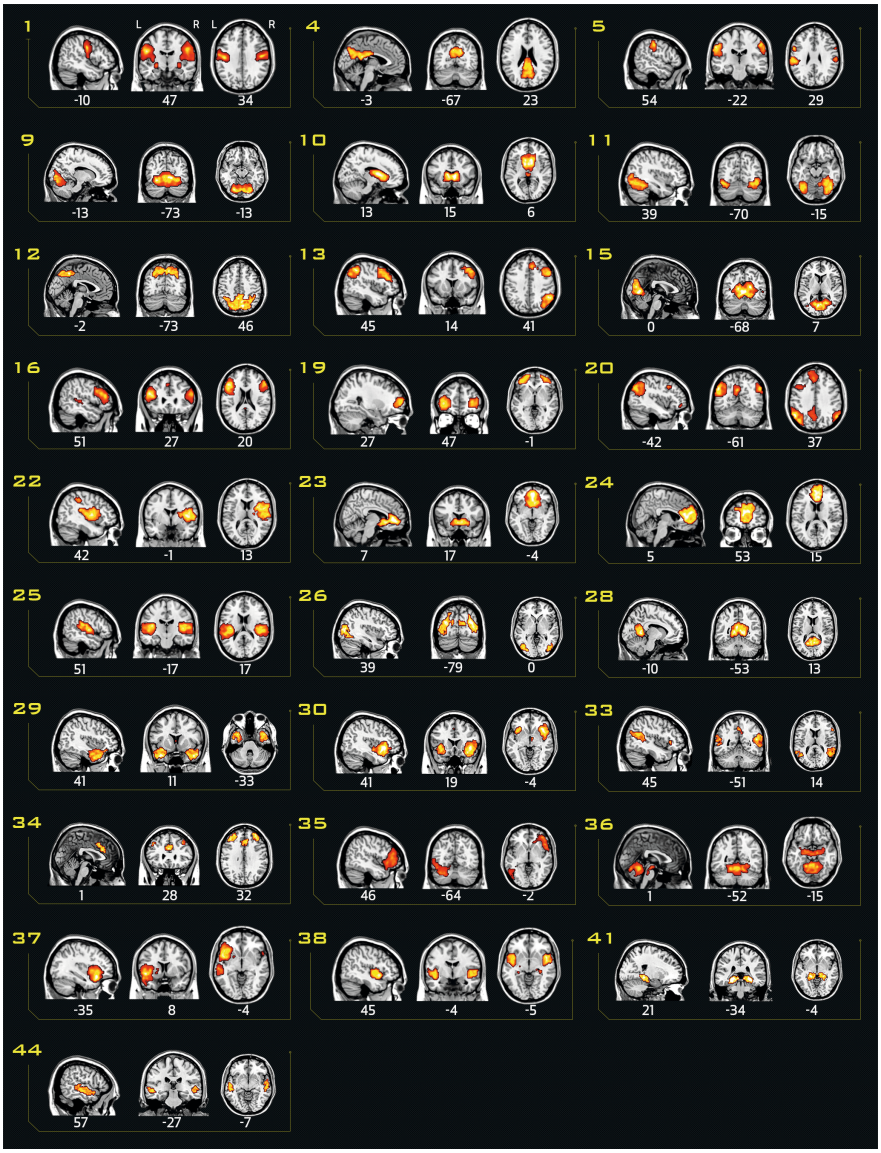

Figure 1. Overview all independent components with neural activity. The MNI coordinates refer to the slices shown

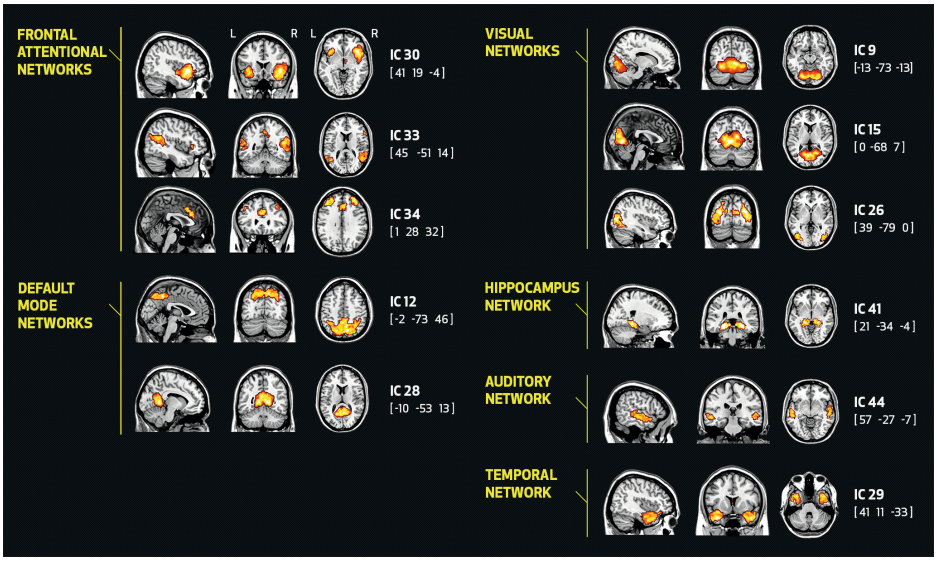

Figure 2. Networks of interest: frontal/attentional networks (ICs 30, 33, 34), default mode networks (ICs 12 and 28), visual networks (ICs 9, 15, 26), hippocampus network (IC 41), auditory network (IC 44) and temporal network (IC 29). The MNI coordinates refer to the slices shown, component labeling follows Allen conventions (Allen et al.2011)

We assessed β-values to ascertain the degree of engagement of networks during go or no-go events (Meda et al. 2009b). The analyses showed that activity in IC 30 and IC 34 (frontal/attentional network) were related to no-go events, while the default mode network components were anti-correlated with both go and no-go events (Online Resource 1).

Functional connectivity

Multivariate and univariate tests showed no effect of diagnosis on the spatial map of components, the timecourse spectra or between-network connectivity, with only small effect sizes (ranging from d = .17 to .23). As there was no significant main effect of diagnosis or age, we reran the MANCOVAN analysis without the interaction term. The results remained not significant. Spatial maps of the networks of interest are depicted in Fig. 3, illustrating the similarities between groups.

We ran a power analysis to estimate the sample size that would be needed to show between-group differences if there was in fact a meaningful difference (pFDR < .05, 2-sided). This told us that a sample of N = 788 would be required to reach a power level of .80 and confirmed our conclusion that any differences were minimal and more likely related to noise.

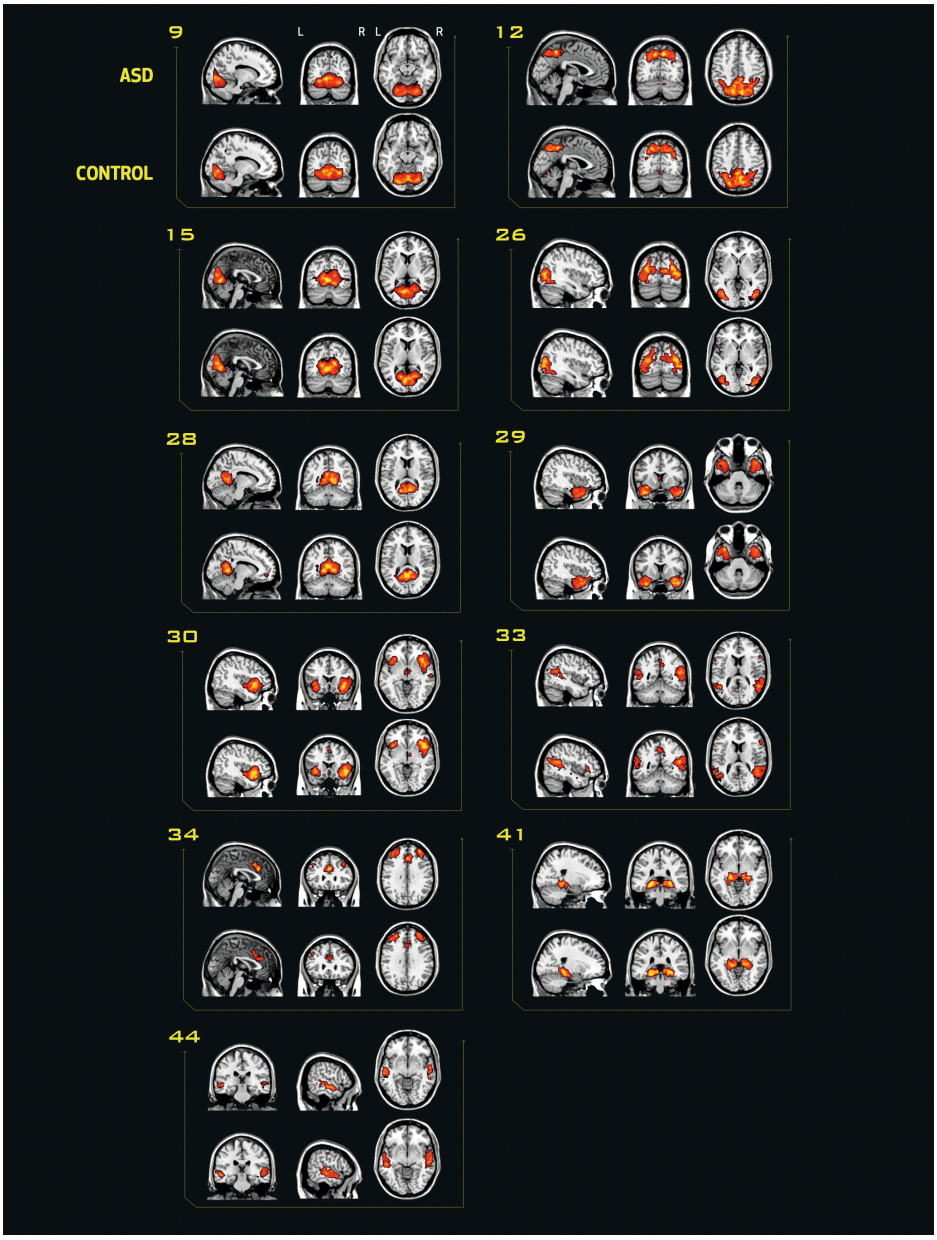

Figure 3. Networks of interest in subjects with ASD and typically developing controls

Component spatial maps of the networks of interest are shown in both groups separately to illustrate the between-group similarities. For each network, the first row of images belongs to the ASD group and the second row to the control group. The MNI coordinates refer to the slices shown

In addition, we performed a standard GLM analysis of the fMRI task, which further confirmed that there were no differences between groups in brain activation during performance of the task (details are provided in Online Resource 2).

We found no significant correlation between the RBS-R total score of subjects with ASD and functional connectivity measures of the components of interest. Average activity from the networks of interest was plotted against total RBS-R scores to illustrate the lack of relation (Fig. 4).

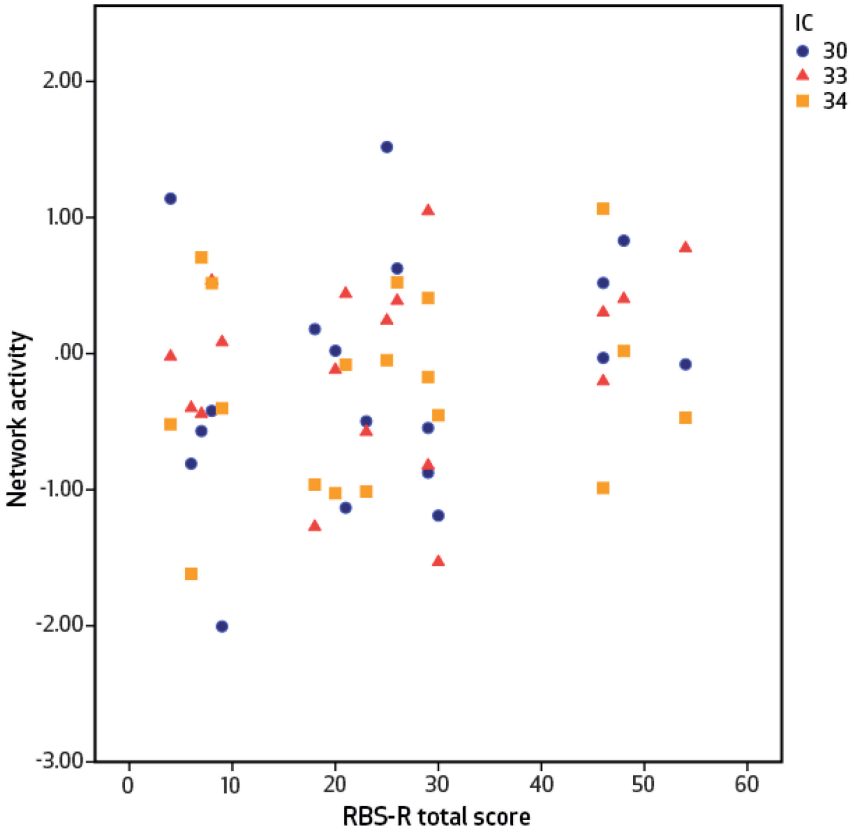

Figure 4. There is no relation between total RBS-R score and activity in frontal/attentional networks

DISCUSSION

In this study we examined functional connectivity during the performance of a cognitive control task (go/no-go) in a population of high-functioning boys with ASD and age-matched typically developing boys using a multivariate data-driven approach (ICA). We found no evidence for changes in functional connectivity in ASD. This is consistent with ROI-based research in children performing a similar paradigm (Lee et al. 2009), but contrasts with studies of adolescents and adults with ASD that have reported decreased functional connectivity in cognitive control networks (Just et al. 2007; Kana et al. 2007; Agam et al. 2010; Solomon et al. 2009).

The findings of dysfunctional connectivity in adults, but not in children, with ASD suggests that changes in connectivity patterns related to cognitive control may appear relatively late in the disorder. This is in keeping with research showing that immature brain activity may be characterized by less structured and more diffuse patterns than in adults (Durston et al. 2006; Supekar et al. 2009). It also implies that detecting subtle differences in the functional connectivity of cognitive control network between children with ASD and typically developing controls may be a particularly difficult challenge. Perhaps it is therefore not entirely surprising that the present study converges with an increasing body of literature reporting only limited changes in functional connectivity in children with ASD, both during rest (Bos et al. under revision) and cognitive control (Lee et al. 2009). Furthermore, we found no evidence for an association between the severity of rigid behavior in our subjects and either functional connectivity or task performance.

There are some strong points to our study, but also some limitations that need to be taken into consideration. One strong point is that we standardized our data analysis as much as possible to limit the number of arbitrary decisions. We did this by using a data-driven approach (ICA) and a hypothesis-free procedure for network selection. A weak point is the limited sensitivity of the RBS-R questionnaire to detect symptoms of rigidity in typically developing subjects. Therefore, correlations between rigidity and functional connectivity measures could only be assessed in children with ASD. A possible further limitation was our relatively small sample size. However, the two groups were well matched and similar to samples in other reports on functional connectivity (Just et al. 2007; Kana et al. 2007; Agam et al. 2010; Solomon et al. 2009). Furthermore, a post-hoc power analysis showed that we would need an enormous number of subjects (788) to show between-group differences in connectivity on this task if there is indeed a true difference. This further supports our interpretation that differences in functional connectivity of cognitive control networks between typically developing children and children with ASD are minimal. In conclusion, we assessed functional connectivity in a well-characterized cohort of children with and without ASD during the performance of a cognitive control task, using a data-driven multivariate approach. We confirmed

previous findings of no differences in connectivity in children with ASD. These findings do not support hypotheses that there are changes in cognitive control and the networks underlying it in children with ASD.

ACKNOWLEDGMENTS

The authors would like to thank all the participants and their families of this study. We wish to thank Juliette Weusten for the assistance with subject recruitment and MRI assessment. This work was financially supported by the Hersenstichting Nederland, grant number F2009(1)-17.

DISCLOSURES

The authors declare that they have no conflicts of interest.

REFERENCES

Agam Y, Joseph RM, Barton JJ, Manoach DS. 2010. Reduced cognitive control of response inhibition by the anterior cingulate cortex in autism spectrum disorders. Neuroimage 1;52(1):336-347. doi: 10.1016/j.neuroimage.2010.04.010

Allen EA, Erhardt EB, Damaraju E, Gruner W, Segall JM, Silva RF, Havlicek M, Rachakonda S, Fries J, Kalyanam R, Michael AM, Caprihan A, Turner JA, Eichele T, Adelsheim S, Bryan AD, Bustillo J, Clark VP, Feldstein Ewing SW, Filbey F, Ford CC, Hutchison K, Jung RE, Kiehl KA, Kodituwakku P, Komesu YM, Mayer AR, Pearlson GD, Phillips JP, Sadek JR, Stevens M, Teuscher U, Thoma RJ, Calhoun VD. 2011. A baseline for the multivariate comparison of resting-state networks. Front Syst Neurosci 4;5:2. doi: 10.3389/fnsys.2011.00002

American Psychiatric Association. 2000. Diagnostic and Statistical Manual of Mental Disorders, Fourth Edition: DSM-IV-TR®. American Psychiatric Publishing

Arbabshirani MR, Havlicek M, Kiehl KA, Pearlson GD, Calhoun VD. 2013. Functional network connectivity during rest and task conditions: A comparative study. Hum Brain Mapp 34(11):2959-2971. doi: 10.1002/hbm.22118

Balsters JH, O'Connell RG, Galli A, Nolan H, Greco E, Kilcullen SM, Bokde AL, Lai R, Upton N, Robertson IH. 2013a. Changes in resting connectivity with age: a simultaneous electroencephalogram and functional magnetic resonance imaging investigation. Neurobiol Aging 34(9):2194-2207. doi: 10.1016/j.neurobiolaging.2013.03.004

Balsters JH, Robertson IH, Calhoun VD. 2013b. BOLD Frequency Power Indexes Working Memory Performance. Front Hum Neurosci 16;7:207. doi: 10.3389/fnhum.2013.00207

Beckmann CF, DeLuca M, Devlin JT, Smith SM. 2005. Investigations into resting-state connectivity using independent component analysis. Philos Trans R Soc Lond B Biol Sci 29;360(1457):1001-1013

Beldzik E, Domagalik A, Daselaar S, Fafrowicz M, Froncisz W, Oginska H, Marek T. 2013. Contributive sources analysis: A measure of neural networks' contribution to brain activations. Neuroimage 76:304–312. doi: 10.1016/j.neuroimage.2013.03.014

Bell AJ, Sejnowski TJ. 1995. An information maximization approach to blind separation and blind deconvolution. Neural Comput 7:1129-1159

Bodfish JW, Symons FW, & Lewis MH. 1999. The Repetitive Behavior Scale. Western Carolina Center Re- search Reports

Bodfish JW, Symons FJ, Parker DE, & Lewis MH. 2000. Varieties of repetitive behavior in autism: Comparisons to mental retardation. J Autism Dev Disord 30(3):237-243

Buckner RL, Andrews-Hanna JR, Schacter DL. 2008. The brain's default network: anatomy, function, and relevance to disease. Ann N Y Acad Sci 1124:1-38. doi: 10.1196/annals.1440.011

Calhoun VD, Adali T. 2006. 'Unmixing' Functional Magnetic Resonance Imaging with Independent Component Analysis. IEEE Eng Med Biol 25(2):79-90

Calhoun VD, Adali T, Pearlson GD, Pekar JJ. 2001. A method for making group inferences from functional MRI data using independent component analysis. Hum Brain Mapp 14(3):140-151

Calhoun VD, Adali T, Pearlson GD, van Zijl PC, Pekar JJ. 2002a. Independent component analysis of fMRI data in the complex domain. Magn Reson Med 48:180–192

Calhoun VD, Adali T, Pekar JJ. 2004a. A method for comparing group fMRI data using independent component analysis: Application to visual, motor and visuomotor tasks. Magn Reson Imaging 22:1181-1191

Calhoun VD, Liu J, Adali T. 2009. A review of group ICA for fMRI data and ICA for joint inference of imaging, genetic, and ERP data. Neuroimage 45(1 Suppl):S163-172. doi: 10.1016/j.neuroimage.2008.10.057

Calhoun VD, Pekar JJ, McGinty VB, Adali T, Watson TD, Pearlson GD. 2002b. Different activation dynamics in multiple neural systems during simulated driving. Hum Brain Mapp 16:158-167

Calhoun VD, Pekar JJ, Pearlson GD. 2004b. Alcohol intoxication effects on simulated driving: Exploring alcohol-dose effects on brain activation using functional MRI. Neuropsychopharmacol 29:2097-2117

Calhoun VD, Sui J, Kiehl K, Turner J, Allen E, Pearlson G. 2012. Exploring the psychosis functional connectome: aberrant intrinsic networks in schizophrenia and bipolar disorder. Front Psychiatry 10;2:75. doi: 10.3389/fpsyt.2011.00075

Chan RC, Shum D, Toulopoulou T, Chen EY. 2008. Assessment of executive functions: review of instruments and identification of critical issues. Arch Clin Neuropsychol 23(2):201-216

Cole MW, Schneider W. 2007. The cognitive control network: Integrated cortical regions with dissociable functions. Neuroimage 1;37(1):343-360

Congdon E, Mumford JA, Cohen JR, Galvan A, Aron AR, Xue G, Miller E, Poldrack RA. 2010. Engagement of large-scale networks is related to individual differences in inhibitory control. Neuroimage 53:653–663

Dichter GS. 2012. Functional magnetic resonance imaging of autism spectrum disorders. Dialogues Clin Neurosci 14(3):319-351

Durston S, Casey BJ. 2006. What have we learned about cognitive development from neuroimaging? Neuropsychologia 44(11):2149-2157

Durston S, Davidson MC, Tottenham N, Galvan A, Spicer J, Fossella JA, Casey BJ. 2006. A shift from diffuse to focal cortical activity with development. Dev Sci 9:1-8

Durston S, Nederveen H, van Dijk S, van Belle J, de Zeeuw P, Langen M, van Dijk A. 2009. Magnetic resonance simulation is effective in reducing anxiety related to magnetic resonance scanning in children. J Am Acad Child Adolesc Psychiatry 48(2):206-207. doi: 10.1097/CHI.0b013e3181930673

Durston S, Thomas KM, Worden MS, Yang Y, Casey BJ. 2002b. The effect of preceding context on inhibition: an event-related fMRI study. Neuroimage 16(2):449-453

Durston S, Thomas K, Yang Y, Uluğ AM, Zimmerman RD, Casey BJ. 2002a. A neural basis for the development of inhibitory control. Dev Sci 5(4):F9-F16

Durston S, Tottenham N, Thomas K, Davidson M, Eigsti I, Yang Y, Ulug A, Casey B. 2003. Differential patterns of striatal activation in young children with and without ADHD. Biol Psychiatry 53(10):871-878

Erhardt EB, Rachakonda S, Bedrick EJ, Allen EA, Adali T, Calhoun VD. 2011. Comparison of multi-subject ICA methods for analysis of fMRI data. Hum Brain Mapp 32:2075-2095. doi: 10.1002/hbm.21170

Friston K, Ashburner J, Frith CD, Poline JP, Heather JD, Frackowiak RS. 1995. Spatial registration and normalization of images. Hum Brain Mapp 2:165-189

Genovese CR, Lazar NA, Nichols T. 2002. Thresholding of statistical maps in functional neuroimaging using the false discovery rate. Neuroimage 15:870-878

Geschwind DH, Levitt P. 2007. Autism spectrum disorders: developmental disconnection syndromes. Curr Opin Neurobiol 17:103-111

Hill EL. 2004. Executive dysfunction in autism. Trends Cogn Sci 8(1):26-32

Himberg J, Hyvrinen A, Esposito F. 2004. Validating the independent components of neuroimaging time series via clustering and visualization. Neuroimage 22(3):1214-1222

Jafri MJ, Pearlson GD, Stevens M, Calhoun VD. 2008. A method for functional network connectivity among spatially independent resting-state components in schizophrenia. Neuroimage 39:1666-1681

Just MA, Cherkassky VL, Keller TA, Kana RK, Minshew NJ. 2007. Functional and anatomical cortical underconnectivity in autism: evidence from an FMRI study of an executive function task and corpus callosum morphometry. Cereb Cortex 17(4):951-961

Kana RK, Keller TA, Minshew NJ, Just MA. 2007. Inhibitory control in high-functioning autism: decreased activation and underconnectivity in inhibition networks. Biol Psychiatry 1;62(3):198-206

Kim DI, Manoach DS, Mathalon DH, Turner JA, Mannell M, Brown GG, Ford JM, Gollub RL, White T, Wible C, Belger A, Bockholt HJ, Clark VP, Lauriello J, O'Leary D, Mueller BA, Lim KO, Andreasen N, Potkin SG, Calhoun VD. 2009. Dysregulation of working memory and default-mode networks in schizophrenia using independent component analysis, an fBIRN and MCIC study. Hum Brain Mapp 30:3795-3811. doi: 10.1002/hbm.20807

Langen M, Kas MJ, Staal WG, van Engeland H, Durston S. 2011a. The neurobiology of repetitive behavior: of mice…. Neurosci Biobehav Rev 35(3):345-355. doi: 10.1016/j.neubiorev.2010.02.004

Langen M, Durston S, Kas MJ, van Engeland H, Staal WG. 2011b. The neurobiology of repetitive behavior: …and men. Neurosci Biobehav Rev 35(3):356-365. doi: 10.1016/j.neubiorev.2010.02.005

Lee PS, Yerys BE, Della Rosa A, Foss-Feig J, Barnes KA, James JD, VanMeter J, Vaidya CJ, Gaillard WD, Kenworthy LE. 2009. Functional connectivity of the inferior frontal cortex changes with age in children with autism spectrum disorders: a fcMRI study of response inhibition. Cereb Cortex 19(8):1787-1794. doi: 10.1093/cercor/bhn209

Lord C, Rutter M, Le Couteur A. 1994. Autism Diagnostic Interview-Revised: a revised version of a diagnostic interview for caregivers of individuals with possible pervasive developmental disorders. J Autism Dev Disord 24:659-685

McKeown MJ, Jung TP, Makeig S, Brown G, Kindermann SS, Lee TW, Sejnowski TJ. 1998. Spatially independent activity patterns in functional MRI data during the stroop color-naming task. Proc Natl Acad Sci USA 95:803-810

McKeown MJ, Sejnowski TJ. 1998. Independent Component Analysis of fMRI Data: Examining the Assumptions 372:368–372

Meda SA, Calhoun VD, Astur RS, Turner BM, Ruopp K, Pearlson GD. 2009a. Alcohol dose effects on brain circuits during simulated driving: an fMRI study. Hum Brain Mapp 30(4):1257-1270. doi: 10.1002/hbm.20591

Meda SA, Stevens MC, Folley BS, Calhoun VD, Pearlson GD. 2009b. Evidence for anomalous network connectivity during working memory encoding in schizophrenia: An ICA based analysis. PLoS One 4:e7911. doi: 10.1371/journal.pone.0007911

Menon V, Uddin L. 2010. Saliency, switching, attention and control: a network model of insula function. Brain Struct Funct 214:655-667. doi: 10.1007/s00429-010-0262-0

Mosconi MW, Kay M, D'Cruz AM, Seidenfeld A, Guter S, Stanford LD, Sweeney JA. 2009. Impaired inhibitory control is associated with higher-order repetitive behaviors in autism spectrum disorders. Psychol Med 39:1559-1566. doi: 10.1017/S0033291708004984

Power JD, Barnes KA, Snyder AZ, Schlaggar BL, Petersen SE. 2012. Spurious but systematic correlations in functional connectivity MRI networks arise from subject motion. Neuroimage 1;59(3):2142-2154. doi: 10.1016/j.neuroimage.2011.10.018

Raichle ME, MacLeod AM, Snyder AZ, Powers WJ, Gusnard DA, and Shulman GL. 2001. A default mode of brain function. Proc Natl Acad Sci U S A 16;98(2):676-682

Segall JM, Allen EA, Jung RE, Erhardt EB, Arja SK, Kiehl K, Calhoun VD. 2012. Correspondence between structure and function in the human brain at rest. Front Neuroinform 27;6:10. doi: 10.3389/fninf.2012.00010

Shaffer D, Fisher P, Lucas CP, Dulcan MK, Schwab-Stone ME. 2000. NIMH Diagnostic Interview Schedule for Children Version IV (NIMH DISC-IV): description, differences from previous versions, and reliability of some common diagnoses. J Am Acad Child Adolesc Psychiatry 39(1):28-38

Sladky R, Friston KJ, Tröstl J, Cunnington R, Moser E, Windischberger C. 2011. Slice-timing effects and their correction in functional MRI. Neuroimage 15;58(2):588-594. doi: 10.1016/j.neuroimage.2011.06.078

Solomon M, Ozonoff SJ, Cummings N, Carter CS. 2008. Cognitive control in autism spectrum disorders. Int J Dev Neurosci 26(2):239-247

Solomon M, Ozonoff SJ, Ursu S, Ravizza S, Cummings N, Ly S, Carter CS. 2009. The neural substrates of cognitive control deficits in autism spectrum disorders. Neuropsychologia 47(12):2515-2526. doi: 10.1016/j.neuropsychologia.2009.04.019

Supekar K, Musen M, Menon V. 2009. Development of large-scale functional brain networks in children. PLoS Biology 7(7):e1000157. doi: 10.1371/journal.pbio.1000157

Van Dijk KR, Sabuncu MR, Buckner RL. 2012. The influence of head motion on intrinsic functional connectivity MRI. Neuroimage 2;59(1):431-438. doi: 10.1016/j.neuroimage.2011.07.044

Wechsler D. 2005. Wechsler Intelligence Scale for Children – Derde Editie NL. Handleiding en Verantwoording. (Wechsler Intelligence Scale for Children – Third Edition, Dutch Version, Manual). London: Harcourt Assessment

Xu J, Potenza MN, Calhoun VD. 2013a. Spatial ICA reveals functional activity hidden from traditional fMRI GLM-based analyses. Front Neurosci 7:154

Xu J, Zhang S, Calhoun VD, Monterosso J, Li CS, Worhunsky PD, Stevens M, Pearlson GD, Potenza MN. 2013b. Task-related concurrent but opposite modulations of overlapping functional networks as revealed by spatial ICA. Neuroimage 1;79:62-71. doi: 10.1016/j.neuroimage.2013.04.038

Zhang S, Li CR. 2012. Functional Networks for Cognitive Control in a Stop Signal Task: Independent Component Analysis. Hum Brain Mapp 33(1): 89-104. doi: 10.1002/hbm.21197

SUPPLEMENTARY MATERIAL

GLM analysis of fMRI data during task performance

As described in the main paper, the fMRI data were preprocessed using a standard pipeline in SPM8 (Wellcome Dept. of Cognitive Neurology, www.fil.ion.ucl.ac.uk). Following this, the preprocessed data were cleaned before the statistical analyses using single-subject ICA. This is an effective method for removing noise from the data, and as such is also advantageous to GLM analyses.

fMRI task analyses – GLM methods

The design matrices used in the GLM analyses were identical to the ones we used in the ICA analysis (see the main paper for a description). At the first level, five event types were defined: initial fixation, go trials, correct and incorrect no-go trials, and a parametric factor representing the number of go trials preceding a no-go event. These events included two events of interest (go and no-go trials) and three events of no interest (errors, fixation and the parametric factor). The event-types were time-locked to stimuli by a canonical synthetic hemodynamic response function (HRF) and its first-order temporal derivative (tHRF).

Table S1. Relationship between activity in networks and task events (go and no-go trials)

Independent component		**β: M/SD**		**p-value correlation with task[a]**	
Name	**num**	**go**	**no-go**	**go**	**no-go**
Frontal / Attentional networks	**30**	.71/2.31	2.55/2.61	.065	<.001
	33	-2.04/2.79	-1.47/2.76	<.001	.002
	34	.44/2.94	1.93/3.12	.364	<.001
Default mode networks	**12**	-2.89/3.13	-2.76/3.33	<.001	<.001
	28	-2.48/2.53	-3.72/2.74	<.001	<.001
Visual networks	**9**	-2.66/3.26	-3.49/3.14	<.001	<.001
	15	-5.07/3.40	-4.87/3.20	<.001	<.001
	26	-2.23/2.41	-3.37/2.50	<.001	<.001
Hippocampus network	**41**	-1.12/1.57	-1.09/1.83	<.001	.001
Auditory network	**44**	-.69/2.19	-1.40/2.29	.058	<.001
Temporal network	**29**	-1.61/1.91	-2.11/2.16	<.001	<.001

[a]One-sample t-test to determine whether β differed from zero, uncorrected p-values

For the group analysis, a random effects model was used in SPM8 to compute a voxelwise T-statistic for the contrast no-go trials > go trials. Regions of Interest included the all voxels that were activated in the ASD and typically developing group during

the no-go > go condition, tested with a one-sample T-test with age as covariate, at a threshold of $p < .001$ (uncorrected), $k > 10$ voxels. Group differences in activation were again tested with a random effects model, using two-sample T-tests at a False Discovery Rate-corrected threshold of $p < .05$, with age entered as a covariate to the design.

fMRI task analyses – GLM results

The one-sample T-test over all participants showed the usual pattern of activation in cognitive control areas, such as the anterior cingulate cortex, bilateral inferior frontal gyrus, bilateral orbitofrontal gyrus, bilateral insula and areas in the bilateral inferior parietal cortex (Supplemental Fig. 1). Two-sample T-test showed that there were no group differences in activation during no-go trials, even when the threshold was liberalized to $p < .001$ (uncorrected), $k > 10$ voxels. Taken together, these results indicate that our paradigm successfully engaged cognitive control areas, both for children with ASD and typically developing controls and that there were no differences in brain activity between diagnostic groups.

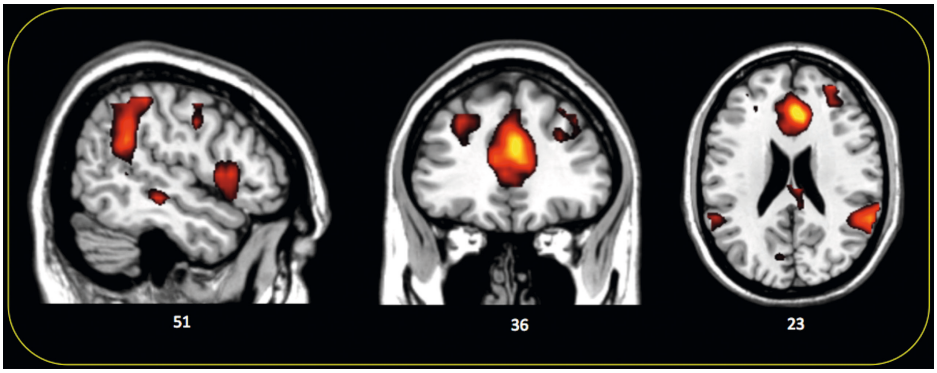

Figure S1. Activation in cognitive control areas during no-go trials. Maps of brain activity for the whole group for the contrast no-go > go, SPM(T) overlaid on a single subject T1 template. The MNI slice location is provided below each image.

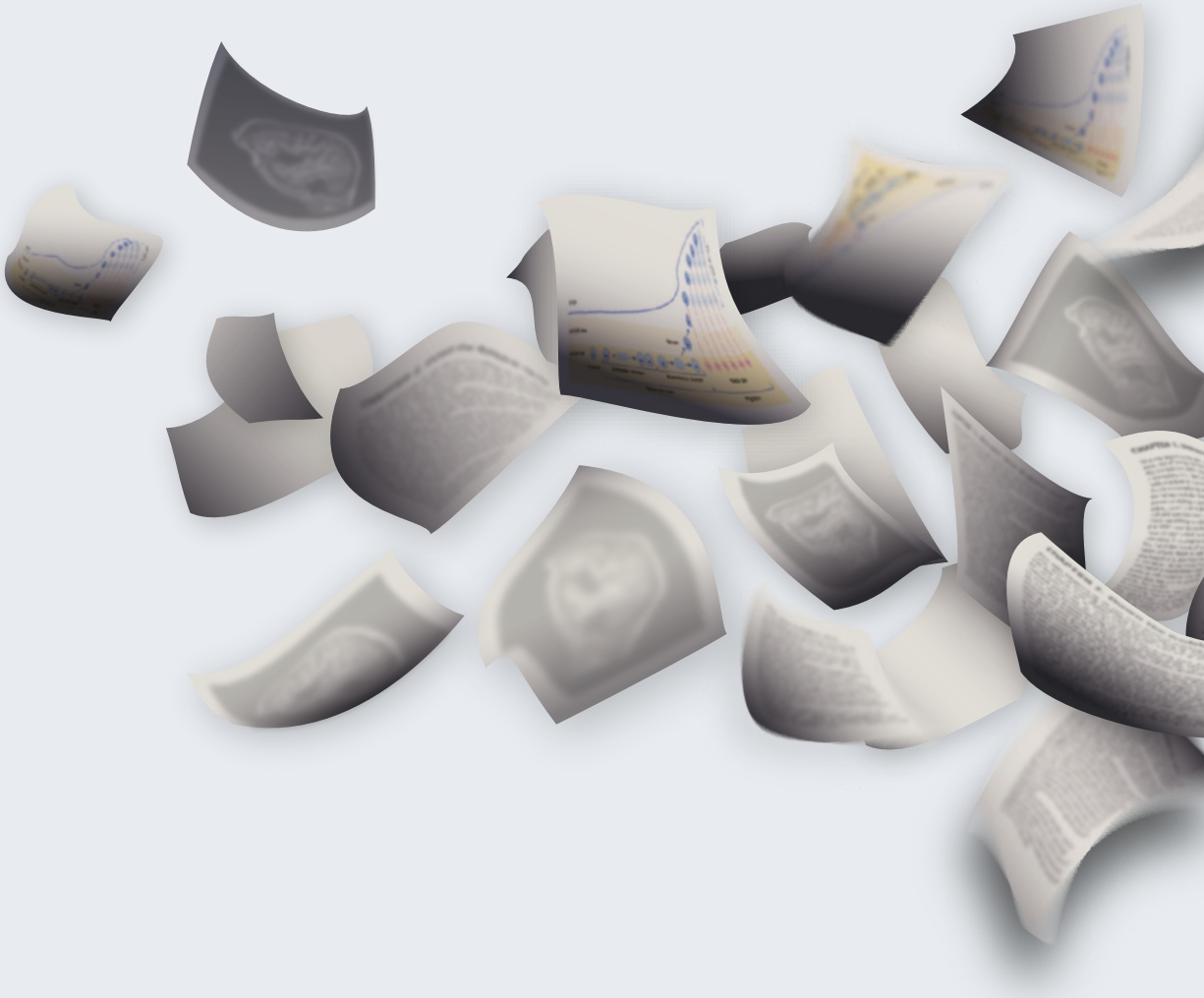

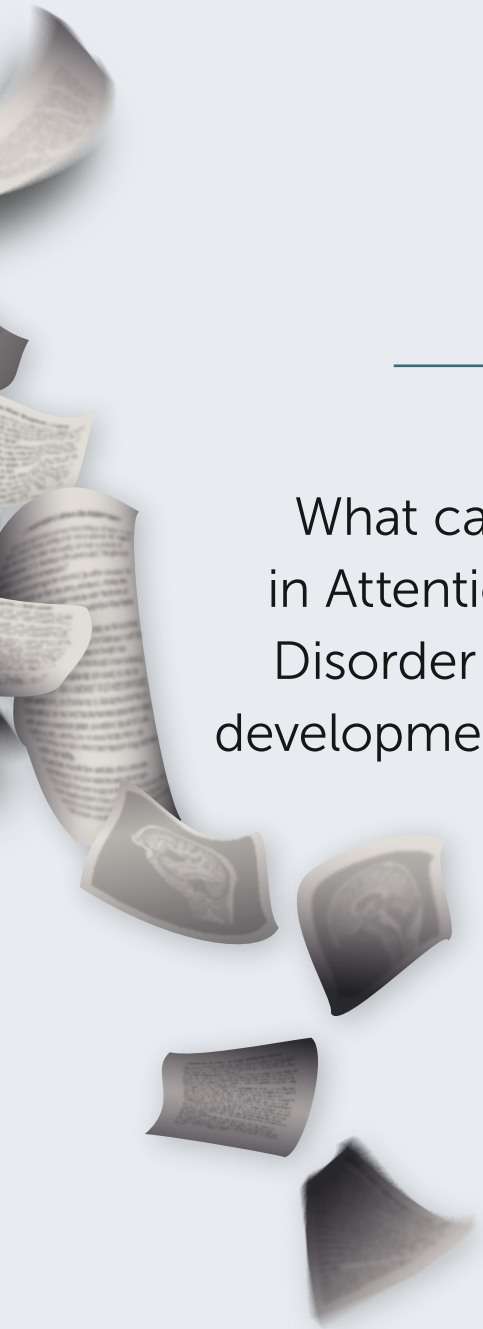

CHAPTER 3

What can cortical development in Attention-Deficit/ Hyperactivity Disorder teach us about the early developmental mechanisms involved?

Sara Ambrosino, Patrick de Zeeuw & Lara Marise Wierenga,
Sarai van Dijk, Sarah Durston

Cerebral Cortex, September 2017;27: 4624–4634

ABSTRACT

Studies of Attention-Deficit/Hyperactivity Disorder (ADHD) have shown developmental changes in the cortical mantle. Different dimensions of cortical morphology, such as surface area and thickness, relate to different neurodevelopmental mechanisms. As such, studying multiple dimensions may inform us about the developmental origins of ADHD. Furthermore, results from existing longitudinal samples await replication.

Therefore, we conducted a longitudinal study of multiple cortical dimensions in a sizable, independent ADHD sample. We analyzed 297 anatomical MRI scans from two matched groups of 94 subjects with ADHD and 94 controls, aged 6–28 years. We estimated the developmental trajectories of cortical volume, surface, thickness and gyrification for 68 regions using mixed-effects regression analysis. Subjects with ADHD had smaller overall cortical volume, predominantly driven by decreases in frontal lobe volume that were associated with reduced surface area and gyrification. Nearly all decreases were stable across development. Only a few decreases survived stringent Bonferroni correction for multiple comparisons, with the smallest detectable Cohen's d |0.43|. There were no between-group differences in cortical thickness, or in subcortical volumes. Our results suggest that ADHD is associated with developmentally persistent reductions in frontal cortical volume, surface area, and gyrification. This may implicate early neurodevelopmental mechanisms regulating cortical expansion and convolution in ADHD.

INTRODUCTION

Studies of brain development in Attention-Deficit/Hyperactivity Disorder (ADHD) have shown developmental changes in volume of cortical and subcortical areas (Valera et al. 2007; Durston et al. 2009a; Nakao et al. 2011; Frodl and Skokauskas 2012; Greven et al. 2015; Vilgis et al. 2016; Hoogman et al. 2017). However, the developmental mechanisms underlying these changes are still unclear. Relatively new analysis approaches may provide the opportunity to address these mechanisms: distinct dimensions of the cortex, such as surface area and thickness, relate to different cytoarchitectonic properties, which in turn are hypothesized to be determined by partially distinct neurodevelopmental mechanisms (Rakic 1995; Panizzon et al. 2009; Chen et al. 2013). For example, the radial unit hypothesis of early development (Rakic 1995) postulates that cortical surface area is related to the number of columnar units (Mountcastle 1997; Jones 2000), which is regulated by the number of neural progenitor cells dividing symmetrically during early phase of neuronal proliferation: at each round of symmetric division, each progenitor generates two progenitor cells, with exponential increase of the founders of cortical columns. In contrast, cortical thickness is hypothesized to be regulated by the number of postmitotic neurons that arise from asymmetric cell division and then migrate within a column during embryonic neurodevelopment (Rakic 1995, 2000). Therefore, the symmetric cell proliferation would relate to the expansion of cortical surface area, whereas asymmetric division would determine its thickness. As such, studying these markers of cortical morphology, for example, cortical surface area and thickness, separately in ADHD may potentially inform us on the developmental stage at which early cortical changes occur.

There have been numerous studies on brain development in ADHD, with those from the research group at National Institute of Mental Health (NIMH) perhaps being the most prolific. They have reported reductions in cortical thickness (Shaw et al. 2006) that have been (partially) replicated (Sowell et al. 2003; Narr et al. 2009; Batty et al. 2010; Schweren et al. 2015) but not always (Wolosin et al. 2009; de Zeeuw et al. 2012). The first studies to investigate different dimensions of cortical morphology (surface area and gyrification) have reported either reduced (Wolosin et al. 2009) or delayed (Shaw et al. 2012) cortical surface expansion in ADHD, whereas results for gyrification have been less unequivocal (Li et al. 2007; Shaw et al. 2012). The findings from NIMH of a simultaneous delay in the development of cortical thickness (Shaw et al. 2007) and surface area (Shaw et al. 2012) suggest that there may be a global perturbation of cortical maturation in ADHD (Shaw et al. 2012). To date, no studies have assessed all relevant cortical markers simultaneously (cortical volume, thickness, surface area and gyrification) in a single, longitudinal sample. Doing so may permit a more refined characterization of cortical development in ADHD, as it will permit us to assess the

interplay between multiple architectonic features that represent different aspects of early development. Furthermore, studies of longitudinal brain development in ADHD are scarce and often come from overlapping samples (Castellanos et al. 2002; Shaw et al. 2007, 2012). Therefore, there is a call in the field for replication in other, independent longitudinal samples (Horga et al. 2014).

In the current study, we investigated brain development in ADHD, using comprehensive markers of cortical development, in a European, longitudinal sample. We hypothesized that subjects with ADHD would show decreases in cortical volume, in particular in frontal areas. We had no specific expectations regarding which aspects of cortical morphology (e.g., thickness or surface area) would be most affected.

MATERIALS AND METHODS

The Institutional Review Board of the University Medical Center Utrecht, the Netherlands, approved the study and its procedures. For subjects under the age of 18 years, written informed consent was obtained from the parents after full disclosure of the study purpose and procedure. Children provided written and/or verbal assent. Subjects aged 18 years or above gave written informed consent themselves.

Participants and Clinical Measures

We acquired 410 whole-brain MRI scans from 260 subjects (129 with ADHD and 131 typically developing controls). We used propensity score matching (PSM) to equalize gender, socioeconomic status (SES), and the number of longitudinal scans between groups. We chose not to match the groups for intelligence quotient (IQ) as changes in IQ are intrinsically related to ADHD (Frazier et al. 2004). Therefore, matching for IQ would have led to unrepresentative samples of both the ADHD and control populations (i.e., selection bias). Such bias would likely remove variability in the dependent variables of interest (e.g., brain volume) and possibly generate anomalous findings (Dennis et al. 2009). PSM resulted in a sample of 188 closely matched subjects (94 in each group), aged between 6 and 28 years. There were a total of 297 MRI scans available, with 73 participants (34 subjects with ADHD; 39 controls) scanned twice or more. There was no difference in mean age between groups at each wave of scanning. Longitudinal scans were acquired with a similar average interval in both groups (ADHD: M (SD) = 3.6 (2.0) years, controls: M (SD) = 3.4 (2.3) years; P = 0.739).

The Diagnostic Interview Schedule for Children (DISC, version 2.3 or IV), parent version (Shaffer et al. 2000), was administered to parents in order to confirm the clinical diagnosis of ADHD or to exclude psychiatric comorbidity in controls at study entry. Parents and teachers completed broadband psychiatric screeners at each time point:

Child Behavior Checklist (CBCL) and Teacher Report Form (TRF) respectively, to provide a dimensional measure of behavioral symptoms (Verhulst et al. 1996, 1997). Total IQ was estimated using a short form of the Dutch version of the Wechsler intelligence scales (WISC-R/WISC-III or WAIS-III as appropriate), including the subtests Vocabulary, Block Design, Similarities, and Object Assembly (Wechsler 2005). Controls were excluded in case of psychiatric morbidity or first-degree relatives with a history of psychiatric problems. Children with ADHD were excluded if they met DSM criteria for any co-morbid disorder other than Oppositional Defiant Disorder (ODD) or Conduct Disorder (CD) on the DISC at study entry. In both groups, additional exclusion criteria were IQ below 70, any major physical or neurological illnesses or the presence of metals in the body that precluded the MRI session. Table 1 lists participant characteristics for both samples. Medication status based on parental- and self-report could reliably be assessed at study entry for 89% of ADHD cases. At study entry, 75% of the subjects with ADHD were using psychostimulant medication. The vast majority (94%) was taking methylphenidate preparations. The proportion of medicated subjects declined slightly at follow-up: 73% of subjects with ADHD were medicated at the time of their second scan, 67% were medicated at scan 3.

Prior to the MRI scan, children under 13 years of age were acclimated to the MRI procedure in a practice session using a dummy scanner as described previously (Durston et al. 2009b); children over 13 years were also offered the opportunity to do a practice session.

Propensity Score Matching

PSM is a statistical matching technique that pairs cases and controls with similar values on a propensity score (PS) from a pool of participants. The PS is the probability of group membership conditional on a set of observed non-random confounders. PSs were estimated using logistic regression, including gender, SES, and a dummy variable for the presence of longitudinal scans as covariates, implemented in SPSS 20.0.0 and R 3.0.2 (Thoemmes 2012). Subjects were then matched using 1:1 nearest neighbor matching. The caliper width (maximum permitted difference between two subjects) was set to the recommended value (Austin 2011) of 0.20 standard deviations of the logit of the PS.

Table 1. Demographic and clinical characteristics of the sample

		ADHD (N=94)	Controls (N=94)	Group Differences[e]
Gender	N Male - Female	78 - 16	80 - 14	ns
Age at scan	N scans Wave 1 / years M (SD)	94 / 11.4 (2.9)	94 / 11.2 (4.0)	ns
	N scans Wave 2 / years M (SD)	34 / 15.1 (2.6)	39 / 14.5 (3.4)	ns
	N scans Wave 3+ / years M (SD)	13 / 18.5 (2.7)	23 / 18.1 (2.7)	ns
Hand preference	N Righthanded/Other	70 / 24	77 / 17	ns
SES	Parental education years M (SD)	12.8 (2.2)	13.1 (2.0)	ns
Total IQ	M (SD) at baseline*	100.9 (16.8)	109.8 (16.8)	*
DISC[a]	N ADHD-I	23	0	-
	N ADHD-HI	16	0	-
	N ADHD-C	55	0	-
	N ODD	34	0	-
	N CD	1	0	-
CBCL[b]	Internalising raw score M (SD)	9.3 (5.6)	4.4 (4.9)	**
	Externalising raw score M (SD)	16.6 (9.5)	4.5 (5.0)	**
	Attention problem raw score M (SD)	9.2 (4.0)	3.1 (2.5)	**
TRF[c]	Internalising raw score M (SD)	7.5 (5.9)	3.5 (4.6)	**
	Externalising raw score M (SD)	13.1 (10.6)	3.0 (5.0)	**
	Attention problem raw score M (SD)	16.9 (9.4)	6.0 (7.0)	**
Medication	N Medicated / Unmedicated / No Reliable Info Avalaible at			
	Wave 1	64[d] / 20 / 10	0 / 94 / 0	**
	Wave 2	22 / 12 / 0	0 / 39 / 0	**
	Wave 3+	6 / 4 / 3	0 / 23 / 0	*

Abbreviations: ADHD, Attention-Deficit/Hyperactivity Disorder (I=inattentive type, HI=hyperactive/impulsive type, C=combined type); N, number; M, mean; SD, standard deviation; SES, Socio-Economic Status; IQ, intelligence quotient; DISC, Diagnostic Interview Schedule for Children; ODD, Oppositional Defiant Disorder; CD, Conduct Disorder; CBCL, Child Behavior Checklist; TRF, Teacher Report Form. Note. [a]DISC repeated at follow-up for 36% of the subjects; [b]CBCL unavailable for 9 controls and 13 ADHD subjects; [c]TRF unavailable for 19 controls and 30 ADHD subjects; [d]63 subjects on psychostimulants (59 on methylphenidate, 3 on dexamphetamine, 1 on atomoxetine), 1 subject on desipramine; [e]t-Test for age at scan at each wave of scanning and total IQ; X^2 for Gender and Handedness; nonparametric statistical test for SES, CBCL and TRF; Fisher's exact test for Medication status at each wave of scanning; ns, not significant; *p < .001; **p < .0001.

MRI Acquisition

All imaging was performed over the time span of 15 years using a 1.5-T MRI-scanner (Philips). A T1-weighted 3-dimensional fast field echo scan of the whole head was acquired with 130 to 150 1.5-mm contiguous coronal slices (earlier scans; 58 scans from subjects with ADHD and 51 scans from controls) or 160 to 180 1.2- mm contiguous coronal slices (later scans; 83 scans from subjects with ADHD and 105 scans from controls) (echo time 4.6ms; repetition time 30ms; flip angle 30°; field of view 256mm; in-lane voxel size 1 mm x 1 mm). There were no major hardware upgrades during the study, and all the appropriate quality control procedures (e.g., use of phantoms) were applied on a regular basis, as well as before and after each software upgrade. Groups did not differ with respect to the distribution of scan acquisition date (Levene's test P = 0.168), or MRI protocols (slice thickness 1.5 vs. 1.2mm), for either baseline (P = 0.770) or longitudinal measures (P = 0.133). Independent neuroradiologists evaluated all MRI scans and no gross morphological abnormalities were reported for any of the participants.

MRI Processing

All scans were coded in order to ensure rater blindness to subject identity and diagnosis at all times during analysis. The T1-weighted images were processed using FreeSurfer v5.1.0 (Fischl 2012), a well validated and widely used segmentation and image analysis software package (http://surfer.nmr.mgh.harvard.edu/fswiki).

The package contains a fully automated structural imaging pipeline for the quantitative assessment of brain anatomy including volumetry of subcortical structures and a complete assessment of cortical morphometry, along the entire surface and with accuracy comparable to manual methods (Fischl et al. 2002) and postmortem studies (Fischl and Dale 2000). The brain segmentation and cortical reconstruction pipelines in FreeSurfer have been described in more detail elsewhere (Dale et al. 1999; Fischl et al. 1999, 2002; Fischl and Dale 2000, 2004a, 2004b). In short, brain segmentation consists of registering the brain into Talaraich space (Talairach and Tournoux 1988), removing nonbrain tissue using a deformable template model (skull stripping), and neuroanatomical labeling, based on both voxel intensity values and a probabilistic atlas (Fischl et al. 2002). The reconstruction of cortical surfaces involves the segmentation of white matter, used to derive a surface representing the gray-white matter boundary (white surface). The white surface is then refined and deformed to locate the pial surface (gray matter/cerebrospinal fluid boundary) (Dale et al. 1999). Finally, by incorporating both geometric information derived from the cortical model and standard neuroanatomical conventions (Desikan et al. 2006; Destrieux et al. 2010), the procedure automatically assigns a neuroanatomical label to each location on the cortical surface (cortical parcellation). The automated cortical reconstruction

is described in more detail in the Supplementary Material. The FreeSurfer pipeline requires that output is checked individually at multiple points during the processing stream, in order to correct errors, if necessary. Given the sensitivity of cortical markers to movement and other acquisition artifacts, this post-processing quality control procedure ensures robustness and reliability of the results across participants (Dewey et al. 2010; Ducharme et al. 2016). Accordingly, we inspected the Talaraich registration, tissue segmentations, surface reconstructions and cortical parcellation for accuracy. If necessary, manual edits were performed by experienced operators (S.A. and L.M.W.) following the standardized procedures documented on the FreeSurfer website (http://surfer.nmr.mgh.harvard.edu/fswiki). The types of errors that frequently required user editing were incomplete skull stripping and mis-classification of white matter.

We acquired the volume of 24 noncortical regions, including 6 subcortical structures per hemisphere (caudate, putamen, pallidum, accumbens, thalamus, and amygdala), the corpus callosum (anterior, mid-anterior, central, mid-posterior, and posterior segments), bilateral hippocampus, bilateral cerebellar gray and white matter and the brain stem. For simplicity, we refer to these as "subcortical" structures.

For cortical morphometry, we analyzed 34 regions per hemisphere from the Desikan-Killiany atlas (Desikan et al. 2006) (see Supplementary Material). The FreeSurfer outputs of interest were cortical volume (CV, mm^3), cortical surface area (CS, mm^2), cortical thickness (CT, mm), and local gyrification index (LGI, dimensionless) of the cortex as a whole and within the predefined areas (Fig. 1).

For each area, CS was measured along the white surface; CV and CT were measured as the volume and the average distance, respectively, between parcellated portions of white and pial surfaces (Fischl and Dale 2000). LGI is a measure of gyral complexity that is calculated at each point of the pial surface and was averaged across each area. LGI refers to the ratio between the surface of a circular patch of the pial surface and the corresponding patch on the outer smoothed surface of the brain (Schaer et al. 2008).

Total, left (lh) and right (rh) hemisphere values were obtained for cortical volume, surface, thickness and gyrification by summing or averaging each measure across all areas included. Average thickness throughout the cortex was computed applying the formula:

Total CT = ((lh.CT * lh.CS) + (rh.CT * rh.CS)) / lh.CS + rh.CS
(http://surfer.nmr.mgh.harvard.edu/fswiki).

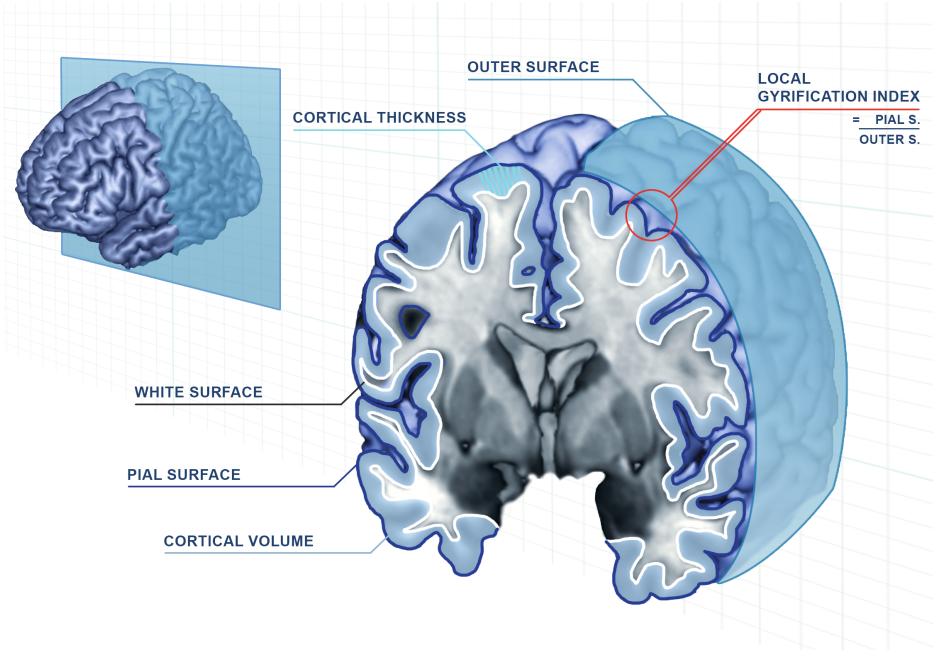

Figure 1. Morphometric parameters of the cerebral cortex.

For every defined region of interest, cortical thickness was estimated as the average distance (in mm) between the white and pial surfaces; cortical surface was the area of the white surface (in mm^2); cortical volume was calculated as the volume contained between the white and pial surfaces (in mm^3); local gyrification index (dimensionless) was computed as the ratio between the pial and outer surface.

Statistical Analysis

SPSS Statistics 20.0.0 for Mac OS X (SPSS Inc.) was used to test for between-group differences in demographic and clinical data using parametric or non-parametric tests as appropriate.

The developmental trajectories of each measure were estimated using (generalized) Linear Mixed Models as implemented in the lme4 library (Bates et al. 2011) in the R statistical package (R Development Core Team 2012). This method permits the inclusion of multiple scans per person, to combine both inter- and intra-individual differences in the growth parameters (i.e., intercepts and slopes), while accounting for unbalanced data structure due to irregular time intervals between scans and unequal numbers of scans between subjects.

The best-fit model was determined in two phases following the procedure described previously (Wierenga et al. 2014a, b). First, a growth model was determined using a step-down selection procedure. Each brain measure of the i^{th} individual at the j^{th} time point was modeled using cubic, quadratic and linear age effects (with age centered

around the mean of the whole group: 13 years), with gender as a covariate, according to the formula:

$$Measure_{ij} = Intercept + d_{ij} + \beta_1 (gender) + \beta_2 (age) + \beta_3 (age)^2 + \beta_4 (age)^3 + e_{ij}$$

where d_{ij} represents the within person dependence and the e_{ij} term is the residual error. Gender and age effects were fixed, while the intercept and the d_{ij} term were modeled as random effects. If the cubic age effect was not significant at $p < .05$, it was removed from the model in order to test the quadratic age effect and so on.

Second, we examined whether the growth model differed between subjects with ADHD and controls. The selected growth model was expanded to include a dichotomous variable "ADHD" and its interaction with the age term(s) as fixed factors. For example, measures where the cubic model was appropriate were modeled as:

$$Measure_{ij} = Intercept + d_{ij} + \beta_1 (gender) + \beta_2 (age) + \beta_3 (age)^2 + \beta_4 (age)^3 + \beta_5 (ADHD) + \beta_6 (ADHD)*(age) + \beta_7 (ADHD)*(age)^2 + \beta_8 (ADHD)*(age)^3 + e_{ij}$$

We tested whether the full model fit the data better than a simpler model including only the main effects of the ADHD and age. If it did not (indicating that there was no group by age interaction), the simpler model was compared to the selected growth model including the age terms only (i.e., this would denote that ADHD had no effect at all). Coefficients were estimated using the full Maximum Likelihood criterion and models were compared using the Bayesian Information Criterion (BIC). If the difference between the BIC of two nested models was greater than 2, the model with the lower BIC was selected; if ($\Delta BIC \leq 2$), the simplest model was selected on the grounds of parsimony. This procedure permitted us to achieve a balance between model complexity and goodness of fit (Kass and Raftery 1995).

We calculated effect sizes for the ADHD predictor by dividing the fixed effect estimate by the square root of the variance at the within-subject level (Tymms 2004). This estimate of effect size is equivalent to Cohen's d (Cohen 1992).

We applied Bonferroni correction to control for multiple comparisons for ADHD main effects (adjusted p-value .00008). However, such correction is likely to be overly conservative given interdependency between brain regions and measures. Combined with the multi-dimensional nature of the data this makes it near impossible to compute the effective number of degrees of freedom in the data. Hence, we report both corrected and uncorrected results here.

In addition, we performed robustness analyses to assess the robustness of our findings in the face of potential confounders. First, a dummy variable for slice thickness (1.5 vs 1.2 mm) was included as an additional fixed term in the growth models. To

enable inferences about local changes un-confounded by global brain measures, further analyses with intracranial volume (ICV), total cortical surface area, average cortical thickness, or average local gyrification to correct local measures of cortical and subcortical volumes, cortical surface area, cortical thickness and local gyrification, respectively, were run. However, given collinearity between gender and ICV, any analysis including both measures must be interpreted with caution. We did not add IQ to the model due to the problems of controlling for characteristics that are intrinsic to the phenotype of interest (Dennis et al. 2009). Finally, since there were only few data points over age 25 years, we reran the analysis without older participants. Since this did not lead to any meaningful changes in the results and interpretation, we report the results from all participants here.

RESULTS

Total cortical volume, surface, thickness and gyrification

The developmental trajectories of total cortical volume and its geometric properties (surface area, thickness and gyrification) are shown in Figure 2. The regression coefficients are provided in the Supplementary Material (Table S2). There was a quadratic effect of age and a main effect of ADHD on total cortical volume, but no interaction between ADHD and age. Mean total cortical volume was 5% smaller for subjects with ADHD than controls and this difference was stable across development. Total cortical surface area followed a cubic trajectory for the entire group; total cortical thickness and total gyrification both showed a linear decrease with age for the group as a whole. There were no main effects or interaction between age and diagnostic group for these measures.

The analysis for each hemisphere separately showed that there was a reduction of cortical volume in the left hemisphere for ADHD, and a reduction of cortical volume and surface area in the right hemisphere (Table S2).

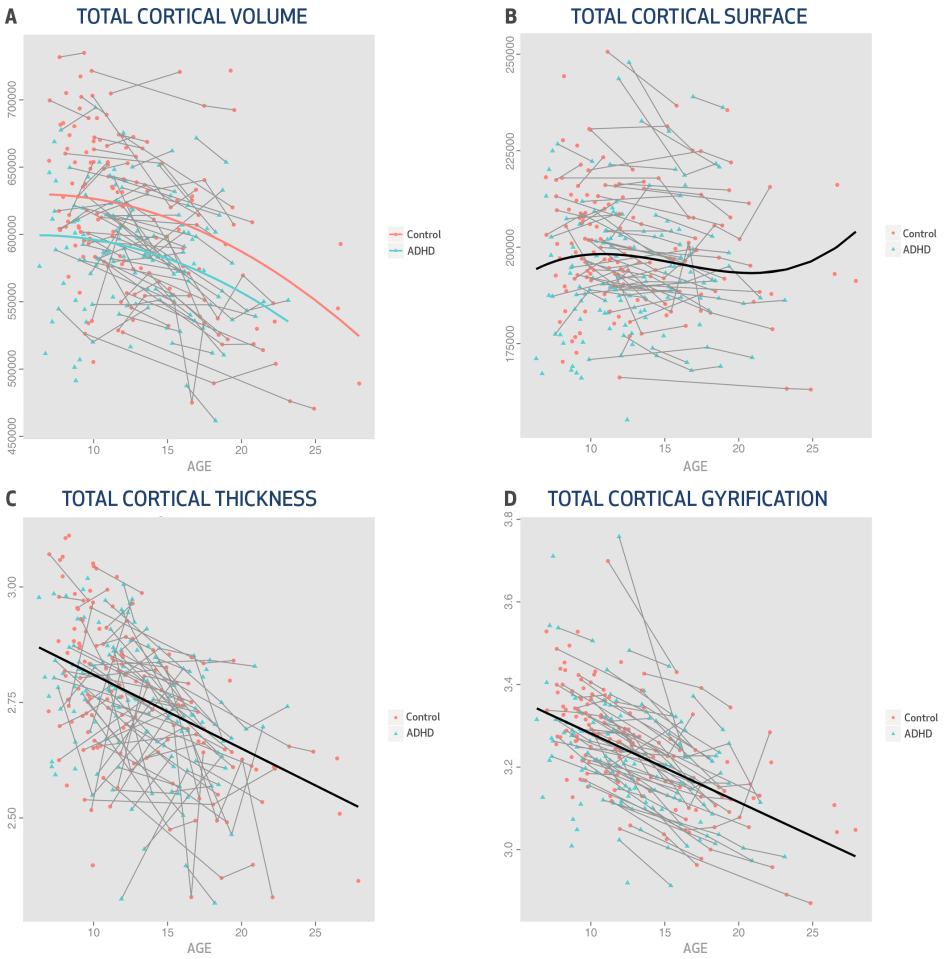

Figure 2. Developmental trajectories of total cortical volume (panel A, mm^3), total surface area (panel B, mm^2), total cortical thickness (panel C, mm) and total gyrification index (panel D, dimensionless). Abbreviations: ADHD, Attention-Deficit/Hyperactivity Disorder.

Local differences in cortical volume, surface area, thickness and gyrification

Subjects with ADHD had reduced cortical volume in several areas throughout the cortex, predominantly in frontal lobes (caudal anterior cingulate and rostral middle frontal cortex of the left hemisphere, bilateral medial and lateral orbitofrontal cortex, bilateral precentral cortex, right superior frontal, caudal middle frontal and pars opercularis of the inferior frontal gyrus). There were no group by age interaction effects on regional cortical volumes, indicating that the main effects of diagnosis were stable across development. Surface area and gyrification were also reduced in a number of areas. There were no differences in thickness in any cortical area. Table 2 and Figure

3 summarize these differences; parameters for developmental trajectories and effect sizes are provided in the Supplementary Material Table S3.

Reductions in volumes were particularly pronounced in the caudal middle frontal and isthmus cingulate cortices of the right hemisphere, where volume reductions of more than 10% (>4 SD below the mean of the controls) were found. Effect sizes ranged from -.43 to -.78, and are therefore 'small' to 'medium' according to Cohen's criteria (Cohen 1992). In many regions, the reduction of surface area occurred together with a reduction of cortical volume (left caudal anterior cingulate, rostral middle frontal and superior temporal cortices; right caudal middle frontal cortex, isthmus cingulate cortex, pars opercularis and lateral occipital cortex). In two regions with decreased cortical volume and surface area, we also found reduced gyrification (left rostral middle frontal cortex and right pars opercularis).

For nearly all areas, there were no differences in the shape of developmental trajectories between the ADHD and control groups. As such, the reductions in cortical surface area and gyrification described above were stable over development. We found only two group by age interactions: for gyrification in the left cuneus and right pars opercularis. In these regions, the gyrification was reduced in the younger age ranges in ADHD, but declined less steeply in subjects with ADHD than controls, which led to convergence of the gyrification index at later age ranges (see: Supplementary Figure S3).

Subcortical areas

There were no differences between groups in the developmental trajectories of any subcortical areas, nor were there any main effects of diagnosis.

Results with Stringent Bonferroni Correction for Multiple Comparisons and Robustness Analyses

Between-group differences in cortical volume reached Bonferroni-corrected significance for the following regions: left, right, and total cortical volume (see Supplementary Table S2), and locally for left rostral middle frontal cortex, left superior parietal, left superior temporal, left supra marginal cortices, right isthmus cingulate, and right lateral occipital cortices (Table 2 and Fig. 3; see Supplementary Table S3). These results were deemed robust, as they retained significance when slice thickness and ICV were included in the model as additional covariates, except for left cortical volume. Between-group differences in cortical surface area and gyrification failed to reach Bonferroni-corrected significance, or when total cortical surface area or average local gyrification (respectively) were added to the model (Supplementary Table S4). As such, they were deemed less robust.

Table 2. Only significant between-group differences for regional measures at the time of the first scan (baseline values)

Left hemisphere						Right hemisphere					
Volume (mm^3)	**Controls M (SD)**	**ADHD M (SD)**	**Δ%**	**t(186)**	**p value**	**Volume (mm^3)**	**Controls M (SD)**	**ADHD M (SD)**	**Δ%**	**t(186)**	**p value**
caudalanteriorcingulate	2364.17 (620.95)	2131.25 (512.94)	9.85	-2.804	.006	**caudalmiddlefrontal**	8693.085 (1611.33)	7785,415 (1416.34)	10.44	-4.102	<.0001
lateralorbitofrontal	9645.06 (1280.61)	9152.60 (1186.19)	5.11	-2.735	.007	**cuneus**	3895.93 (588.77)	3591.45 (634.43)	7.82	-3.411	<.001
medialorbitofrontal	6648.14 (942.18)	6231.90 (953.22)	6.26	-3.011	.003	**isthmuscingulate**[B]	3460.10 (724.36)	3094.21 (509.83)	10.57	-4.005	<.0001
middletemporal	14873.34 (2070.92)	14144.67 (1836.65)	4.90	-2.552	.012	**lateraloccipital**[B]	14491.13 (2097.74)	13229.42 (1734.95)	8.71	-4.494	<.0001
precentral	16023.61 (1836.40)	15349.56 (1794.82)	4.21	-2.545	.012	**lateralorbitofrontal**	9458.86 (1279.44)	8952.87 (1146.93)	5.35	-2.855	.005
precuneus	13796.31 (1792.36)	12977.44 (1730.64)	5.94	-3.187	.002	**medialorbitofrontal**	6273.25 (848.37)	5873.16 (829.83)	6.38	-3.269	.001
rostralmiddlefrontal[B]	23282.65 (3312.90)	21494.06 (2341.65)	7.68	-4.274	<.0001	**parsopercularis**	5787.43 (963.86)	5300.62 (921.71)	8.41	-3.539	.001
superiorparietal[B]	18177.81 (2473.67)	16961.56 (2000.78)	6.69	-3.706	<.001	**precentral**	16002.22 (1931.85)	15119.47 (1740.48)	5.52	-3.291	.001
superiortemporal[B]	16179.76 (1955.96)	15048.86 (1788.64)	6.99	-4.137	<.0001	**precuneus**	14164.17 (1972.88)	13387.95 (1859.06)	5.48	-2.776	.006
supramarginal[B]	15878.93 (2151.64)	14688.31 (2096.45)	7.50	-3.843	<.001	**superiorfrontal**	30092.40 (3711.68)	28745.44 (2876.46)	4.48	-2.781	.006
						superiorparietal	18074.09 (2442.41)	17086.73 (2046.77)	5.46	-3.004	.003
						superiortemporal	15571.57 (1965.54)	14801.53 (1580.31)	4.95	-2.960	.003
Surface Area (mm^2)	**Controls M (SD)**	**ADHD M (SD)**	**Δ%**	**t(186)**	**p value**	**Surface Area (mm^2)**	**Controls M (SD)**	**ADHD M (SD)**	**Δ%**	**t(186)**	**p value**
caudalanteriorcingulate	705.61 (153.51)	645.12 (153.51)	8.57	-2.908	.004	**caudalmiddlefrontal**	2692.20 (539.24)	2407.82 (439.15)	10.56	-3.965	<.001
rostralanteriorcingulate	922.50 (156.31)	857.87 (179.75)	7.01	-2.630	.009	**isthmuscingulate**	1044.27 (185.54)	949.76 (174.11)	9.05	-3.601	<.001
rostralmiddlefrontal	6791.60 (909.71)	6341.90 (906.39)	6.62	-3.395	.001	**lateraloccipital**	5649.27 (755.85)	5291.44 (682.30)	6.33	-3.407	.001
superiortemporal	4436.60 (487.06)	4180.88 (472.39)	5.76	-3.654	<.001	**parsopercularis**	1647.07 (273.67)	2407.82 (278.47)	9.57	-3.916	<.001
Gyrification	**Controls M (SD)**	**ADHD M (SD)**	**Δ%**	**t(186)**	**p value**	**Gyrification**	**Controls M (SD)**	**ADHD M (SD)**	**Δ%**	**t(186)**	**p value**
cuneus	3.03 (0.18)	2.99 (0.23)	1.29	-1.298	.196	**parsopercularis**	4.80 (0.34)	4.67 (0.32)	2.77	-2.775	.006
rostralmiddlefrontal	3.01 (0.17)	2.93 (0.17)	2.60	-3.116	.002	**transversetemporal**	5.39 (0.36)	5.23 (0.38)	2.97	-2.953	.004

Abbreviations and symbols: ADHD, Attention-Deficit/Hyperactivity Disorder; M, mean; SD, standard deviation; Δ%, percentage change, determined by dividing the difference of the ADHD and control values by the control value, multiplied by 100; [B]between-group differences in developmental trajectories reaching Bonferroni-corrected significance.

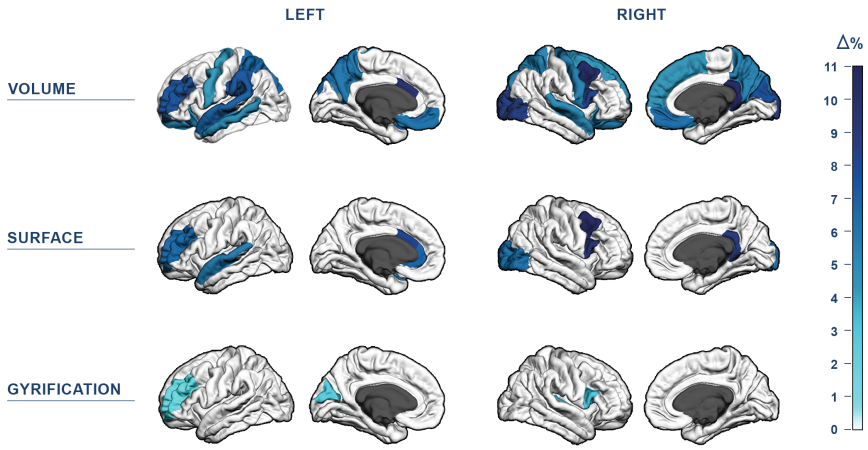

Figure 3. Group differences for regional measures.

Note. The darker the color, the greater the reduction in Attention-Deficit/Hyperactivity Disorder compared to controls. References to color in this figure legend are provided in Table 2.

DISCUSSION

In this study, we investigated brain development in an independent, longitudinal sample of subjects with ADHD and matched, typically developing controls. We found reduced cortical volume in ADHD, predominantly in the frontal lobes, in line with previous studies (Castellanos et al. 2002; Durston et al. 2009a; Wolosin et al. 2009; Batty et al. 2010). More detailed examination of cortical markers suggested that the reductions in volume were primarily driven by a reduction in surface area, rather than thinning of the cortex, and that these differences persisted across development.

We found changes with development in cortical and subcortical areas for both controls and ADHD subjects, reflecting structural maturation of the brain. Furthermore, we observed different developmental trajectories for the different cortical dimensions (surface area, thickness and gyrification), supporting earlier studies (Raznahan et al. 2011; Wierenga et al. 2014b) and suggesting that they may be driven, at least in part, by distinct regulatory processes (Panizzon et al. 2009; White et al. 2010).

Our data suggest that ADHD is primarily associated with developmentally stable changes in the volume of the cortical mantle as a whole and of specific cortical regions proportionally, as these changes did not seem to be driven by more global reductions in brain volume.

These changes appear to be mostly due to decreased surface expansion, as evidenced by reductions in surface area, and less convolution, as evidenced by reductions in gyrification. This pattern of results particularly implicates the

neurodevelopmental mechanisms that govern the tangential growth and sulcation of the cortex in ADHD.

According to the radial unit hypothesis (Rakic 1995), cortical surface area is determined by the number of columns, which in turn depend on the number of neural progenitors within the proliferative zones. The proliferation phase of embryonic brain development is governed by mechanisms that either promote the number of neurons that can migrate to target cortical areas (neurogenesis) or restrict it (cell death) (Rakic 2000). Therefore, either lower production or excessive loss of cells during proliferation could lead to a lower degree of cortical expansion. Disorders of late neuronal proliferation have been associated with congenital anomalies such as primary microcephaly, characterized by small brain size with normal to thin cortex and simplified, but grossly conserved, gyral patterning (Barkovich et al. 2012). We speculate that a possible mechanism underlying the reduction in surface area with preserved cortical thickness in ADHD may represent a minor perturbation of late neuronal proliferation, leading to a subtle but stable reduction of cortical surface area, with largely preserved cortical layering. Any reflection on the mechanisms underlying such a perturbation is of necessity speculative. However, it is noteworthy that teratogenic substances targeting neuronal precursors, such as nicotine and alcohol have been linked to ADHD (Linnet et al. 2003; Banerjee et al. 2007), as have a number of genetic and molecular factors regulating neuronal proliferation and differentiation (e.g., *DIRAS2* (Reif et al. 2011), *CDH13* (Poelmans et al. 2011; Rivero et al. 2013), *UPF3B* (Jolly et al. 2013), BDNF (Shim et al. 2008) and other neurotrophins (Syed et al. 2007).

Our results of decreases in cortical surface area and gyrification contrast with earlier findings of decreased cortical thickness (Sowell et al. 2003; Shaw et al. 2006; Narr et al. 2009; Schweren et al. 2015) and smaller striatum volume in ADHD (Durston et al. 2009a; Nakao et al. 2011; Frodl and Skokauskas 2012; Greven et al. 2015; Hoogman et al. 2017). Furthermore, we did not replicate longitudinal results showing delays in the maturation of cortical thickness and surface area in the NIMH longitudinal sample (Shaw et al. 2007, 2012). In the field, there is a call for replication in independent samples, particularly for longitudinal studies. As such, it is noteworthy that we do not fully replicate their findings, but rather report different ones in this independent sample. It underscores that earlier results do not necessarily generalize to other samples of subjects with ADHD, but that differences between ADHD and controls may vary as a function of sample characteristics. Important differences between the NIMH sample and ours are in geographical location, average IQ and SES. The NIMH studies have typically matched groups for IQ and SES (e.g., Shaw et al. 2007), whereas we matched for SES only. Demographic differences within and between studies are increasingly being recognized as an important caveat in conducting and comparing neuroimaging studies in developmental disorders (Horga et al. 2014). Another factor contributing to

these differences might be methodology; the NIMH studies investigated between-group differences in the mean age of the peak of their developmental models. We applied a rigorous post-processing quality control procedure (Ducharme et al. 2016) and a stringent statistical method to determine the best developmental model for our data, resulting in different models than those used in the NIMH sample. Furthermore, we investigated cortical markers per area, rather than per vertex, to preserve statistical power. In doing so, we may have missed small effects in highly localized cortical areas.

There are some limitations to our study. First, a sensitivity analysis using G*Power (Faul et al. 2007) showed that the smallest effect size detectable with our data for 80% power was |.43|, at the Bonferroni-corrected alpha-level. Therefore, although our sample was sufficiently sensitive to small to medium effects (Cohen 1992), we were unable to detect differences of the magnitude that have been reported previously (i.e. <-0.2) in meta- and mega-analyses of cortical and subcortical measures and their developmental trajectories (Valera et al. 2007; Hoogman et al. 2017). Second, the majority of subjects with ADHD in our sample were using psychostimulants. There was insufficient power to statistically investigate the effect of medication on our results. Third, we could not examine developmental trajectories in more homogeneous clinical subgroups based on gender, IQ, subtype or severity of the clinical presentation.

In conclusion, our findings show developmentally persistent reductions in cortical volume, surface area, and gyrification in our sample of subjects with ADHD, particularly in frontal areas. These findings contrast with other studies in different samples and underscore the importance of replication in independent samples, particularly for longitudinal data. Furthermore, they suggest that, at least for some children with ADHD, the disorder may be associated with an early (prenatal) disruption of cortical development leading to changes in surface area and gyrification that are stable across development.

FUNDING

The Netherlands Organisation for Scientific Research (Nederlandse Organisatie voor Wetenschappelijk Onderzoek [NWO]) (VIDI 91776384 and VICI 453-10-005 grants to S.D.).

NOTES

We would like to thank all participants and their families for participating in this study. We further wish to thank Juliette Weusten, Lizanne Schweren, Fenny S. Zwart, Sanne

Veerhoek, Janna van Belle and Nathalie Vessaz for their assistance with subject recruitment and acquisition of MRI scans throughout the running time of this study, Yumas Hankouri and René Mandl for the technical assistance with MRI processing, and Vincenzo Ambrosino for the graphic design of the Figures.

CONFLICT OF INTEREST

SD has received a research grant from Unilever Foods that is unrelated to this manuscript. The other authors report no biomedical financial interests or potential conflicts of interest.

REFERENCES

Austin PC. 2011. Optimal caliper widths for propensity-score matching when estimating differences in means and differences in proportions in observational studies. Pharm Stat. 10(2):150-161.

Banerjee TD, Middleton F, Faraone SV. 2007. Environmental risk factors for attention-deficit hyperactivity disorder. Acta Paediatr. 96(9):1269-1274.

Barkovich AJ, Guerrini R, Kuzniecky RI, Jackson GD, Dobyns WB. 2012. A developmental and genetic classification for malformations of cortical development: update 2012. Brain. 135(5):1348-1369.

Bates D, Maechler M, Bolker B. 2011. Lme4: Linear Mixed-Effects Models using S4 Classes. R Package Version 0.999375-39.

Batty MJ, Liddle EB, Pitiot A, Toro R, Groom MJ, Scerif G, Liotti M, Liddle PF, Paus T, Hollis C. 2010. Cortical gray matter in attention-deficit/hyperactivity disorder: a structural magnetic resonance imaging study. J Am Acad Child Adolesc Psychiatry. 49(3):229-238.

Castellanos FX, Lee PP, Sharp W, Jeffries NO, Greenstein DK, Clasen LS, Blumenthal JD, James RS, Ebens CL, Walter JM, Zijdenbos A, Evans AC, Giedd JN, Rapoport JL. 2002. Developmental trajectories of brain volume abnormalities in children and adolescents with attention-deficit/hyperactivity disorder. JAMA. 288(14):1740-1748.

Chen CH, Fiecas M, Gutiérrez ED, Panizzon MS, Eyler LT, Vuoksimaa E, Thompson WK, Fennema-Notestine C, Hagler DJ Jr, Jernigan TL, et al. 2013. Genetic topography of brain morphology. Proc Natl Acad Sci USA. 110:17089-17094.

Cohen J. 1992. A power primer. Psychol Bull. 112(1):155-159.

Dale AM, Fischl B, Sereno MI. 1999. Cortical surface-based analysis I. Segmentation and surface reconstruction. NeuroImage. 9(2):179-194.

de Zeeuw P, Schnack HG, van Belle J, Weusten J, van Dijk S, Langen M, Brouwer RM, van Engeland H, Durston S. 2012. Differential brain development with low and high IQ in Attention-Deficit/Hyperactivity Disorder. PLoS One. 7:e35770.

Dennis M, Francis DJ, Cirino PT, Schachar R, Barnes MA, Fletcher JM. 2009. Why IQ is not a covariate in cognitive studies of neurodevelopmental disorders. J Int Neuropsychol Soc. 15(3):331-343.

Desikan RS, Ségonne F, Fischl B, Quinn BT, Dickerson BC, Blacker D, Buckner RL, Dale AM, Maguire RP, Hyman BT, Albert MS, Killiany RJ. 2006. An automated labeling system for subdividing the human cerebral cortex on MRI scans into gyral based regions of interest. NeuroImage. 31(3):968-980.

Destrieux C, Fischl B, Dale A, Halgren E. 2010. Automatic parcellation of human cortical gyri and sulci using standard anatomical nomenclature. Neuroimage. 15;53(1):1-15.

Dewey J, Hana G, Russell T, Price J, McCaffrey D, Harezlak J, Sem E, Anyanwu JC, Guttmann CR, Navia B, Cohen R, Tate DF, HIV Neuroimaging Consortium. 2010. Reliability and validity of MRI-based automated volumetry software relative to auto-assisted manual measurement of subcortical structures in HIV-infected patients from a multisite study. Neuroimage. 15;51(4):1334-1344.

Ducharme S, Albaugh MD, Nguyen TV, Hudziak JJ, Mateos-Pérez JM, Labbe A, Evans AC, Karama S, Brain Development Cooperative Group. 2016. Trajectories of cortical thickness maturation in normal brain development--The importance of quality control procedures. Neuroimage. 15;125: 267-279.

Durston S, de Zeeuw P, Staal WG. 2009a. Imaging genetics in ADHD: a focus on cognitive control. Neurosci Biobehav Rev. 33(5):674-689.

Durston S, Nederveen H, van Dijk S, van Belle J, de Zeeuw P, Langen M, van Dijk A. 2009b. Magnetic resonance simulation is effective in reducing anxiety related to magnetic resonance scanning in children. J Am Acad Child Adolesc Psychiatry. 48(2):206-207.

Faul F, Erdfelder E, Lang AG, Buchner A. 2007. G*Power 3: a flexible statistical power analysis program for the social, behavioral, and biomedical sciences. Behav Res Methods. 39(2):175-191.

Fischl B. 2012. FreeSurfer. Neuroimage. 15;62(2):774-781.

Fischl B, Dale AM. 2000. Measuring the thickness of the human cerebral cortex from magnetic resonance images. Proc Natl Acad Sci USA. 97(20):11050-11055.

Fischl B, Sereno MI, Dale AM. 1999. Cortical surface-based analysis ii: inflation, flattening, and a surface-based coordinate system. NeuroImage. 9(2):195-207.

Fischl B, Salat DH, Busa E, Albert M, Dieterich M, Haselgrove C, van der Kouwe A, Killiany R, Kennedy D, Klaveness S, Montillo A, Makris N, Rosen B, Dale AM. 2002. Whole brain segmentation: automated labeling of neuroanatomical structures in the human brain. Neuron. 33(3):341-355.

Fischl B, Salat DH, van der Kouwe AJW, Makris N, Ségonne F, Quinn BT, Dale AM. 2004a. Sequence-independent segmentation of magnetic resonance images. NeuroImage. 23 (Suppl 1):S69-S84.

Fischl B, van der Kouwe A, Destrieux C, Halgren E, Ségonne F, Salat DH, Busa E, Seidman LJ, Goldstein J, Kennedy D, Caviness V, Makris N, Rosen B, Dale AM. 2004b. Automatically parcellating the human cerebral cortex. Cereb Cortex. 14(1):11-22.

Frazier TW, Demaree HA, Youngstrom EA. 2004. Meta-analysis of intellectual and neuropsychological test performance in attention-deficit/hyperactivity disorder. Neuropsychology. 18(3):543-555.

Frodl T, Skokauskas N. 2012. Meta-analysis of structural MRI studies in children and adults with attention deficit hyperactivity disorder indicates treatment effects. Acta Psych Scand. 125:114-126.

Greven CU, Bralten J, Mennes M, O'Dwyer L, van Hulzen KJ, Rommelse N, Schweren LJ, Hoekstra PJ, Hartman CA, Heslenfeld D, et al. 2015. Developmentally stable whole-brain volume reductions and developmentally sensitive caudate and putamen volume alterations in those with attention-deficit/hyperactivity disorder and their unaffected siblings. JAMA Psychiatry. 72(5):490-499.

Hoogman M, Bralten J, Hibar DP, Mennes M, Zwiers MP, Schweren LS, van Hulzen KJ, Medland SE, Shumskaya E, Jahanshad N, Zeeuw P, et al. 2017. Subcortical brain volume differences in participants with attention deficit hyperactivitydisorder in children and adults: a cross-sectional mega-analysis. Lancet Psychiatry. 4(4):310-319.

Horga G, Kaur T, Peterson BS. 2014. Annual Research Review: Current limitations and future directions in MR studies of child- and adult-onset developmental psychopathologies. J Child Psychol Psychiatry. 55:659-680.

Jolly LA, Homan CC, Jacob R, Barry S, Gecz J. 2013. The UPF3B gene, implicated in intellectual disability, autism, ADHD and childhood onset schizophrenia regulates neural progenitor cell behaviour and neuronal outgrowth. Hum Mol Genet. 1;22(23):4673-4687.

Jones EG. 2000. Microcolumns in the cerebral cortex. Proc Natl Acad Sci USA. 9;97(10):5019-5021.

Kass RE, Raftery AE. 1995. Bayes Factors. J Am Statist Assoc. 90(430):773-795.

Li X, Jiang J, Zhu W, Yu C, Sui M, Wang Y, Jiang T. 2007. Asymmetry of prefrontal cortical convolution complexity in males with attention-deficit/ hyperactivity disorder using fractal information dimension. Brain Dev. 29:649-655.

Linnet KM, Dalsgaard S, Obel C, Wisborg K, Henriksen TB, Rodriguez A, Kotimaa A, Moilanen I, Thomsen PH, Olsen J, Jarvelin MR. 2003. Maternal lifestyle factors in pregnancy risk of attention deficit hyperactivity disorder and associated behaviors: review of the current evidence. Am J Psychiatry. 160(6):1028-1040.

Mountcastle VB. 1997. The columnar organization of the neocortex. Brain. 120(4):701-722.

Nakao T, Radua J, Rubia K, Mataix-Cols D. 2011. Gray matter volume abnormalities in ADHD: voxel-based meta-analysis exploring the effects of age and stimulant medication. Am J Psychiatry. 168(11):1154-1163.

Narr KL, Woods RP, Lin J, Kim J, Phillips OR, Del'Homme M, Caplan R, Toga AW, McCracken JT, Levitt JG. 2009. Widespread cortical thinning is a robust anatomical marker for attention-deficit/hyperactivity disorder. J Am Acad Child Adolesc Psychiatry. 48:1014-1022.

Panizzon MS, Fennema-Notestine C, Eyler LT, Jernigan TL, Prom-Wormley E, Neale M, Jacobson K, Lyons MJ, Grant MD, Franz CE, et al. 2009. Distinct genetic influences on cortical surface area and cortical thickness. Cereb Cortex. 19(11):2728-2735.

Poelmans G, Pauls DL, Buitelaar JK, Franke B. 2011. Integrated genome-wide association study findings: identification of a neurodevelopmental network for attention deficit hyperactivity disorder. Am J Psychiatry. 168(4):365-377.

Rakic P. 1995. A small step for the cell, a giant leap for mankind: a hypothesis of neocortical expansion during evolution. Trends Neurosci. 18:383-388.

Rakic P. 2000. Radial unit hypothesis of neocortical expansion. Novartis Found Symp. 228:30–42; discussion 42-52.

Raznahan A, Shaw P, Lalonde F, Stockman M, Wallace GL, Greenstein D, Clasen L, Gogtay N, Giedd JN. 2011. How does your cortex grow? J Neurosci. 11;31(19):7174-7177.

Reif A, Nguyen TT, Weissflog L, Jacob CP, Romanos M, Renner TJ, Buttenschon HN, Kittel-Schneider S, Gessner A, Weber H, et al. 2011. DIRAS2 is associated with adult ADHD, related traits, and co-morbid disorders. Neuropsychopharmacology. 36(11):2318-2327.

Rivero O, Sich S, Popp S, Schmitt A, Franke B, Lesch KP. 2013. Impact of the ADHD-susceptibility gene CDH13 on development and function of brain networks. Eur Neuropsychopharmacol. 23(6):492-507.

Schaer M, Cuadra MB, Tamarit L, Lazeyras F, Eliez S, Thiran JP. 2008. A surface-based approach to quantify local cortical gyrification. IEEE Trans Med Imaging. 27(2):161-170.

Schweren LJ, Hartman CA, Heslenfeld DJ, van der Meer D, Franke B, Oosterlaan J, Buitelaar JK, Faraone SV, Hoekstra PJ. 2015. Thinner Medial Temporal Cortex in Adolescents With Attention-Deficit/Hyperactivity Disorder and the Effects of Stimulants. J Am Acad Child Adolesc Psychiatry. 54(8):660-667.

Shaffer D, Fisher P, Lucas CP, Dulcan MK, Schwab-Stone ME. 2000. NIMH Diagnostic Interview Schedule for Children Version IV (NIMH DISC-IV): description, differences from previous versions, and reliability of some common diagnoses. J Am Acad Child Adolesc Psychiatry. 39(1):28-38.

Shaw P, Eckstrand K, Sharp W, Blumenthal J, Lerch JP, Greenstein D, Clasen L, Evans A, Giedd J, Rapoport JL. 2007. Attention-deficit/hyperactivity disorder is characterized by a delay in cortical maturation. Proc Natl Acad Sci USA. 4;104(49):19649-19654.

Shaw P, Lerch J, Greenstein D, Sharp W, Clasen L, Evans A, Giedd J, Castellanos FX, Rapoport J. 2006. Longitudinal mapping of cortical thickness and clinical outcome in children and adolescents with attention-deficit/hyperactivity disorder. Arch Gen Psychiatry. 63:540-549.

Shaw P, Malek M, Watson B, Sharp W, Evans A, Greenstein D. 2012. Development of cortical surface area and gyrification in attention-deficit/hyperactivity disorder. Biol Psychiatry. 1;72(3):191-197.

Shim SH, Hwangbo Y, Kwon YJ, Jeong HY, Lee BH, Lee HJ, Kim YK. 2008. Increased levels of plasma brain-derived neurotrophic factor (BDNF) in children with attention deficit-hyperactivity disorder (ADHD). Prog Neuropsychopharmacol Biol Psychiatry. 12;32(8):1824-1828.

Sowell ER, Thompson PM, Welcome SE, Henkenius AL, Toga AW, Peterson BS. 2003. Cortical abnormalities in children and adolescents with attention-deficit hyperactivity disorder. Lancet. 362:1699-1707.

Syed Z, Dudbridge F, Kent L. 2007. An investigation of the neurotrophic factor genes GDNF, NGF, and NT3 in susceptibility to ADHD. Am J Med Genet B. 144B:375-378.

Talaraich J, Tournoux P. 1988. Co-planar stereotaxic atlas of the human brain: 3-dimensional proportional system: an approach to cerebral imaging. Stuttgart: Thieme Medical Publishers.

Thoemmes F. 2012. Propensity score matching in SPSS. arXiv:1201.6385.

Tymms P. 2004. Effect sizes in multilevel models. In I. Schagen & K. Elliot (Eds.), But what does it mean? The use of effect sizes in educational research. Slough: UK: National Foundation for Educational Research.

Valera EM, Faraone SV, Murray KE, Seidman LJ. 2007. Meta-analysis of structural imaging findings in attention-deficit/hyperactivity disorder. Biol Psychiatry. 61:1361-1369.

Verhulst F, Van Der Ende J, Koot H. 1996. Handleiding voor de CBCL/4-18 (Manual for the CBCL/4-18). Rotterdam: Department of Child and Adolescent Psychiatry, Erasmus Academic Medical Center.

Verhulst F, Van Der Ende J, Koot H. 1997. Handleiding voor de Teacher's Report Form (TRF) (Manual for the Teacher Report Form (TRF)). Rotterdam: Department of Child and Adolescent Psychiatry, Erasmus Academic Medical Center.

Vilgis V, Sun L, Chen J, Silk TJ, Vance A. 2016. Global and local grey matter reductions in boys with ADHD combined type and ADHD inattentive type. Psychiatry Res. 30;254:119-126.

Wechsler D. 2005. Wechsler Intelligence Scale for Children – Derde Editie NL. Handleiding en Verantwoording. (Wechsler Intelligence Scale for Children – Third Edition, Dutch Version, Manual). London: Harcourt Assessment.

White T, Su S, Schmidt M, Kao CY, Sapiro G. 2010. The development of gyrification in childhood and adolescence. Brain & Cognition. 72(1):36-45.

Wierenga LM, Langen M, Ambrosino S, van Dijk S, Oranje B, Durston S. 2014a. Typical development of basal ganglia, hippocampus, amygdala and cerebellum from age 7 to 24. Neuroimage. 1;96:67-72.

Wierenga LM, Langen M, Oranje B, Durston S. 2014b. Unique developmental trajectories of cortical thickness and surface area. Neuroimage. 15;87:120-126.

Wolosin SM, Richardson ME, Hennessey JG, Denckla MB, Mostofsky SH. 2009. Abnormal cerebral cortex structure in children with ADHD. Hum Brain Mapp. 30(1):175-184.

SUPPLEMENTAL INFORMATION

MRI processing

The FreeSurfer v5.1.0 package [http://surfer.nmr.mgh.harvard.edu/fswiki] contains a fully automated structural imaging pipeline for the quantitative study of cortical and subcortical neuroanatomy. The cortical surface reconstruction pipeline is complex and consists of several stages for each individual scan. First, the scan is automatically placed in the Talaraich orientation, by registering it to a model brain in Talairach space (1) (*Talaraich registration*). Next, the intensity variations due to magnetic field inhomogeneities are corrected and a normalized intensity image is created (*intensity normalization*). The extra-cerebral voxels (skull and meningeal surfaces) are removed using a deformable template model, leaving only the brain and the overlying pial surface (*skull stripping*). Voxels are then classified as white matter or other tissues based on their intensity and their neighbour constraints (*white matter segmentation*). Based on the expected Talairach location of the corpus callosum and pons, sagittal and axial cutting planes are computed in order to separate the cerebral hemispheres from each other. This procedure also separates the cerebellum and brain stem from the cerebrum (*cutting planes procedure*). Any interior cavities inside the white matter volume are filled (ventricles, lacunes) to generate two solid masses of connected voxels, each representing the hemispheric subcortical mass (*connected components procedure*). These resulting volumes are then covered with a triangular tessellation (approximately 160.000 meshes), representing the surface topology of the corresponding volume (*surface tessellation*). To reduce metric distortions, this initial jagged surface is refined guided by the local MRI intensity gradients between the white and gray matter: the smoothed reconstructed surface is referred to as the white surface (*surface refinement procedure*). Next, for the pial surface reconstruction, the white surface is deformed, following a function that specifies the direction of movement of the tessellation towards the gray matter/CSF border (*surface deformation*) (2). In order to establish a surface-based coordinate system, the reconstructed cortical surface of each hemisphere is morphed ("inflated") into a spherical surface (*spherical transformation*). This representation allows identification of the same point on the pial and the white surface of any participant using the same standard spherical coordinates systems (e.g., longitude and colatitude), which increases the accuracy of anatomical localization across scans (3). The distance between the white and pial surfaces at any point on the cortex gives the thickness of the cortical mantle at that location (4). In the final procedure, both geometric information derived from the cortical model and standard neuroanatomical conventions are integrated to automatically assign a probabilistic neuroanatomical label to each location on the cortical surface (cortical parcellation). Figure S1 summarizes the main FreeSurfer processing stages.

FreeSurfer performs two distinct parcellations, based on the Desikan-Killiany and the Destrieux cortical atlases, which differ in the number and designation criteria of regions of interest (ROIs) (34 gyral-based and 74 surface-based areas per hemisphere respectively) (5,6). In the current study, we used the Desikan-Killiany ROIs, listed according to the lobes in Table S1 and depicted in Figure S2.

REFERENCES

1. Talaraich J, Tournoux P. 1988. Co-planar Stereotaxic Atlas of the Human Brain: 3-dimensional Proportional System: An Approach To Cerebral Imaging. Thieme Medical Publishers, Stuttgart.
2. Dale AM, Fischl B, Sereno MI. 1999. Cortical surface-based analysis I. Segmentation and surface reconstruction. NeuroImage 9(2): 179-194.
3. Fischl B, Sereno MI, Dale AM. 1999. Cortical Surface-Based Analysis II: Inflation, Flattening, and a Surface-Based Coordinate System. NeuroImage 9(2): 195-207.
4. Fischl B, Dale AM. 2000. Measuring the Thickness of the Human Cerebral Cortex from Magnetic Resonance Images. Proc Natl Acad Sci U.S.A. 97 (20): 11050-11055.
5. Desikan RS, Segonne F, Fischl B, Quinn BT, Dickerson BC, Blacker D, et al. 2006. An automated labeling system for subdividing the human cerebral cortex on MRI scans into gyral based regions of interest. NeuroImage 31(3): 968-980.
6. Destrieux C, Fischl B, Dale A, Halgren E. 2010. Automatic parcellation of human cortical gyri and sulci using standard anatomical nomenclature. Neuroimage 15, 53(1): 1-15.

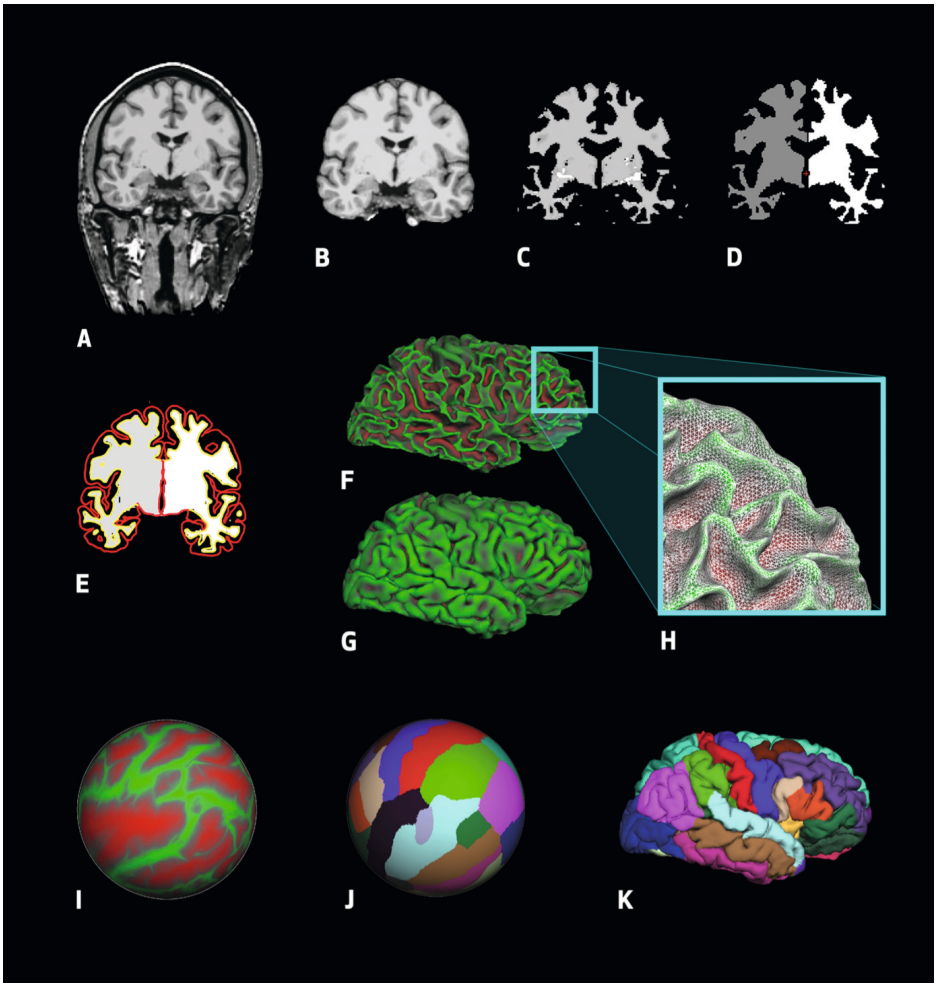

Figure S1. Main FreeSurfer processing stages

Note. A: T1 normalized volume; B: skull stripping; C: white matter segmentation; D: connected components; E yellow line and F: white surface; E red line and G: pial surface; H: surface tessellation I: spherical transformation; J, K: cortical parcellation (Desikan-Killiany atlas) [http://surfer.nmr.mgh.harvard.edu].

Table S1. List of Desikan-Killiany regions for each lobe

Cerebral Lobes	Desikan-Killiany regions
Frontal	caudal anterior cingulate, caudal middle frontal, frontal pole, lateral orbitofrontal, medial orbitofrontal, pars opercularis, pars orbitalis, pars triangularis, paracentral, precentral, rostral anterior cingulate, rostral middle frontal, superior frontal
Parietal	inferior parietal, isthmus cingulate, postcentral, precuneus, posterior cingulate, superior parietal, supramarginal
Temporal	banks of the superior temporal sulcus (banks sts), entorhinal, fusiform, inferior temporal, insula, middle temporal, parahippocampal, superior temporal, temporal pole, transverse temporal
Occipital	cuneus, lateral occipital, lingual, pericalcarine

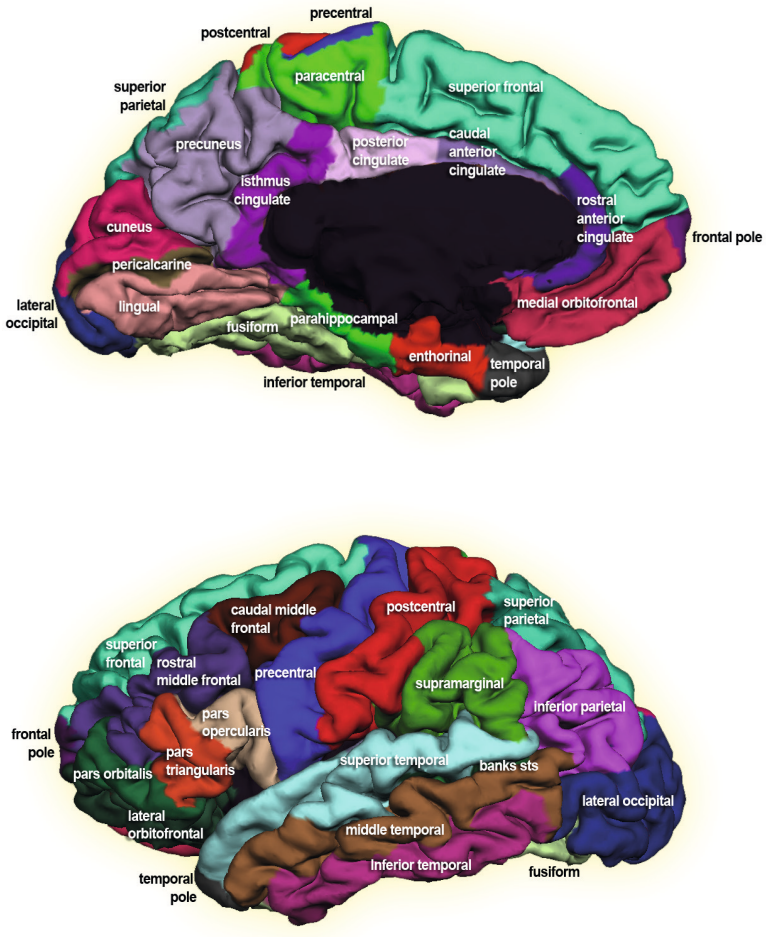

Figure S2. Desikan-Killiany atlas

Table S2. Parameters for developmental trajectories of cerebral cortex markers, overall and per hemisphere

	Cortical parameter	Growth model	Intercept (s.e.)	Gender (s.e.)	Age (s.e.)	Age^2 (s.e.)	Age^3 (s.e.)	ADHD (s.e.)
Total	Volume	Quadratic	565660.46 (9692.59) **	53595.44 (9341.07) **	-3044.85 (507.49) **	-221.46 (88.33) **		-30378.30 (6845.15) **[B]
	Surface	Cubic	174784.82 (3087.81) **	22948.58 (3296.46) **	-495.76 (167.21) **	-83.58 (40.32) **	9.73 (4.32) **	
	Thickness	Linear	2.80 (.02) **	-.04 (.02)	-.02 (.00) **			
	Gyrification	Linear	3.16 (.02) **	.08 (.02) **	-.02 (.00) **			
Left	Volume	Linear	279266.4 (4629.14) **	27914.02 (4649.35) **	-1990.65 (206.02) **			-13911.16 (3406.79) **[B]
	Surface	Linear	87014.38 (1465.24) **	11318.41 (1600.21) **	-149.57 (60.01) *			
	Thickness	Linear	2.80 (.02) **	-.04 (.02)	-.02 (.00) **			
	Gyrification	Linear	3.16 (.02) **	.07 (.02) **	-.02 (.00) **			
Right	Volume	Quadratic	282856.88 (4895.91) **	26968.03 (4709.06) **	-1408.72 (264.43) **	-115.17 (45.76) **		-15495.12 (3451.47) **[B]
	Surface	Cubic	89458.58 (1697.83) **	11268.54 (1658.71) **	-242.65 (87.19) **	-45.09 (20.83) **	4.62 (2.23) **	-3438.28 (1216.87) **
	Thickness	Linear	2.79 (.02) **	-.03 (.02)	-.02 (.00) **			
	Gyrification	Quadratic	3.14 (.02) **	.09 (.02) **	-.02 (.00) **	.00 (.00) **		

Note. Cortical volume values in mm^3, surface values in mm^2, thickness values in mm, gyrification values dimensionless;
*p < .05; **p < .01, [B]results surviving Bonferroni correction for multiple comparisons. Abbreviations: s.e., standard error; ADHD, Attention-Deficit/Hyperactivity Disorder.

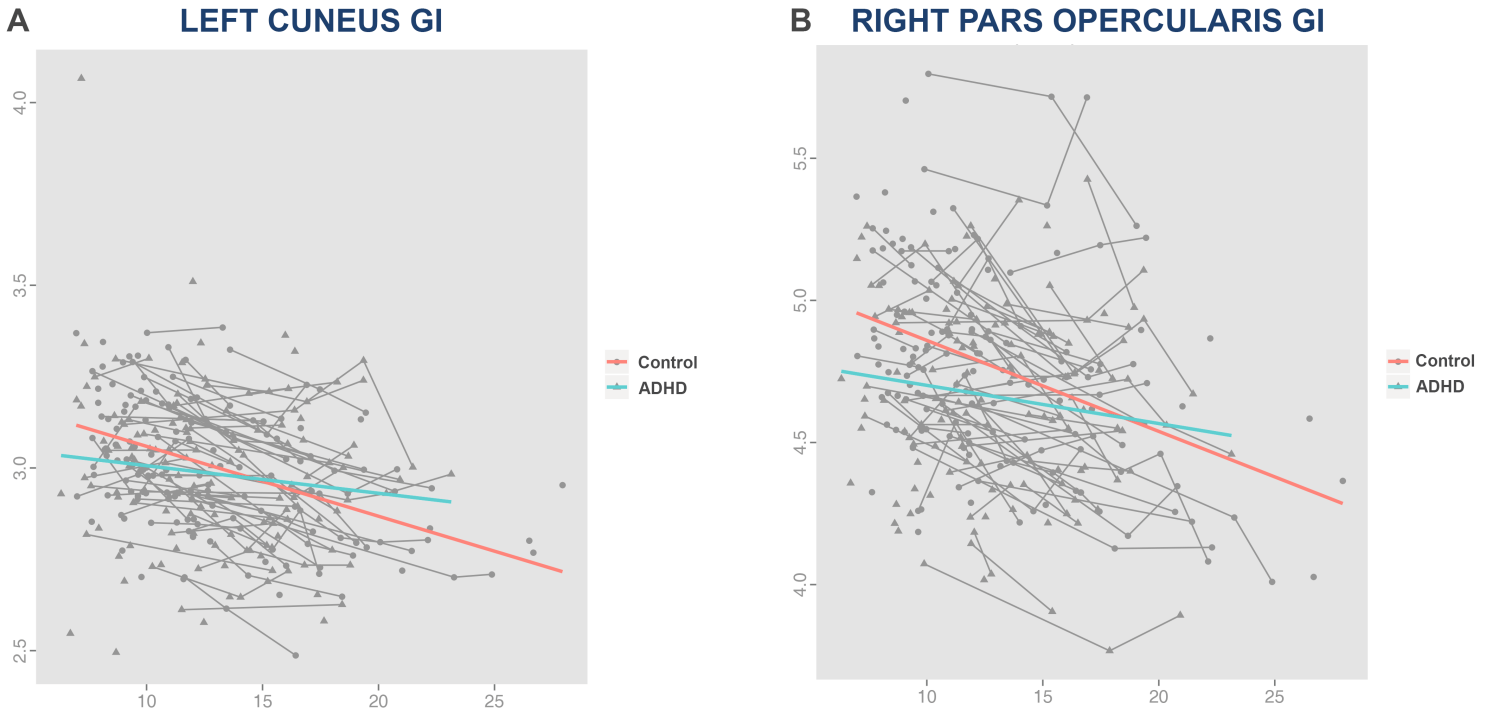

Figure S3. ADHD by age interaction effects on the developmental trajectories of cortical gyrification (panel A, left cuneus; panel B, right pars opercularis)
Abbreviations: GI, gyrification index; ADHD, Attention-Deficit/Hyperactivity Disorder.

Table S3. Parameters for developmental trajectories reflecting significant differences between groups. Findings highlighted in grey were robust across all robustness analyses (Table S4).

	Primary analysis											
	Cortical volume				Cortical Surface Area				Cortical Gyrification					
Cortical region	Growth Model	ADHD	(s.e.)	d	Growth Model	ADHD	(s.e.)	d	Growth Model	ADHD	(s.e.)	d	ADHD x Age	(s.e.)
Total cortex	Quadratic	-30378.302	(6845.152)**[B]	-.70	Cubic				Linear					
Left Hemisphere	Linear	-13911.164	(3406.794)**[B]	-.64	Linear				Linear					
caudalanteriorcingulate	Quadratic	-247.755	(79.718)**	-.46	Linear	-59.018	(19.607)**		Linear					
cuneus	Linear				Linear				Linear				.012	(.003)**
lateralorbitofrontal	Linear	-469.482	(161.502)**	-.49	Linear				Linear					
medialorbitofrontal	Linear	-359.546	(120.486)**	-.62	Linear				Linear					
middletemporal	Quadratic	-74.055	(263.443)**	-.43	Linear				Linear					
precentral	Linear	-704.923	(244.695)**	-.55	Linear				Linear					
precuneus	Cubic	-723.306	(224.500)**	-.51	Linear				Linear					
rostralanteriorcingulate	Quadratic				Linear	-68.469	(23.769)**	-.46	Linear					
rostralmiddlefrontal	Quadratic	-1857.419	(38.178)**[B]	-.78	Linear	-40.654	(12.725)**	-.53	Linear	-.067	(.022)*	-.53		
superiorparietal	Linear	-1228.321	(295.477)**[B]	-.71	Cubic				Linear					
superiortemporal	Cubic	-1122.874	(255.754)**[B]	-.68	Linear	-221.665	(64.526)**	-.53	Linear					
supramarginal	Cubic	-1172.661	(282.945)**[B]	-.66	Cubic				Linear					
Right Hemisphere	Quadratic	-15495.125	(3451.470)**[B]	-.72	Cubic	-3438.275	(1216.870)**	-.44	Quadratic					
caudalmiddlefrontal	Linear	-921.245	(214.547)**	-.68	Linear	-252.481	(66.754)**	-.60	Linear					
cuneus	Linear	-279.887	(79.349)**	-.56	Linear				Linear					
isthmuscingulate	Linear	-342.842	(83.376)**[B]	-.64	Linear	-88.771	(25.320)**	-.55	Quadratic					
lateraloccipital	Linear	-1192.241	(245.651)**[B]	-.77	Linear	-356.887	(94.855)**	-.59	Cubic					
lateralorbitofrontal	Quadratic	-556.099	(165.271)**	-.55	Linear				Linear					
medialorbitofrontal	Linear	-366.866	(112.561)**	-.57	Linear				Linear					

Table S3. Continued

	Primary analysis											
	Cortical volume				Cortical Surface Area				Cortical Gyrification					
Cortical region	**Growth Model**	**ADHD**	**(s.e.)**	**d**	**Growth Model**	**ADHD**	**(s.e.)**	**d**	**Growth Model**	**ADHD**	**(s.e.)**	**d**	**ADHD x Age**	**(s.e.)**
parsopercularis	Linear	-476.220	(133.735)**	-.55	Linear	-155.221	(39.211)**	-.60	Linear				.019	(.006)**
precentral	Linear	-796.882	(235.315)**	-.63	Linear				Linear					
precuneus	Linear	-705.108	(247.449)**	-.44	Linear				Quadratic					
superiorfrontal	Quadratic	-1541.425	(437.092)**	-.56	Linear				Linear					
superiorparietal	Linear	-887.752	(299.179)**	-.51	Linear				Linear					
superiortemporal	Quadratic	-854.851	(248.854)**	-.54	Linear				Linear					
transversetemporal	Linear				Linear				Linear	-.147	(.050)**	-.45		

Note. Cortical volume values in mm^3; Cortical surface area values in mm^2; Cortical gyrification values dimensionless. *p < .05; **p < .01; Bresults surviving Bonferroni correction for multiple comparisons.

Abbreviations: ADHD, Attention-Deficit/Hyperactivity Disorder (main factor); ADHD x Age, ADHD by age interaction; s.e., standard error; d, Cohen's d effect sizes.

Table S4. Robustness analyses: parameters for developmental trajectories reflecting significant differences between groups.

	Additional covariates									
	Slice Thickness								ICV	
	Cortical Volume		Cortical Surface Area		Cortical Gyrification				Cortical Volume	
Cortical region	ADHD	(s.e.)	ADHD	(s.e.)	ADHD	(s.e.)	ADHD x Age	(s.e.)	ADHD	(s.e.)
Total cortex	-27985.589	(681.411)**[B]							-20598.10	(443.310)**[B]
Left Hemisphere	-13710.237	(3398.507)**[B]								
caudalanteriorcingulate	-245.177	(79.924)**	-58.410	(19.655)**					-220.258	(78.240)**
cuneus							.012	(.003)**		
lateralorbitofrontal	-450.892	(162.283)**								
medialorbitofrontal	-363.188	(121.170)**								
middletemporal										
precentral										
precuneus	-672.814	(217.530)**							-606.073	(198.996)**
rostralanteriorcingulate			-69.098	(23.845)**						
rostralmiddlefrontal	-1848.916	(380.813)**[B]	-40.112	(12.109)**	-.064	(.021)**			-1406.340	(30.577)**[B]
superiorparietal	-1133.739	(287.625)**							-1075.922	(274.906)**
superiortemporal	-1088.032	(253.684)**[B]	-217.520	(64.634)**					-960.013	(220.537)**[B]
supramarginal	-1111.813	(277.577)**[B]							-964.261	(242.232)**[B]
Right Hemisphere	-14281.354	(3438.098)**[B]	-3417.824	(1220.322)**					-1047.242	(2246.001)**[B]
caudalmiddlefrontal	-902.793	(215.217)**[B]	-258.120	(66.478)**					-830.191	(195.745)**[B]
cuneus	-276.289	(79.493)**							-244.289	(75.005)**
isthmuscingulate	-339.353	(83.337)**[B]	-88.454	(25.366)**					-309.839	(77.061)**[B]
lateraloccipital	-1191.63	(246.399)**[B]	-356.310	(95.118)**					-1070.93	(226.205)**[B]
lateralorbitofrontal	-549.755	(165.871)**								
medialorbitofrontal	-371.517	(112.925)**							-272.242	(96.406)**
parsopercularis	-466.519	(134.490)**	-155.706	(39.289)**			.019	(.006)**	-437.149	(129.918)**

Table S4. Continued

	Additional covariates									
	Slice Thickness								ICV	
	Cortical Volume		Cortical Surface Area		Cortical Gyrification				Cortical Volume	
Cortical region	ADHD	(s.e.)	ADHD	(s.e.)	ADHD	(s.e.)	ADHD x Age	(s.e.)	ADHD	(s.e.)
precentral	-720.407	(230.883)**							-592.419	(197.234)**
precuneus										
superiorfrontal	-1488.435	(431.994)**							-1257.070	(375.519)**
superiorparietal										
superiortemporal	-786.926	(249.123)**							-639.481	(218.234)**
transversetemporal					-.142	(.050)**				

Note. Cortical volume values in mm^3; Cortical surface area values in mm^2; Cortical gyrification values dimensionless. *p < .05; **p < .01; Bresults surviving Bonferroni correction for multiple comparisons.

Abbreviations: ADHD, Attention-Deficit/Hyperactivity Disorder (main factor); ADHD x Age, ADHD by age interaction; s.e., standard error; ICV, Intracranial volume.

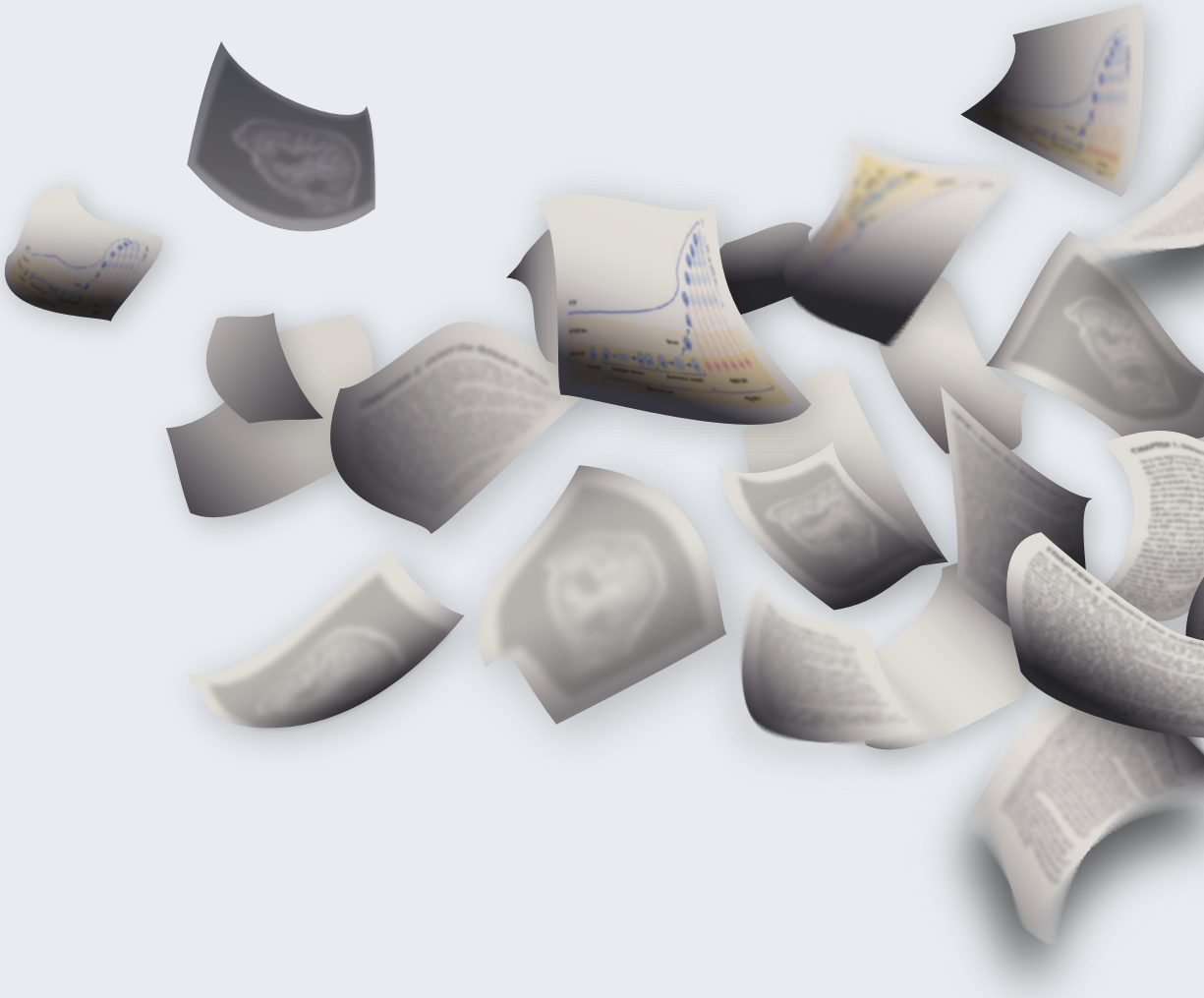

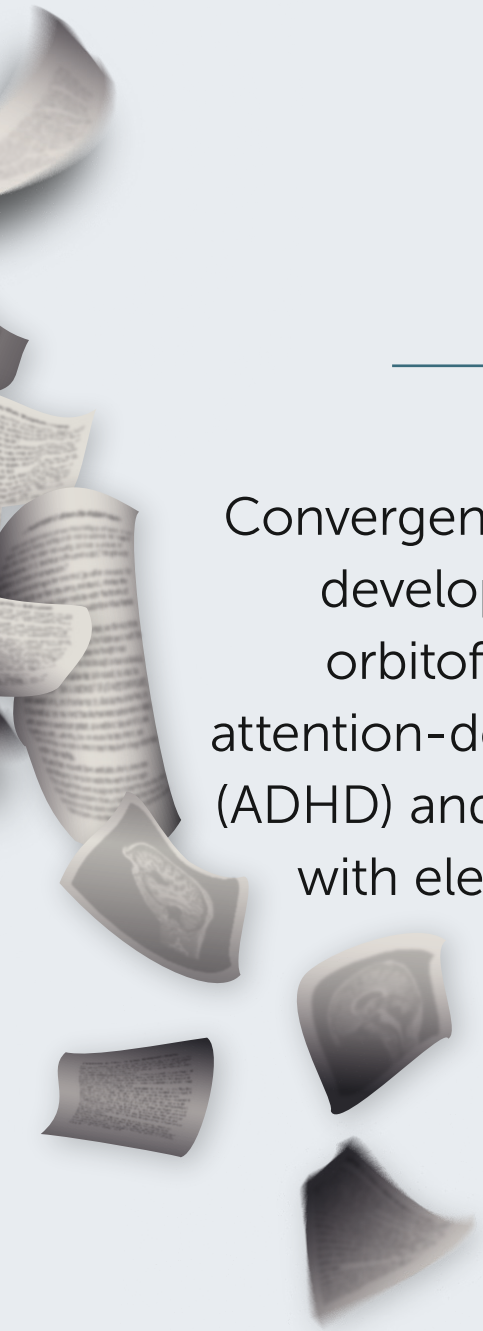

CHAPTER 4

Convergence in the neuroanatomical developmental trajectories of orbitofrontal cortex between attention-deficit/hyperactivity disorder (ADHD) and autism spectrum disorder with elevated ADHD symptoms

Sara Ambrosino, Dienke Bos, Branko van Hulst,
Bob Oranje, Sarah Durston

Under review in *Cerebral Cortex*

ABSTRACT

Autism Spectrum Disorder (ASD) and Attention-Deficit/Hyperactivity Disorder (ADHD) are genetically related neurodevelopmental conditions with high comorbidity. Conceptually, they may be viewed as two extremes of one overarching, trans-diagnostic continuum, possibly with common neurobiological pathways involved in the development of both conditions. Structural neuroimaging studies investigating ASD and ADHD concurrently are scarce and have used cross-sectional designs. Hence it is not established whether these conditions share developmental pathways. We conducted a longitudinal MRI study investigating brain development in a well-matched sample of 210 children and adolescents, including individuals with ADHD, individuals with ASD and high or low levels of ADHD symptoms, and typically developing controls. We estimated the developmental trajectories of brain structures using mixed-effects regression analysis. We found developmentally stable reductions of cortical volume and surface area within bilateral orbital prefrontal cortex (OFC) in ADHD, specifically in right orbital gyri and left orbital sulci. We found a similar effect in left orbital sulci for children with ASD and elevated ADHD symptoms. Our results point to shared neuroanatomical changes in left OFC related to ADHD, both as a primary diagnosis and comorbidly in ASD. This implicates early developmental mechanisms of left OFC expansion in ADHD symptoms in these two neurodevelopmental conditions.

INTRODUCTION

Autism Spectrum Disorder (ASD, autism) and Attention-Deficit/Hyperactivity Disorder (ADHD) are considered to be distinct neurodevelopmental conditions in our diagnostic classification systems (DSM-5, American Psychiatric Association 2013; ICD-10, World Health Organization 1993). ASD is diagnosed based on deficits in social communication and repetitive and restricted behaviors and interests, whereas ADHD is characterized by symptoms of inattention, motor restlessness and impulsivity (American Psychiatric Association 2013). However, these conditions show vast overlap in terms of their clinical presentation and often co-occur in individuals: about one third of individuals with a primary diagnosis of autism has comorbid ADHD (Simonoff 2008), and up to half of all individuals with ADHD meet full diagnostic criteria for autism (Rommelse et al. 2010). In line with this observation, ASD and ADHD have been reported to be highly genetically correlated (Rommelse et al. 2010). These observations have led to the suggestion that autism and ADHD may perhaps be better conceptualized as two extremes of one overarching, trans-diagnostic condition, with distinct subtypes, based on clinical severity and comorbid symptoms. This potentially has implications for neurodevelopmental changes associated with both conditions, as different subtypes may be associated with both overlapping and differing neurobiological developmental pathways (Rommelse et al. 2017).

Despite extensive studies of neurobiology in autism and ADHD, no biological markers for have been established for either condition, nor for any co-morbid subtypes (Bethlehem et al. 2017). This is related, at least in part, to the substantial clinical and etiological heterogeneity that characterizes both disorders, similar to most psychiatric conditions (Wardenaar and de Jonge 2013). Neurobiological differences with small effect sizes have been associated with both diagnoses at the group level, yet none of these characterize all affected individuals. Furthermore, neuroimaging studies have shown common and distinct patterns of findings between autism and ADHD (Hoogman et al. 2020). The most consistent neurobiological findings in ADHD have been reductions in the volume of the whole brain, and cortico-frontal and striatal regions, particularly (Valera et al. 2007; Ellison-Wright et al. 2008; Nakao et al. 2011; Frodl and Skokauskas 2012; Norman et al. 2016; Hoogman et al. 2017; Hoogman et al. 2019). Studies of ASD have reported similar changes in striatum (Hoogman et al. 2020), more specific cortical effects in frontal and temporal areas (Zielinski et al. 2014; Foster et al. 2015), and an increased rate of brain growth during early childhood (Courchesne et al. 2011). However, any inferences from comparing the literature on autism and ADHD are speculative of necessity, as traditionally, studies of one condition have excluded individuals with the other. A trans-diagnostic theoretical framework would therefore benefit greatly from

studies investigating ASD, ADHD, and a third group with co-occurring symptoms, in a single design (Hoogman et al. 2020).

A few neuroimaging studies have examined ASD and ADHD concurrently, mostly in relatively small samples (N=45 to 96) (Brieber et al. 2007; Lim et al. 2015; Nickel et al. 2018; Albajara Sáenz et al. 2020). Of these, Nickel and colleagues' (2018) was the only (preliminary) report to include both individuals with ASD or ADHD, and individuals with autism and comorbid ADHD. They reported a specific effect of ADHD in orbital left inferior frontal gyrus (Nickel et al. 2018), a key region for response inhibition and attentional modulation (Chong et al. 2008; Swick et al. 2008). Other studies investigating brain anatomy in individuals with ASD and comorbid ADHD symptoms did not include individuals with isolated autism or ADHD as comparison groups (Mahajan et al. 2016; Mizuno et al. 2019). Furthermore, it is of note that all existing studies directly comparing autism and ADHD used cross-sectional study designs (Brieber et al. 2007; Lim et al. 2015; Nickel et al. 2018; Albajara Sáenz et al. 2020), and therefore did not investigate these conditions from a developmental perspective. Arguably, longitudinal studies are of particular importance in investigating autism and ADHD, given the developmental nature of these conditions and the large inter-individual variation associated with them.

In this study, we aimed to address this gap in the literature by performing a longitudinal structural MRI study of brain development in a large sample of individuals, from children to late adolescents (7.4-19.8 years), with autism, ADHD, and typically developing controls (TD). We first investigated developmental trajectories of cortical and subcortical areas in the three primary diagnostic groups. We then created more clinically homogeneous subgroups, by comparing subjects with ASD and high or low levels of comorbid ADHD-symptoms. Finally, we moved beyond the traditional categorical distinction between diagnostic groups and tested whether dimensional measures of ADHD were a better predictor of brain development than a categorical effect of diagnosis.

We based our hypotheses on the framework of ADHD and ASD as extremes on an overarching, trans-diagnostic condition, and focused on the overlap in ADHD symptoms. This led us to hypothesize that changes in brain development would overlap for the group of individuals with ADHD and the group with both ASD and elevated ADHD symptoms. Based on prior research relating ADHD, and especially attentional problems, to prefrontal networks (Chong et al. 2008; Arnsten 2009), and preliminary evidence of a specific effect of ADHD in left orbital cortex (Nickel et al. 2018), we expected shared changes to be predominant in left prefrontal areas.

MATERIALS AND METHODS

The study was approved by the Institutional Review Board of the University Medical Center Utrecht (UMCU), the Netherlands. For participants under the age of 18 years, written informed consent was obtained from the parents after full disclosure of the study purpose and procedure. Children provided written and/or verbal assent. Participants aged 18 years or above provided written informed consent themselves.

Participants and clinical measures

There was a total of 416 scans available, acquired from 320 participants: 119 individuals with ADHD, 79 with ASD, and 122 TD. Participants were then statistically matched at the group level for age and sex using Propensity Score Matching (PSM) (Thoemmes 2012). This resulted in a sample of 280 MRI scans from 210 participants, 70 per group, aged 7.4 to 19.8 years. Demographic and clinical characteristics of the sample are provided in Table 1. 70 participants (33%) were scanned twice, equally distributed between the three groups ($p = .844$, Table 1). There were no differences between the groups in age at each wave of scanning ($p > .753$), and in the time interval between the first and the second scan ($p = .255$).

The clinical diagnosis of ASD or ADHD was established by an expert clinician based on DSM-IV-TR/ICD-10 (American Psychiatric Association 2000; World Health Organization 1993) or DSM-5 criteria (American Psychiatric Association 2013). The Diagnostic Interview Schedule for Children (DISC, version 2.3 or IV) parent version (Shaffer et al. 2000) was administered to parents by a qualified researcher in order to confirm the primary or comorbid diagnosis of ADHD, or to exclude psychiatric comorbidity in controls at study entry.

At each scan, parents completed the Child Behavior Checklist (CBCL), a well-validated and widely used psychiatric screener that provides a dimensional measure of a broad range of symptoms (Verhulst et al. 1996, 1997). The CBCL includes a subscale on attentional problems, generating a T-score that, when equal or greater than 67, indicates the presence of clinically relevant symptoms of inattention. Based on this cut-off at study entry, individuals with ASD were further divided in two subgroups: individuals with a higher level of ADHD-symptoms (ASD+), and individuals with fewer ADHD symptoms (ASD-).

We estimated intelligence quotient (IQ) using an abbreviated version of the Wechsler intelligence scales (WISC-R/WISC-III or WAIS-III as appropriate, Dutch versions), including the subtests Vocabulary, Block Design, Similarities and Object Assembly (Wechsler 2005). There were no differences between groups in Total, Verbal or Performance IQ.

Typically developing controls were excluded in case of psychiatric morbidity or first-degree relatives with a history of psychiatric problems. Additional exclusion criteria in

all groups were an estimated IQ below 70, any major physical or neurological illnesses, or the presence of metals in the body that precluded the MRI session.

At study entry, 54/70 (77%) participants with ADHD, and 17/34 (50%) participants with ASD+ were using psychostimulant medications (e.g., methylphenidate). None of the controls were using any form of psychoactive medications.

Prior to the MRI scan, children under 13 years of age were acclimated to the MRI procedure in a practice session using a dummy scanner as described previously by Durston and colleagues (2009); children over 13 years were also offered the opportunity to do a practice session.

MRI acquisition

We acquired all scans on a single 3.0-T Philips Achieva MRI scanner (Philips Medical Systems, Best, The Netherlands) using the following T1-weighted parameters: TR/TE 10/4.6 ms, flip angle 8°, matrix 304 x 299, FOV 24 cm, voxel size 0.75 x 0.75 x 0.8 mm^3. To avoid ambiguities in the correct left/right orientation of the processed images, we marked the right side of the forehead of participants with a vitamin E pill, hyperintense on T1-weighted images. Independent clinical neuroradiologists evaluated all scans; no gross morphological or signal abnormalities were found.

MRI processing

All T1-weighted brain scans were coded, to ensure rater blindness to subject identity and diagnosis for the entire analysis, and then processed on the computer cluster of the UMCU using FreeSurfer v6 (Fischl 2012). This is a well-validated online image analysis suite (http://surfer.nmr.mgh.harvard.edu/fswiki) for a fully automated quantitative assessment of brain anatomy including volumetry of subcortical structures and a detailed assessment of cortical morphometry, with accuracy comparable to manual methods (Fischl et al. 2002) and post-mortem studies (Fischl and Dale 2000). For a detailed description of the reconstruction pipelines in FreeSurfer, please refer to previous publications (Dale et al. 1999; Fischl et al. 1999; Fischl and Dale 2000; Fischl et al. 2002, 2004a, 2004b).

Next, all processed scans (including single time points) were put through the longitudinal pipeline embedded in FreeSurfer (Reuter et al. 2012). This process creates an unbiased within-subject template from all its time points. Then, a number of processing steps were initialized (including skull stripping, Talairach transformation, atlas registration, spherical surface maps and parcellations) on all individual scans at all time points using the common information from the within-subject template. Eventually, this process reduces the random intra-individual variation in the processing procedure, and thereby significantly improves reliability and statistical power of the longitudinal analysis (Reuter et al. 2012).

Table 1. Demographic and clinical characteristics of the study sample

		ASD	ADHD	TD	p[d]	Effect	ASD-	ASD+	ADHD	TD	p[d]	Effect
Subjects / scans	N	70 / 92	70 / 96	70 / 92	ns	-	33 / 44	33 / 38	64 / 82	64 / 80	ns	-
Sex	N Male - Female	67 - 3	59 - 11	60 - 10	ns	-	32 - 1	33 - 0	54 - 10	55 - 9	**.035**	ASD+
Age at scan years	M (SD)	11.72 (2.24)	11.83 (2.65)	11.86 (2.58)	ns	-	11.65 (1.61)	10.76 (1.44)	11.00 (1.80)	11.11 (1.74)	ns	-
	range	7.43 - 19.45	7.53 - 18.85	7.95 - 19.78			7.43 - 14.61	8.21 - 14.33	7.53 - 15.03	7.95 - 15.01		
Hand preference[a]	N Right - Other	69 - 0	67 - 3	68 - 2	ns	-	33 - 0	32 - 0	62 - 2	62 - 2	ns	-
Total IQ at baseline	M (SD)	112.24 (17.03)	106.34 (16.66)	112.76 (17.23)	**.050**	ns	116.36 (15.00)	109.91 (17.35)	106.73 (17.00)	113.16 (17.35)	**.040**	ADHD < ASD-
DISC[b] at baseline	ADHD-I	7	18	0	-	-	-	7	15	0	-	-
	ADHD-HI	2	8	0			-	2	8	0		
	ADHD-C	7	34	0			-	6	33	0		
CBCL AP T-score[c] at baseline	M (SD)	66.60 (8.45)	65.06 (7.40)	52.02 (2.78)	**<.001**	ADHD > TD ASD > TD	60.00 (4.36)	72.94 (6.32)	65.38 (7.46)	52.00 (2.78)	**<.001**	ASD+ > ADHD ADHD > ASD- ASD- > TD
	range	51 - 92	52 - 88	50 - 66			51 - 66	67 - 92	52 - 88	50 - 66		

Note. On the left side are the characteristics of the main study sample divided into the three primary diagnostic groups of interest.
On the right side, are the characteristics of the age-matched subsample divided into four (sub)groups based on symptoms of ADHD (see main text).

Abbreviations: ASD, Autism Spectrum Disorder; ADHD, Attention-Deficit/Hyperactivity Disorder (I=inattentive type, HI=hyperactive/impulsive type, C=combined type); TD, typically developing controls; ASD-, Autism Spectrum Disorder with fewer symptoms of ADHD; ASD+, Autism Spectrum Disorder with greater symptoms of ADHD; p, group differences p-value; N, number; ns, not significant; M, mean; SD, standard deviation; IQ, intelligence quotient; DISC, Diagnostic Interview Schedule for Children; CBCL, Child Behaviour Checklist; AP, Attention Problems.
Note. [a] Hand preference unavailable for 1 subject with ASD; [b] DISC unavailable for 10 ADHD and 18 ASD+ subjects; [c] CBCL unavailable for 7 controls and 6 ADHD subjects; [d] X^2 for N of scans; Fisher's exact test for sex and hand preference; One-way ANOVA with *post-hoc* Tukey's test for age at scan, IQ, and CBCL AP T-score.

Quality control procedure

All the FreeSurfer data passed an extensive qualitative assessment (QA), depicted in supplementary Figure S1. Given the sensitivity of cortical markers to motion and other acquisition artifacts, this post-processing QA procedure is critical for a more precise and robust estimation of brain measures across participants (Dewey et al. 2010; Ducharme et al. 2016). Accordingly, all FreeSurfer outputs were inspected by an experienced operator (SA) for accuracy of the reconstructed gray-white matter segmentation and surfaces. Where appropriate, errors were corrected following the standardized procedures documented on the FreeSurfer website (http://surfer.nmr.mgh.harvard.edu/fswiki), and then re-processed. The types of errors that typically required manual editing were incomplete skull stripping and mis-classification of white matter. There were no differences between groups in the proportion of edited scans. Scans with inaccuracies in reconstruction which persisted after manual editing were excluded. This QA procedure was applied to all cross-sectional, within-subject templates, and final longitudinal scans. As such, only high-quality scans were included in the final analysis.

Regions and measures of interest

We acquired the volume of 25 non-cortical regions, including seven subcortical structures per hemisphere (caudate, putamen, pallidum, accumbens, thalamus, ventral diencephalon and amygdala), corpus callosum (anterior, mid-anterior, central, mid-posterior and posterior segments), bilateral hippocampus, and bilateral cerebellar gray and white matter. For simplicity, these regions will be indicated as 'subcortical' structures henceforth.

Next, we parcellated the cerebral cortex into 74 anatomical regions per hemisphere using the sulco-gyral-based atlas provided by Destrieux (Destrieux et al. 2010) (see supplementary table S1 and Figure S2). This high number of cortical regions enabled us to examine the complex folded anatomy of the cerebral cortex in greater detail also within sulci (for comparison, the Desikan-Killiany atlas defines 34, gyral-based, regions per hemisphere). This is important, since a larger proportion of the cortical surface (from one half to two thirds) is hidden within the sulci, so the brain is more 'sulcal' than 'gyral' (Zilles et al. 1997; Van Essen 2005).

We characterized cortical morphology comprehensively by measuring cortical volume (mm^3), cortical surface area (mm^2), cortical thickness (mm), and local gyrification index (*l*GI, dimensionless), of the cortex as a whole and within the predefined regions. For each region, cortical surface area was measured along the gray-white matter boundary (white surface). Cortical volume and thickness were measured as the volume and the average distance, respectively, between parcellated portions of white and pial surfaces (Fischl and Dale 2000). *l*GI is a measure of folding complexity that is calculated at each point of the pial surface and averaged across each cortical area. *l*GI refers to the

ratio between the surface of a circular region of the pial surface, and the corresponding region on the outer smoothed surface of the brain (Schaer et al. 2008).

Statistical analysis

SPSS Statistics 25.0 for Mac OS X (SPSS Inc., Chicago, Illinois) was used to test for differences between diagnostic groups in demographic and clinical data using one-way ANOVA with post-hoc Tukey's test, X^2 or Fisher's exact tests, as appropriate.

We estimated developmental trajectories of the brain measures of interest using mixed-effects model analyses as implemented in the *nlme* package (Pinheiro et al. 2017) in R v3.3.3 (R Core Team 2017). This method permitted us to include participants with multiple scans, and to combine both inter- and intra-individual differences in the growth parameters (e.g., intercepts), while accounting for unequal number of scans per subject, and uneven temporal spacing of scans between them. The best-fit model was estimated in two phases as described previously (Wierenga et al. 2014a, 2014b; Ambrosino et al. 2017).

First, a growth model was determined using a step-down selection procedure. Each brain measure of the i^{th} individual at the j^{th} time point was modeled using cubic, quadratic and linear age effects, with sex as a covariate, according to the formula:

$$Measure_{ij} = Intercept + d_{ij} + \beta_1 (sex) + \beta_2 (age) + \beta_3 (age)^2 + \beta_4 (age)^3 + e_{ij}$$

where d_{ij} represents the within subject dependence and the e_{ij} term is the residual error. Age terms were centered around the mean across groups (11.8 years) to improve the interpretability of the coefficients. Sex and age effects were fixed, while the intercept and the d_{ij} term were modeled as random factors. If the cubic age effect was not significant at $p<.05$, it was removed from the model in order to test the quadratic age effect and so on.

Second, we examined whether the growth model differed between individuals with a primary diagnosis of ADHD, ASD, and typically developing controls. To this aim, the selected growth model was expanded to include a trichotomous variable 'diagnosis' and its interaction with the age term(s) as fixed factors. We tested whether the full model fit the data better than a simpler model including only the main effects of the primary diagnosis and age. If not, the simpler model was compared to the selected growth model including the age terms only.

We estimated coefficients using the full Maximum Likelihood criterion. Best-fit models were selected based on the principle of parsimony, aiming to explain the most amount of variance with the least number of parameters. This was achieved by a stringent model selection procedure according to the smallest Bayesian Information Criterion value (BIC; Schwarz 1978).

In the case of a significant effect of the diagnosis predictor, we performed post-hoc pairwise analyses using Tukey's HSD test. This method accounts for multiple comparisons by correcting for family-wise error rate (Maxwell and Delaney 1990).
We computed effect sizes of diagnosis, equivalent to Cohen's d (Cohen 1992), by dividing the fixed effect estimate by the square root of the variance at the within-subject level (Tymms 2004).

Additionally, we ran sensitivity analyses to control for potential confounders, such as hand preference and IQ, by including respective covariates. We further report on analyses including estimated total intracranial volume, total cortical surface area, average cortical thickness, or average local gyrification as additional covariates, in order to correct local cortical and subcortical measures for global values as appropriate.

Next, to investigate the impact of comorbid symptoms of ADHD on brain development, we ran the same mixed model analysis and selection procedure described above, but now with the sample divided into four diagnostic groups, according to the CBCL Attention Problems T-score: ADHD, ASD+, ASD-, and controls. As the ASD+ subgroup was younger on average (age range 8.21-14.33 years, mean 10.70 years) than the ASD- subgroup (range 7.43-19.45 years, mean 12.46 years, p=.009), we resampled the data by including only participants up to 15 years, and then matched the four (sub)groups for age using PSM. This resulted in a closely matched subsample of 194 children and adolescents, with a total of 244 MRI scans. Their demographics are included in Table 1.

Further, we examined how group differences in brain development were related to developmental changes in ADHD symptoms. To this aim, we first explored developmental trajectories of attention problems (T-scores) in the age-matched four diagnostic (sub)groups. We used mixed model analysis with diagnostic group as a fixed factor, and subject as a random factor. As the CBCL T-scores take age and sex into account, these variables were not included as covariates in the behavioral model. Post-hoc pairwise comparisons were performed using Tukey's HSD test.

We then investigated the longitudinal relation between attention problems and brain measures. For brain regions showing significant group effects, we compared the best-fitting developmental model to a model including regression residuals extracted from the behavioral model as an additional covariate. This enabled us to control for collinearity between attention problems and diagnostic status. Best-fit models were selected using BIC values.

The impact of attention problems on brain development was further investigated in separate models exploring the main effect of attention problems (T-scores), with age, and sex as covariates, but now without including diagnostic status. Models

with attention problems were then compared with the best-fitting developmental models with diagnostic group using Cox test for non-nested models (Greene 2003) implemented in the *lmtest* package in R (Zeileis and Hothorn 2002).

RESULTS

Results are summarized in Table 2. We first compared brain development between the three primary diagnostic groups: ADHD, ASD, and TD. We found a main effect of diagnosis in the volume of left orbital sulci, a composite H-shaped sulcal cortex consisting of two longitudinal (medial and lateral) sulci linked by a transverse one (Destrieux et al. 2010). Post-hoc analyses (accounting for multiple comparisons), showed that this region was smaller in individuals with ADHD and ASD compared to TD (d=-.68, p<.001 and d=-.49, p=.016), and that there was no difference between groups with ADHD and ASD (p=.506).

We also found a group difference in volume of right orbital gyri, a region comprising right anterior, posterior, medial and lateral orbital gyri (Destrieux et al. 2010). Post-hoc analyses showed that this region was reduced in ADHD compared to TD (d=-.84, p<.001), but not in ASD (ASD vs TD p=.070). Nor was it different between groups with ASD and ADHD (p=.053).

In both of these cortical regions, the reduction in the volume was accompanied by a concordant decrease in cortical surface area, shown in Fig. 1 (all p<.001, see Table 2).

Developmental trajectories of cortical volume and surface area followed a quadratic curve in right orbital gyri, whereas they decreased linearly in left orbital sulci. We found no interaction effect between age and diagnosis for any of these cortical measures, reflected by parallel developmental trajectories between the three groups. As such, all reductions described above appeared to be present at baseline and developmentally stable (i.e., not increasing or decreasing over time). Notably, results remained consistent when covarying for total brain measures, hand preference, and total IQ. We found no differences between groups in cortical thickness and gyrification of any cortical area, nor in the volume of any subcortical structure.

We extended our analysis from primary diagnostic groups to subgroups based on comorbid symptoms of ADHD, derived from the Attention Problems subscale of the CBCL at study entry: ADHD, ASD+, ASD-, and TD. There was a difference between the four (sub)groups, which followed a stepwise pattern: ASD+ > ADHD > ASD- > TD, where the ASD+ subgroup had the most the severe ADHD symptoms, and the ASD- subgroup had higher symptoms than TD (all p<.001, see Table 1).

Mixed model analysis on brain development showed that the reductions in volume and surface area of left orbital sulci observed in ASD compared to TD were driven by the subgroup of individuals with autism and greater comorbid ADHD symptoms (ASD+) (p=.022 for volume; p=.005 for surface area). In this region, the ASD+ and ADHD groups differed from the TD group, but not from each other (ADHD = ASD+ < TD). No differences in brain development were found for the subgroup with autism and fewer ADHD symptoms (ASD-) compared to the other (sub)groups (p>.202).

To rule out the possibility that our results were driven by the difference in age between the ASD+ and the ASD- subgroups (p=.009), we repeated the analysis on a slightly smaller, closely age-matched subsample, which yielded consistent results (d=-.59, p=.048 for left orbital sulci volume; d=-.70, p=.015 for surface area) shown in Table 2 and Fig. 1.

Table 2. Group differences for cortical measures between the three primary diagnostic groups (left side), and the four age-matched (sub)groups based on ADHD symptoms (right side).

		ADHD ASD TD				ADHD ASD+ ASD- TD			
Cortical Area	**Measure**	**Model**	**Group Effect**	**d°**	**p***	**Model**	**Group Effect**	**d°**	**p***
Left orbital sulci	Volume	Linear	ADHD < TD	-.68	<.001	Linear	ADHD < TD	-.68	<.001
			ASD < TD	-.49	.016		ASD+ < TD	-.59	.048
	Surface area	Linear	ADHD < TD	-.77	<.001	Linear	ADHD < TD	-.77	<.001
			ASD < TD	-.53	<.001		ASD+ < TD	-.70	.015
Right orbital gyri	Volume	Quadratic	ADHD < TD	-.84	<.001	Linear	ADHD < TD	-.84	<.001
	Surface area	Quadratic	ADHD < TD	-.85	<.001	Linear	ADHD < TD	-.85	<.001

Abbreviations: ADHD, Attention-Deficit/Hyperactivity Disorder; ASD, Autism Spectrum Disorder; TD, typically developing controls; ASD+, Autism Spectrum Disorder with more symptoms of ADHD; ASD-, Autism Spectrum Disorder with fewer symptoms of ADHD. Note. ° Cohen's d effect size; * Tukey's test p-value.

Finally, we examined whether the developmental patterns observed in the four (sub) groups related to a dimensional measure of ADHD. Mixed model analysis of attention problems (T-scores) over development showed a significant main effect of diagnosis (p<.001). Tukey's test showed that all pairwise comparisons remained significant over development (p<.001), following the stepwise pattern observed at baseline (see supplementary Fig. S3). Mixed model analysis on brain development showed no additive effect of attention problems (residuals) on the diagnostic group effects on left orbital sulci and right orbital gyri. Separate models testing attention problems on brain development did not improve on the best-fit developmental model including diagnostic status.

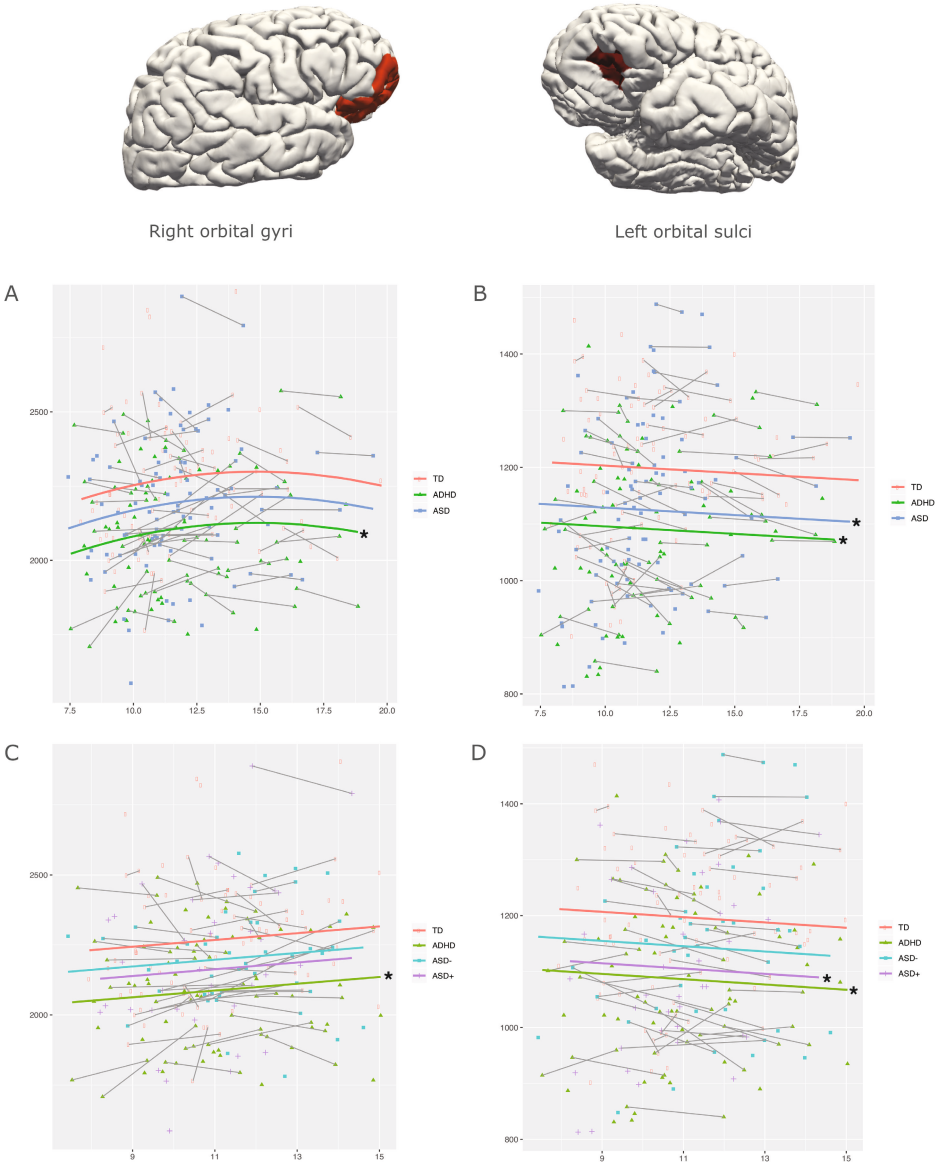

Figure 1. Developmental differences in cortical surface area in the right orbital gyri (left side) and the left orbital sulci (right side) between individuals with Autism Spectrum Disorder (ASD), Attention-Deficit/Hyperactivity Disorder (ADHD), and typically developing controls (TD) (panels A and B). Differences in ASD with more and fewer comorbid symptoms of ADHD (ASD+ and ASD-, respectively) compared to ADHD and TD are shown in panels C and D.

Note: cortical surface area in mm^2 (y-axis) by age in years (x-axis); *Asterisks indicate statistically significant differences compared to TD (see Table 2)

DISCUSSION

In this study, we compared brain developmental trajectories in a large (N=210) longitudinal sample of well-matched children and adolescents with a primary diagnosis of ADHD or ASD, and typically developing controls. We conceptualized ASD and ADHD as two extremes on an overarching, trans-diagnostic continuum and investigated whether changes in brain development were related to symptomatic overlap between the ADHD and ASD groups. We found developmentally stable reductions in cortical volume and surface area within bilateral orbital prefrontal cortex (OFC) in individuals with an ADHD diagnosis compared to typical developing individuals. Furthermore, we found a similar developmental pattern in left orbital sulci for individuals with autism and elevated ADHD symptoms. This suggests that there may be similar neuroanatomical developmental pathways associated with ADHD symptoms in these two neurodevelopmental conditions.

Our results were consistent with our hypothesis in that they showed changes in OFC in individuals with ASD and elevated ADHD symptoms that were similar to those in individuals with a primary diagnosis of ADHD, particularly in the left hemisphere. This suggests that developmental changes in left OFC may be related to ADHD symptoms in both neurodevelopmental conditions, in line with the trans-diagnostic hypothesis (Rommelse et al. 2017). Yet, our dimensional analysis of ADHD symptoms did not yield significant results, indicating that in our study the variance in left OFC morphology was better captured by a categorical definition of ADHD and ASD with elevated ADHD symptoms than by ADHD symptoms *per se*. This result suggests that the relation between changes in cortical development and ADHD symptoms is not linear within a hypothesized overarching continuum, but still differs between diagnostic groups. This is echoed by our observation that individuals with ASD and elevated ADHD symptoms had most symptoms overall, and were most severely affected, whereas individuals with a primary ADHD diagnosis had the greatest reductions in OFC measures.

The involvement of OFC, located on the ventral surface of the frontal lobe (Destrieux et al. 2010) is plausible in ADHD neurobiology, as it is one of the most connected regions of the brain and involved in several functional networks modulated by dopamine (Kahnt and Tobler 2017), including those regulating reward expectation, attention, and impulsive behavior (Winstanley et al. 2010). Impairments of these cognitive functions have been frequently reported in ADHD (Arnsten 2009). Interestingly, the only neuroimaging study to date to compare four clinical (sub)groups (including individuals with ADHD and elevated ASD symptoms in addition to the other three groups), albeit cross-sectionally and in a smaller sample, found an effect of ADHD, both as a primary and as a co-morbid diagnosis to ASD, in left pars orbitalis (Nickel et al. 2018). This cortical region

is anatomically contiguous with, and for some individuals not clearly separable from, OFC (Destrieux et al. 2010).

Our findings further showed that a reduction of surface area was the principal morphometric determinant of smaller orbitofrontal volumes in ADHD and in ASD with elevated ADHD symptoms. According to the radial unit hypothesis of Rakic, cortical surface area, and thus the size of any cortical region, is determined by the number of ontogenetic units (Rakic 1995). Speculatively, our findings therefore suggest that a perturbation of early proliferative mechanisms increasing the number of ontogenetic units that will form the mature OFC, may be involved in the development of clinically relevant ADHD symptoms. Mechanisms regulating the expansion of cortical surface area are hypothesized to modulate the pattern and complexity of cortical folding (White et al. 2010). OFC is a morphologically highly complex and variable region that has been found to show both common and distinct qualitative sulco-gyral patterns in multiple neuropsychiatric conditions with developmental origins, such as autism and ADHD (Watanabe et al. 2014; Patti and Troiani 2018).

Our study has several methodological strengths, including the use of a large sample of closely matched participants across all primary diagnostic groups and clinical subgroups, the acquisition of all 3-T scans on a single scanner, a longitudinal study design and longitudinal processing of the data which passed a stringent quality control procedure. However, this study should also be viewed in the context of some limitations. First, effect size estimates in our study ranged from 0.49 to 0.85 and were therefore 'medium' to 'large' according to Cohen's criteria (Cohen 1992). While this highlights the strength of our findings, it can also be taken to suggest that we may have been underpowered to detect smaller, more subtle, morphometric changes. It is also of note that clinical confirmation of comorbid ADHD was not available for our ASD sample, so we used a questionnaire-derived proxy. Although our approach worked well for achieving sample homogeneity for ADHD symptoms, caution is called for when interpreting questionnaire scores, as individuals with an ASD diagnosis and elevated levels of ADHD symptoms do not necessarily meet full criteria for (comorbid) ADHD. Moreover, we did not evaluate the possible presence of ASD comorbidity or elevated ASD symptoms in our sample with a primary ADHD diagnosis. Therefore, our study cannot fully rule out the possibility of a specific effect of ASD on brain development across diagnoses. To disentangle the complex interplay between autism and ADHD, further investigations using clinically confirmed co-occurrence of the two conditions are necessary. Furthermore, our participants with ADHD and ASD with elevated ADHD symptoms were not medication-naïve, and this may have mitigated their symptom levels. However, meta-analyses have shown that long-term psychotropic treatment contributes to 'normalization' of brain volumes in ADHD (Shaw et al. 2009), whereas our study showed that OFC is smaller in

ADHD and ASD with elevated ADHD symptoms. This suggests that changes in cortical morphology persist in relation to ADHD symptoms *despite* the influence of psychotropic medication. Lastly, longitudinal scans were not available for all participants in our study, although this was partly controlled for by the mixed model analysis.

In conclusion, we report reductions in the expansion of left OFC that were stable across development and shared between individuals with a primary diagnosis of ADHD and individuals with a primary diagnosis of ASD and elevated ADHD symptoms. These findings suggest that the neurobiological pathways that regulate early OFC development may be related to ADHD symptoms in both neurodevelopmental conditions, in line with hypotheses conceptualizing both disorders as extremes on an overarching, trans-diagnostic continuum.

FUNDING

This work was supported by the Netherlands Organisation for Scientific Research (NWO) VIDI 91776384 and VICI 453-10-005 grants to Sarah Durston.

ACKNOWLEDGMENTS

We would like to thank all participants and their families for participating in this study. We further wish to thank Rosanne van Diepen, Yvonne Rijks, Sanne Veerhoek, and Chantal Vlaskamp for their assistance with subject recruitment and acquisition of MRI scans throughout the running time of this study.

REFERENCES

Albajara Sáenz A, Van Schuerbeek P, Baijot S, Septier M, Deconinck N, Defresne P, et. al. 2020. Disorder-specific brain volumetric abnormalities in Attention-Deficit/Hyperactivity Disorder relative to Autism Spectrum Disorder. PLoS One. Nov 9;15(11):e0241856. doi: 10.1371/journal.pone.0241856. PMID: 33166335; PMCID: PMC7652272.

Ambrosino S, de Zeeuw P, Wierenga LM, van Dijk S, Durston S. 2017. What can cortical development in Attention-Deficit/Hyperactivity Disorder teach us about the early developmental mechanisms involved? Cereb Cortex. Sep 1;27(9):4624-4634. doi: 10.1093/cercor/bhx182. PMID: 28922857.

American Psychiatric Association. 2013. Diagnostic and statistical manual of mental disorders (DSM-5®). American Psychiatric Pub.

American Psychiatric Association. 2000. Diagnostic and statistical manual of mental disorders. 4th ed. Washington, DC: American Psychiatric Association.

Arnsten AF. 2009. The Emerging Neurobiology of Attention Deficit Hyperactivity Disorder: The Key Role of the Prefrontal Association Cortex. J Pediatr. May 1;154(5):I-S43. doi: 10.1016/j.jpeds.2009.01.018. PMID: 20596295; PMCID: PMC2894421.

Bethlehem RAI, Romero-Garcia R, Mak E, Bullmore ET, Baron-Cohen S. 2017. Structural Covariance Networks in Children with Autism or ADHD. Cereb Cortex. Aug 1;27(8):4267-4276. doi: 10.1093/cercor/bhx135. PMID: 28633299; PMCID: PMC5903412.

Brieber S, Neufang S, Bruning N, Kamp-Becker I, Remschmidt H, Herpertz-Dahlmann B, et al. 2007. Structural brain abnormalities in adolescents with autism spectrum disorder and patients with attention deficit/hyperactivity disorder. J Child Psychol Psychiatry. Dec;48(12):1251-1258. doi: 10.1111/j.1469-7610.2007.01799.x. PMID: 18093031.

Chong TT, Williams MA, Cunnington R, Mattingley JB. 2008. Selective attention modulates inferior frontal gyrus activity during action observation. Neuroimage. Mar 1;40(1):298-307. doi: 10.1016/j.neuroimage.2007.11.030. Epub 2007 Dec 3. PMID: 18178107.

Cohen J. 1992. A power primer. Psychol Bull. 112(1):155–159.

Courchesne E, Campbell K, & Solso S. 2011. Brain growth across the life span in autism: age-specific changes in anatomical pathology. Brain Res. J. 1380:138–145. https://doi.org/10.1016/j.brainres.2010.09.10

Dale AM, Fischl B, Sereno MI. 1999. Cortical surface-based analysis I. Segmentation and surface reconstruction. Neuroimage. 9(2):179–194.

Destrieux C., Fischl B., Dale A., Halgren E. 2010. Automatic parcellation of human cortical gyri and sulci using standard anatomical nomenclature. Neuroimage.15;53(1):1-15.

Dewey J, Hana G, Russell T, Price J, McCaffrey D, Harezlak J, et al. 2010. Reliability and validity of MRI-based automated volumetry software relative to auto-assisted manual measurement of subcortical structures in HIV-infected patients from a multisite study. Neuroimage. 51(4):1334–1344.

Ducharme S, Albaugh MD, Nguyen TV, Hudziak JJ, Mateos-Pérez JM, Labbe A, et al. 2016. Trajectories of cortical thickness maturation in normal brain development–The importance of quality control procedures. Neuroimage. 125:267–279.

Durston S, Nederveen H, van Dijk S, van Belle J, de Zeeuw P, Langen M, van Dijk A. 2009. Magnetic resonance simulation is effective in reducing anxiety related to magnetic resonance scanning in children. J Am Acad Child Adolesc Psychiatry. 48(2):206–207.

Ellison-Wright I, Ellison-Wright Z, Bullmore E. 2008. Structural brain change in Attention Deficit Hyperactivity Disorder identified by meta-analysis. BMC Psychiatry. Jun 30:8-51. doi: 10.1186/1471-244X-8-51. PMID: 18590567; PMCID: PMC2453122.

Fischl B. 2012. FreeSurfer. Neuroimage. 62(2):774–781.

Fischl B, Dale AM. 2000. Measuring the thickness of the human cerebral cortex from magnetic resonance images. Proc Natl Acad Sci USA. 97(20):11050–11055.

Fischl B, Salat DH, Busa E, Albert M, Dieterich M, Haselgrove C, et al. 2002. Whole brain segmentation: automated labeling of neuroanatomical structures in the human brain. Neuron. 33(3):341–355.

Fischl B, Salat DH, van der Kouwe AJW, Makris N, Ségonne F, Quinn BT, Dale AM. 2004a. Sequence-independent segmentation of magnetic resonance images. Neuroimage. 23(Suppl 1): S69–S84.

Fischl B, Sereno MI, Dale AM. 1999. Cortical surface-based analysis ii: inflation, flattening, and a surface-based coordinate system. Neuroimage. 9(2):195–207.

Fischl B, van der Kouwe A, Destrieux C, Halgren E, Ségonne F, Salat DH, et al. 2004b. Automatically parcellating the human cerebral cortex. Cereb Cortex. 14(1):11–22.

Foster NE, Doyle-Thomas KA, Tryfon A, Ouimet T, Anagnostou E, Evans AC, et al. 2015. Structural Gray Matter Differences During Childhood Development in Autism Spectrum Disorder: A Multimetric Approach. Pediatr Neurol. Oct;53(4):350-359. doi: 10.1016/j.pediatrneurol.2015.06.013. Epub 2015 Jun 25. PMID: 26231265.

Frodl T, Skokauskas N. 2012. Meta-analysis of structural MRI studies in children and adults with attention deficit hyperactivity disorder indicates treatment effects. Acta Psych Scand. 125:114–126.

Greene W. H. 2003. Econometric Analysis, 5th ed. New Jersey: Prentice Hall.

Hoogman M, Bralten J, Hibar DP, Mennes M, Zwiers MP, Schweren LS, et al. 2017. Subcortical brain volume differences in participants with attention deficit hyperactivitydisorder in children and adults: a cross-sectional mega-analysis. Lancet Psychiatry. 4(4):310–319.

Hoogman M, Muetzel R, Guimaraes JP, Shumskaya E, Mennes M, Zwiers MP, et al. 2019. Brain Imaging of the Cortex in ADHD: A Coordinated Analysis of Large-Scale Clinical and Population-Based Samples. Am J Psychiatry. Jul 1;176(7):531-542. doi: 10.1176/appi.ajp.2019.18091033. Epub 2019 Apr 24. PMID: 31014101; PMCID: PMC6879185.

Hoogman M, van Rooij D, Klein M, Boedhoe P, Ilioska I, Li T, et al. 2020. Consortium neuroscience of attention deficit/hyperactivity disorder and autism spectrum disorder: The ENIGMA adventure. Hum Brain Mapp. May 18. doi: 10.1002/hbm.25029. Epub ahead of print. PMID: 32420680.

Kahnt T, Tobler PN. 2017. Dopamine Modulates the Functional Organization of the Orbitofrontal Cortex. J Neurosci. 37(6):1493-1504. doi:10.1523/JNEUROSCI.2827-16.2016

Lim L, Chantiluke K, Cubillo AI, Smith AB, Simmons A, Mehta MA, Rubia K. 2015. Disorder-specific grey matter deficits in attention deficit hyperactivity disorder relative to autism spectrum disorder. Psychol Med. Apr;45(5):965-976. doi: 10.1017/S0033291714001974. Epub 2014 Sep 17. PMID: 25229248; PMCID: PMC4413819.

Mahajan R, Dirlikov B, Crocetti D, Mostofsky SH. 2016. Motor Circuit Anatomy in Children with Autism Spectrum Disorder With or Without Attention Deficit Hyperactivity Disorder. Autism Res. 9: 67-81. https://doi-org.proxy.library.uu.nl/10.1002/aur.1497

Maxwell SE, Delaney HD. 1990. Designing Experiments and Analyzing Data: A Model Comparison Perspective. p 210.

Mizuno Y, Kagitani-Shimono K, Jung M, Makita K, Takiguchi S, Fujisawa TX, et al. 2019. Structural brain abnormalities in children and adolescents with comorbid autism spectrum disorder and attention-deficit/hyperactivity disorder. Transl Psychiatry. Dec 9;9(1):332. doi: 10.1038/s41398-019-0679-z. PMID: 31819038; PMCID: PMC6901569.

Nakao T, Radua J, Rubia K, Mataix-Cols D. 2011. Gray matter volume abnormalities in ADHD: voxel-based meta-analysis exploring the effects of age and stimulant medication. Am J Psychiatry. 168(11):1154–1163.

Nickel K, Tebartz van Elst L, Manko J, Unterrainer J, Rauh R, Klein C, et al. 2018. Inferior Frontal Gyrus Volume Loss Distinguishes Between Autism and (Comorbid) Attention-Deficit/Hyperactivity Disorder-A FreeSurfer Analysis in Children. Front Psychiatry. Oct 23;9:521. doi: 10.3389/fpsyt.2018.00521. PMID: 30405459; PMCID: PMC6206215.

Norman LJ, Carlisi C, Lukito S, Hart H, Mataix-Cols D, Radua J, Rubia K. 2016. Structural and Functional Brain Abnormalities in Attention-Deficit/Hyperactivity Disorder and Obsessive-Compulsive Disorder: A Comparative Meta-analysis. JAMA Psychiatry. Aug 1;73(8):815-825. doi: 10.1001/jamapsychiatry.2016.0700. Erratum in: JAMA Psychiatry. 2017 Oct 1;74(10):1079. Erratum in: JAMA Psychiatry. 2018 Mar 1;75(3):303. PMID: 27276220.

Patti MA, Troiani V. 2017. Orbitofrontal sulcogyral morphology is a transdiagnostic indicator of brain dysfunction. Neuroimage Clin. Dec 18;17:910-917. doi: 10.1016/j.nicl.2017.12.021. PMID: 29527495; PMCID: PMC5842758.

Pinheiro J, Bates D, DebRoy S, Sarkar D, and R Core Team. 2017. _nlme: Linear and Nonlinear Mixed Effects Models_. R package version 3.1-131, URL: https://CRAN.R-project.org/package=nlme

R Core Team. 2017. R: A language and environment for statistical computing. R Foundation for Statistical Computing, Vienna, Austria. URL https://www.R-project.org/.

Rakic P. 1995. A small step for the cell, a giant leap for mankind: a hypothesis of neocortical expansion during evolution. Trends Neurosci. Sep;18(9):383-388. doi: 10.1016/0166-2236(95)93934-p. PMID: 7482803.

Reuter M, Schmansky NJ, Rosas HD, Fischl B. 2012. Within-Subject Template Estimation for Unbiased Longitudinal Image Analysis. NeuroImage 61(4):1402-1418.

Rommelse N, Buitelaar JK, Hartman CA. 2017. Structural brain imaging correlates of ASD and ADHD across the lifespan: a hypothesis-generating review on developmental ASD-ADHD subtypes. J Neural Transm. Feb;124(2):259-271. doi: 10.1007/s00702-016-1651-1. Epub 2016 Dec 21. PMID: 28000020; PMCID: PMC5285408.

Rommelse NN, Franke B, Geurts HM, Hartman CA, Buitelaar JK. 2010. Shared heritability of attention-deficit/hyperactivity disorder and autism spectrum disorder. Eur Child Adolesc Psychiatry. Mar;19(3):281-295. doi: 10.1007/s00787-010-0092-x. Epub 2010 Feb 11. PMID: 20148275; PMCID: PMC2839489.

Schaer M, Cuadra MB, Tamarit L, Lazeyras F, Eliez S, Thiran JP. 2008. A surface-based approach to quantify local cortical gyrification. IEEE Trans Med Imaging. Feb;27(2):161-170. doi: 10.1109/TMI.2007.903576. PMID: 18334438.

Schwarz G. 1978. Estimating the dimension of a model. Annals of Statistics. 6:461-464. http://dx.doi.org/10.1214/aos/1176344136

Shaffer D, Fisher P, Lucas CP, Dulcan MK, Schwab-Stone ME. 2000. NIMH Diagnostic Interview Schedule for Children Version IV (NIMH DISC-IV): description, differences from previous versions, and reliability of some common diagnoses. J Am Acad Child Adolesc Psychiatry. Jan;39(1):28-38. doi: 10.1097/00004583-200001000-00014. PMID: 10638065.

Shaw P, Sharp WS, Morrison M, Eckstrand K, Greenstein DK, Clasen LS, et al. 2009. Psychostimulant treatment and the developing cortex in attention deficit hyperactivity disorder. Am J Psychiatry. Jan;166(1):58-63. doi: 10.1176/appi.ajp.2008.08050781. Epub 2008 Sep 15. PMID: 18794206; PMCID: PMC2700349.

Simonoff E, Pickles A, Charman T, Chandler S, Loucas T, Baird G. 2008. Psychiatric disorders in children with autism spectrum disorders: prevalence, comorbidity, and associated factors in a population-derived sample. J Am Acad Child Adolesc Psychiatry. Aug;47(8):921-929. doi: 10.1097/CHI.0b013e318179964f. PMID: 18645422.

Swick D, Ashley V, Turken AU. 2008. Left inferior frontal gyrus is critical for response inhibition. BMC Neurosci. Oct 21;9:102. doi: 10.1186/1471-2202-9-102. PMID: 18939997; PMCID: PMC2588614.

Thoemmes F. 2012. Propensity score matching in SPSS. arXiv:1201.6385.

Tymms P. 2004. Effect sizes in multilevel models. In: Schagen I, Elliot K, editors. But what does it mean? The use of effect sizes in educational research. Slough: UK: National Foundation for Educational Research.

Valera EM, Faraone SV, Murray KE, Seidman LJ. 2007. Metaanalysis of structural imaging findings in attention-deficit/ hyperactivity disorder. Biol Psychiatry. 61:1361–1369.

Van Essen DC. 2005. A Population-Average, Landmark- and Surface-based (PALS) atlas of human cerebral cortex. Neuroimage. Nov 15;28(3):635-662. doi: 10.1016/j.neuroimage.2005.06.058. Epub 2005 Sep 19. PMID: 16172003.

Verhulst F, Van Der Ende J, Koot H. 1996. Handleiding voor de CBCL/4–18 (Manual for the CBCL/4–18). Rotterdam: Department of Child and Adolescent Psychiatry, Erasmus Academic Medical Center.

Verhulst F, Van Der Ende J, Koot H. 1997. Handleiding voor de Teacher's Report Form (TRF) (Manual for the Teacher Report Form (TRF)). Rotterdam: Department of Child and Adolescent Psychiatry, Erasmus Academic Medical Center.

Wardenaar KJ, de Jonge P. 2013. Diagnostic heterogeneity in psychiatry: towards an empirical solution. BMC Med. Sep 12;11:201. doi: 10.1186/1741-7015-11-201. PMID: 24228940; PMCID: PMC3846412.

Watanabe H, Nakamura M, Ohno T, Itahashi T, Tanaka E, Ohta H, et al. 2014. Altered orbitofrontal sulcogyral patterns in adult males with high-functioning autism spectrum disorders. Soc Cogn Affect Neurosci. Apr;9(4):520-528. doi: 10.1093/scan/nst016. Epub 2013 Feb 5. PMID: 23386741; PMCID: PMC3989135.

Wechsler D. 2005. Wechsler Intelligence Scale for Children – Derde Editie NL. Handleiding en Verantwoording. London: Harcourt Assessment. (Wechsler Intelligence Scale for Children – Third Edition, Dutch Version, Manual).

White T, Su S, Schmidt M, Kao CY, Sapiro G. 2010. The development of gyrification in childhood and adolescence. Brain Cogn. Feb;72(1):36-45. doi: 10.1016/j.bandc.2009.10.009. Epub 2009 Nov 25. PMID: 19942335; PMCID: PMC2815169.

Wierenga L, Langen M, Ambrosino S, van Dijk S, Oranje B, Durston S. 2014a. Typical development of basal ganglia, hippocampus, amygdala and cerebellum from age 7 to 24. Neuroimage. Aug 1;96:67-72. doi: 10.1016/j.neuroimage.2014.03.072. Epub 2014 Apr 4. PMID: 24705201.

Wierenga LM, Langen M, Oranje B, Durston S. 2014b. Unique developmental trajectories of cortical thickness and surface area. Neuroimage. Feb 15;87:120-126. doi: 10.1016/j.neuroimage.2013.11.010. Epub 2013 Nov 15. PMID: 24246495.

Winstanley CA, Zeeb FD, Bedard A, Fu K, Lai B, Steele C, Wong AC. 2010. Dopaminergic modulation of the orbitofrontal cortex affects attention, motivation and impulsive responding in rats performing the five-choice serial reaction time task. Behav Brain Res. Jul 11;210(2):263-272. doi: 10.1016/j.bbr.2010.02.044. Epub 2010 Mar 3. PMID: 20206211.

World Health Organization (WHO). 1993. The ICD-10 classification of mental and behavioural disorders. World Health Organization.

Zeileis A, Hothorn T. 2002. "Diagnostic Checking in Regression Relationships." *R News*, 2(3), 7–10. https://CRAN.R-project.org/doc/Rnews/.

Zielinski BA, Prigge MB, Nielsen JA, Froehlich AL, Abildskov TJ, Anderson JS, et al. 2014. Longitudinal changes in cortical thickness in autism and typical development. Brain. Jun;137(Pt 6):1799-1812. doi: 10.1093/brain/awu083. Epub 2014 Apr 22. PMID: 24755274; PMCID: PMC4032101.

Zilles K, Schleicher A, Langemann C, Amunts K, Morosan P, Palomero-Gallagher N, et al. 1997. Quantitative analysis of sulci in the human cerebral cortex: development, regional heterogeneity, gender difference, asymmetry, intersubject variability and cortical architecture. Hum Brain Mapp. 5(4):218-221. doi: 10.1002/(SICI)1097-0193(1997)5:4<218::AID-HBM2>3.0.CO;2-6. PM

SUPPLEMENTARY MATERIAL

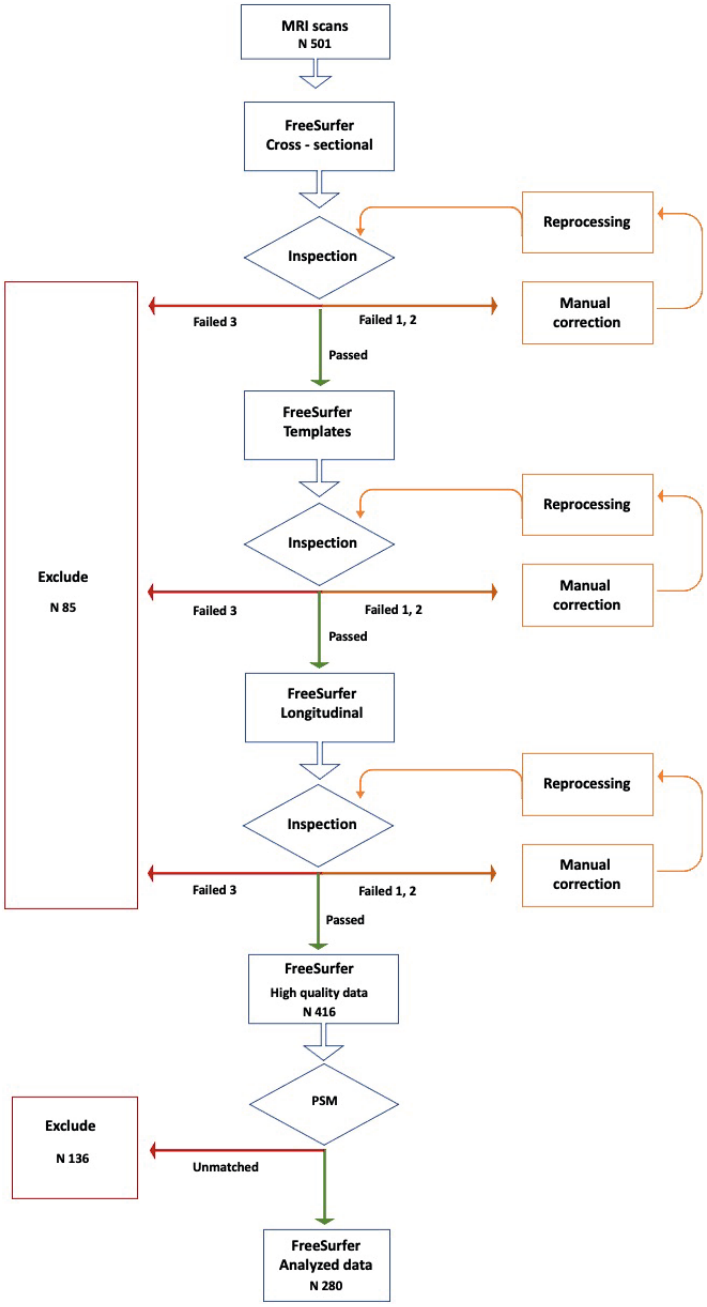

Figure S1. Longitudinal processing, qualitative assessment, and matching of data.
Abbreviation: PSM, Propensity Score Matching.

Table S1 and Figure S2. Destrieux anatomical regions per hemisphere

Index	Short Name	Long name (TA nomenclature is bold typed)	Visible on views	Lobe
1	G_and_S_frontomargin	Fronto-marginal gyrus (of Wernicke) and sulcus	A, L, I	Frontal
2	G_and_S_occipital_inf	Inferior occipital gyrus (O3) and sulcus	L, P, I	Occipital
3	G_and_S_paracentral	Paracentral lobule and sulcus	S, P, M	Front-Par
4	G_and_S_subcentral	Subcentral gyrus (central operculum) and sulci	L	Frontal
5	G_and_S_transv_ frontopol	Transverse frontopolar gyri and sulci	A, L, M, I	Frontal
6	G_and_S_cingul-Ant	Anterior part of the ***cingulate gyrus and sulcus*** (ACC)	M	Frontal
7	G_and_S_cingul-Mid-Ant	Middle-anterior part of the ***cingulate gyrus and sulcus*** (aMCC)	M	Frontal
8	G_and_S_cingul-Mid-Post	Middle-posterior part of the ***cingulate gyrus and sulcus*** (pMCC)	M	Front-Par
9	G_cingul-Post-dorsal	Posterior-dorsal part of the ***cingulate gyrus*** (dPCC)	M	Parietal
10	G_cingul-Post-ventral	Posterior-ventral part of the cingulate gyrus (vPCC, ***isthmus of the cingulate gyrus***)	M, I	Parietal
11	G_cuneus	***Cuneus*** (O6)	S, P, M	Occipital
12	G_front_inf-Opercular	***Opercular part of the inferior frontal gyrus***	L, I	Frontal
13	G_front_inf-Orbital	***Orbital part of the inferior frontal gyrus***	L, I	Frontal
14	G_front_inf-Triangul	***Triangular part of the inferior frontal gyrus***	L, I	Frontal
15	G_front_middle	***Middle frontal gyrus*** (F2)	S, A, L	Frontal
16	G_front_sup	***Superior frontal gyrus*** (F1)	S, A, L, M	Frontal
17	G_Ins_lg_and_S_cent_ ins	***Long insular gyrus and central sulcus of the insula***	L	Insula
18	G_insular_short	***Short insular gyri***	L	Insula
19	G_occipital_middle	Middle occipital gyrus (O2, lateral occipital gyrus)	S, L, P	Occipital
20	G_occipital_sup	Superior occipital gyrus (O1)	S, L, P	Occipital
21	G_oc-temp_lat-fusifor	***Lateral occipito-temporal gyrus*** (fusiform gyrus, O4-T4)	I	Temporal
22	G_oc-temp_med-Lingual	***Lingual gyrus,*** ligual part of the ***medial occipito-temporal gyrus***, (O5)	P, M, I	Occipital
23	G_oc-temp_med-Parahip	***Parahippocampal gyrus***, parahippocampal part of the ***medial occipito-temporal gyrus*** (T5)	M, I	Temporal
24	G_orbital	***Orbital gyri***	A, L, I	Frontal
25	G_pariet_inf-Angular	***Angular gyrus***	S, L, P	Parietal
26	G_pariet_inf-Supramar	***Supramarginal gyrus***	S, L, P	Parietal
27	G_parietal_sup	***Superior parietal lobule*** (lateral part of P1)	S, L, P, M	Parietal
28	G_postcentral	***Postcentral gyrus***	S, L, P	Parietal
29	G_precentral	***Precentral gyrus***	S, A, L	Frontal
30	G_precuneus	***Precuneus*** (medial part of P1)	S, P, M	Parietal
31	G_rectus	***Straight gyrus***, Gyrus rectus	A, M, I	Frontal
32	G_subcallosal	***Subcallosal area, subcallosal gyrus***	M, I	Limbic

Table S1 Continued

Index	Short Name	Long name (TA nomenclature is bold typed)	Visible on views	Lobe
33	G_temp_sup-G_T_ transv	***Anterior transverse temporal gyrus*** (of Heschl)	A, L	Temporal
34	G_temp_sup-Lateral	Lateral aspect of the ***superior temporal gyrus***	A, L	Temporal
35	G_temp_sup-Plan_polar	Planum polare of the ***superior temporal gyrus***	A, L, M	Temporal
36	G_temp_sup-Plan_ tempo	***Planum temporale or temporal plane*** of the superior temporal gyrus	A, L	Temporal
37	G_temporal_inf	***Inferior temporal gyrus*** (T3)	L, I	Temporal
38	G_temporal_middle	***Middle temporal gyrus*** (T2)	A, L, P, I	Temporal
39	Lat_Fis-ant-Horizont	Horizontal ramus of the ***anterior segment of the lateral sulcus*** (or fissure)	L, I	Frontal
40	Lat_Fis-ant-Vertical	Vertical ramus of the ***anterior segment of the lateral sulcus*** (or fissure)	L, I	Frontal
41	Lat_Fis-post	***Posterior ramus*** (or segment) ***of the lateral sulcus*** (or fissure)	A, L	Insula
42	Pole_occipital	***Occipital pole***	L, P, M, I	Occipital
43	Pole_temporal	***Temporal pole***	A, L, M, I	Temporal
44	S_calcarine	***Calcarine sulcus***	M	Occipital
45	S_central	***Central sulcus*** (Rolando's fissure)	S, A, L, P	Frontal
46	S_cingul-Marginalis	***Marginal branch*** (or part) ***of the cingulate sulcus***	S, P, M	Frontal
47	S_circular_insula_ant	Anterior segment of the ***circular sulcus of the insula***	L, I	Insula
48	S_circular_insula_inf	Inferior segment of the ***circular sulcus of the insula***	A, L	Insula
49	S_circular_insula_sup	Superior segment of the ***circular sulcus of the insula***	L, I	Insula
50	S_collat_transv_ant	Anterior transverse collateral sulcus	I	Temp-Occipital
51	S_collat_transv_post	Posterior transverse collateral sulcus	I	Temp-Occipital
52	S_front_inf	***Inferior frontal sulcus***	S, A, L	Frontal
53	S_front_middle	Middle frontal sulcus	S, A, L	Frontal
54	S_front_sup	***Superior frontal sulcus***	S, A, L	Frontal
55	S_interm_prim-Jensen	Sulcus intermedius primus (of Jensen)	S, L, P	Parietal
56	S_intrapariet_and_P_ trans	***Intraparietal sulcus*** (interparietal sulcus) and transverse parietal sulci	S, L, P	Parietal
57	S_oc_middle_and_ Lunatus	Middle occipital sulcus and lunatus sulcus	S, L, P	Occipital
58	S_oc_sup_and_ transversal	Superior occipital sulcus and ***transverse occipital sulcus***	S, L, P	Occipital
59	S_occipital_ant	Anterior occipital sulcus and ***preoccipital notch*** (temporo-occipital incisure)	L, P	Occipital
60	S_oc-temp_lat	Lateral occipito-temporal sulcus	I	Limbic-Occipital

Table S1 Continued

Index	Short Name	Long name (TA nomenclature is bold typed)	Visible on views	Lobe
61	S_oc-temp_med_and_Lingual	Medial occipito-temporal sulcus (***collateral sulcus***) and lingual sulcus	M, I	Occipital
62	S_orbital_lateral	Lateral orbital sulcus	A, L, I	Frontal
63	S_orbital_med-olfact	Medial orbital sulcus (***olfactory sulcus***)	I	Frontal
64	S_orbital-H_Shaped	***Orbital sulci*** (H-shaped sulci)	I, L	Frontal
65	S_parieto_occipital	***Parieto-occipital sulcus*** (or fissure)	S, P, M	Parietal-Occipital
66	S_pericallosal	Pericallosal sulcus (***S of corpus callosum***)	M	Limbic
67	S_postcentral	***Postcentral sulcus***	S, L, P	Parietal
68	S_precentral-inf-part	Inferior part of the ***precentral sulcus***	S, A, L	Frontal
69	S_precentral-sup-part	Superior part of the ***precentral sulcus***	S, L	Frontal
70	S_suborbital	Suborbital sulcus (sulcus rostrales, supraorbital sulcus)	M	Frontal
71	S_subparietal	***Subparietal sulcus***	M	Parietal
72	S_temporal_inf	***Inferior temporal sulcus***	L, P, I	Temporal
73	S_temporal_sup	***Superior temporal sulcus*** (parallel sulcus)	S, A, L, P	Temporal
74	S_temporal_transverse	***Transverse temporal sulcus***	A, L	Temporal

Note. TA, Terminologia Anatomica; G_, gyral; S_, sulcal; S, superior, I, inferior; A, anterior; P, posterior; L, lateral; M, medial.

Reference:

Destrieux C, Fischl B, Dale A, Halgren E. 2010. Automatic parcellation of human cortical gyri and sulci using standard anatomical nomenclature. Neuroimage.15;53(1):1-15

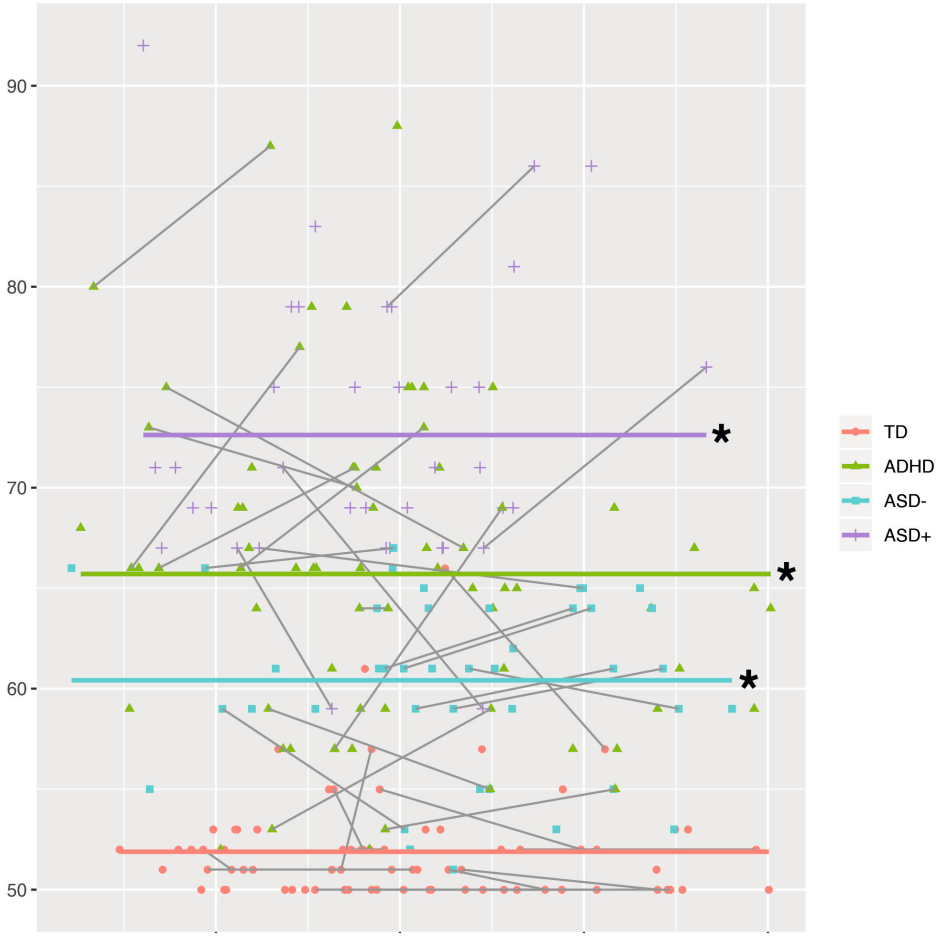

Figure S3. Attention problems across ASD and ADHD

Abbreviations: ADHD, Attention-Deficit/Hyperactivity Disorder; ASD, Autism Spectrum Disorder; ASD+, ASD with symptoms of ADHD (elevated attention problems); ASD-, ASD with fewer symptoms of ADHD; typically developing controls (TD). Note: Mixed model analysis of Attention Problems (CBCL T-scores, y-axis) by age in years (x-axis); *Asterisks indicate significant differences for all clinical (sub)groups from the TD group, as well as with each other.

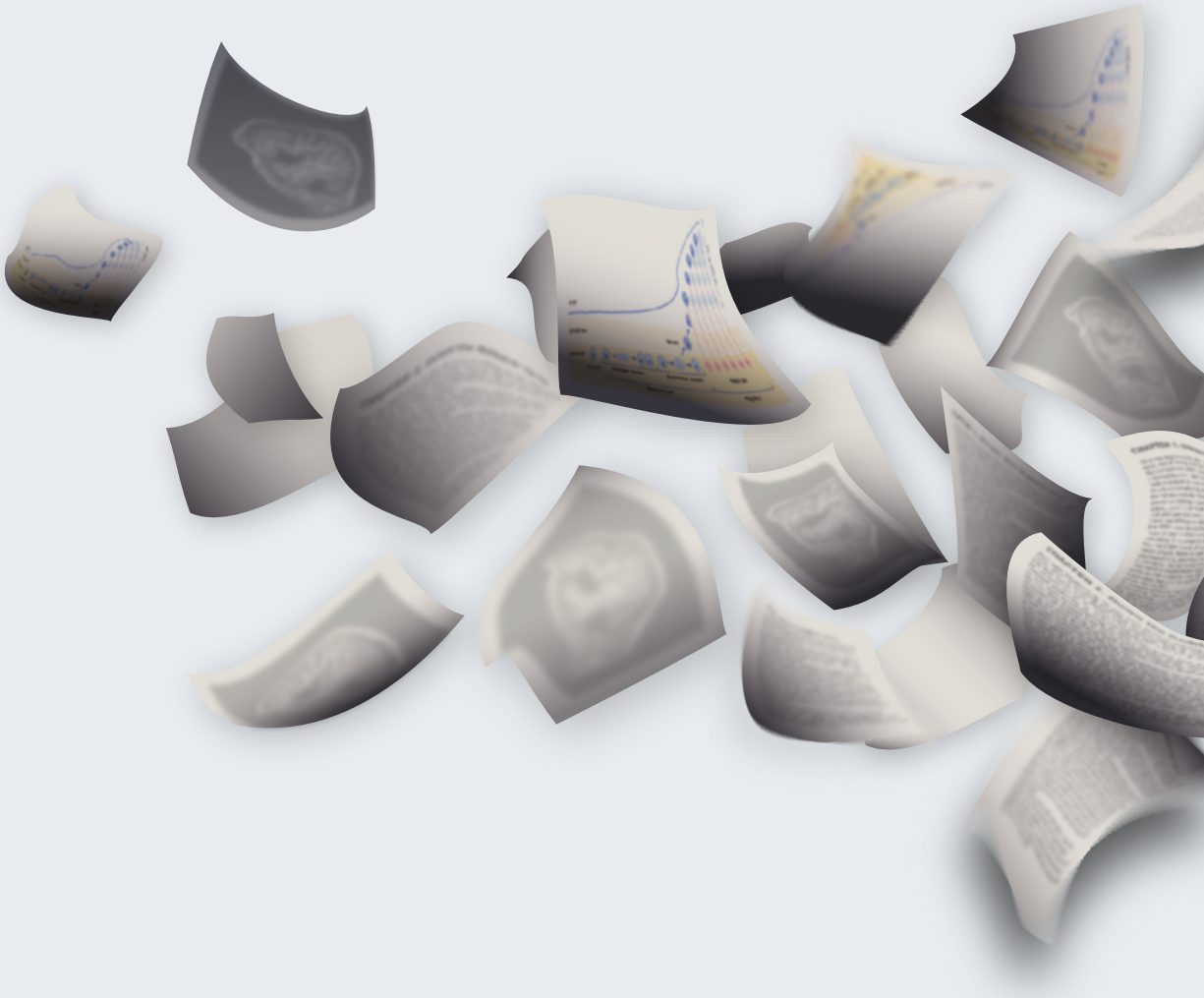

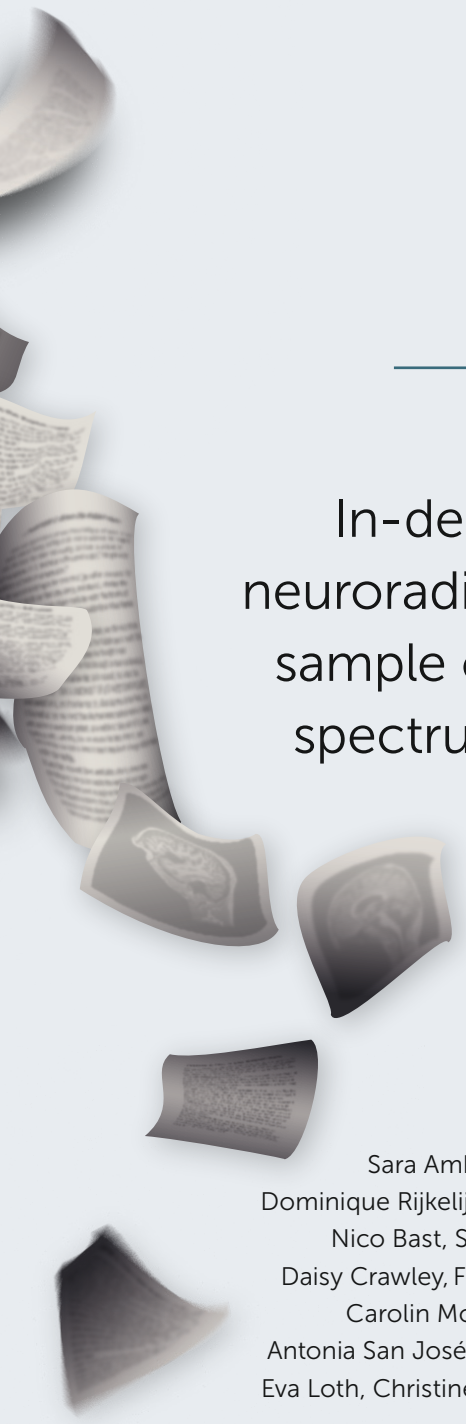

CHAPTER 5

In-depth characterization of neuroradiological findings in a large sample of individuals with autism spectrum disorder and controls

Sara Ambrosino, Hasnaa Elbendary, Maarten Lequin, Dominique Rijkelijkhuizen, Tobias Banaschewski, Simon Baron-Cohen, Nico Bast, Sarah Baumeister, Jan Buitelaar, Tony Charman, Daisy Crawley, Flavio Dell'Acqua, Hannah Hayward, Rosemary Holt, Carolin Moessnang, Antonio M. Persico, Roberto Sacco, Antonia San José Cáceres, Julian Tillmann, the EU-AIMS LEAP Group, Eva Loth, Christine Ecker, Bob Oranje, Declan Murphy & Sarah Durston

Neuroimage Clinical. 2022. 35:103118

ABSTRACT

Background: Autism Spectrum Disorder (ASD) is a group of neurodevelopmental conditions associated with quantitative differences in cortical and subcortical brain morphometry. Qualitative assessment of brain morphology provides complementary information on the possible underlying neurobiology. Studies of neuroradiological findings in ASD have rendered mixed results, and await robust replication in a sizable and independent sample.

Methods: We systematically and comprehensively assessed neuroradiological findings in a large cohort of participants with ASD and age-matched controls (total N=620, 348 ASD and 272 controls), including 70 participants with intellectual disability (47 ASD, 23 controls). We developed a comprehensive scoring system, augmented by standardized biometric measures.

Results: There was a higher incidence of neuroradiological findings in individuals with ASD (89.4%) compared to controls (83.8%, p=.042). Certain findings were also more common in ASD, in particular opercular abnormalities (OR 1.9, 95% CI 1.3-3.6) and mega cisterna magna (OR 2.4, 95% CI 1.4-4.0) reached significance when using FDR, whereas increases in macrocephaly (OR 2.0, 95% CI 1.2-3.2), cranial deformities (OR 2.4, 95% CI: 1.0-5.8), calvarian / dural thickening (OR 1.5, 95% CI 1.0-2.3), ventriculomegaly (OR 3.4, 95% CI 1.3-9.2), and hypoplasia of the corpus callosum (OR 2.7, 95% CI 1.1-6.3) did not survive this correction. Furthermore, neuroradiological findings were more likely to occur in isolation in controls, whereas they clustered more frequently in ASD. The incidence of neuroradiological findings was higher in individuals with mild intellectual disability (95.7%), irrespective of ASD diagnosis.

Conclusion: There was a subtly higher prevalence of neuroradiological findings in ASD, which did not appear to be specific to the condition. Individual findings or clusters of findings may point towards the neurodevelopmental mechanisms involved in individual cases. As such, clinical MRI assessments may be useful to guide further etiopathological (genetic) investigations, and are potentially valuable to fundamental ASD research.

INTRODUCTION

Autism Spectrum Disorder (ASD) is a group of highly heterogeneous neurodevelopmental conditions and is related to differences in brain structure (Chen et al. 2011; Ecker et al. 2015; van Rooij et al. 2018). To date, structural neuroimaging studies in ASD have largely focused on *quantitative* data, with the most common findings being changes in brain morphometry in multiple brain regions (particularly in the striatal and fronto-temporal areas), combined with an atypical trajectory of brain growth in autistic individuals (Ecker et al. 2015; van Rooij et al. 2018). Specifically, enlarged brain volume in young children with ASD is one of the most consistent findings in autism research (Courchesne 2002). The enlargement of the brain in ASD is accompanied by increased head circumference (Lainhart et al. 1997); it occurs during infancy and toddler years, while it is unclear whether it persists into later childhood and adolescence (Courchesne et al. 2001; Aylward et al. 2002). This suggests that the trajectory of early brain growth may be different in ASD (Courchesne et al. 2011). Later studies consistently found that early brain overgrowth in ASD differs between brain regions, mostly affecting frontal and temporal areas (Chen et al. 2011). Additionally, volumetric differences have been reported in numerous subcortical structures in ASD (Li et al. 2021), especially corpus callosum (Bellani et al. 2013; Frazier and Hardan 2009), caudate nucleus (Qiu et al. 2016), and cerebellum (D'Mello et al. 2015), although these findings are less consistent. Discrepancies between quantitative neuroimaging studies in ASD may be due to methodological differences, and, notably, to the established wide phenotypic diversity, both clinical and neurobiological (neuroanatomical), among individuals in the autism group. Assessment of neuroanatomical variation at an individual rather than just at a group level may therefore be more suited to understanding individual differences in the neurobiological underpinnings of the autism spectrum.

Qualitative evaluation of individual scans is the typical approach in clinical neuroradiological practice. Several studies have investigated qualitative neuroradiological findings in ASD (Piven et al. 1990; Zeegers et al. 2006; Boddaert et al. 2009; Vasa et al. 2012; Erbetta et al. 2014; Erbetta et al. 2015; Monterrey et al. 2017; Myers et al. 2020). However, these reported inconsistent prevalence and characteristics of brain abnormalities in ASD, and as such are inconclusive. As a consequence, brain magnetic resonance imaging (MRI) is currently *not* included as a clinical standard when investigating autism (Filipek et al. 2000), although it may be indicated in cases with co-morbid conditions or neurological signs and symptoms (Schaefer et al. 2013; Cooper et al. 2016). Most qualitative studies used relatively small samples (N=26 to 168) (Piven et al. 1990; Zeegers et al. 2006; Boddaert et al. 2009; Erbetta et al. 2014; Erbetta et al. 2015; Monterrey et al. 2017), and the methods were inconsistent between studies, with

different inclusion criteria (e.g., with or without individuals with intellectual disability, ID), and different definitions of 'neuroradiological findings'.

Abnormal findings on brain scans occur fairly commonly, in an estimated 20-25% of the general population (Katzman et al. 1999; Kim et al. 2002; Jansen et al. 2017). However, they are highly heterogenous, and specific findings are infrequent, meaning that while the chances of finding any abnormality might be relatively large, the chances of finding a particular one are not. Studies of neuroradiological findings in ASD have used different categorization systems, and sometimes did deliberately not report certain findings, as they were considered not to be clinically relevant, or a variation of normal brain anatomy (Boddaert et al. 2009). Inevitably, these different approaches have contributed to the heterogenous nature of the findings reported in the literature. Notably, there is *no* agreed-upon definition of what constitutes a deviation from normal: brain structure demonstrates a wide variation in shape and size, and the range of normality is to some degree arbitrary, and, for some structures, simply unknown (Osborn and Preece 2006).

Considering the intrinsic heterogeneity of the clinical and imaging data in ASD, and the relative infrequency of most reported neuroradiological findings as individual entities, studies using a comprehensive characterization of neuroradiological findings, and in large samples of participants, are essential. On a methodological level, it is important to screen brain scans explicitly for neuroradiological findings prior to quantitative analysis for a more comprehensive analytical and interpretative approach of brain morphology. Indeed, the presence of neuroanatomical defects often precludes certain imaging pipelines. Conventional neuroimaging studies in autism are therefore biased towards 'typical' brain anatomy. Furthermore, neuroradiological findings can point to developmental causal mechanisms (e.g., small cerebellum associated with pons hypoplasia, or with a posterior fossa cyst), and may therefore help elucidate the neurodevelopmental processes related to ASD.

Hence, this study aimed to systematically and comprehensively characterize qualitative brain MRI findings in a large sample of individuals with ASD, with and without ID, and matched controls. We capitalized on the large sample of the LEAP cohort (Charman et al. 2017; Loth et al. 2017), and constructed a comprehensive scoring system covering all brain structures and regions, permitting us to characterize in a standardized manner any visible morphological or signal abnormality identified on MRI scans including possible variants (neuroradiological findings), regardless of their clinical relevance. We expected to find an increased prevalence of structural brain abnormalities in individuals with ASD, especially in those with ID. Given the inconsistent literature, we were not able to derive specific hypotheses on which brain regions would be most affected.

MATERIAL AND METHODS

Participants

We included participants of the Longitudinal European Autism Project (LEAP). The study design, methodologies, and clinical characterization of the LEAP cohort have been described extensively in previous publications (Charman et al. 2017; Loth et al. 2017). In short, participants were recruited and assessed across six research centres in Europe: Institute of Psychiatry, Psychology and Neuroscience, King's College London (KCL, United Kingdom); Autism Research Centre, University of Cambridge (UCAM, United Kingdom); University Medical Centre Utrecht (UMCU, the Netherlands); Radboud University Nijmegen Medical Centre (RUNMC, the Netherlands); Central Institute of Mental Health (CIMH, Germany); and University Campus BioMedico (UCBM, Italy).

We included participants aged 6-30 years with intelligence quotient (IQ) in the typical range (75+), and participants with mild ID (IQ 50-74), aged 12-30 years. Females were purposely over-recruited in LEAP, with a targeted Male:Female ratio of 3:1, to enable better analysis of sex effects.

Inclusion criteria for the ASD sample were an existing clinical diagnosis of ASD according to the Diagnostic and Statistical Manual of Mental Disorders (DSM)-IV (American Psychiatric Association 1994), DSM-IV-TR (American Psychiatric Association 2000), DSM-5 (American Psychiatric Association 2013) or ICD-10 (World Health Organization 1993) criteria. In addition, the Autism Diagnostic Observation Schedule (ADOS, Lord et al. 2000; 2012) and the Autism Diagnostic Interview-Revised (ADI-R, Rutter et al. 2003) were administered to support the clinical diagnosis of ASD. However, individuals with a clinical diagnosis of ASD who did not reach cut-off on these instruments were not excluded, as clinical judgement was considered to be more stable and reliable than scores on individual diagnostic instruments per se (Charman and Gotham 2013).

Participants were purposely recruited in LEAP to enable in depth experimental characterization of biological markers including the use of complex methodologies (e.g., MRI), and yet preserve the widest possible clinical diversity of the autism spectrum. Therefore, individuals with very low IQ (< 50) were excluded in LEAP, while IQ ≥ 50 was included, and all psychiatric comorbidities were permitted, except for psychosis or bipolar disorder. Syndromic forms of intellectual disabilities were permitted. Participants on stable medication (minimum 8 weeks) at study entry and over the course of the study were included. Controls were excluded in case of any psychiatric morbidity. In all participants, additional exclusion criteria were uncorrectable hearing or visual impairments, any major neurological disorders, or the presence of metals in the body that precluded the MRI session (see Charman et al. 2017 for more details).

The study was approved by national and local independent ethics committees at each study site. Prior to testing, all participants, and/or their parents/legal guardian, provided written informed consent, as well as participants' assent.

MRI data acquisition and quality assessment

Participants were assessed between January 2014 and March 2017 (LEAP wave 1). We acquired structural MRI scans from 704 participants, including high-resolution three-dimensional T1-weighted (T1w) scans (n=695), T2-weighted (T2w) fast spin-echo scans (n=411), and fluid attenuated inversion recovery (FLAIR) scans (n=357). Scans were acquired on 3T scanners from different manufacturers (Siemens, General Electrics, Philips) across the six participating centers using the same acquisition protocol. The scanning parameters for the T1w, T2w, and FLAIR scans at each site are provided in Appendix A (Table A1).

All scans were assessed by a team of three raters based at the UMCU: one senior pediatric neuroradiologist (ML) with broad expertise in brain congenital anomalies, and two pediatric neurologists experienced in brain development and structural MRI assessment (SA, HE). Specifically, each scan was assessed by SA (rater 1), while the scans of 218/620 (35.2%) participants were independently assessed by HE (rater 2). Additionally, the scans of 104/620 (16.8%) participants were assessed by the neuroradiologist (ML). Agreements between the raters were between 92-98% (see details below).

Scans were coded in order to ensure rater blindness to study site, participant identity and diagnosis at all times during analysis. However, raters were aware of the participants' age at the time of scan to inform the interpretation of brain structure growth and maturation (e.g., myelination).

First, we evaluated the acquisition symmetry and overall quality of each scan using a 0 to 5 rating scale (5 for the best quality scan). In case of multiple acquisitions of the same sequence, the best quality one was carried forward for analysis.

We excluded 80 participants for insufficient data quality (T1w quality < 3) due to missing T1w (n=9), or to the presence of significant movement artifacts, primarily in the ASD group (n=71; 58 ASD, 13 controls; p<.001). We additionally excluded 4 participants due to incomplete demographic information.

Eventually, we retained a final sample of 620 individuals (348 ASD, 272 controls), including 70 participants (11.3%) with mild ID (47 ID-ASD, 23 ID-controls). The details of participant characteristics included in this study are provided in Table 1. The ASD and control groups were matched for age, but not for sex or IQ. The ASD group included more males (p=.048) and had lower full-scale IQ (difference 5.6 points; p<.001). The ID

group included more males (p=.022) and had older participants (p=.002) compared to the group of participants with IQ in the typical range (details provided in Table 2). There were no between-groups differences in the distribution of the available T1w, T2w and FLAIR scans (p=.082).

Table 1. Demographic and clinical characteristics of the sample

		ASD n=348	**Controls** n=272	**Group differences***
Sex	n male - female	252 - 96	176 - 96	**.048**
Age at scan	Years M (SD)	17.6 (5.6)	17.5 (5.8)	.935
ID	n ID - typical IQ	47 - 301	23 - 249	**.049**
Total IQ	M (SD)	99.4 (19.0)	105.0 (18.0)	**< .001**
ADI-R	Social M (SD)	16.3 (6.9)	-	-
	Communication M (SD)	12.9 (5.7)	-	-
	RRB M (SD)	4.3 (2.7)	-	-
ADOS	Social M (SD)	5.9 (2.6)	-	-
	RRB M (SD)	4.7 (2.8)	-	-
	Total M (SD)	5.2 (2.7)	-	-
Scans per participant	n 1	89	91	.082
	n 2	115	86	
	n 3	144	95	
Scans in Total	n	751	548	-

Abbreviations: ASD, autism spectrum disorder; n, number; M, mean; SD, standard deviation; IQ, intelligence quotient; ID, intellectual disability; ADI-R, Autism Diagnostic Interview- Revised; RRB, restricted and repetitive behaviors; ADOS, Autism Diagnostic Observation Scale.
Note: *X^2 for sex and number of scans acquired per person; t test for age and total IQ

In the final, high-quality sample, T1-weighted images were available for 100% of the participants (620 scans); T2-weighted and FLAIR scans were available for 369 (59.5%) and 310 (50%) participants respectively, resulting in a total of 1299 scans. The overall visual quality of the included scans was 4.3/5, and did not differ between the ASD and control group (p=.082).

Brain MRI assessment

Special attention was paid to abnormalities previously described in the literature on neuroradiological findings in ASD (Piven et al. 1990; Taber et al. 2004; Zeegers et al. 2006; Boddaert et al. 2009; Vasa et al. 2012; Erbetta et al. 2014), or in related neuropsychiatric disorders (Nopoulos et al. 2000; Vasa et al. 2012; Sommer et al. 2013), and in healthy adult and pediatric populations (Katzman et al. 1999; Kim et al. 2002; Jansen et al. 2017). But primarily, our aim was to capture all potentially relevant

neuroradiological findings. Arguably, some findings may not be clinically relevant to ASD, yet they may still be scientifically relevant, as they may point to neurodevelopmental mechanisms and provide information on the biological pathways involved. Therefore, we constructed a systematic and comprehensive scoring system (see Appendix B online, doi: 10.1016/j.nicl.2022.103118), covering all brain structures and regions, and characterizing all visibly detectable neuroradiological abnormalities (brain lesions, malformations, and anatomical variants). To enable quantification, we categorized our extensive assessment data into ten categories as follows: anomalies of 1) skull, whole brain, and brain lobes, 2) cerebral cortex, 3) hippocampi, 4) white matter, 5) Virchow-Robin (VR) perivascular spaces, 6) basal ganglia, 7) posterior fossa, 8) cerebral spinal fluid spaces, 9) midline, and 10) other.

Further, we compared the assessments performed by any two raters in each category (on 276 participants, for a total of 2760 observations) using a binary system. Readings were rated as '0' in case of congruent descriptions (both readers rated the category as normal, or described the same type of abnormality), or '1' in case of substantial differences. The agreement between rater 1 and 2, performed on 172 participants, was 92%; the agreement between rater 1 and rater 3 (an experienced neuroradiologist), performed on 57 participants, was 98%. In case of disagreement (a rating of '1'), consensus was reached by discussion.

Finally, we acquired multiple biometric measures from the MR-scan, using standardized methods and age-sex normed values. This permitted us to further characterize specific brain features and to objectively quantify anomalies, while accounting for sex and age effects.

Specifically, we acquired metrics of the whole head shape and size (Allanson et al. 2009; Franco et al. 2013), of the anterior and posterior inter-opercular distances (Chen et al. 1995; Chen et al. 1996), of the corpus callosum (length and thickness) (Garel et al. 2011; Karakaş et al. 2011), and of the lateral ventricles (Sari et al. 2015). Further, we measured perivascular VR spaces (Heier et al. 1989), pineal gland cysts, and the length of the cavum septum pellucidum and cavum vergae (Dremmen et al. 2019) when present. In the posterior fossa, we measured the width of cisterna magna (Limperopoulos et al. 2009), and the extent of tonsillar ectopia in case of Chiari malformation type 1 (Baisden 2012).

All measures were acquired on T1w sequences using the submillimeter caliper of MedINRIA medical image visualization software (https://med.inria.fr). For further details on the measurement's methods and standard references, we refer to Appendix C. Notably, this data is distinct and provides complementary information to measures obtained using standard automated imaging pipelines such as FreeSurfer (Fischl 2012).

In fact, some of these measures, such as the distinct dimensions of the corpus callosum, may be related to different neurodevelopmental mechanisms (De León Reyes et al. 2020).

Statistical analysis

We conducted all statistical analyses using SPSS statistical package v26. We used Chi-squared or Fisher's Exact Test, as appropriate, to analyze differences in the observed MRI findings between diagnostic groups (ASD vs controls), and between individuals with and without ID. Odds ratios [OR] were calculated to estimate the strength of the association between neuroradiological findings and ASD or ID. We applied a false discovery rate (FDR) correction (Benjamini and Hochberg 1995) to control for multiple comparisons, using a significance threshold of $p < .05$. Notably, previous studies on neuroradiological findings in ASD have reported uncorrected results (e.g., Erbetta et al. 2014) due to their small number of comparisons. Hence, to enable better comparisons with previous studies, and in consideration of our novel, more rigorous assessment of the scans, we report both FDR-corrected and uncorrected results here.

Further, we explored the possibility of clustering. We compared the number of neuroradiological findings per individual (clusters) between groups. Then, we investigated the distribution of each type of finding within the clusters using Chi-square goodness of fit test. Post-hoc analyses were performed using adjusted standardized residuals for chi-square tests (Beasley and Schumacker 1995). Finally, we performed pairwise correlations of the frequency distributions of neuroradiological findings in the sample, Bonferroni-corrected for multiple comparisons, and compared these correlations between groups.

RESULTS

Complete demographic and high-quality brain MRI scans were available from 620 participants, aged from 6.8 to 30.6 years (Table 1). Table 2 summarizes the observed neuroradiological findings and between-group differences. Examples of common findings, and of some rarer anomalies encountered in our dataset, are depicted in Figure 1.

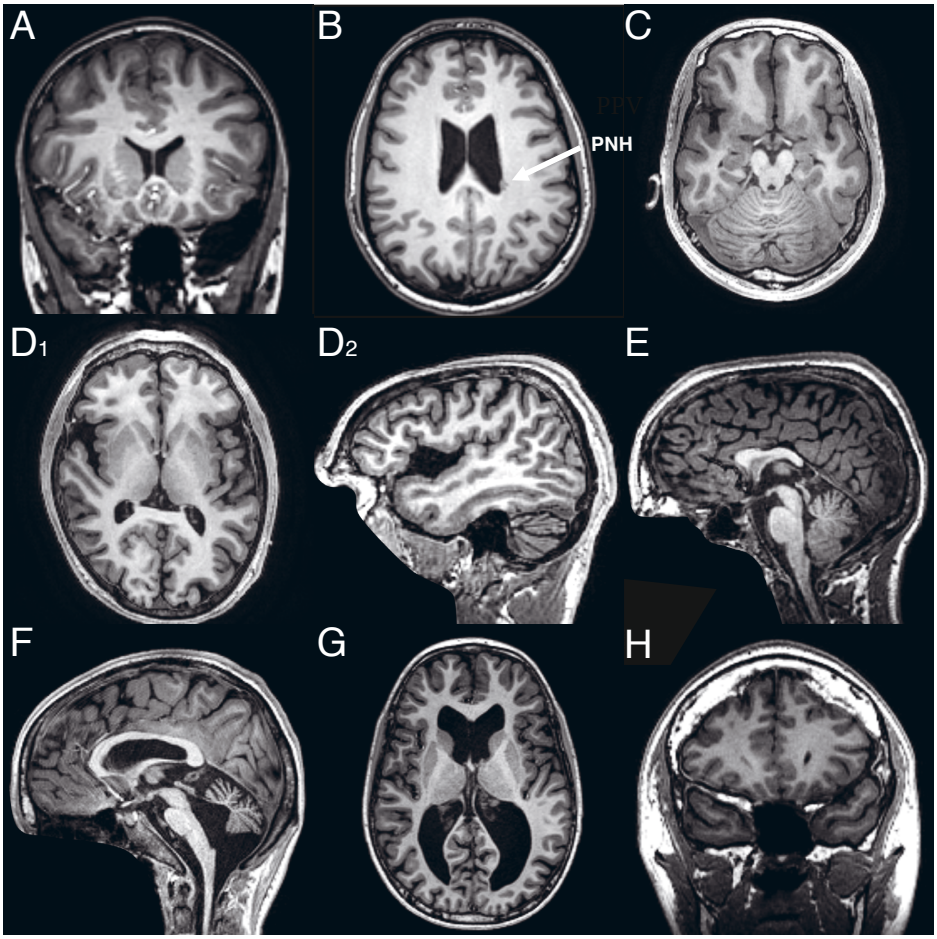

Figure 1. Examples of neuroradiological findings

Panel A: arachnoid cyst in the left temporal pole; Panel B: periventricular nodular heterotopia (PNH, arrow); Panel C: simplified gyral pattern; Panel D_{1-2}: opercular abnormality; Panel E: partial agenesis of the corpus callosum; Panel F: Dandy-Walker variant; Panel G: ventriculomegaly; Panel H: thickening of the dura mater.

Table 2. Neuroradiological findings in the sample

	Total N=620	**ASD** n=348	**Controls** n=272	**Group diff***	**Typical IQ** n=550	**ID** n=70	**IQ diff***
Age (years M (SD))	17.6 (5.7)	17.6 (5.6)	17.5 (5.8)	ns	17.4 (5.8)	18.9 (4.4)	**.002**
Sex (n male – female)	428 - 192	252 - 96	176 - 96	**.048**	388 - 162	40 - 30	**.022**
Head, brain, and lobes							
Cranial deformity All	28 (4.5%)	21 (6.0%)	7 (2.6%)	.039	23 (4.2%)	5 (7.1%)	ns
Plagiocephaly	9 (1.5%)	6 (1.7%)	3 (1.1%)	ns	7 (1.3%)	2 (2.9%)	ns
Hyperbrachycephaly	9 (1.5%)	8 (2.3%)	1 (0.4%)	ns	8 (1.5%)	2 (2.9%)	ns
Hyperdolichocephaly	10 (1.6%)	7 (2.0%)	3 (1.1%)	ns	8 (1.5%)	1 (1.4%)	ns
Cranial volume All	133 (21.5%)	87 (25.0%)	46 (16.9%)	.018	115 (20.9%)	18 (25.7%)	ns
Microcephaly	47 (7.6%)	27 (7.8%)	20 (7.4%)	ns	36 6.5%)	11 (15.7%)	**.007**
Macrocephaly	86 (13.9%)	60 (17.2%)	26 (9.6%)	.007	79 (14.4%)	7 (10%)	ns
Calvarian / dural thickening	126 (20.3%)	81 (23.3%)	45 (16.5%)	.039	99 (18.0%)	27 (38.6%)	**< .001**
Opercular abnormality Bi/unilateral	229 (36.9%)	150/0 (43.1%)	77/2 (29.0%)	**< .001**	191 (34.7%)	38 (54.3%)	**.001**
Cerebral cortex							
Malformations All	8 (1.3%)	7 (2.0%)	1 (0.4%)	ns	5 (0.9%)	3 (4.3%)	ns
Periventricular nodular heterotopia	3 (0.5%)	2 (0.6%)	1 (0.4%)	ns	2 (0.4%)	1 (1.4%)	ns
Simplified gyral pattern	2 (0.3%)	2 (0.6%)	0 (0%)	ns	2 (0.4%)	0 (0%)	ns
Cortical dysplasia	3 (0.5%)	3 (0.9%)	0 (0%)	ns	1 (0.2%)	2 (2.9%)	ns
Lesion	3 (0.5%)	2 (0.6%)	1 (0.4%)	ns	2 (0.4%)	1 (1.4%)	ns
Hippocampi							
Lesion	2 (0.3%)	1 (0.3%)	1 (0.4%)	ns	2 (0.4%)	0 (0%)	ns
White matter							
Lesion	15 (2.4%)	10 (2.9%)	5 (1.8%)	ns	12 (2.2%)	3 (4.3%)	ns

Table 2. Continued

	Total N=620	**ASD** n=348	**Controls** n=272	**Group diff***	**Typical IQ** n=550	**ID** n=70	**IQ diff***
Virchow-Robin spaces							
Dilation All	338 (54.5%)	189 (54.3%)	149 (54.8%)	ns	302 (54.9%)	36 (51.4%)	ns
Deep white matter / subcortical	133 (21.5%)	66 (19.0%)	67 (24.6%)	ns	120 (21.8%)	13 (18.6%)	ns
Lenticulo-striate	300 (48.4%)	171 (49.1%)	129 (47.4%)	ns	268 (48.7%)	32 (45.7%)	ns
Basal ganglia	0 (0%)	0 (0%)	0 (0%)	ns	0 (0%)	0 (0%)	ns
Posterior fossa							
All	115 (18.5%)	80 (23.0%)	35 (12.9%)	**.002**	96 (17.5%)	19 (27.1%)	ns
Dandy-Walker complex	106 (17.1%)	73 (21.0%)	33 (12.1%)	.004	90 (16.4%)	16 (22.9%)	ns
Mega-cisterna magna	82 (13.2%)	60 (17.2%)	22 (8.1%)	**.001**	76 (13.8%)	6 (8.6%)	ns
Dandy-Walker variant	3 (0.5%)	1 (0.3%)	2 (0.7%)	ns	0 (0%)	3 (4.3%)	ns
Blake pouch cyst	1 (0.2%)	1 (0.3%)	0 (0%)	ns	1(0.2%)	0 (0%)	ns
Arachnoid cyst	13 (2.1%)	6 (1.7%)	7 (2.6%)	ns	12 (2.2%)	1 (1.4%)	ns
Vermian hypoplasia	7 (1.1%)	5 (1.4%)	2 (0.7%)	ns	1 (0.2%)	6 (8.6%)	**< .001**
Chiari type 1 malformation	7 (1.1%)	5 (1.4%)	2 (0.7%)	ns	5 (0.9%)	2 (2.9%)	ns
Lesion	1 (0.2%)	1 (0.3%)	0 (0%)	ns	1 (0.2%)	0 (0%)	ns
Vascular anomaly	1 (0.2%)	1 (0.3%)	0 (0%)	ns	0 (0%)	1 (1.4%)	ns
CSF spaces							
Ventriculomegaly	26 (4.2%)	21 (6.0%)	5 (1.8%)	.010	22 (4.0%)	4 (5.7%)	ns
Cavum septum pellucidum / vergae	12 (1.9%)	4 (1.1%)	8 (2.9%)	ns	10 (1.8%)	2 (2.9%)	ns
Choroid plexus cysts	3 (0.5%)	2 (0.6%)	1 (0.4%)	ns	1 (0.2%)	2 (2.9%)	ns
Subarachnoid spaces Enlargement	57 (9.2%)	34 (9.8%)	23 (2.9%)	ns	60 (10.9%)	19 (27.1%)	**< .001**
Calcifications	2 (0.3%)	0 (0%)	2 (0.7%)	ns	2 (0.4%)	0 (0%)	ns

Table 2. Continued

	Total N=620	**ASD** n=348	**Controls** n=272	**Group diff***	**Typical IQ** n=550	**ID** n=70	**IQ diff***
Midline							
CC Hypoplasia All	30 (4.8%)	23 (6.6%)	7 (2.6%)	.020	17 (3.1%)	13 (18.6%)	**< .001**
CC thin	10 (1.6%)	7 (2.0%)	3 (1.1%)	ns	5 (0.9%)	5 (7.1%)	**< .001**
CC short	12 (1.9%)	8 (2.3%)	4 (1.5%)	ns	7 (1.3%)	5 (7.1%)	**.001**
CC short and thin	4 (0.6%)	4 (1%)	0 (0%)	ns	2 (0.4%)	2 (2.9%)	ns
CC partial agenesis	1 (0.2%)	1 (0.3%)	0 (0%)	ns	0 (0%)	1 (1.4%)	ns
CC focal hypoplasia	4 (0.6%)	4 (1.1%)	0 (0%)	ns	3 (0.5%)	1 (1.4%)	ns
Pineal gland cyst All	90 (14.5%)	54 (15.5%)	36 (13.2%)	ns	76 (13.8%)	14 (20%)	ns
≥ 10 mm	14 (2.3%)	8 (2.3%)	6 (2.2%)	ns	9 (1.6%)	5 (7.1%)	.015
< 10 mm	76 (12.3%)	46 (13.2%)	30 (11.0%)	ns	67 (12.2%)	9 (12.9%)	ns
Other							
Vascular anomalies All	10 (1.6%)	7 (2.0%)	3 (1.1%)	ns	10 (1.8%)	2 (2.9%)	ns
DVA	8 (1.3%)	6 (1.7%)	2 (0.7%)	ns	6 (1.1%)	2 (2.9%)	ns
Kissing carotids	1 (0.2%)	0 (0%)	1 (0.4%)	ns	1 (0.2%)	0 (0%)	ns
Capillary teleangectasia	1 (0.2%)	1 (0.3%)	0 (0%)	ns	1 (0.2%)	0 (0%)	ns
Cysts All	8 (1.3%)	5 (1.4%)	3 (1.1%)	ns	7 (1.3%)	1 (1.4%)	ns
Arachnoid**	3 (0.5%)	2 (0.6%)	1 (0.4%)	ns	3 (0.5%)	0 (0%)	ns
Poroencefalic	3 (0.5%)	2 (0.6%)	1 (0.4%)	ns	2 (0.4%)	1 (1.4%)	ns
Neuroglial	1 (0.2%)	0 (0%)	1 (0.4%)	ns	1 (0.2%)	0 (0%)	ns
Inclusion	1 (0.2%)	1 (0.3%)	0 (0%)	ns	1 (0.2%)	0 (0%)	ns

Abbreviations: ASD, autism spectrum disorder; N or n, number; M, mean; SD, standard deviation; ns, not significant; IQ, intelligence quotient; ID, intellectual disability; CSF, cerebral spinal fluid; CC, corpus callosum; DVA, developmental venous anomalies.

Note: *X^2 or Fisher's Exact Test, as appropriate, for testing for groups differences on ASD and ID (raw p-values; results reaching significance when controlling FDR are indicated in bold). **Arachnoid cysts in locations other than the posterior fossa.

Types of neuroradiological findings

Most participants (539/620, 86.9%) had at least one neuroradiological finding, including 331/348 (89.4%) participants with ASD, 95.7% of participants with mild ID (44/47 ID-ASD, 23/23 ID-controls), and 205/249 (82.3%) typically developing controls. Participants with ASD, and participants with mild ID irrespective of ASD diagnosis, were more likely to have a neuroradiological finding compared to their respective controls (X^2_1 =4.1, p=.042 and X^2_1 =5.3, p=.021, respectively). There was no difference in the frequency of total findings between males and females. Preliminary analysis on sex differences is provided in Appendix D. Among a few other results, we found a higher incidence of mega cisterna magna in males (X^2_1 = 17.7; p<.001, *FDRp*<.001; OR 4.2, 95% CI 2.0-8.5) (Table D.1).

In ASD, we found a higher incidence of opercular abnormalities (X^2_1 =12.9, p<.001, FDR-adjusted value of *p (FDRp)*=.017; OR 1.9, 95% CI 1.3-2.6), and mega cisterna magna (X^2_1 =11.1, p=.001, *FDRp*=.026; OR 2.4, 95% CI 1.4-3.9), compared to controls (Table 2). Given the sex mismatch between diagnostic groups in our research population (Table 1), and the sex difference on mega cisterna magna (Table D.1), we repeated the ASD analysis on mega cisterna magna in a male only subgroup (n=428), which yielded consistent results (p=.009).

We additionally found a higher incidence in ASD of cranial deformities (X^2_1 =4.2, p=.039; OR 2.4, 95% CI 1.0-5.8), macrocephaly (X^2_1 =7.5, p=.006; OR 2.0, 95% CI 1.2-3.2), calvarian / dural thickening (X^2_1 =4.3, p=.039; OR 1.5, 95% CI 1.0-2.3), ventriculomegaly (enlarged ventricles; (X^2_1 =6.7, p=.010; OR 3.4, 95% CI 1.3-9.2), and hypoplasia of the corpus callosum (X^2_1 =5.4, p=.020; OR 2.7, 95% CI 1.1-6.3), although these results failed to reach significance after correction for multiple comparison (Table 2). All these differences did not hold in the subsample of participants with mild ID (i.e. when comparing ID-ASD to ID-controls).

Instead, participants with mild ID had a higher incidence of microcephaly (X^2_1 =7.5, p=.006, *FDRp*=.042; OR 2.7, 95% CI 1.3-5.5), calvarian / dural thickening (X^2_1 =16.2, p<.001, *FDRp*=.001; OR 2.9, 95% CI 1.7-4.9), opercular abnormalities (X^2_1 =10.2, p=.001, *FDRp*=.011; OR 2.2, 95% CI 1.4-3.7), vermian hypoplasia (X^2_1 =39.2, p<.001, *FDRp*<.001; OR 51.5, 95% CI 6.1-434.3), enlargement of the subarachnoid spaces (X^2_1 =11.0, p=.001, *FDRp*=.008; OR 3.0, 95% CI 1.5-5.7), and hypoplasia of the corpus callosum (X^2_1 =32.3, p<.001, *FDRp*=.002; OR 7.2, 95% CI 3.3-15.5) compared to participants with IQ in the typical range (ASD and controls combined), see table 2.

Clustering of neuroradiological findings

The number of neuroradiological findings per individual ranged from 0 to 8, regardless of clinical diagnosis. In more than half of cases, any single neuroradiological finding was accompanied by others: of the 620 participants, 81 (13.1%) had no findings at

all ('cluster 0'), 189 (30.5%) had one finding ('cluster 1'), 142 (22.9%) had two findings ('cluster 2'), 119 (19.2%) had three findings ('cluster 3'), and 89 (14.4%) had four or more findings ('cluster 4+').

The number of neuroradiological findings per person differed between ASD and controls (X^2_3 =25.4, p<.001). Post-hoc analysis of the adjusted standardized residuals showed that individuals with 0 or 1 findings were more prevalent in the control group (p<.001), the number of individuals with 2-3 neuroradiological findings did not differ between groups, while individuals with 4 or more neuroradiological findings were more prevalent in the ASD group than in controls (p=.029), see figure 2. These differences were not present in the subsample of participants with mild ID.

Similarly, the number of neuroradiological findings per person differed between individuals with mild ID and individuals with typical IQ, irrespective of ASD diagnosis (X^2_3 =25.0, p<.001). Post-hoc analysis showed that individuals with 0 or 1 finding were more prevalent in the control group (p=.001), the number of individuals with 2-3 neuroradiological findings did not differ between the groups, and individuals with 4+ neuroradiological findings were more prevalent in mild ID than in participants with typical IQ (p=.001). These group differences were not present in the subsample of individuals with ASD (i.e. when comparing ID-ASD vs ASD with typical IQ).

Types by number of neuroradiological findings

We used Chi-square goodness of fit test and post-hoc analyses to explore if there was a difference in the frequency of different types of neuroradiological findings across the (1 to 4+) clusters. We found that macrocephaly, the mega cisterna magna, vermian hypoplasia, enlargement of the subarachnoid spaces and of lateral ventricles were more prevalent in the 4+ cluster (all p_s<.001). In other words, these findings were commonly accompanied by three or more other findings. There were no differences between diagnostic groups in the distribution of any neuroradiological finding within the (1 to 4+) clusters, with the exception of the Virchow-Robin (VR) perivascular spaces: post-hoc analyses showed that the VR spaces were more prevalent (p=.001) in cluster 1 in controls (i.e., they occurred in isolation), whereas they were more prevalent in cluster 4+ (p=.012) in ASD.

Next, we investigated the correlation between each type of neuroradiological finding in the whole group. Due to the large number of comparisons, here we applied Bonferroni correction (adjusted p value=.0002). Results are summarized in Appendix D (Table D.2). We found that macrocephaly was associated with calvarian / dural thickening and with ventriculomegaly, and that the microcephaly was associated with hypoplasia of the corpus callosum. We also found significant correlations between cortical malformations and cystic or WM abnormalities (all p_s<.0001).

Finally, we tested whether correlation coefficients differed between the groups. We found no differences in these correlations in ASD, nor in individuals with mild ID, compared to controls.

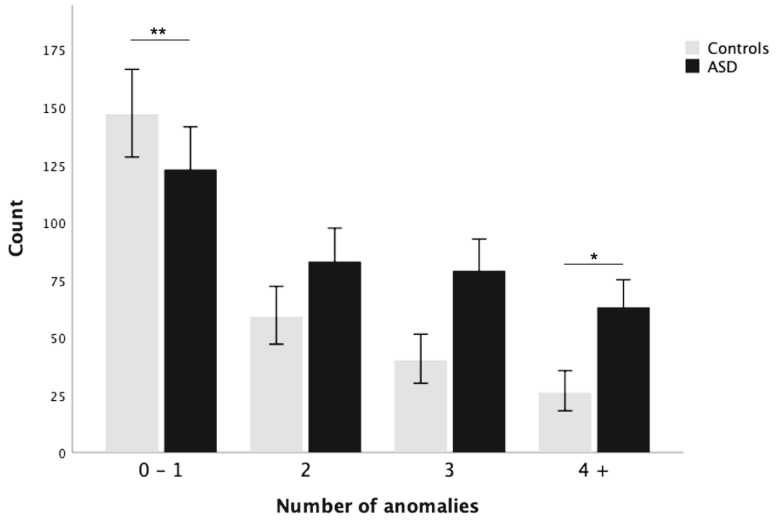

Figure 2. Clustering of neuroradiological findings in ASD vs controls

The number of neuroradiological findings per person differed between ASD and controls (p<.001). Asterisks mark significant group differences from post-hoc analysis: individuals with 0-1 neuroradiological findings were more prevalent in the control group (**p<.001), individuals with 2-3 findings did not differ between groups, individuals with 4 or more findings were significantly more prevalent in ASD compared to controls (*p =.029).

DISCUSSION

We performed a large study (N=620) investigating neuroradiological findings in ASD. We used a systematic and comprehensive scoring system of brain findings on MRI, augmented with standardized biometric measures of brain features. We found that neuroradiological findings were more common and clustered more frequently in ASD, although this did not appear to be specific to the condition.

The incidence of brain MRI findings in ASD in our study was higher (89.4%) than in previous reports, which ranged from 11% (Vasa et al. 2012), 40-54% (Piven et al. 1990; Taber et al. 2004; Zeegers et al. 2006; Boddaert et al. 2009: Erbetta et al. 2014, 2015; Myers et al. 2020), to 68% (Monterrey et al. 2017) in ASD. This is likely related to several factors, such as the inclusion of participants with ID in our study (as there were more findings in ID-participants compared to participants with typical IQ), and

our acquisition of extensive assessment data, which permitted us to report on a wide range of anatomical features, from common to more rare variants in brain anatomy.

The presence of specific neuroradiological markers may hint at the neurodevelopmental processes involved. For example, we found a higher incidence of mega cisterna magna in ASD, consistent with previous neuroradiologic studies (Erbetta et al. 2014; Erbetta et al. 2015). Mega cisterna magna is a cystic malformation of the posterior fossa characterized by a focal enlargement of the subarachnoid space located below the cerebellum (cerebellomedullary cistern), with normal fourth ventricle and cerebellar structures (Whitney et al. 2013; Bosenami et al. 2015). Mega cisterna magna is considered to be on the mild end of the Dandy-Walker (DW) complex, a wide spectrum of congenital abnormalities sharing overlapping radiological features, a similar clinical spectrum, and related developmental origins (Barkovich et al. 1989). Embryologically, the DW complex is thought to be related to insults predominantly involving the developing cerebellar hemispheres (leading to the DW variant, Fig. 1 panel F), or the developing fourth ventricle (associated to the mega cisterna magna), or both (leading to the most severe DW malformation) (Barkovich et al. 1989). Interestingly, in our study, we found a higher incidence of the DW complex as a whole in the autism group, largely driven by the presence of mega cisterna magna. This implicates the developmental period when the fourth ventricle develops, up to 26 weeks' gestation (Brocklehurst 1969), in ASD.

Prior studies on cerebellar morphometry provided variable results on the direction and pattern of differences observed in ASD (Brambilla et al. 2003; Donovan & Basson 2017). Our study reflects such variability as well, as by definition the DW variant and malformation are characterized by varying degrees of malformation of the cerebellar regions, whereas in mega cisterna magna these structures are visually intact (Barkovich et al. 1989). The qualitative assessment of posterior fossa as conducted in our study may be able to help to stratify ASD into subtypes based on cerebellar anomalies at a macroscopic level.

Consistent with previous volumetric studies of the corpus callosum (CC) in ASD (reviewed by Bellani et al. 2013), we found a higher incidence of hypoplasia of the CC in the autism group, although this result did not reach significance when controlling FDR. The CC is the largest commissural white matter tract, involved in the integration of high-order functions and sensory information between the two hemispheres. Anatomically, the CC has four distinct segments (rostrum, genu, body and splenium), all identifiable by 20 weeks post-conception (Edwards et al. 2014). In this study, we extended the identification of the cases with callosal hypoplasia by assessing the presence of these segments, and determining whether the hypoplasia was primarily related to thinning and / or shortening of the CC. We found no between-group differences in the distinct forms of callosal hypoplasia. However, we identified one case with partial agenesis

of the CC (Fig. 1 panel E), characterized by markedly reduced length as a result of missing segments, primarily the splenium. This may result from an early perturbation of callosal development preceding the 20th week of gestation. The remaining cases of callosal hypoplasia are more likely related to insults later in gestation, leading to a reduction in size of the fully formed CC (De León Reyes et al. 2020). The development of the CC is regulated through a complex interplay of genes (see Edwards et al. 2014 for a comprehensive review), a number of which have been already linked to ASD (e.g., 17p13.3 which contains the *LIS1* gene, or 11q13.4 for the *DHCR7* gene; Edwards et al. 2014).

Additionally, we found a higher incidence of qualitative abnormalities of the opercular formation in ASD (Fig. 1 panel $D_{1\text{-}2}$). This finding is unprecedented in ASD research, and is likely due to the fact that we assessed the opercular region explicitly, and objectified our findings by measuring inter-opercular distances. Our result converges with previous automated quantitative studies that repeatedly identified cortical morphometric changes predominantly in fronto-temporal and fronto-parietal regions in ASD (Hadjikhani et al. 2006; Hyde et al. 2010; Ecker et al. 2013). Recently, differences in fronto-temporal cortical thickness were also reported in a large sample derived from the same cohort as the present study (LEAP) (Ecker et al. 2022). Our finding also aligns with a previous report of cortical shape abnormalities specifically in the opercular region in ASD (Nordahl et al. 2007). Investigation of the link between qualitative anomalies of the opercular regions and morphometric changes in the pertaining cortical areas is a fascinating and open area of research.

The operculum is a large cortical structure encompassing parts of the frontal, temporal and parietal lobes, which together cover the insula. Functionally, the operculum is involved in social, sensory, language, and cognitive processing (Chen et al. 1996; Nordahl et al. 2007). Problems with these abilities are some of the core symptoms of ASD (American Psychiatric Association 2013). The open operculum, resulting in an exposed insula, is not merely due to a volumetric reduction of frontal, temporal or parietal regions, but may be related to a disturbed developmental process, starting around 20-22 weeks' gestation period and usually proceeding in a clear and well-orchestrated manner, known as opercularization. Therefore, our refined anatomical characterization of the opercular region may provide clues to the neurodevelopmental mechanisms involved.

In addition to micro- and macrocephaly, we found a few rare malformations of cortical development (MCD) in ASD, namely periventricular nodular heterotopia (PNH, n=2, Fig. 1 panel B), diffuse simplified gyral pattern (n=2, see Fig. 1 panel C), and cortical dysplasia (n=3). Although there were no between-group differences due to the low incidence of these malformations, they are each suggestive of disrupted specific phases of cortical development, possibly related to specific genetic mutations. For

example, PNH are disorders of the last phase of neuronal migration associated to, among others, *FLNA* or *ARFGEF2* mutations. Identification of genes associated with MCD (Barkovich et al. 2012; Desikan and Barkovich 2016) in these participants may link between neuroradiological findings to neurodevelopment, and potentially to individual clinical profiles.

In sum, our study shows high prevalence of specific brain anomalies in ASD that may act as markers of neurodevelopmental processes involved. Furthermore, our results showed that neuroradiological findings were more likely to occur in isolation in controls, whereas they were more commonly associated with multiple findings in ASD. This converges with another recent study of cortical morphometry in the LEAP cohort, which suggested that the total amount of widespread deviation from typical brain anatomy is a better predictor of the clinical outcome in ASD than changes in any specific brain region per se (Pretzsch et al. 2022). Speculatively, these findings suggest a possible 'cumulative effect' of neurodevelopmental events in developing ASD.

Plausibly, some neuroradiological findings may cluster due to shared biological or mechanical factors (i.e., tissue viscoelasticity) which modulate the whole brain and shape of the neurocranium (Bilston 2011). Our study confirms this hypothesis, as we indeed found that there were anomalies that tended to cluster together. For example, we found correlations between macrocephaly and ventriculomegaly, where progressive enlargement of intracranial ventricular system may have resulted in an abnormally large head (Orru' et al. 2018). We also found an association between macrocephaly and thickening of cranial bones, hinting at another possible mechanism for the increase in head size frequently observed in ASD (Lainhart et al.1997; Fombonne et al. 1999; Dementieva et al. 2005; Orru' et al. 2018) in addition to early brain overgrowth (Courchesne 2002).

Yet, we also found that neither the type, nor the number of neuroradiological findings per person, nor the pattern of association between different findings were specifically associated with the autism spectrum. In fact, there were no differences in neuroradiological findings between ASD and controls within the subsample of participants with mild ID, although this sample was relatively small. Previous studies including individuals with ID did not perform direct pairwise comparisons between diagnostic groups (Zeegers et al. 2006; Erbetta et al. 2015). Nevertheless, the literature on neuroradiological findings in ASD unanimously concurs that there are *no* specific individual (or association of) findings that are unique to ASD (Piven et al.1990; Zeegers et al. 2006; Boddaert et al. 2009; Vasa et al. 2012; Erbetta et al. 2014, 2015; Monterrey et al. 2017; Myers et al. 2020). Our study corroborates this, further supporting the notion that brain imaging *per se* does not a have a direct role in the diagnosis of autism.

However, neuroradiological findings may be related to specific etiopathological mechanisms, which in turn, may be linked to ASD. Hence, our study illustrates that brain imaging has potential clinical relevance, particularly for evaluation of individual subjects (e.g. clinical genetics), and certainly in case of accompanying neurological and clinical signs and symptoms. From a methodological perspective, our study shows that detailed qualitative radiological screening of MRI scans is a valuable complement to automated (quantitative) assessments of brain morphometry.

Strengths of this study were its large sample size, and the use of a systematic and comprehensive scoring system of brain anomalies on MRI, augmented with standardized biometric measures of brain features. However, our findings must also be interpreted in the light of several limitations. First, T2w and FLAIR sequences were not available for all participants. However, these are not strictly necessary for identifying most of the MRI findings (e.g., persistent cavum septum pellucidum (Dremmen et al. 2019)). In addition, the acquisition parameters of the MRI scans used in this study were sub-optimal for assessing hippocampus. Therefore, analyses in this region must be interpreted with caution. Nonetheless, we ensured that all the reported findings in this study were adequately characterized by the available MRI sequences, and the number of scans missing did not differ between participants with and without ASD. Furthermore, not all scans in this study were reviewed independently by more than one rater. However, we worked in an interdisciplinary team, with one experienced, senior neuroradiologist supervising two pediatric neurologists with experience in brain imaging and development. Difficult scans were reviewed for consensus, and estimates of interrater agreement were remarkably high.

CONCLUSIONS

We used a systematic and comprehensive scoring system of brain anomalies on MRI, augmented with standardized biometric measures of brain features, and found a high incidence of neuroradiological findings in individuals with and without ASD. We found that neuroradiological findings were more common and clustered more frequently in ASD. Also, individual findings or clusters of findings may point towards the timing of neurodevelopmental mechanisms involved in individual cases. As such, clinical MRI assessments may be useful in the context of (genetic) diagnoses, and are potentially valuable to further elucidate the pathogenesis of autism.

ACKNOWLEDGMENTS

We would like to thank all participants and their families for participating in this study. We further wish to thank Miriam Douma, Tabitha Koops, Sara Post, Iris Selten, Alyssia Spaan, Maarten Steffers, and Anna Ver Loren van Themaat for their assistance with subject recruitment and acquisition of MRI scans throughout the running time of this study. We gratefully acknowledge the contributions of the EU-AIMS LEAP Group: Jumana Ahmad, Sara Ambrosino, Bonnie Auyeung, Tobias Banaschewski, Simon Baron-Cohen, Sarah Baumeister, Christian F. Beckmann, Sven Bölte, Thomas Bourgeron, Carsten Bours, Michael Brammer, Daniel Brandeis, Claudia Brogna, Yvette de Bruijn, Jan K. Buitelaar, Bhismadev Chakrabarti, Tony Charman, Mario Cirillo, Ineke Cornelissen, Daisy Crawley, Flavio Dell'Acqua, Francesco Di Salle, Guillaume Dumas, Sarah Durston, Christine Ecker, Fabrizio Esposito, Jessica Faulkner, Vincent Frouin, Pilar Garcés, David Goyard, Lindsay Ham, Hannah Hayward, Joerg Hipp, Rosemary Holt, Mark H. Johnson, Emily J.H. Jones, Prantik Kundu, Meng-Chuan Lai, Xavier Liogier D'ardhuy, Michael V. Lombardo, Eva Loth, David J. Lythgoe, René Mandl, Andre Marquand, Luke Mason, Maarten Mennes, Andreas Meyer-Lindenberg, Carolin Moessnang, Nico Mueller, Declan G.M. Murphy, Bethany Oakley, Laurence O'Dwyer, Marianne Oldehinkel, Bob Oranje, Gahan Pandina, Antonio M. Persico, Barbara Ruggeri, Annika Rausch, Amber Ruigrok, Jessica Sabet, Roberto Sacco, Antonia San José Cáceres, Emily Simonoff, Will Spooren, Giacchino Tedeschi, Julian Tillmann, Roberto Toro, Heike Tost, Jack Waldman, Steve C.R. Williams, Caroline Wooldridge, and Marcel P. Zwiers. The primary contact for the EU-AIMS LEAP Group is Declan G. Murphy (Email: pa-dmurphy@kcl.ac.uk).

FUNDING

The results leading to this publication have received funding from the Innovative Medicines Initiative 2 Joint Undertaking under grant agreement No 777394 for the project AIMS-2-TRIALS. This Joint Undertaking receives support from the European Union's Horizon 2020 research and innovation programme and EFPIA and AUTISM SPEAKS, Autistica, SFARI. The funders had no role in the design of the study; in the collection, analyses, or interpretation of data; in the writing of the manuscript, or in the decision to publish the results. Any views expressed are those of the author(s) and not necessarily those of the funders.

DECLARATION OF INTEREST

TB served in an advisory or consultancy role for ADHS digital, Infectopharm, Lundbeck, Medice, Neurim Pharmaceuticals, Oberberg GmbH, Roche, and Takeda. He received conference support or speaker's fee by Medice and Takeda. He received royalities from Hogrefe, Kohlhammer, CIP Medien, Oxford University Press; the present work is unrelated to these relationships. JKB has been in the past 3 years a consultant to / member of advisory board of / and/or speaker for Takeda/Shire, Roche, Medice, Angelini, Janssen, and Servier. He is not an employee of any of these companies, and not a stock shareholder of any of these companies. He has no other financial or material support, including expert testimony, patents, royalties. ASJC has worked with Servier and been a member of advisory boards for Servier and Roche. JT is an employee of F. Hoffmann–La Roche Ltd. The other authors report no biomedical financial interests or potential conflicts of interest.

REFERENCES

Allanson JE, Cunniff C, Hoyme HE, McGaughran J, Muenke M, Neri G. 2009. Elements of morphology: standard terminology for the head and face. Am. J. Med. Genet. A. Jan;149A(1), 6-28. doi: 10.1002/ajmg.a.32612.

American Psychiatric Association. 2013. Diagnostic and statistical manual of mental disorders (5th ed.). Arlington, VA: Author.

American Psychiatric Association. 1994. Diagnostic and statistical manual of mental disorders (4th ed.) Washington, DC: Author.

American Psychiatric Association. 2000. Diagnostic and statistical manual of mental disorders (4th ed., text rev.) Washington, DC: Author.

Aylward EH, Minshew NJ, Field K, Sparks BF, Singh N. 2002. Effects of age on brain volume and head circumference in autism. Neurology. 59(2), 175–183. https://doi.org/10.1212/wnl.59.2.175

Baisden J. 2012. Controversies in Chiari I malformations. Surg. Neurol. Int. 3(Suppl 3), S232–S237. https://doi.org/10.4103/2152-7806.98580

Barkovich AJ, Guerrini R, Kuzniecky RI, Jackson GD, Dobyns WB. 2012. A developmental and genetic classification for malformations of cortical development: update 2012. Brain, 135(Pt 5), 1348–1369. https://doi.org/10.1093/brain/aws019

Barkovich AJ, Kjos BO, Norman D, Edwards MS. 1989. Revised classification of posterior fossa cysts and cystlike malformations based on the results of multiplanar MR imaging. AJR Am. J. Roentgenol. Dec;153(6), 1289-300. doi: 10.2214/ajr.153.6.1289. PMID: 2816648.

Beasley TM, Schumacker RE. 1995. Multiple Regression Approach to Analyzing Contingency Tables: Post Hoc and Planned Comparison Procedures. J. Exp. Educ. 64, 79-93. https://doi.org/10.1080/00220973.1995.9943797

Bellani M, Calderoni S, Muratori F, Brambilla P. 2013. Brain anatomy of autism spectrum disorders I. Focus on corpus callosum. Epidemiol. Psychiatr. Sci. 22(3), 217–221. https://doi.org/10.1017/S2045796013000139

Benjamini Y, Hochberg Y. 1995. Controlling the False Discovery Rate: A Practical and Powerful Approach to Multiple Testing. J. R. Stat. Soc. Series B (Methodological), 57(1), 289–300. http://www.jstor.org/stable/2346101

Bilston LE. 2011. Brain Tissue Mechanical Properties. In: Miller K. (eds) Biomechanics of the Brain. Biological and Medical Physics, Biomedical Engineering. Springer, New York, NY. https://doi-org.proxy.library.uu.nl/10.1007/978-1-4419-9997-9_4

Boddaert N, Zilbovicius M, Philipe A, Robel L, Bourgeois M, Barthélemy C, Seidenwurm D, Meresse I, Laurier L, Desguerre I, Bahi-Buisson N, Brunelle F, Munnich A, Samson Y, Mouren MC, Chabane N. 2009. MRI findings in 77 children with non-syndromic autistic disorder. PLoS One. 4(2), e4415. doi: 10.1371/journal.pone.0004415.

Bosemani T, Orman G, Boltshauser E, Tekes A, Huisman TA, Poretti A. 2015. Congenital abnormalities of the posterior fossa. Radiographics. Jan-Feb;35(1), 200-220. doi: 10.1148/rg.351140038. PMID: 25590398.

Brambilla P, Hardan A, di Nemi SU, Perez J, Soares JC, Barale F. 2003. Brain anatomy and development in autism: review of structural MRI studies. Brain Res. Bull. 61(6), 557–569. https://doi.org/10.1016/j.brainresbull.2003.06.001

Brocklehurst G. 1969. The development of the human cerebrospinal fluid pathway with particular reference to the roof of the fourth ventricle. J. Anat. Nov;105(Pt 3), 467-475. PMID: 4187088; PMCID: PMC1232183.

Charman T, Gotham K. 2013. Measurement Issues: Screening and diagnostic instruments for autism spectrum disorders - lessons from research and practise. Child. Adolesc. Ment. Health. 18(1), 52–63. https://doi.org/10.1111/j.1475-3588.2012.00664.x

Charman T, Loth E, Tillmann J, Crawley D, Wooldridge C, Goyard D, Ahmad J, Auyeung B, Ambrosino S, Banaschewski T, et al. 2017. The EU-AIMS Longitudinal European Autism Project (LEAP): clinical characterisation. Mol. Autism. Jun 23, 8:27. doi: 10.1186/s13229-017-0145-9. PMID: 28649313; PMCID: PMC5481972.

Chen R, Jiao Y, Herskovits EH. 2011. Structural MRI in autism spectrum disorder. Pediatr. Res. 69 (5Pt 2), 63R–8R. https://doi.org/10.1203/PDR.0b013e318212c2b3

Chen CY, Zimmerman RA, Faro S, Parrish B, Wang Z, Bilaniuk LT, Chou TY. 1995. MR of the cerebral operculum: topographic identification and measurement of interopercular distances in healthy infants and children. AJNR Am. J. Neuroradiol. Sep;16(8), 1677-1687. PMID: 7502974.

Chen CY, Zimmerman RA, Faro S, Parrish B, Wang Z, Bilaniuk LT, Chou TY. 1996. MR of the cerebral operculum: abnormal opercular formation in infants and children. AJNR Am. J. Neuroradiol. Aug;17(7), 1303-1311. PMID: 8871716.

Cooper AS, Friedlaender E, Levy SE, Shekdar KV, Bradford AB, Wells KE, Mollen C. 2016. The Implications of Brain MRI in Autism Spectrum Disorder. J. Child Neurol. 31(14), 1611–1616. https://doi.org/10.1177/0883073816665548

Courchesne E. 2002. Abnormal early brain development in autism. Mol. Psychiatry, 7 Suppl 2, S21–S23. https://doi.org/10.1038/sj.mp.4001169

Courchesne E, Campbell K, Solso S. 2011. Brain growth across the life span in autism: age-specific changes in anatomical pathology. Brain Res. J. 1380, 138–145. https://doi.org/10.1016/j.brainres.2010.09.10

Courchesne E, Karns CM, Davis HR, Ziccardi R, Carper RA, Tigue ZD, Chisum HJ, Moses P, Pierce, K, Lord C, Lincoln AJ, Pizzo S, Schreibman L, Haas RH, Akshoomoff NA, Courchesne RY. 2001. Unusual brain growth patterns in early life in patients with autistic disorder: an MRI study. Neurology, 57(2), 245–254. https://doi.org/10.1212/wnl.57.2.245

De León Reyes NS, Bragg-Gonzalo L, Nieto M. 2020. Development and plasticity of the corpus callosum. Development. Sep 28, 147(18), dev189738. doi: 10.1242/dev.189738. PMID: 32988974.

Dementieva YA, Vance DD, Donnelly SL, Elston LA, Wolpert CM, Ravan SA, DeLong GR, Abramson RK, Wright HH, Cuccaro ML. 2005. Accelerated head growth in early development of individuals with autism. Pediatr. Neurol. Feb;32(2), 102-108. doi: 10.1016/j.pediatrneurol.2004.08.005. PMID: 15664769.

Desikan RS, Barkovich AJ. 2016. Malformations of cortical development. Ann. Neurol. 80(6), 797–810. https://doi.org/10.1002/ana.24793

D'Mello AM, Crocetti D, Mostofsky SH, Stoodley CJ. 2015. Cerebellar gray matter and lobular volumes correlate with core autism symptoms. NeuroImage Clin, 7, 631–639. https://doi.org/10.1016/j.nicl.2015.02.007

Donovan AP, Basson MA. 2017. The neuroanatomy of autism - a developmental perspective. J. Anat. 230(1), 4–15. https://doi.org/10.1111/joa.12542

Dremmen MHG, Bouhuis RH, Blanken LME, Muetzel RL, Vernooij MW, Marroun HE, Jaddoe VWV, Verhulst FC, Tiemeier H, White T. 2019. Cavum Septum Pellucidum in the General Pediatric Population and Its Relation to Surrounding Brain Structure Volumes, Cognitive Function, and Emotional or Behavioral Problems. AJNR Am. J .Neuroradiol. Feb;40(2), 340-346. doi: 10.3174/ajnr.A5939. Epub 2019 Jan 24. PMID: 30679220; PMCID: PMC7028615.

Ecker C, Pretzsch CM, Bletsch A, Mann C, Schaefer T, Ambrosino S, Tillmann J, Yousaf A, Chiocchetti A, Lombardo M, Warrier V, Bast N, Moessnang C, Baumeister S, Dell'Acqua F, Floris DL, Zabihi M, Marquand A, Cliquet F, Leblond C, Moreau C, Puts N, Banaschewski T, Jones EJH, Mason L, Bölte S, Meyer-Lindenberg A, Persico AM, Durston S, Baron-Cohen S, Spooren W, Loth E, Freitag CM, Charman T, Dumas G, Bourgeron T, Beckmann CF, Buitelaar JK, Murphy DGM. 2022. Interindividual Differences in Cortical Thickness and Their Genomic Underpinnings in Autism Spectrum Disorder. Am. J. Psychiatry. 179(3), 242–254. https://doi.org/10.1176/appi.ajp.2021.20050630

Ecker C, Bookheimer SY, Murphy DG. 2015. Neuroimaging in autism spectrum disorder: brain structure and function across the lifespan. Lancet Neurol. 14(11), 1121-1134.

Ecker C, Ginestet C, Feng Y, Johnston P, Lombardo MV, Lai MC, Suckling J, Palaniyappan L, Daly E, Murphy CM, Williams SC, Bullmore ET, Baron-Cohen S, Brammer M, Murphy DG, & MRC AIMS Consortium. 2013. Brain surface anatomy in adults with autism: the relationship between surface area, cortical thickness, and autistic symptoms. JAMA psychiatry, 70(1), 59–70. https://doi.org/10.1001/jamapsychiatry.2013.265

Edwards TJ, Sherr EH, Barkovich AJ, Richards LJ. 2014. Clinical, genetic and imaging findings identify new causes for corpus callosum development syndromes. Brain. Jun;137(Pt 6), 1579-1613. doi: 10.1093/brain/awt358. Epub 2014 Jan 28. PMID: 24477430; PMCID: PMC4032094.

Erbetta A, Bulgheroni S, Contarino VE, Chiapparini L, Esposito S, Annunziata S, Riva D. 2015. Low-Functioning Autism and Nonsyndromic Intellectual Disability: Magnetic Resonance Imaging (MRI) Findings. J. Child Neurol. Oct;30(12), 1658-1663. doi: 10.1177/0883073815578523. Epub 2015 Apr 20. PMID: 25895913.

Erbetta A, Bulgheroni S, Contarino VE, Chiapparini L, Esposito S, Vago C, Riva D. 2014. Neuroimaging findings in 41 low-functioning children with autism spectrum disorder: a single-center experience. J. Child Neurol. 29(12), 1626-1631.

Filipek PA, Accardo PJ, Ashwal S, Baranek GT, Cook EH Jr, Dawson G, Gordon B, Gravel JS, Johnson CP, Kallen RJ, Levy SE, Minshew NJ, Ozonoff S, Prizant BM, Rapin I, Rogers SJ, Stone WL, Teplin SW, Tuchman RF, Volkmar FR. 2000. Practice parameter: screening and diagnosis of autism: report of the Quality Standards Subcommittee of the American Academy of Neurology and the Child Neurology Society. Neurology. Aug 22;55(4), 468-479. doi: 10.1212/wnl.55.4.468. PMID: 10953176.

Fischl B. 2012. FreeSurfer. Neuroimage. Aug 15;62(2):774-781. doi: 10.1016/j.neuroimage.2012.01.021. Epub 2012 Jan 10. PMID: 22248573; PMCID: PMC3685476.

Fombonne E, Rogé B, Claverie J, Courty S, Frémolle J. 1999. Microcephaly and macrocephaly in autism. J. Autism Dev. Disord. Apr;29(2), 113-119. doi: 10.1023/a:1023036509476. PMID: 10382131.

Franco FC, de Araujo TM, Vogel CJ, Quintão CC. 2013. Brachycephalic, dolichocephalic and mesocephalic: Is it appropriate to describe the face using skull patterns? Dental Press J Orthod. May-Jun;18(3), 159-163. doi: 10.1590/s2176-94512013000300025. PMID: 24094027.

Frazier TW, Hardan AY. 2009. A meta-analysis of the corpus callosum in autism. Biol. Psychiatry. Nov 15;66(10), 935-941. doi: 10.1016/j.biopsych.2009.07.022. Epub 2009 Sep 12. PMID: 19748080; PMCID: PMC2783565.

Garel C, Cont I, Alberti C, Josserand E, Moutard ML, Ducou le Pointe H. 2011. Biometry of the corpus callosum in children: MR imaging reference data. AJNR Am. J. Neuroradiol. Sep;32(8), 1436-1443. doi: 10.3174/ajnr.A2542. Epub 2011 Jul 28. PMID: 21799035; PMCID: PMC7964359.

Hadjikhani N, Joseph RM, Snyder J, Tager-Flusberg H. 2006. Anatomical differences in the mirror neuron system and social cognition network in autism. Cereb cortex (New York, N.Y. : 1991), 16(9), 1276–1282. https://doi.org/10.1093/cercor/bhj069

Heier LA, Bauer CJ, Schwartz L, Zimmerman RD, Morgello S, Deck MD. 1989. Large Virchow-Robin spaces: MR-clinical correlation. AJNR Am. J. Neuroradiol. Sep-Oct;10(5), 929-936. PMID: 2505536.

Hyde KL, Samson F, Evans AC, Mottron L. 2010. Neuroanatomical differences in brain areas implicated in perceptual and other core features of autism revealed by cortical thickness analysis and voxel-based morphometry. Hum Brain Mapp. 31(4), 556–566. https://doi.org/10.1002/hbm.20887

Jansen PR, Dremmen M, van den Berg A, Dekkers IA, Blanken L, Muetzel RL, Bolhuis K, Mulder RM, Kocevska D, Jansen TA, de Wit MY, Neuteboom RF, Polderman T, Posthuma D, Jaddoe V, Verhulst FC, Tiemeier H, van der Lugt A, White T. 2017. Incidental Findings on Brain Imaging in the General Pediatric Population. N. Engl. J. Med. 377(16), 1593–1595. https://doi.org/10.1056/NEJMc1710724

Karakaş P, Koç Z, Koç F, Gülhal Bozkır M. 2011. Morphometric MRI evaluation of corpus callosum and ventricles in normal adults. Neurol Res. Dec;33(10), 1044-1049. doi: 10.1179/1743132811Y.0000000030. PMID: 22196757.

Katzman GL, Dagher AP, Patronas NJ. 1999. Incidental findings on brain magnetic resonance imaging from 1000 asymptomatic volunteers. JAMA. Jul 7;282(1), 36-39.

Kim BS, Illes J, Kaplan RT, Reiss A, Atlas SW. 2002. Incidental findings on pediatric MR images of the brain. AJNR Am. J. Neuroradiol. 23(10), 1674-1677.

Lainhart JE, Piven J, Wzorek M, Landa R, Santangelo SL, Coon H, Folstein SE. 1997. Macrocephaly in children and adults with autism. J Am Acad Child Adolesc Psychiatry. 36(2), 282–290. https://doi.org/10.1097/00004583-199702000-00019

Li X, Zhang K, He X, Zhou J, Jin C, Shen L, Gao Y, Tian M, Zhang H. 2021. Structural, Functional, and Molecular Imaging of Autism Spectrum Disorder. Neurosci Bull. 37(7), 1051–1071. https://doi.org/10.1007/s12264-021-00673-0

Limperopoulos C, Robertson RL, Jr Khwaja OS, Robson CD, Estroff JA, Barnewolt C, Levine D, Morash D, Nemes L, Zaccagnini L, du Plessis AJ. 2008. How accurately does current fetal imaging identify posterior fossa anomalies?. AJR. Am. J. Roentgenol. 190(6), 1637–1643. https://doi.org/10.2214/AJR.07.3036

Lord C, Risi S, Lambrecht L, Cook EH, Leventhal BL, DiLavore PC, Pickles A, Rutter M. 2000. The Autism Diagnostic Observation Schedule—Generic: a standard measure of social and communication deficits associated with the spectrum of autism. J. Autism Dev. Disord. 30, 205–223.

Lord C, Rutter M, DiLavore PC, Risi S, Gotham K, Bishop S. 2012. Autism Diagnostic Observation Schedule, Second Edition (ADOS-2) manual (part I): modules 1–4. Torrance: Western Psychological Services.

Loth E, Charman T, Mason L, Tillmann J, Jones EJH, Wooldridge C, Ahmad J, Auyeung B, Brogna C, Ambrosino S, Banaschewski T, Baron-Cohen S, Baumeister S, Beckmann C, Brammer M, Brandeis D, Bölte S, Bourgeron T, Bours C, de Bruijn Y, Chakrabarti B, Crawley D, Cornelissen I, Dell'Acqua F, Dumas G, Durston S, Ecker C, Faulkner J, Frouin V, Garces P, Goyard D, Hayward H, Ham LM, Hipp J, Holt RJ, Johnson MH, Isaksson J, Kundu P, Lai MC, D'ardhuy XL, Lombardo MV, Lythgoe DJ, Mandl R, Meyer-Lindenberg A, Moessnang C, Mueller N, O'Dwyer L, Oldehinkel M, Oranje B, Pandina G, Persico AM, Ruigrok ANV, Ruggeri B, Sabet J, Sacco R, Cáceres ASJ, Simonoff E, Toro R, Tost H, Waldman J, Williams SCR, Zwiers MP, Spooren W, Murphy DGM, Buitelaar JK. 2017. The EU-AIMS Longitudinal European Autism Project (LEAP): design and methodologies to identify and validate stratification biomarkers for autism spectrum disorders. Mol. Autism. Jun 23, 8:24. doi: 10.1186/s13229-017-0146-8. PMID: 28649312; PMCID: PMC5481887.

Monterrey JC, Philips J, Cleveland S, Tanaka S, Barnes P, Hallmayer JF, Reiss AL, Lazzeroni LC, Hardan AY. 2017. Incidental brain MRI findings in an autism twin study. Autism Res. Jan;10(1), 113-120. doi: 10.1002/aur.1720. Epub 2016 Nov 22. PMID: 27874265.

Myers L, Ho ML, Cauvet E, Lundin K, Carlsson T, Kuja-Halkola R, Tammimies K, Bölte S. 2020. Actionable and incidental neuroradiological findings in twins with neurodevelopmental disorders. Sci. Rep. 10, 22417. https://doi-org.proxy.library.uu.nl/10.1038/s41598-020-79959-8

Nopoulos P, Berg S, Castellenos FX, Delgado A, Andreasen NC, Rapoport JL. 2000. Developmental brain anomalies in children with attention-deficit hyperactivity disorder. J. Child Neurol. 15(2), 102-108.

Nordahl CW, Dierker D, Mostafavi I, Schumann CM, Rivera SM, Amaral DG, Van Essen DC. 2007. Cortical folding abnormalities in autism revealed by surface-based morphometry. J. Neurosci. 27(43), 11725-11735.

Orrù E, Calloni SF, Tekes A, Huisman TAGM, Soares BP. 2018. The Child With Macrocephaly: Differential Diagnosis and Neuroimaging Findings. AJR Am. J. Roentgenol. Apr;210(4), 848-859. doi: 10.2214/AJR.17.18693. Epub 2018 Feb 22. PMID: 29470161.

Osborn AG, Preece MT. 2006. Intracranial cysts: radiologic-pathologic correlation and imaging approach. Radiology. 239(3), 650-664.

Piven J, Berthier ML, Starkstein SE, Nehme E, Pearlson G, Folstein S. 1990. Magnetic resonance imaging evidence for a defect of cerebral cortical development in autism. Am. J. Psychiatry 147(6), 734-739.

Pretzsch CM, Schäfer T, Lombardo MV, Warrier V, Mann C, Bletsch A, Chatham CH, Floris DL, Tillmann J, Yousaf A, Jones E, Charman T, Ambrosino S, Bourgeron T, Dumas G, Loth E, Oakley B, Buitelaar JK, Cliquet F, Leblond CS, … Ecker C. 2022. Neurobiological Correlates of Change in Adaptive Behavior in Autism. Am. J. Psychiatry 179(5), 336–349. https://doi.org/10.1176/appi.ajp.21070711

Qiu T, Chang C, Li Y, Qian L, Xiao CY, Xiao T, Xiao X, Xiao YH, Chu KK, Lewis MH, Ke X. 2016. Two years changes in the development of caudate nucleus are involved in restricted repetitive behaviors in 2-5-year-old children with autism spectrum disorder. Dev. Cogn. Neurosci. 19, 137–143. https://doi.org/10.1016/j.dcn.2016.02.010

Rutter M, Le Couteur A, Lord C. 2003. Autism Diagnostic Interview-Revised. Los Angeles: Western Psychological Services.

Sarı E, Sarı S, Akgün V, Özcan E, İnce S, Babacan O, Saldır M, Açıkel C, Başbozkurt G, Yeşilkaya Ş, Kılıc C, Kara K, Vurucu S, Kocaoğlu M, Yeşilkaya E. 2015. Measures of ventricles and evans' index: from neonate to adolescent. Pediatr. Neurosurg. 50(1), 12-7. doi: 10.1159/000370033. Epub 2015 Jan 22. PMID: 25613691.

Schaefer GB, Mendelsohn NJ, & Professional Practice and Guidelines Committee. 2013. Clinical genetics evaluation in identifying the etiology of autism spectrum disorders: 2013 guideline revisions. Genet. Med. 15(5), 399–407. https://doi.org/10.1038/gim.2013.32

Sommer IE, de Kort GA, Meijering AL, Dazzan P, Hulshoff Pol HE, Kahn RS, & van Haren NE. 2013. How frequent are radiological abnormalities in patients with psychosis? A review of 1379 MRI scans. Schizophr. Bull. 39(4), 815–819. https://doi.org/10.1093/schbul/sbs037

Taber KH, Shaw JB, Loveland KA, Pearson DA, Lane DM, Hayman LA. 2004. Accentuated Virchow-Robin spaces in the centrum semiovale in children with autistic disorder. J. Comput. Assist. Tomogr. Mar-Apr;28(2), 263-268. doi: 10.1097/00004728-200403000-00017. PMID: 15091132.

van Rooij D, Anagnostou E, Arango C, Auzias G, Behrmann M, Busatto GF, Calderoni S, Daly E, Deruelle C, Di Martino A, Dinstein I, Duran F, Durston S, Ecker C, Fair D, Fedor J, Fitzgerald J, Freitag CM, Gallagher L, Gori I, … Buitelaar J. K. 2018. Cortical and Subcortical Brain Morphometry Differences Between Patients With Autism Spectrum Disorder and Healthy Individuals Across the Lifespan: Results From the ENIGMA ASD Working Group. Am. J. Psychiatry. 175(4), 359–369. https://doi.org/10.1176/appi.ajp.2017.17010100

Vasa RA, Ranta M, Huisman TA, Pinto PS, Tillman RM, Mostofsky SH. 2012. Normal rates of neuroradiological findings in children with high functioning autism. J. Autism Dev. Disord. 42(8), 1662-1670.

Whitney N, Sun H, Pollock JM, Ross DA. 2013. The human foramen magnum--normal anatomy of the cisterna magna in adults. Neuroradiology. Nov;55(11), 1333-9. doi: 10.1007/s00234-013-1269-z. Epub 2013 Sep 15. PMID: 24036927.

World Health Organization (WHO). 1993. The ICD-10 classification of mental and behavioural disorders. World Health Organization.

Zeegers M, Van Der Grond J, Durston S, Nievelstein RJ, Witkamp T, Van Daalen E, Buitelaar J, Engeland HV. 2006. Radiological findings in autistic and developmentally delayed children. Brain Dev. 28(8), 495-499.

Table A1. Scanner details and acquisition parameters at each participating site

Site	Manufacturer	Model	Software version	Acquisition sequence	Slices (n)	TR (s)	TE (ms)	FA (°)	Coverage	Voxel size (mm^3)	FOV (mm)
Cambridge	Siemens	Verio	Syngo MR B17	Tfl3d1_ns	176	2.30	2.95	9	256*256	1.1*1.1*1.2	270
				Ax FLAIR	27	7.84	96	150	240*320	0.7*0.7*4	224
KCL	GE Medical systems	Discovery mr750	LX MR DV23.1_V02_ 1317.c	SAG ADNI GO ACC SPGR	196	7.31	3.02	11	256*256	1.1*1.1*1.2	270
				Ax T2 FRFSE	72	4.38	60	/	512*512	0.5*0.5*2	240
				Ax T2 FLAIR	36	8.00	120	/	512*512	0.4*0.4*4	220
Mannheim	Siemens	TimTrio	Syngo MR B17	MPRAGE ADNI	176	2.30	2.93	9	256*256	1.1*1.1*1.2	270
Nijmegen	Siemens	Skyra	Syngo MR D13	Tfl3d1_16ns	176	2.30	2.93	9	256*256	1.1*1.1*1.2	270
				T2	25	1.50	80	150	320*320	0.7*0.7*4	220
Rome	GE Medical systems	Signa HDxt	24/LX/MR HD16.0_V02_ 1131.a	SAG ADNI GO ACC SPGR	172	5.96	1.76	11	256*256	1.1*1.1*1.2	270
				ACPC T2	72	5.78	127	90	512*512	0.5*0.5*2	240
				Ax T2 FLAIR	36	9.00	122	90	512*512	0.5*0.5*4	240
Utrecht	Philips Medical Systems	Achieva	3.2.3/3.2.3.1	ADNI GO 2	170	6.76	3.1	9	256*256	1.1*1.1*1.2	270

Abbreviations: n, number; TR, repetition time; TE, echo time; FA, flip angle; FOV, field of view

APPENDIX C: BIOMETRIC ASSESSMENTS

Head size and proportions

To assess head size and shape, we measured the greatest Anterior-posterior (AP) diameter from the T1 mid-sagittal plane, and the greatest Bi-parietal (BP) diameter from the T1 axial plane that most closely aligned with the AP diameter. Both diameters usually went through or were close to the thalami.

The Cranial Index (CI) was calculated as the ratio of head-width (BP) expressed as a percentage of head-length (AP). Accordingly, CI was computed as: CI = (BP / AP) * 100.

Head circumference was computed: HC= (BP + AP) * Π / 2.

Extreme deviations from the three main head shapes (brachycephalic, mesocephalic, and dolichocephalic types) were estimated. Hyperdolichocephaly was defined as CI < 71, hyperbrachycephaly was defined as CI > 90 (Franco et al. 2013). Plagiocephaly was confirmed by measuring Cranial Vault Asymmetry (CVA) > 5 mm.

Macro- and microcephaly were defined in case of HC > 97th or < 3rd percentiles, respectively (Allanson et al. 2009).

Inter-opercular distances

Underdevelopment of the opercular region (an "open" operculum) was defined as an increased mean distance (> 3.5 mm) between the posterior-inferior border of the inferior frontal gyrus and the superior-anterior border of the temporal lobe (anterior open operculum) on sagittal (*a*) and axial (*b*) planes, or an increased mean distance (> 0.5 mm) between the inferior border of the parietal operculum and the superior border of the temporal operculum (posterior open operculum) in sagittal (*c*) or coronal (*d*) planes. Mean anterior and posterior interopercular distances of each hemisphere were calculated by averaging *a* and *b*, or *c* and *d*, respectively (Chen et al. 1995, Chen et al. 1996).

The **corpus callosum** is the largest commissural tract, structurally divided into four segments: rostrum, genu, body and splenium. We assessed the anterior-posterior diameter of the corpus callosum by measuring the distance between the anterior aspect of the genu and the posterior aspect of the splenium on midline sagittal sections. The thickness of the corpus callosum was measured at the level of the body. Callosal measures that were less than the 3rd percentile or greater than the 97th percentile (Garel et al. 2011; Karakaş et al. 2011) were considered to be short/thin or long/thick corpus callosum, respectively.

On the midsagittal plane we also measured the largest diameter of **pineal gland** cysts, if present.

In the posterior fossa, **mega cisterna magna** was defined as a ≥10 mm enlargement of the retro and infra-cerebellar cerebrospinal fluid (CSF) space measured between the inferior margin of the vermis and the posterior rim of the foramen magnum perpendicular to the occipital dura on the midsagittal plane, in the presence of an intact vermis and a normal 4th ventricle (Limperopoulos et al. 2009).

Chiari malformation type 1 was defined in case of herniation of cerebellar tonsils ≥ 5 mm below the foramen magnum (Baisden 2012).

Ventriculomegaly

Evans' index was measured on transverse images as the ratio between the maximum diameter of the frontal horns of the lateral ventricles and the maximum inner diameter of the skull in the same section. Ventriculomegaly was graded as follows: 0, normal (Evans' index < 0.3); 1, slight dilation (Evans' index 0.3–0.35); or 2, dilation (Evans' index > 0.35) (Sari et al. 2015).

The septum pellucidum is a vertical double membrane separating the anterior horns of the lateral ventricles. The two layers are separated at birth and typically fuse into a single septum within 5 months, likely due to the growth of the surrounding brain structures (Sarwar 1989). Occasionally, this process fails leaving a persistent cavum. A cavum length 1-4 mm is common in a large proportion of healthy subjects. In accordance to most previous studies, we defined an enlarged **cavum septum pellucidum** in case of a cavum length of ≥ 6 mm (Dremmen et al. 2019).

Measurements of the **subarachnoid space** width were taken on coronal images, in cuts passing through the frontal horns of the lateral ventricles, as the maximum width of the CSF from the crest of a gyrus to the nearest point on the inner table of the skull. Subarachnoid CSF space enlargement was defined in case of a cranio-cortical width ≥ 6 mm (Marino et al.2014).

Finally, we measured the size (largest diameter) of perivascular **Virchow-Robin (VR) spaces** in subcortical and deep white matter, and associated with the lenticulostriate arteries. According to the reference work of Heier and colleagues (1989), VR spaces were considered dilated if they were larger than 3 mm.

REFERENCES

Allanson, J.E., Cunniff, C., Hoyme, H.E., McGaughran, J., Muenke, M., Neri, G. 2009. Elements of morphology: standard terminology for the head and face. Am. J. Med. Genet. A. Jan;149A(1), 6-28. doi: 10.1002/ajmg.a.32612. PMID: 19125436; PMCID: PMC2778021.

Baisden, J. 2012. Controversies in Chiari I malformations. Surg. Neurol. Int. 3(Suppl 3), S232–S237. https://doi.org/10.4103/2152-7806.98580

Chen, C.Y., Zimmerman, R.A., Faro, S., Parrish, B., Wang, Z., Bilaniuk, L.T., Chou, T.Y. 1995. MR of the cerebral operculum: topographic identification and measurement of interopercular distances in healthy infants and children. AJNR Am. J. Neuroradiol. Sep;16(8), 1677-87. PMID: 7502974.

Chen, C.Y., Zimmerman, R.A., Faro, S., Parrish, B., Wang, Z., Bilaniuk, L.T., Chou T.Y. 1996. MR of the cerebral operculum: abnormal opercular formation in infants and children. AJNR Am. J. Neuroradiol. Aug;17(7), 1303-11. PMID: 8871716.

Dremmen, M.H.G., Bouhuis, R.H., Blanken, L.M.E., Muetzel, R.L., Vernooij, M.W., Marroun, H.E., Jaddoe, V.W.V., Verhulst, F.C., Tiemeier, H., White T. 2019. Cavum Septum Pellucidum in the General Pediatric Population and Its Relation to Surrounding Brain Structure Volumes, Cognitive Function, and Emotional or Behavioral Problems. AJNR Am. J. Neuroradiol. Feb;40(2), 340-346. doi: 10.3174/ajnr.A5939. PMID: 30679220; PMCID: PMC7028615.

Franco, F.C., de Araujo, T.M., Vogel, C.J., Quintão, C.C. 2013. Brachycephalic, dolichocephalic and mesocephalic: Is it appropriate to describe the face using skull patterns? Dental Press J. Orthod. May-Jun;18(3):159-63. doi: 10.1590/s2176-94512013000300025. PMID: 24094027.

Garel, C., Cont, I., Alberti, C., Josserand, E., Moutard, M.L., Ducou le Pointe, H. 2011. Biometry of the corpus callosum in children: MR imaging reference data. AJNR Am. J. Neuroradiol. Sep;32(8), 1436-43. doi: 10.3174/ajnr.A2542. Epub 2011 Jul 28. PMID: 21799035; PMCID: PMC7964359.

Heier, L.A., Bauer, C.J., Schwartz, L., Zimmerman, R.D., Morgello, S., Deck M.D. 1989. Large Virchow-Robin spaces: MR-clinical correlation. AJNR Am. J. Neuroradiol. Sep-Oct;10(5), 929-36. PMID: 2505536.

Karakaş, P., Koç, Z., Koç, F., Gülhal Bozkır, M. 2011. Morphometric MRI evaluation of corpus callosum and ventricles in normal adults. Neurol. Res. Dec;33(10), 1044-9. doi: 10.1179/1743132811Y.0000000030. PMID: 22196757.

Limperopoulos, C., Robertson, R. L., Jr Khwaja, O. S., Robson, C. D., Estroff, J. A., Barnewolt, C., Levine, D., Morash, D., Nemes, L., Zaccagnini, L., du Plessis, A. J. 2008. How accurately does current fetal imaging identify posterior fossa anomalies?. AJR. Am. J. Roentgenol. 190(6), 1637–1643. https://doi.org/10.2214/AJR.07.3036

Marino, M.A., Morabito R., Vinci, S., Germanò, A., Briguglio, M., Alafaci, C., Mormina, E., Longo, M., & Granata F. 2014. Benign external hydrocephalus in infants. A single centre experience and literature review. Neuroradiol. J. 27(2), 245–250. https://doi.org/10.15274/NRJ-2014-10020

Sarı, E., Sarı, S., Akgün, V., Özcan, E., İnce, S., Babacan, O., Saldır, M., Açıkel, C., Başbozkurt, G., Yeşilkaya, Ş., Kılıc, C., Kara, K., Vurucu, S., Kocaoğlu, M., Yeşilkaya, E. 2015. Measures of ventricles and evans' index: from neonate to adolescent. Pediatr. Neurosurg. 50(1), 12-7. doi: 10.1159/000370033. Epub 2015 Jan 22. PMID: 25613691.

Sarwar, M. 1989. The septum pellucidum: normal and abnormal. AJNR Am. J. Neuroradiol. Sep-Oct;10(5), 989-1005. PMID: 2505543; PMCID: PMC8335275.

APPENDIX D: SUPPLEMENTARY RESULTS

Table D.1. Neuroradiological findings – sex differences

	Total N=620	**Male** n=428	**Female** n=192	**Sex diff*** *p* value
Head, brain, and lobes				
Cranial deformity All	28 (4.5%)	18 (4.2%)	10 (5.2%)	ns
Plagiocephaly	9 (1.5%)	8 (1.9%)	1 (0.5%)	ns
Hyperbrachycephaly	9 (1.5%)	6 (1.4%)	3 (1.6%)	ns
Hyperdolichocephaly	10 (1.6%)	6 (1.4%)	4 (2.1%)	ns
Cranial volume All	133 (21.5%)	86 (20.1%)	47 (24.5%)	ns
Microcephaly	47 (7.6%)	7 (1.6%)	40 (20.8%)	**< .001**
Macrocephaly	86 (13.9%)	79 (18.5%)	7 (3.6%)	**< .001**
Calvarian / dural thickening	126 (20.3%)	95 (22.2%)	31 (16.1%)	ns
Opercular abnormalities	229 (36.9%)	160 (37.4%)	69 (35.9%)	ns
Cerebral cortex				
Malformations All	8 (1.3%)	7 (1.6%)	1 (0.5%)	ns
Periventricular nodular Heterotopia	3 (0.5%)	3 (0.7%)	0 (0%)	ns
Simplified gyral pattern	2 (0.3%)	2 (0.5%)	0 (0%)	ns
Cortical dysplasia	3 (0.5%)	2 (0.5%)	1 (0.5%)	ns
Lesions	3 (0.5%)	3 (0.7%)	0 (0%)	ns
Hippocampi				
Lesions	2 (0.3%)	1 (0.2%)	1 (0.5%)	ns
White matter				
Lesions	15 (2.4%)	12 (2.8%)	3 (1.6%)	ns
Virchow-Robin spaces				
Dilation All	338 (54.5%)	243 (56.8%)	95 (49.5%)	ns
Deep white matter / subcortical	133 (21.5%)	104 (24.3%)	29 (15.1%)	.010
Lenticulo-striate	300 (48.4%)	216 (50.5%)	84 (43.8%)	ns
Basal ganglia	0 (0%)	0 (0%)	0 (0%)	ns
Posterior fossa				
All	115 (18.5%)	96 (22.4%)	19 (9.9%)	**< .001**
Dandy-Walker complex	106 (17.1%)	92 (21.5%)	14 (7.3%)	**< .001**
Mega cisterna magna	82 (13.2%)	73 (17.1%)	9 (4.7%)	**< .001**
Dandy-Walker variant	3 (0.5%)	3 (0.7%)	0 (0%)	ns
Blake pouch cyst	1 (0.2%)	1 (0.2%)	0 (0%)	ns
Arachnoid cyst	13 (2.1%)	12 (2.8%)	1 (0.5%)	ns
Vermian hypoplasia	7 (1%)	3 (0.7%)	4 (2.1%)	ns
Chiari type 1 malformation	7 (1.1%)	3 (0.7%)	4 (2.1%)	ns
Lesion	1 (0.2%)	1 (0.2%)	0 (0%)	ns

Table D.1. Continued

	Total N=620	**Male** n=428	**Female** n=192	**Sex diff*** *p* value
Vascular anomaly	1 (0.2%)	0 (0%)	1 (0.5%)	ns
CSF spaces				
Ventriculomegaly	26 (4.2%)	21 (4.9%)	5 (2.6%)	ns
Cavum septum pellucidum / vergae	12 (1.9%)	9 (2.1%)	3 (1.6%)	ns
Choroid plexus cysts	3 (0.5%)	3 (0.7%)	0 (0%)	ns
Subarachnoid spaces Enlargement	57 (9.2%)	19 (4.4%)	38 (19.8%)	ns
Calcifications	2 (0.3%)	2 (0.5%)	0 (0%)	ns
Midline				
CC Hypoplasia All	30 (4.8%)	16 (3.7%)	14 (7.3%)	ns
CC thin	10 (1.6%)	3 (0.7%)	7 (3.6%)	.012
CC short	12 (1.9%)	8 (1.9%)	4 (2.1%)	ns
CC short and thin	4 (0.6%)	3 (0.7%)	1 (0.5%)	ns
CC partial agenesis	1 (0.2%)	1 (0.2%)	0 (0%)	ns
CC focal hypoplasia	4 (0.6%)	2 (0.5%)	2 (1.0%)	ns
Pineal gland cyst All	90 (14.5%)	58 (13.6%)	32 (16.7%)	ns
≥ 10 mm	14 (2.3%)	9 (2.1%)	5 (2.6%)	ns
< 10 mm	76 (12.3%)	49 (11.4%)	27 (14.1%)	ns
Other				
Vascular anomalies All	10 (1.6%)	4 (0.9%)	6 (3.1%)	ns
DVA	8 (1.3%)	3 (0.7%)	5 (2.6%)	ns
Kissing carotids	1 (0.2%)	0 (0%)	1 (0.5%)	ns
Capillary teleangectasia	1 (0.2%)	1 (0.2%)	0 (0%)	ns
Cysts All	8 (1.3%)	6 (1.4%)	2 (1.0%)	ns
Arachnoid**	3 (0.5%)	3 (0.7%)	0 (0%)	ns
Poroencefalic	3 (0.5%)	2 (0.5%)	1 (0.5%)	ns
Neuroglial	1 (0.2%)	1 (0.2%)	0 (0%)	ns
Inclusion	1 (0.2%)	0 (0%)	1 (0.5%)	ns

Abbreviations: ASD, autism spectrum disorder; n, number; M, mean; SD, standard deviation; ns, not significant; IQ, intelligence quotient; ID, intellectual disability; CSF, cerebral spinal fluid; CC, corpus callosum; DVA, developmental venous anomalies. Note: *X^2 or Fisher's Exact Test, as appropriate, for testing for sex differences (raw p-values; results reaching significance when controlling FDR are indicated in bold). **Arachnoid cysts in locations other than the posterior fossa.

Table D.2. Correlations between neuroradiological findings (p-values).

	1	2	3	4	5	6	7	8	9	10	11	12	13	14	15	16	17	18	19	20	21	22	23	24	25
1. Cranial deformity	-	ns	ns	ns	ns	ns	ns	ns	ns	ns	ns	ns	ns	.036	ns	ns	ns	ns	ns		ns	ns	ns	ns	ns
2. Microcephaly	ns	-	-	ns	ns	ns	ns	ns	ns	ns	ns	ns	ns	ns	ns	ns	ns	ns	ns	ns	ns	**< .0001**	ns	ns	ns
3. Macrocephaly	ns	-	-	**< .0001**	.047	ns	ns	ns	.017	ns	ns	ns	ns	ns	ns	ns	**< .0001**	ns	ns	ns	ns	ns	ns	ns	ns
4. Thickening dura / skull	ns	ns	**< .0001**	-	**< .0001**	ns	ns	ns	ns	ns	ns	ns	ns	.034	.034	ns	ns	ns	ns	.027	ns	ns	ns	ns	ns
5. Opercula abnormality	ns	ns	.047	**< .0001**	-	ns	ns	ns	ns	ns	ns	ns	ns	ns	ns	ns	.002	ns	ns	.004	ns	.002	ns	ns	ns
6. Cortical malformation	ns	ns	ns	ns	ns	-	ns	**< .0001**	ns	ns	ns	ns	ns	ns	ns	ns	ns	ns	ns	ns	ns	ns	ns	ns	**< .0001**
7. Hippocampi	ns	ns	ns	ns	ns	ns	-	ns	ns	ns	ns	ns	ns	ns	ns	ns	ns	.038	ns	ns	ns	ns	ns	ns	.026
8. White Matter lesions	ns	ns	ns	ns	ns	**< .0001**	ns	-	ns	ns	ns	ns	ns	ns	.011	ns	ns	ns	ns	ns	ns	ns	ns	ns	.001
9. Virchow-Robin spaces	ns	ns	ns	ns	ns	ns	ns	ns	-	ns	ns	ns	ns	ns	ns	ns	ns	ns	ns	ns	ns	ns	ns	ns	ns
10. Mega cisterna magna	ns	ns	ns	ns	ns	ns	ns	ns	ns	-	-	-	-	-	ns	ns	ns	ns	ns	.025	.017	ns	ns	ns	ns
11. Dandy-Walker variant	ns	ns	ns	ns	ns	ns	ns	ns	ns	-	-	-	-	-	ns	ns	.005	ns	ns	.023	ns	ns	ns	ns	ns
12. Blake cyst	ns	ns	ns	ns	ns	ns	ns	ns	ns	-		-	-	-	ns	ns	.042	ns	ns	ns	ns	.048	ns	ns	ns
13. Cerebellar cysts	ns	ns	ns	ns	ns	ns	ns	ns	ns	-	-	-	-	-	ns	ns	.014	ns	ns	ns	ns	ns	ns	ns	ns
14. Vermis hypoplasia	.036	ns	ns	.034	ns	ns	ns	ns	ns	-	-	-	-	-	ns	ns	ns	ns	ns	ns	ns	.041	ns	ns	ns
15. Chiari 1 malformation	ns	ns	ns	.034	ns	ns	ns	.011	ns	ns	ns	ns	ns	ns	-	ns	ns	ns	ns	ns	ns	ns	ns	ns	ns
16. Cerebellar lesions	ns	ns	ns	ns	ns	ns	ns	ns	ns	ns	ns	ns	ns	ns	ns	-	ns	ns	ns	ns	ns	ns	ns	.032	ns
17. Ventriculomegaly	ns	ns	**< .0001**	ns	.002	ns	ns	ns	ns	ns	.005	.042	.013	ns	ns	ns	-	ns	ns	.001	ns	ns	ns	ns	ns
18. Cavum septum	ns	ns	ns	ns	ns	ns	.038	ns	ns	ns	ns	ns	ns	ns	ns	ns	ns	-	ns	ns	ns	ns	ns	ns	ns
19. Choroid cysts	ns	ns	ns	ns	ns	ns	ns	ns	ns	ns	ns	ns	ns	ns	ns	ns	ns	ns	-	ns	ns	.007	ns	ns	ns
20. Periencephalic spaces	ns	ns	ns	.027	.004	ns	ns	ns	ns	.025	.023	ns	ns	ns	ns	ns	.001	ns	ns	-	ns	ns	ns	ns	ns
21. Calcifications	ns	ns	ns	ns	ns	ns	ns	ns	ns	.017	ns	ns	ns	ns	ns	ns	ns	ns	ns	ns	-	ns	ns	ns	ns
22. CC hypoplasia	ns	**< .0001**	ns	ns	.002	ns	ns	ns	ns	ns	ns	.048	ns	.041	ns	ns	ns	ns	.007	ns	ns	-	ns	ns	ns
23. Pineal gland cyst	ns	ns	ns	ns	ns	ns	ns	ns	ns	ns	ns	ns	ns	ns	ns	ns	ns	ns	ns	ns	ns	ns	-	ns	ns
24. Vascular abnormality	ns	ns	ns	ns	ns	ns	ns	ns	ns	ns	ns	ns	ns	ns	ns	.032	ns	ns	ns	ns	ns	ns	ns	-	ns
25. Other Cysts	ns	ns	ns	ns	ns	**< .0001**	.026	.001	ns	ns	ns	ns	ns	ns	ns	ns	ns	ns	ns	ns	ns	ns	ns	ns	-

Note. Correlations reaching Bonferroni-corrected significance are indicated in bold.

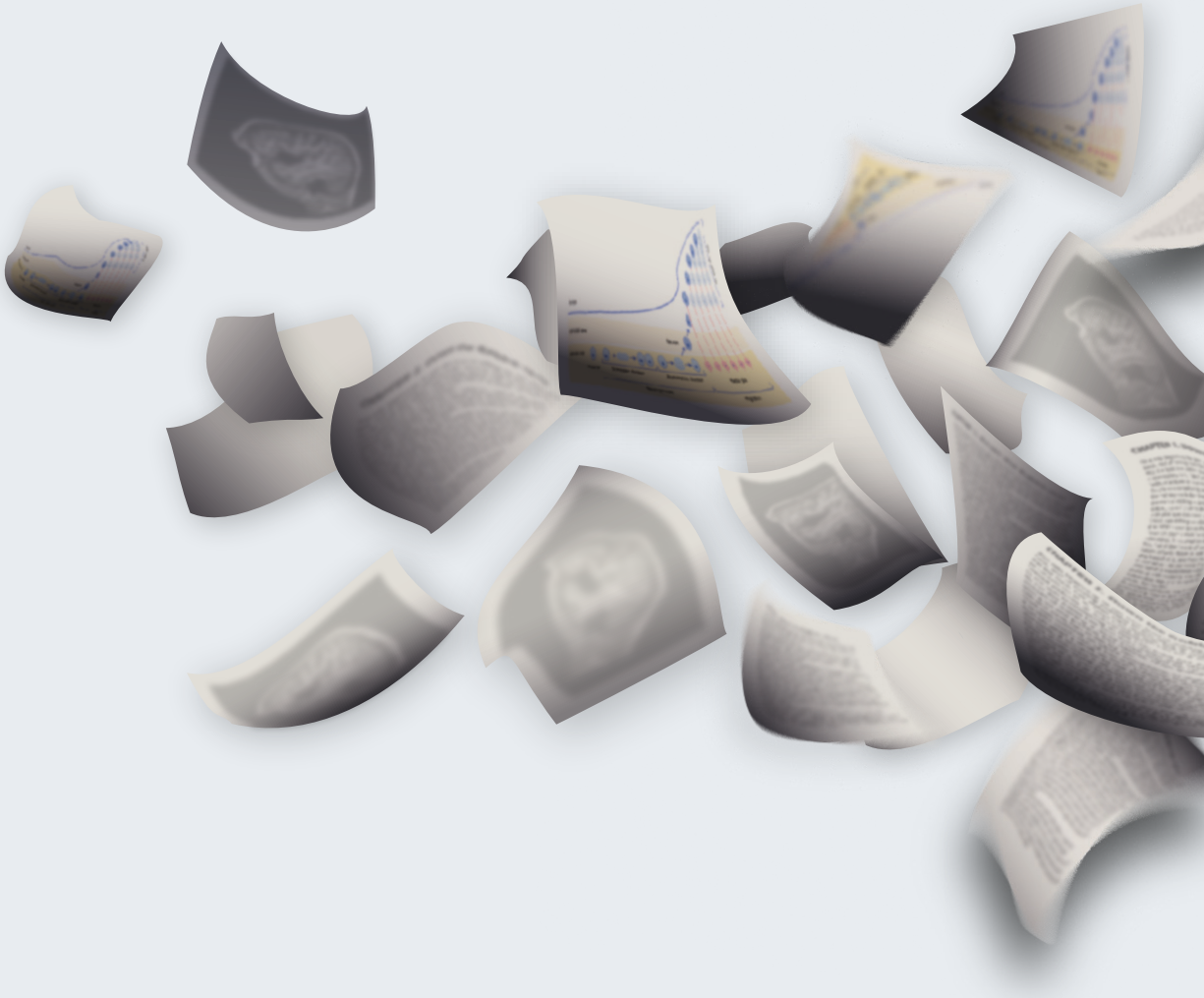

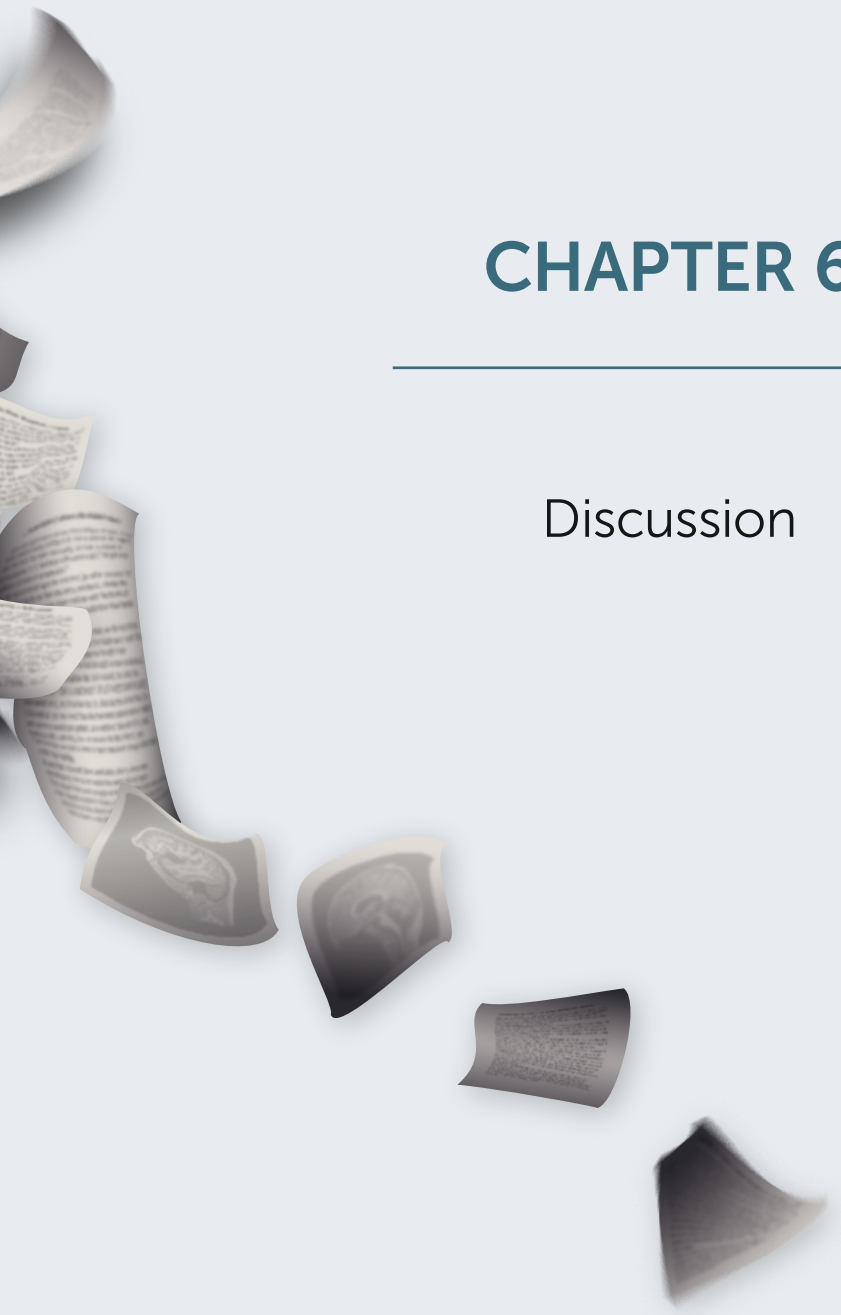

CHAPTER 6

Discussion

As the title of this thesis suggests, neuroimages should be not regarded as mere pictures of the brain; rather, brain MRI can be extremely eloquent and provide valuable insights into neurobiological models of developmental disorders. This can be achieved when neuroimaging data are assessed comprehensively, taking the complexity of neuroanatomical features and dynamic frameworks of brain development into account. Modern image processing techniques permit the measurement of different dimensions of cerebral cortex, for example. But what does a reduction of cortical thickness really *mean*? By itself, this finding has only very limited value for uncovering the neurobiological changes associated with any developmental condition, if it is not placed in the context of the other brain features, such as which brain areas are involved (primarily), and how they change over time. As such, longitudinal analyses of multiple features of the brain are pivotal for neuroimaging studies of developmental disorders. In this thesis, we examined functional and structural MRI measures in the two most frequently diagnosed developmental conditions, ASD and ADHD (Elsabbagh et al. 2012; Polanczyk et al. 2014).

In **chapter 2,** we investigated functional connectivity networks in children with ASD during the performance of a cognitive control task using a multivariate data-driven approach. We found no differences in functional connectivity between children with autism and typically developing controls. This negative finding may be related to immature brain activity in children, which is characterized by less structured and more diffuse patterns of activity (less connected and interconnected) than in adults. These results emphasize that functional, like structural, neuroimaging data are dependent on age and/or developmental stage. This study was too limited in its age-range (9 to 14 years) and size (N = 19 + 19) to permit adequate investigation of developmental changes in brain connectivity.

We carefully addressed these limitations in our following studies of brain development in autism and ADHD. We investigated developmental trajectories of brain structures using longitudinal study designs in large and independent samples across a broader age range, allowing for higher accuracy and greater generalizability of the data. Specifically, in **chapter 3** we assessed developmental trajectories of subcortical volumes and multiple cortical dimensions in a large longitudinal sample of children, adolescents and adults with ADHD and matched typically developing controls (N = 188, 297 scans). We found stable reductions in overall cortical volume in ADHD, but predominantly in frontal areas, which were driven by reductions in cortical surface area and gyrification. This may implicate early developmental mechanisms regulating the tangential growth and sulcation of the frontal cortex in the neurobiological changes associated with ADHD.

We further investigated these changes in cortical development in **chapter 4**, where we compared individuals with ADHD, individuals with autism spectrum disorder (ASD) with

high and low levels of co-occurring ADHD symptoms (ASD+ and ASD-), and matched typically developing controls (N = 210, 280 scans). We found similar reductions in the volume and surface area of left orbitofrontal cortex (OFC) in ADHD and ASD+ compared to controls. This may implicate early developmental mechanisms specifically involving left OFC expansion in ADHD symptoms in both conditions. This is plausible neurobiologically, as ASD and ADHD are frequently comorbid and there is substantial overlap in their clinical presentation. In fact, it has been suggested that ASD and ADHD may be better conceptualized as two extremes of one overarching, trans-diagnostic condition (Rommelse et al. 2017). Our findings suggest that similar pathways regulating early OFC development may be related to ADHD symptoms in both conditions, providing a possible neurobiological correlate for a trans-diagnostic framework.

The involvement of frontal areas has been reported repeatedly in ADHD (Arnsten 2009), and this was confirmed by our findings in chapters 3 and 4. The cerebral cortex has a columnar structure; our finding of volumetric reduction caused by a reduction of cortical surface area (determined by the number of columns) but not of cortical thickness (related to the number of neurons within the columns) is of importance, because it points towards specific neurobiological mechanisms that may be involved in ADHD, namely those involved in lateral expansion of cortex.

In terms of phylogeny, the evolutionary expansion of cerebral cortex is believed to primarily be the result of an increase in the number of columnar modules, rather than an increase of their thickness. This is in line with the observation that cortical surface area differs enormously across species, whereas the variation in cortical thickness is small. This implies that, during evolution, the cortex expanded laterally rather than vertically (Geschwind and Rakic 2013). This may be particularly true for the human brain, which has disproportionally large surface area in relation to its volume. The expansion of unique progenitor populations, and the protracted developmental timeline over which neuronal progenitors' proliferation and migration occur, are widely believed to be the evolutionary basis for the relatively large cortex and complex connections that characterize the human brain. Inevitably, this increase in size and complexity also creates greater vulnerability to errors in the development at any point in the process (Subramanian et al. 2020).

It is therefore not surprising that malformations of the brain, and particularly of cerebral cortex, are not rare, with an estimated prevalence of approximately 1:1000 births in Europe (Morris et al. 2019). Malformations of cortical development (MCD) encompass a large group of conditions, and are highly heterogenous in nature, severity and etiopathogenesis. They may arise from disruption during any of the three coordinated stages of cortical development.

The earliest stage consists of the proliferation and differentiation of neural progenitors within the ventricular (VZ) and subventricular zones (SVZ) of the dorsal telencephalon and in the ganglionic eminences. Prior to six weeks of embryonic life, neural progenitors begin symmetric cell division, with each stem cell producing two identical stem cells with each mitotic cycle (Rajkowska & Goldman-Rakic 1995), resulting in exponential cellular growth. Then, at approximately six weeks gestational age, the neural progenitors gradually shift to asymmetric division. During asymmetric cell division, one daughter cell continues as an undifferentiated stem cell and undergoes further replication, while the other daughter cell matures into a neuron and migrates outward to the cortex. In the second stage of cortical development, neurons migrate radially from VZ and SVZ, and tangentially from the ganglionic eminences toward the meningeal surface. Later generation cells pass through the previously developed neurons before reaching their final positions (Sidman & Rakic 1973), forming the six layers of the neocortex in a characteristic inside-out columnar pattern. The third stage concerns the organization of cortex, and involves the establishing of intercellular connections through a complex interplay of processes involving neurite outgrowth, synaptogenesis, synaptic pruning, and cell death. These overlapping stages, and examples of related MCDs, are depicted in figure 1.

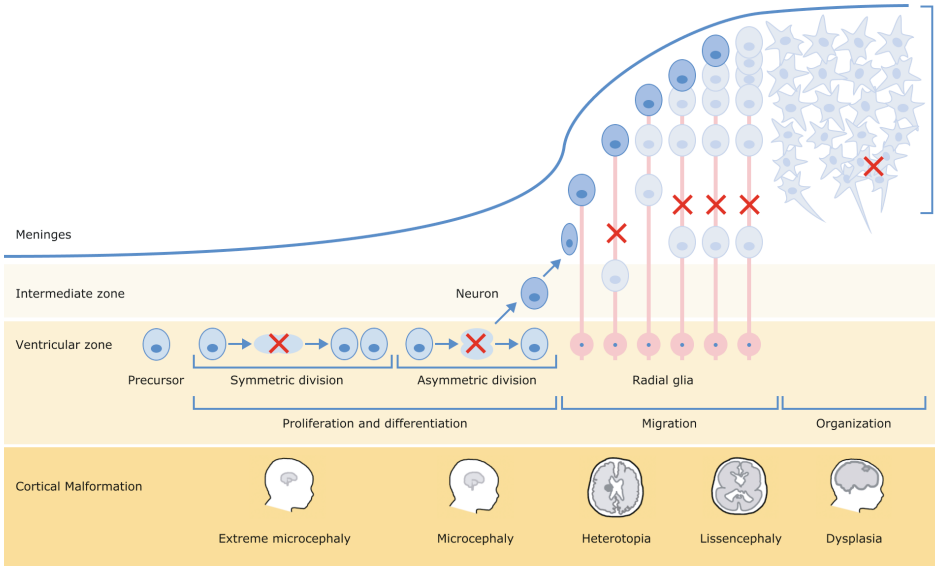

Figure 1. Cortical developmental stages and examples of associated malformations

Stage 1: Neuronal proliferation and differentiation; timing: 2-4 months; associated malformations: (extreme) microcephaly, megalencephaly (not depicted);
Stage 2: Radial and tangential migration; timing: 3-5 months; associated malformations: lissencephaly, agyria-pachygyria (not depicted), neuronal heterotopias;
Stage 3: Neuronal organization; timing: 5 months-post-natal; associated malformations: cortical dysplasias, polymicrogyria and schizencephaly (not depicted).

MCDs are initially diagnosed on neuroimaging features, and further characterized using clinical phenotyping and genetic analyses; ultimately, more precise information may be obtained by neuropathological examination of the brain tissue (Severino et al. 2020). In fact, updated classifications of MCDs are based on both morphological and genetic criteria (Barkovich et al. 2012). The study of neuroradiological, genetic, and neuropathological aspects of MCDs may therefore offer valuable opportunities to decipher complex developmental processes of the human brain by pointing to where they go awry. This idea was first formulated as a general principle in 1657 by William Harwey (English physician):

> *"Nature is nowhere accustomed more openly to display her secret mysteries than in cases where she shows tracings of her workings apart from the beaten paths; nor is there any better way to advance the proper practice of medicine than to give our minds to the discovery of the usual law of nature, by careful investigation of cases of rarer forms of disease."*

In other words, the best way to elucidate any fundamental biological mechanisms involved in common disorders is to investigate them in their extreme forms, in rare cases.

Congenital microcephalies are rare disorders of the proliferation phase (Barkovich et al. 2012) that are characterized by a significantly smaller brain size (cranial circumference more than 2SD below the mean) and a normal to slightly thinner cortex (primary microcephaly), or by an extreme small brain (cranial circumference more than 3SD below the mean) with a particularly thin cortex (extreme microcephaly). In the former case, only the asymmetric cell division seems to be impaired, whereas in the latter, both precursor cell proliferation and late cell division are implicated (Francis et al. 2006). As such, congenital microcephalies clearly exemplify errors in the fundamental processes of cortical expansion. Clinically, microcephalies may be characterized by developmental delay, intellectual disability, seizures, and behavioural problems including ADHD (Aagaard et al. 2018).

ADHD is one of the most common developmental disorders in children and adolescents worldwide (Polanczyk et al. 2015). We can only speculate whether and which cellular mechanisms may be involved in the pattern of reduction of cortical surface area with normal thickness we observed in (normocephalic) ADHD subjects in **chapter 3** and **4**. Lessons from congenital microcephalies suggest that a plausible mechanism may be a minor perturbation of the later phase of neuronal proliferation (asymmetric cell division), leading to a subtle, but statistically significant reduction of the cortical volume, with substantially preserved cortical layering. Notably, teratogenic substances targeting neuronal precursors, such as nicotine and alcohol have been

linked to ADHD (Linnet et al. 2003; Banerjee et al. 2007), as have several genetic and molecular factors essential for neuronal proliferation and differentiation including neurotrophins (Syed et al. 2007).

Given the potentially valuable contribution of studying MCDs and other congenital brain anomalies for uncovering neurobiological mechanisms involved in developmental disorders, we explicitly investigated them in **chapter 5**. Here, we comprehensively and systematically characterized any visible morphological or signal abnormality on MRI scans, including possible variants (neuroradiological findings), in one of the largest cohorts of individuals with ASD and matched controls worldwide (N = 620). We found that neuroradiological findings were more frequent and tended to co-occur (cluster) more in individuals with ASD. However, the type of variation, the number of neuroradiological findings per individual, and the pattern of association between various findings were not specifically associated with ASD (as there were no differences between subjects with ASD and controls in the subsample of subjects with mild intellectual disability).

Clustering is a key diagnostic criterium in syndromology, where multiple (three or more) minor anomalies are taken to indicate significant defects in morphogenesis and are highly correlated with a major congenital anomaly presumably due to a single underlying aetiology (Verma 2021). Our study showed that a wide variety of (and clustering of) anomalies in brain development are associated with ASD and intellectual disability, emphasizing the role of neurobiological development in these conditions.

In the light of the findings in chapter 5, it could be helpful to reconsider the assessment structural brain MRI in both clinical practice and research on ASD. Currently, according to the guidelines of the American Academy of Neurology and Child Neurology Society (Filipek et al. 2000), brain imaging is not recommended in the clinical assessment of autism spectrum conditions. This was justified by the low incidence and inconsistent localization of neuroradiological findings in previous reports (Filipek et al. 1992; Damasio et al. 1980), which led to the conclusion that they were merely coincidental and unrelated to the disorder. Rather, our data show that neuroradiological findings, carefully examined in a large sample, are more prevalent and cluster in ASD. We corroborate previous findings in that neuroradiological findings in ASD are highly heterogenous in nature, extent and site, and, as such, cannot be considered pathognomonic of the condition (Piven et al. 1990). However, they may point to specific developmental mechanisms, which in turn, could be linked to ASD in individual cases. These findings suggest that brain imaging may potentially be useful in a clinical context, for individual subjects, and that it could certainly form a valuable contribution to autism research.

Together, the findings in this thesis support the hypothesis that clinical heterogeneity in ASD and ADHD is accompanied by similar variation in the associated neurobiological substrates: these range from anomalies large enough to be qualitatively noticeable in anatomical MRI scans (**chapter 5**), to more subtle changes at the group level that are invisible to the human eye, but can be characterized with quantitative assessments (**chapter 3 and 4**).

FUTURE RESEARCH

We used either qualitative *or* quantitative methodologies in our studies. Ideally, for a more comprehensive analytical and interpretative approach to brain morphology, it would be beneficial to combine both methodologies as they are complementary. We identified a variety of structural anomalies by qualitative evaluation of scans at the individual level that were not evident in the quantitative assessments. Contrarily, small changes at the group level cannot be detected by visual assessment, and only become evident in large datasets with quantitative evaluation. Typically, structural anomalies would either be ignored in quantitative neuroimaging studies or these scans would be excluded from the analyses. If neuroradiological findings are not investigated explicitly and systematically, the latter approach leads to selection bias. Alternatively, researchers may aim to preserve the intrinsic complexity of such datasets by including anomalies as predictors in their analyses. Our findings in chapter 5 could be used in such analyses, as we identified novel, and potentially relevant anomalies (e.g., distinct dimensions of the corpus callosum, or interopercular distances), that neuroimaging software developers could implement in their pipelines.

All methodologies have intrinsic limits to their sensitivity and, as such, generate false negative findings. Therefore, the absence of findings in qualitative and/or quantitative assessments does not preclude the possibility of micro-structural or functional changes. Notably, cortical malformations are found in ASD at a higher rate, ex-vivo, upon post-mortem evaluation than on in-vivo MRI (Blackmon et al. 2015). Neuropathological studies may be helpful in interpretating the changes found on MRI: is cortical thinning at the group level related to fewer and / or smaller neurons, glial cells, dendritic arborization, synaptic density in individuals? Casanova et al. (2013) found multiple circumscribed dysplastic changes throughout the cortex in post-mortem brains of individuals with autism, predominantly in prefrontal areas; these changes corresponded to cortical thinning on MRI compared to typically developing controls, smaller pyramidal cells throughout the cortical width, and fewer interneurons. This preliminary study was

insufficient in size (N = 14, 7 ASD and 7 controls), yet it indicates a promising direction for interpreting neurobiological changes on MRI in ASD.

Further studies are necessary linking qualitative and quantitative methods, as well as neuroimaging and neuropathology, in representative samples to investigate the inherently complex, heterogeneous and interconnected nature of developmental disorders, such as autism and ADHD.

CONCLUSION

In this thesis, we used different neuroimaging techniques to characterize neurobiological (neuroanatomical) substrates of two highly frequent developmental conditions: ASD and ADHD. Our findings suggest that brain changes may constitute a spectrum of neuropathological features, possibly reflecting the well-established clinical heterogeneity that characterize both conditions. These findings may aid our understanding of the underpinning biological mechanisms, and may be not only relevant for research, but potentially also clinically.

REFERENCES

Aagaard K, Bach CC, Henriksen TB, Larsen RT, Matthiesen NB. 2018. Head circumference at birth and childhood developmental disorders in a nationwide cohort in Denmark. Paediatr Perinat Epidemiol. Sep;32(5):458-466. doi: 10.1111/ppe.12479. Epub 2018 Jun 8. PMID: 29882976.

Arnsten AF. 2009. The Emerging Neurobiology of Attention Deficit Hyperactivity Disorder: The Key Role of the Prefrontal Association Cortex. J Pediatr. May 1;154(5):I-S43. doi: 10.1016/j.jpeds.2009.01.018. PMID: 20596295; PMCID: PMC2894421.

Banerjee TD, Middleton F, Faraone SV. 2007. Environmental risk factors for attention-deficit hyperactivity disorder. Acta Paediatr. Sep;96(9):1269-74. doi: 10.1111/j.1651-2227.2007.00430.x. PMID: 17718779.

Barkovich AJ, Guerrini R, Kuzniecky RI, Jackson GD, Dobyns WB. 2012. A developmental and genetic classification for malformations of cortical development: update 2012. Brain. May;135(Pt 5):1348-69. doi: 10.1093/brain/aws019. Epub 2012 Mar 16. PMID: 22427329; PMCID: PMC3338922.

Blackmon K, Ben-Avi E, Wang X, Pardoe HR, Di Martino A, Halgren E, Devinsky O, Thesen T, Kuzniecky R. 2015. Periventricular white matter abnormalities and restricted repetitive behavior in autism spectrum disorder. Neuroimage Clin. Oct 31;10:36-45. doi: 10.1016/j.nicl.2015.10.017. PMID: 26693400; PMCID: PMC4660377.

Casanova MF, El-Baz AS, Kamat SS, Dombroski BA, Khalifa F, Elnakib A, Soliman A, Allison-McNutt A, Switala AE. 2013. Focal cortical dysplasias in autism spectrum disorders. Acta Neuropathol Commun. Oct 11;1:67. doi: 10.1186/2051-5960-1-67. PMID: 24252498; PMCID: PMC3893372.

Damasio H., Maurer R.G., Damasio A.R., Chui H.C. 1980. Computerized tomographic scan findings in patients with autistic behavior. Arch Neurol. Aug;37(8):504-10. doi: 10.1001/archneur.1980.00500570052008. PMID: 6968201.

Elsabbagh M, Divan G, Koh YJ, Kim YS, Kauchali S, Marcín C, Montiel-Nava C, Patel V, Paula CS, Wang C, Yasamy MT, Fombonne E. 2012. Global prevalence of autism and other pervasive developmental disorders. Autism Res. Jun;5(3):160-79. doi: 10.1002/aur.239. Epub 2012 Apr 11. PMID: 22495912; PMCID: PMC3763210.

Filipek PA, Accardo PJ, Ashwal S, Baranek GT, Cook EH Jr, Dawson G, Gordon B, Gravel JS, Johnson CP, Kallen RJ, Levy SE, Minshew NJ, Ozonoff S, Prizant BM, Rapin I, Rogers SJ, Stone WL, Teplin SW, Tuchman RF, Volkmar FR. 2000. Practice parameter: screening and diagnosis of autism: report of the Quality Standards Subcommittee of the American Academy of Neurology and the Child Neurology Society. Neurology. Aug 22;55(4):468-79. doi: 10.1212/wnl.55.4.468. PMID: 10953176.

Filipek PA, Richelme C, Kennedy DN, Rademacher J, Pitcher DA, Zidel SY, Caviness VS. 1992. Morphometric analysis of the brain in developmental language disorders and autism. Ann Neurol;32:475. Abstract. (Class II).

Francis F, Meyer G, Fallet-Bianco C, Moreno S, Kappeler C, Socorro AC, Tuy FP, Beldjord C, Chelly J. 2006. Human disorders of cortical development: from past to present. European Journal of Neuroscience, 23(4), 877-93.

Geschwind DH, Rakic P. 2013. Cortical evolution: judge the brain by its cover. Neuron. Oct 30;80(3):633-47. doi: 10.1016/j.neuron.2013.10.045. PMID: 24183016; PMCID: PMC3922239.

Linnet KM, Dalsgaard S, Obel C, Wisborg K, Henriksen TB, Rodriguez A, Kotimaa A, Moilanen I, Thomsen PH, Olsen J, Jarvelin MR. 2003. Maternal lifestyle factors in pregnancy risk of attention deficit hyperactivity disorder and associated behaviors: review of the current evidence. Am J Psychiatry. Jun;160(6):1028-40. doi: 10.1176/appi.ajp.160.6.1028. PMID: 12777257.

Morris JK, Wellesley DG, Barisic I, Addor MC, Bergman JEH, Braz P, Cavero-Carbonell C, Draper ES, Gatt M, Haeusler M, Klungsoyr K, Kurinczuk JJ, Lelong N, Luyt K, Lynch C, O'Mahony MT, Mokoroa O, Nelen V, Neville AJ, Pierini A, Randrianaivo H, Rankin J, Rissmann A, Rouget F, Schaub B, Tucker DF, Verellen-Dumoulin C, Wiesel A, Zymak-Zakutnia N, Lanzoni M, Garne E. 2019. Epidemiology of congenital cerebral anomalies in Europe: a multicentre, population-based EUROCAT study. Arch Dis Child. Dec;104(12):1181-1187. doi: 10.1136/archdischild-2018-316733. Epub 2019 Jun 26. PMID: 31243007.

Piven J, Berthier ML, Starkstein SE, Nehme E, Pearlson G, Folstein S. 1990. Magnetic resonance imaging evidence for a defect of cerebral cortical development in autism. Am J Psychiatry 147(6):734-739.

Polanczyk GV, Salum GA, Sugaya LS, Caye A, Rohde LA. Annual research review: A meta-analysis of the worldwide prevalence of mental disorders in children and adolescents. 2015. J Child Psychol Psychiatry. Mar;56(3):345-65. doi: 10.1111/jcpp.12381. Epub 2015 Feb 3. PMID: 25649325.

Polanczyk GV, Willcutt EG, Salum GA, Kieling C, Rohde LA. 2014. ADHD prevalence estimates across three decades: an updated systematic review and meta-regression analysis. Int J Epidemiol. Apr;43(2):434-42. doi: 10.1093/ije/dyt261. Epub 2014 Jan 24. PMID: 24464188; PMCID: PMC4817588.

Rajkowska, G., Goldman-Rakic, P. S. 1995. Cytoarchitectonic definition of prefrontal areas in the normal human cortex: I. Remapping of areas 9 and 46 using quantitative criteria. Cerebral Cortex, 5(4), 307–322.

Rommelse N, Buitelaar JK, Hartman CA. 2017. Structural brain imaging correlates of ASD and ADHD across the lifespan: a hypothesis-generating review on developmental ASD-ADHD subtypes. J Neural Transm. Feb;124(2):259-271. doi: 10.1007/s00702-016-1651-1. Epub 2016 Dec 21. PMID: 28000020; PMCID: PMC5285408.

Severino M, Geraldo AF, Utz N, Tortora D, Pogledic I, Klonowski W, Triulzi F, Arrigoni F, Mankad K, Leventer RJ, Mancini GMS, Barkovich JA, Lequin MH, Rossi A. 2020. Definitions and classification of malformations of cortical development: practical guidelines. Brain. Oct 1;143(10):2874-2894. doi: 10.1093/brain/awaa174. Erratum in: Brain. 2020 Dec 1;143(12):e108. PMID: 32779696; PMCID: PMC7586092.

Sidman RL, Rakic P. 1973. Neuronal migration, with special reference to developing human brain: a review. Brain Res. Nov 9;62(1):1-35. doi: 10.1016/0006-8993(73)90617-3. PMID: 4203033.

Subramanian L, Calcagnotto ME, Paredes MF. 2020. Cortical Malformations: Lessons in Human Brain Development. Front Cell Neurosci. Jan 24;13:576. doi: 10.3389/fncel.2019.00576. PMID: 32038172; PMCID: PMC6993122.

Syed Z, Dudbridge F, Kent L. 2007. An investigation of the neurotrophic factor genes GDNF, NGF, and NT3 in susceptibility to ADHD. American Journal of Medical Genetics parts B, Neuropsychiatric Genetics, 144B(3), 375-8.

Verma RP. 2021. Introductory Chapter: Epidemiology, Evaluation and Risk Assessment of Congenital Anomalies. In (Ed.), Congenital Anomalies in Newborn Infants - Clinical and Etiopathological Perspectives. IntechOpen. https://doi.org/10.5772/intechopen.97181

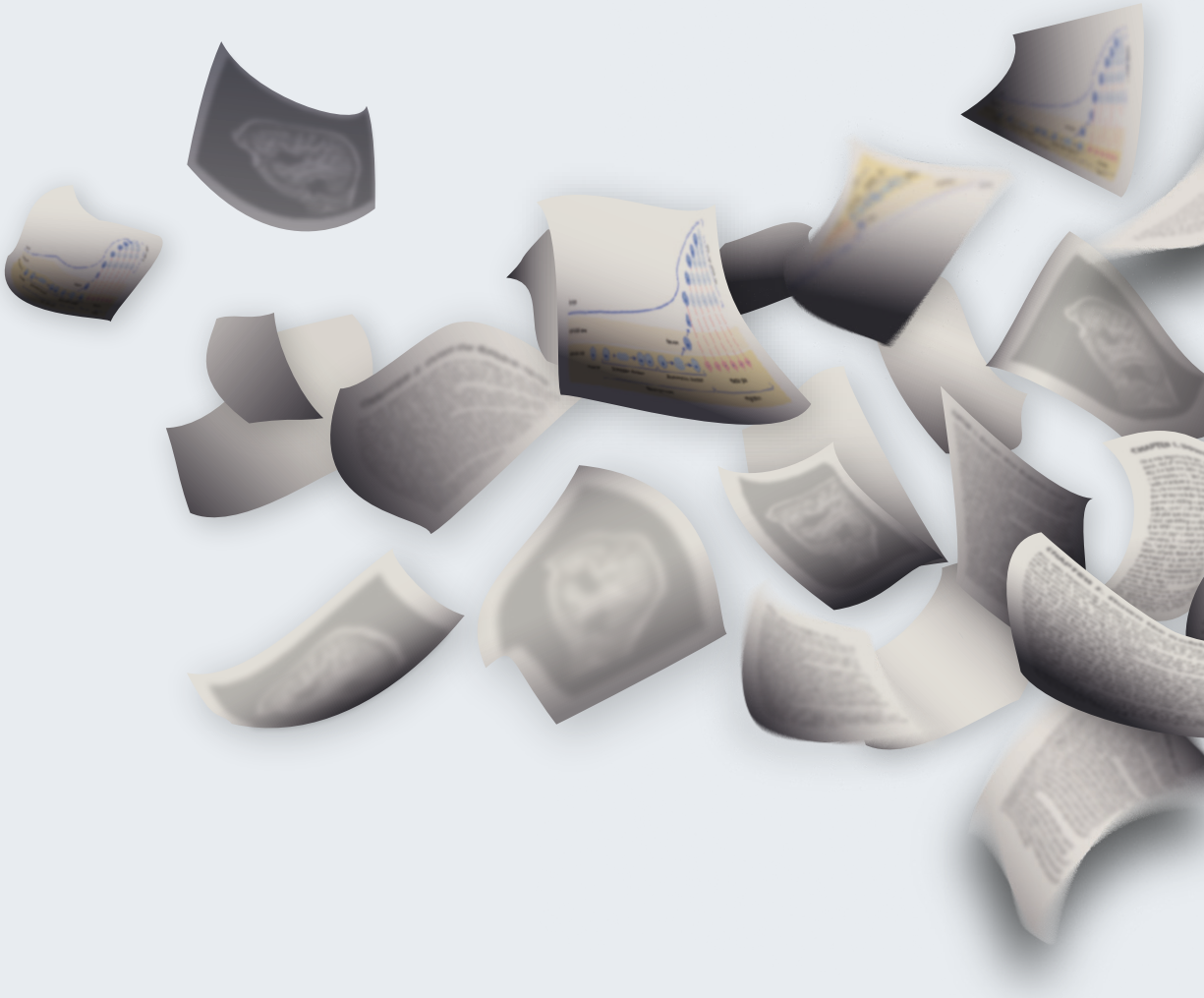

APPENDICES

Nederlandse samenvatting

Publications

Acknowledgements

Curriculum Vitae

NEDERLANDSE SAMENVATTING

Ontwikkelingsstoornissen omvatten een brede groep aandoeningen, gedefinieerd in DSM-5, die beginnen tijdens de ontwikkeling (American Psychiatric Association 2022). Op dit moment zijn Autisme Spectrum Stoornis (ASS) en Attention-Deficit/Hyperactivity Disorder (ADHD) de twee meest gediagnosticeerde ontwikkelingsstoornissen. (Elsabbagh et al. 2012; Polanczyk et al. 2014).

ASS wordt doorgaans vastgesteld in de vroege kindertijd en wordt gekenmerkt door aanhoudende gebreken in sociale communicatie, beperkende en repetitieve gedragspatronen en interesses, en ongebruikelijke sensorische reacties (DSM-5-TR, American Psychiatric Association 2022). Er is echter een grote variatie in de klinische presentatie van autisme, zowel in termen van symptoomprofielen als in de ernst daarvan, vandaar de term "spectrum". (Lai et al. 2013). Bovendien heeft ongeveer 70% van de individuen met ASS één of meer psychiatrische comorbiditeiten, (Simonoff et al. 2008), waarvan ADHD de meest voorkomende is (Kaat et al. 2013; Joshi et al. 2017).

ADHD daarentegen wordt voornamelijk gekenmerkt door een belemmerende mate van onoplettendheid, desorganisatie en/of hyperactiviteit-impulsiviteit die aanwezig is vóór de leeftijd van twaalf jaar. Hoewel ADHD-symptomen de neiging hebben zich te groeperen, kunnen sommige individuen worden geclassificeerd als overwegend onoplettend en anderen als overwegend hyperactief en impulsief. Personen die zowel de kernsymptomen van onoplettendheid als hyperactiviteit-impulsiviteit vertonen, voldoen aan de criteria voor het gecombineerde type. Net als bij ASS komt ADHD vaak voor in combinatie met andere ontwikkelingsstoornissen.

ASS en ADHD zijn relatief veelvoorkomende aandoeningen, met naar schatting wereldwijde prevalentiecijfers tussen respectievelijk 1-2,8% en 5-7% (Baird et al. 2006; Faraone et al. 2015; Thomas et al. 2015; Xu et al. 2019). Gezien hun hoge prevalentie, frequente chronische morbiditeit en gerelateerde functionele beperkingen zijn ASS en ADHD belangrijke aandachtspunten voor de volksgezondheid. Dit rechtvaardigt aanzienlijke inspanningen om naar neurobiologische verbanden te zoeken die kunnen dienen als aangrijpingspunt voor het ontwikkelen van nieuwe behandelingen en interventiestrategieën.

Magnetische Resonantie Imaging (MRI) studies naar structuren in de hersenen heeft ons begrip van de typische hersenontwikkeling en veranderingen daarin bij ontwikkelingsstoornissen zoals autisme en ADHD, aanzienlijk verbeterd (zie kader 1).

Kader 1. Structurele beeldvorming van de hersenen bij ASS en ADHD

Structurele MRI-studies rapporteren op groepsniveau consistent een groter hersenvolume bij kinderen met ASS in de leeftijd van 2-4 jaar, vergeleken met kinderen met een typische ontwikkeling (Courchesne et al. 2001; Courchesne 2002). Deze vroege hersenvergroting, die tevens gepaard gaat met een grotere omvang van het hoofd (Lainhart et al. 1997), houdt aan tot de leeftijd van 5-6 jaar, en het is tot niet duidelijk of dit op latere leeftijd continueert (Courchesne et al. 2001; Aylward et al. 2002). Dit suggereert dat de ontwikkelingstrajecten van hersenrijping atypisch zouden kunnen zijn bij ASS, met mogelijk een periode van vroege overgroei gevolgd door een gestagneerd en afnemend hersenvolume op latere leeftijd (Courchesne et al. 2011). Deze overgroei in ASS lijkt weer gerelateerd te zijn aan een vergroot volume van de witte stof (Carper et al. 2002; Hazlett et al. 2005; Schumann et al. 2010), alsmede aan een uitbreiding van het corticaal oppervlak, maar niet aan de dikte van de cortex (Hazlett et al. 2011). In de hersenschors lijken de frontale en temporale kwabben voor de grootste volumetrische toename verantwoordelijk te zijn in ASS (Chen et al. 2011), hoewel er ook verschillen gerapporteerd worden in verscheidene subcorticale volumes (Li et al. 2021), maar met minder consistentie tussen studies.

Omgekeerd, hebben de meeste structurele MRI-studies bij ADHD afnames in volume van subcorticale structuren gevonden vergeleken met zich typisch ontwikkelende individuen, met name in (delen van) het striatum, (Nakao et al. 2011; Frodl and Skokauskas 2012; Hoogman et al. 2017). Studies naar corticale ontwikkeling in ADHD suggereren een mogelijk vertraagde rijping van de hersenen, waarbij corticale dikte en oppervlakte een paar jaar later piekten dan bij typisch ontwikkelende controles, met name in prefrontale gebieden (Shaw et al.2007, 2012).

Zoals de titel al aangeeft, hebben we in dit proefschrift geprobeerd om "**beyond pictures"** te gaan in ons MRI-onderzoek naar ASS en ADHD: we hebben daarmee beoogd een bijdrage te leveren aan de huidige kennis van zowel structurele als functionele neuroimaging bij ASS en ADHD, en de mogelijke neurobiologische implicaties daarvan onderzocht en bediscussieerd.

In **hoofdstuk 2**, onderzochten we functionele connectiviteit bij kinderen met ASS tijdens het uitvoeren van een cognitieve controletaak, met behulp van een multivariate, data-gestuurde analyse. Een kern-kenmerk van ASS is repetitief en stereotiep gedrag. We veronderstelden dat dit kenmerk weerspiegeld zouden worden in de prestaties op een respons-inhibitietaak, samen met een verminderde connectiviteit van cognitieve controlenetwerken. Opmerkelijk genoeg vonden we echter geen verschillen in functionele connectiviteit of in prestatie op deze inhibitietaak tussen kinderen met autisme en typisch ontwikkelende controles. Dergelijke verschillen zijn echter wel gevonden bij volwassenen met ASS. Onze negatieve bevinding kan gerelateerd zijn aan de zich nog ontwikkelende hersenactiviteit bij kinderen in het algemeen, die gekenmerkt wordt door minder gestructureerde en meer diffuse activiteitspatronen dan bij volwassenen. Subtiele verschillen in zowel cognitieve controle, als in patronen van functionele connectiviteit kunnen daarom op deze leeftijd nog onopgemerkt kunnen blijven. Onze resultaten benadrukken daarom dat functionele, overigens net als structurele, neuroimaging data gerelateerd zijn aan leeftijd en/of ontwikkelingsfase

van de proefpersonen. Onze studie was te beperkt in leeftijdsbereik en omvang om adequaat veranderingen in hersenconnectiviteit met ontwikkeling te onderzoeken.

We hebben deze beperking grondig aangepakt in de hierop volgende studies naar de ontwikkeling van de hersenen bij autisme en ADHD. We onderzochten in deze studies ontwikkelingstrajecten van hersenstructuren met longitudinale designs in grote en meestal onafhankelijke steekproeven over een breder leeftijdsbereik, waardoor een hogere nauwkeurigheid en een grotere generaliseerbaarheid van de resultaten mogelijk was.

Specifiek hebben we de ontwikkelingstrajecten van corticale en subcorticale hersenstructuren onderzocht in twee onafhankelijke, grote cohorten van individuen met ADHD (**hoofdstuk 3**) en individuen met ASS en/of ADHD (**hoofdstuk 4**), in vergelijking met typisch ontwikkelende controles. Zoals hierboven al aangegeven, hebben we in beide onderzoeken gebruik gemaakt van een longitudinaal design. Dit is belangrijk, omdat hersenstructuren aanzienlijk variëren in grootte en vorm, en zich verschillend ontwikkelen gedurende de levensloop. Longitudinale studies zijn daarom meer geschikt om de ontwikkelingstrajecten binnen individuen in de tijd te onderzoeken dan zogenaamde "cross-sectionele" studies, die hersenstructuren vergelijken tussen individuen van specifieke leeftijdsgroepen. ASS en ADHD zijn ontwikkelingsstoornissen en longitudinale neuroimaging studies zijn daarom bijzonder belangrijk voor onderzoek naar deze aandoeningen.

In **hoofdstuk 3**, vonden we stabiele afnames in het totale corticale volume bij ADHD, voornamelijk in frontale gebieden, die gerelateerd waren aan afnames in corticaal oppervlak en gyrificatie. De timing van de ontwikkeling van deze hersenkenmerken suggereert dat er bij ADHD mogelijk vroege stoornissen zijn in de ontwikkelingsprocessen die de tangentiële groei en sulcatie van de frontale cortex reguleren.

In **hoofdstuk 4**, hebben we deze stoornissen in corticale ontwikkeling verder onderzocht door individuen met ADHD, individuen met autismespectrumstoornis (ASS) in combinatie met veel en weinig ADHD-symptomen (ASS+ en ASS-), en gematchte typisch ontwikkelende controles met elkaar te vergelijken. We vonden vergelijkbare afnames in volume en oppervlakte van de linker orbitofrontale cortex (OFC) bij ADHD en ASS+ vergeleken met controles. Dit wijst mogelijk op vroege ontwikkelingsstoornissen specifiek in OFC links, gekoppeld aan ADHD-symptomen in beide ontwikkelingsstoornissen. Dit is neurobiologisch aannemelijk, gezien de hoge comorbiditeit van ASS en ADHD en de aanzienlijke overlap in hun klinische presentatie. Er is zelfs gesuggereerd dat ASS en ADHD beter kunnen worden begrepen als twee uitersten van één overkoepelende, trans-diagnostische aandoening (Rommelse et

al. 2017). Onze bevindingen suggereren dat vergelijkbare trajecten in vroege OFC-ontwikkeling, gerelateerd zijn aan ADHD-symptomen bij beide aandoeningen, wat een mogelijke neurobiologische correlaat biedt voor een dergelijk trans-diagnostisch kader.

Een beperking van kwantitatieve neuroimaging studies is dat ze inherent een beperkt vermogen hebben om onderscheid te maken tussen de mogelijke verschillende oorzaken van de gevonden morfologische verschillen. Bovendien zouden computationele neuroimaging methoden onvoorspelbare afwijkingen kunnen missen, zoals bijvoorbeeld neuronale heterotopieën binnen de witte stof, of zelfs slecht in staat kunnen zijn om beelden te verwerken in geval van grote afwijkingen van de typische hersengeometrie. Dus, paradoxaal genoeg, is een belangrijke beperking van computationele neuroimaging dat het geen rekening houdt met de mogelijke aanwezigheid van grove afwijkingen. Dit betekent dat het bevooroordeeld zou kunnen zijn in de richting van typische hersenanatomie. Dit zou de identificatie van neuroimaging markers voor welke hersenaandoening dan ook aanzienlijk belemmeren, omdat het de intrinsieke complexiteit van neuroimaging data onderschat. De beoordeling van kwalitatieve afwijkingen vormt een aantrekkelijk alternatief en is potentieel een waardevolle bron van informatie over inter-individuele variabiliteit in de hersenmorfologie, omdat dergelijke afwijkingen kunnen wijzen op specifieke ontwikkelingsmechanismen. Als zodanig moeten ze expliciet en zeer gedetailleerd worden onderzocht met behulp van geschikte methodologieën.

In **hoofdstuk 5**, hebben we daarom systematisch kwalitatieve MRI-bevindingen in de hersenen gekarakteriseerd in een van 's werelds grootste cohorten individuen met ASS met en zonder verstandelijke beperking, met behulp van een uitgebreid scoringssysteem. We vonden dat neuroradiologische bevindingen vaker voorkomen en ook vaker sàmen voorkomen (clusteren) bij mensen met ASS. Het type variatie, het aantal neuroradiologische bevindingen per individu en het patroon van verbanden tussen verschillende bevindingen bleken alle echter niet specifiek voor ASS. Clustering is een belangrijk diagnostisch criterium in de syndromologie, waarbij de aanwezigheid van meerdere (drie of meer) kleine afwijkingen wordt gezien als een aanwijzing voor significante stoornissen in de morfogenese en sterk gecorreleerd is met grote aangeboren afwijkingen die vermoedelijk het gevolg zijn van één onderliggende etiologie (Verma 2021). Onze studie liet zien dat een grote verscheidenheid aan (en clustering van) afwijkingen in de hersenontwikkeling geassocieerd is met ASS en met een verstandelijke beperking. Dit benadrukt de relevantie van hersenontwikkeling bij deze aandoening.

De bevindingen in dit proefschrift ondersteunen de hypothese dat klinische heterogeniteit in ASS en ADHD gepaard gaat met een even zo grote variatie in neurobiologische correlaten: deze variëren van afwijkingen die groot genoeg zijn om kwalitatief op te vallen op anatomische MRI-scans (**hoofdstuk 5**), tot subtielere veranderingen op groepsniveau die onzichtbaar zijn voor het menselijk oog, maar wel gekarakteriseerd kunnen worden met kwantitatieve methoden (**hoofdstuk 3** en **4**).

Concluderend, hebben we in dit proefschrift verschillende neuroimagingtechnieken gebruikt om de neurobiologische (neuroanatomische) correlaten van twee veelvoorkomende ontwikkelingsstoornissen, ASS en ADHD, te karakteriseren. Onze resultaten suggereren dat veranderingen in de hersenen een spectrum van biologische veranderingen vormen, dat mogelijk de bekende klinische heterogeniteit reflecteert. Deze resultaten dragen bij aan ons begrip van de biologische mechanismen die betrokken zijn bij ASS en ADHD, en zijn mogelijk relevant voor zowel wetenschappelijk vervolgonderzoek als klinische toepassingen.

REFERENCES

American Psychiatric Association. 2022. Diagnostic and statistical manual of mental disorders: DSM-5-TR (Fifth edition, text revision). American Psychiatric Association Publishing.

Aylward EH, Minshew NJ, Field K, Sparks BF, & Singh N. 2002. Effects of age on brain volume and head circumference in autism. Neurology. 59(2), 175–183. https://doi.org/10.1212/wnl.59.2.175

Baird G, Simonoff E, Pickles A, Chandler S, Loucas T, Meldrum D, Charman T. 2006. Prevalence of disorders of the autism spectrum in a population cohort of children in South Thames: the Special Needs and Autism Project (SNAP). Lancet. Jul 15;368(9531):210-5. doi: 10.1016/S0140-6736(06)69041-7. PMID: 16844490.

Carper RA, Moses P, Tigue ZD, Courchesne E. 2002. Cerebral lobes in autism: early hyperplasia and abnormal age effects. Neuroimage. Aug;16(4):1038-51. doi: 10.1006/nimg.2002.1099. PMID: 12202091.

Chen R, Jiao Y, Herskovits EH. 2011. Structural MRI in autism spectrum disorder. Pediatr. Res. 69 (5Pt 2), 63R–8R. https://doi.org/10.1203/PDR.0b013e318212c2b3

Courchesne E. 2002. Abnormal early brain development in autism. Mol. Psychiatry, 7 Suppl 2, S21–S23. https://doi.org/10.1038/sj.mp.4001169

Courchesne E, Karns CM, Davis HR, Ziccardi R, Carper RA, Tigue ZD, Chisum HJ, Moses P, Pierce K, Lord C, Lincoln AJ, Pizzo S, Schreibman L, Haas RH, Akshoomoff NA, & Courchesne RY. 2001. Unusual brain growth patterns in early life in patients with autistic disorder: an MRI study. Neurology, 57(2), 245–254. https://doi.org/10.1212/wnl.57.2.245

Courchesne E, Campbell K, & Solso S. 2011. Brain growth across the life span in autism: age-specific changes in anatomical pathology. Brain Res. J. 1380, 138–145. https://doi.org/10.1016/j.brainres.2010.09.10

Elsabbagh M, Divan G, Koh YJ, Kim YS, Kauchali S, Marcín C, Montiel-Nava C, Patel V, Paula CS, Wang C, Yasamy MT, Fombonne E. 2012. Global prevalence of autism and other pervasive developmental disorders. Autism Res. Jun;5(3):160-79. doi: 10.1002/aur.239. Epub 2012 Apr 11. PMID: 22495912; PMCID: PMC3763210.

Faraone SV, Asherson P, Banaschewski T, Biederman J, Buitelaar JK, Ramos-Quiroga JA, Rohde LA, Sonuga-Barke EJ, Tannock R, Franke B. 2015. Attention-deficit/hyperactivity disorder. Nat Rev Dis Primers. Aug 6;1:15020. doi: 10.1038/nrdp.2015.20. PMID: 27189265.

Frodl T, Skokauskas N. 2012. Meta-analysis of structural MRI studies in children and adults with attention deficit hyperactivity disorder indicates treatment effects. Acta Psych Scand. 125:114-126.

Hazlett HC, Poe M, Gerig G, Smith RG, Provenzale J, Ross A, Gilmore J, Piven J. 2005. Magnetic resonance imaging and head circumference study of brain size in autism: birth through age 2 years. Arch Gen Psychiatry. Dec;62(12):1366-76. doi: 10.1001/archpsyc.62.12.1366. PMID: 16330725.

Hazlett HC, Poe MD, Gerig G, Styner M, Chappell C, Smith RG, Vachet C, Piven J. 2011. Early brain overgrowth in autism associated with an increase in cortical surface area before age 2 years. Arch Gen Psychiatry. May;68(5):467-76. doi: 10.1001/archgenpsychiatry.2011.39. PMID: 21536976; PMCID: PMC3315057.

Hoogman M, Bralten J, Hibar DP, Mennes M, Zwiers MP, Schweren LS, van Hulzen KJ, Medland SE, Shumskaya E, Jahanshad N, Zeeuw P, et al. 2017. Subcortical brain volume differences in participants with attention deficit hyperactivitydisorder in children and adults: a cross-sectional mega-analysis. Lancet Psychiatry. 4(4):310-319.

Joshi G, Faraone SV, Wozniak J, Tarko L, Fried R, Galdo M, Furtak SL, Biederman J. 2017. Symptom Profile of ADHD in Youth With High-Functioning Autism Spectrum Disorder: A Comparative Study in Psychiatrically Referred Populations. J Atten Disord. Aug;21(10):846-855. doi: 10.1177/1087054714543368. Epub 2014 Aug 1. PMID: 25085653; PMCID: PMC4312732.

Kaat AJ, Gadow KD, Lecavalier L. 2013. Psychiatric symptom impairment in children with autism spectrum disorders. J Abnorm Child Psychol. Aug;41(6):959-69. doi: 10.1007/s10802-013-9739-7. PMID: 23605958.

Lai MC, Lombardo MV, Chakrabarti B, Baron-Cohen S. 2013. Subgrouping the autism "spectrum": reflections on DSM-5. PLoS Biol.;11(4):e1001544. doi: 10.1371/journal.pbio.1001544. Epub 2013 Apr 23. PMID: 23630456; PMCID: PMC3635864.

Lainhart JE, Piven J, Wzorek M, Landa R, Santangelo SL, Coon H, & Folstein SE. 1997. Macrocephaly in children and adults with autism. J Am Acad Child Adolesc Psychiatry. 36(2), 282–290. https://doi.org/10.1097/00004583-199702000-00019

Li X, Zhang K, He X, Zhou J, Jin C, Shen L, Gao Y, Tian M, & Zhang H. 2021. Structural, Functional, and Molecular Imaging of Autism Spectrum Disorder. Neurosci Bull. 37(7), 1051–1071. https://doi.org/10.1007/s12264-021-00673-0

Nakao T, Radua J, Rubia K, Mataix-Cols D. 2011. Gray matter volume abnormalities in ADHD: voxel-based meta-analysis exploring the effects of age and stimulant medication. Am J Psychiatry. 168(11):1154–1163.

Polanczyk GV, Willcutt EG, Salum GA, Kieling C, Rohde LA. 2014. ADHD prevalence estimates across three decades: an updated systematic review and meta-regression analysis. Int J Epidemiol. Apr;43(2):434-42. doi: 10.1093/ije/dyt261. Epub 2014 Jan 24. PMID: 24464188; PMCID: PMC4817588.

Rommelse N, Buitelaar JK, Hartman CA. 2017. Structural brain imaging correlates of ASD and ADHD across the lifespan: a hypothesis-generating review on developmental ASD-ADHD subtypes. J Neural Transm. Feb;124(2):259-271. doi: 10.1007/s00702-016-1651-1. Epub 2016 Dec 21. PMID: 28000020; PMCID: PMC5285408.

Schumann CM, Bloss CS, Barnes CC, Wideman GM, Carper RA, Akshoomoff N, Pierce K, Hagler D, Schork N, Lord C, Courchesne E. 2010. Longitudinal magnetic resonance imaging study of cortical development through early childhood in autism. J Neurosci. Mar 24;30(12):4419-27. doi: 10.1523/JNEUROSCI.5714-09.2010. PMID: 20335478; PMCID: PMC2859218.

Shaw P, Eckstrand K, Sharp W, Blumenthal J, Lerch JP, Greenstein D, Clasen L, Evans A, Giedd J, Rapoport JL. 2007. Attention-deficit/hyperactivity disorder is characterized by a delay in cortical maturation. Proc Natl Acad Sci USA. 4;104(49):19649-19654.

Shaw P, Malek M, Watson B, Sharp W, Evans A, Greenstein D. 2012. Development of cortical surface area and gyrification in attention-deficit/hyperactivity disorder. Biol Psychiatry. 1;72(3):191-197.

Simonoff E, Pickles A, Charman T, Chandler S, Loucas T, Baird G. 2008. Psychiatric disorders in children with autism spectrum disorders: prevalence, comorbidity, and associated factors in a population-derived sample. J Am Acad Child Adolesc Psychiatry. Aug;47(8):921-9. doi: 10.1097/CHI.0b013e318179964f. PMID: 18645422.

Thomas R, Sanders S, Doust J, Beller E, Glasziou P. 2015. Prevalence of attention-deficit/hyperactivity disorder: a systematic review and meta-analysis. Pediatrics. Apr;135(4):e994-1001. doi: 10.1542/peds.2014-3482. Epub 2015 Mar 2. PMID: 25733754.

Verma RP. 2021. Introductory Chapter: Epidemiology, Evaluation and Risk Assessment of Congenital Anomalies. In (Ed.), Congenital Anomalies in Newborn Infants - Clinical and Etiopathological Perspectives. IntechOpen. https://doi.org/10.5772/intechopen.97181

Xu G, Strathearn L, Liu B, O'Brien M, Kopelman TG, Zhu J, Snetselaar LG, Bao W. 2019. Prevalence and Treatment Patterns of Autism Spectrum Disorder in the United States, 2016. JAMA Pediatr. Feb 1;173(2):153-159. doi: 10.1001/jamapediatrics.2018.4208. PMID: 30508021; PMCID: PMC6439607.

PUBLICATIONS

First authored:

Ambrosino S, Elbendary H, Lequin M, Rijkelijkhuizen D, Banaschewski T, Baron-Cohen S, Bast N, Baumeister S, Buitelaar J, Charman T, Crawley D, Dell'Acqua F, Hayward H, Holt R, Moessnang C, Persico AM, Sacco R, San José Cáceres A, Tillmann J; EU-AIMS LEAP Group; Loth E, Ecker C, Oranje B, Murphy D, Durston S. **2022**. In-depth characterization of neuroradiological findings in a large sample of individuals with autism spectrum disorder and controls. *Neuroimage Clin*. 35:103118.

Ambrosino S, de Zeeuw P, Wierenga LM, van Dijk S, Durston S. **2017**. What can Cortical Development in Attention-Deficit/Hyperactivity Disorder Teach us About the Early Developmental Mechanisms Involved? *Cereb Cortex*. Sep 1;27(9):4624-4634.

Ambrosino S, Bos DJ, van Raalten TR, Kobussen NA, van Belle J, Oranje B, Durston S. **2014**. Functional connectivity during cognitive control in children with autism spectrum disorder: an independent component analysis. *J Neural Transm*. Sep;121(9):1145-55.

Ambrosino S, Bos D, van Hulst B, Oranje B, Durston S. Convergence in the neuroanatomical developmental trajectories of orbitofrontal cortex between attention-deficit/hyperactivity disorder (ADHD) and autism spectrum disorder with elevated ADHD symptoms. Under review in *Cereb Cortex*.

Co-authored:

Baumeister S, Moessnang C, Bast N, Hohmann S, Aggensteiner P, Kaiser A, Tillmann J, Goyard D, Charman T, Ambrosino S, [...]; EU-AIMS LEAP Group. **2023**. Processing of social and monetary rewards in autism spectrum disorders. *Br J Psychiatry*. Mar;222(3):100-111.

Hollestein V, Poelmans G, Forde NJ, Beckmann CF, Ecker C, Mann C, Schäfer T, Moessnang C, Baumeister S, Banaschewski T, [...], Ambrosino S, [...], Naaijen J. **2023**. Excitatory/inhibitory imbalance in autism: the role of glutamate and GABA gene-sets in symptoms and cortical brain structure. *Transl Psychiatry*. Jan 21;13(1):18.

Looden T, Floris DL, Llera A, Chauvin RJ, Charman T, Banaschewski T, Murphy D, Marquand AF, Buitelaar JK, Beckmann CF; AIMS-2-TRIALS group. **2022**. Patterns of connectome variability in autism across five functional activation tasks: findings from the LEAP project. Mol Autism. Dec 27;13(1):53.

Pretzsch CM, Floris DL, Schäfer T, Bletsch A, Gurr C, Lombardo MV, Chatham CH, Tillmann J, Charman T, Arenella M, Jones E, Ambrosino S, [...], Ecker C. **2023**. Cross-sectional and longitudinal neuroanatomical profiles of distinct clinical (adaptive) outcomes in autism. *Mol Psychiatry*. Mar 29.

Haartsen R, Mason L, Garces P, Gui A, Charman T, Tillmann J, Johnson MH, Buitelaar JK, Loth E, Murphy D, Jones EJH; EU-AIMS LEAP group. **2022**. Qualitative differences in the spatiotemporal brain states supporting configural face processing emerge in adolescence in autism. *Cortex*. Oct;155:13-29.

Laidi C, Floris DL, Tillmann J, Elandaloussi Y, Zabihi M, Charman T, Wolfers T, Durston S, Moessnang C, Dell'Acqua F, [...]; EU-AIMS LEAP Group. **2022**. Cerebellar Atypicalities in Autism? *Biol Psychiatry*. Oct 15;92(8):674-682.

Mei T, Forde NJ, Floris DL, Dell'Acqua F, Stones R, Ilioska I, Durston S, Moessnang C, Banaschewski T, Holt RJ, [...]; EU-AIMS LEAP group; Beckmann CF, Llera A, Buitelaar JK. **2022**. Autism Is Associated With Interindividual Variations of Gray and White Matter Morphology. *Biol Psychiatry Cogn Neurosci Neuroimaging*. Sep 6:S2451-9022(22)00212-9.

Pretzsch CM, Schäfer T, Lombardo MV, Warrier V, Mann C, Bletsch A, Chatham CH, Floris DL, Tillmann J, Yousaf A, Jones E, Charman T, Ambrosino S, [...], Murphy DGM, Ecker C. **2022**. Neurobiological Correlates of Change in Adaptive Behavior in Autism. *Am J Psychiatry*. May;179(5):336-349.

Vann SD, Zachiu C, Meys KME, Ambrosino S, Durston S, de Vries LS, Groenendaal F, Lequin MH. **2022**. Normative mammillary body volumes: From the neonatal period to young adult. *Neuroimage Rep*. Dec;2(4):None.

Bast N, Mason L, Freitag CM, Smith T, Portugal AM, Poustka L, Banaschewski T, Johnson M; EU-AIMS LEAP Group. **2021**. Saccade dysmetria indicates attenuated visual exploration in autism spectrum disorder. *J Child Psychol Psychiatry*. Feb;62(2):149-159.

Del Bianco T, Mason L, Charman T, Tillman J, Loth E, Hayward H, Shic F, Buitelaar J, Johnson MH, Jones EJH; EU-AIMS LEAP Group. **2021**. Temporal Profiles of Social Attention Are Different Across Development in Autistic and Neurotypical People. *Biol Psychiatry Cogn Neurosci Neuroimaging*. Aug;6(8):813-824.

Ecker C, Pretzsch CM, Bletsch A, Mann C, Schaefer T, Ambrosino S, Tillmann J, Yousaf A, Chiocchetti A, Lombardo MV, [...], Murphy DGM. **2021**. Interindividual Differences in Cortical Thickness and Their Genomic Underpinnings in Autism Spectrum Disorder. *Am J Psychiatry*. Sep 10:appiajp202120050630.

Floris DL, Wolfers T, Zabihi M, Holz NE, Zwiers MP, Charman T, Tillmann J, Ecker C, Dell'Acqua F, Banaschewski T, [...]; EU-AIMS Longitudinal European Autism Project Group. **2021**. Atypical Brain Asymmetry in Autism-A Candidate for Clinically Meaningful Stratification. *Biol Psychiatry Cogn Neurosci Neuroimaging*. Aug;6(8):802-812.

Li T, van Rooij D, Roth Mota N, Buitelaar JK; ENIGMA ADHD Working Group; Hoogman M, Arias Vasquez A, Franke B. **2021**. Characterizing neuroanatomic heterogeneity in people with and without ADHD based on subcortical brain volumes. *J Child Psychol Psychiatry*. Sep;62(9):1140-1149.

Postema MC, Hoogman M, Ambrosino S, Asherson P, Banaschewski T, Bandeira CE, Baranov A, Bau CHD, Baumeister S, Baur-Streubel R, [...], Francks C. **2021**. Analysis of structural brain asymmetries in attention-deficit/hyperactivity disorder in 39 datasets. *J Child Psychol Psychiatry*. Oct;62(10):1202-1219.

Zhang-James Y, Helminen EC, Liu J; ENIGMA-ADHD Working Group; Franke B, Hoogman M, Faraone SV. **2021**. Evidence for similar structural brain anomalies in youth and adult attention-deficit/hyperactivity disorder: a machine learning analysis. *Transl Psychiatry*. Feb 1;11(1):82.

Moessnang C, Baumeister S, Tillmann J, Goyard D, Charman T, Ambrosino S, Baron-Cohen S, Beckmann C, Bölte S, Bours C, [...]; EU-AIMS LEAP group. **2020**. Social brain activation during mentalizing in a large autism cohort: the Longitudinal European Autism Project. *Mol Autism*. Feb 22;11(1):17.

Tillmann J, Uljarevic M, Crawley D, Dumas G, Loth E, Murphy D, Buitelaar J, Charman T; AIMS-2-TRIALS LEAP group. **2020**. Dissecting the phenotypic heterogeneity in sensory features in autism spectrum disorder: a factor mixture modelling approach. *Mol Autism*. Aug 31;11(1):67. doi: 10.1186/s13229-020-00367-w. PMID: 32867850; PMCID: PMC7457751.

Hoogman M, Muetzel R, Guimaraes JP, Shumskaya E, Mennes M, Zwiers MP, Jahanshad N, Sudre G, Wolfers T, Earl EA, [...], Ambrosino S, [...], Franke B. **2019**. Brain Imaging of the

Cortex in ADHD: A Coordinated Analysis of Large-Scale Clinical and Population-Based Samples. *Am J Psychiatry*. Jul 1;176(7):531-542.

Oldehinkel M, Mennes M, Marquand A, Charman T, Tillmann J, Ecker C, Dell'Acqua F, Brandeis D, Banaschewski T, Baumeister S, [...]; EU-AIMS LEAP group. **2019**. Altered Connectivity Between Cerebellum, Visual, and Sensory-Motor Networks in Autism Spectrum Disorder: Results from the EU-AIMS Longitudinal European Autism Project. *Biol Psychiatry Cogn Neurosci Neuroimaging*. Mar;4(3):260-270.

Tillmann J, San José Cáceres A, Chatham CH, Crawley D, Holt R, Oakley B, Banaschewski T, Baron-Cohen S, Bölte S, Buitelaar JK, Durston S, [...]; EU-AIMS LEAP group. **2019**. Investigating the factors underlying adaptive functioning in autism in the EU-AIMS Longitudinal European Autism Project. *Autism Res*. Apr;12(4):645-657.

Bos DJ, Oranje B, Achterberg M, Vlaskamp C, Ambrosino S, de Reus MA, van den Heuvel MP, Rombouts SARB, Durston S. **2017**. Structural and functional connectivity in children and adolescents with and without attention deficit/hyperactivity disorder. *J Child Psychol Psychiatry*. Jul;58(7):810-818.

Charman T, Loth E, Tillmann J, Crawley D, Wooldridge C, Goyard D, Ahmad J, Auyeung B, Ambrosino S, Banaschewski T, [...], Buitelaar JK. **2017**. The EU-AIMS Longitudinal European Autism Project (LEAP): clinical characterisation. *Mol Autism*. Jun 23;8:27.

Hoogman M, Bralten J, Hibar DP, Mennes M, Zwiers MP, Schweren LSJ, van Hulzen KJE, Medland SE, Shumskaya E, Jahanshad N, , [...], Ambrosino S, [...], Franke B. **2017**. Subcortical brain volume differences in participants with attention deficit hyperactivity disorder in children and adults: a cross-sectional mega-analysis. *Lancet Psychiatry*. Apr;4(4):310-319.

Loth E, Charman T, Mason L, Tillmann J, Jones EJH, Wooldridge C, Ahmad J, Auyeung B, Brogna C, Ambrosino S, [...], Buitelaar JK. **2017**. The EU-AIMS Longitudinal European Autism Project (LEAP): design and methodologies to identify and validate stratification biomarkers for autism spectrum disorders. *Mol Autism*. Jun 23;8:24.

Wierenga L, Langen M, Ambrosino S, van Dijk S, Oranje B, Durston S. **2014**. Typical development of basal ganglia, hippocampus, amygdala and cerebellum from age 7 to 24. *Neuroimage*. Aug 1;96:67-72.

ACKNOWLEDGEMENTS

Wow. What a journey. What a long, exhausting, satisfying, amazing experience. I arrived in the Netherlands in summer 2011 with the desire of diving into research. For expanding my knowledge in neuroscience and methodology, for learning English (finally). For the adventure I always dreamed of as a child, between the lines of my favorite book:

> *"What new treasures lay here for science to unfold? I was prepared for any surprise, my imagination was ready for any astonishment however astounding". (Journey to the Center of the Earth, Jules Verne)*

What I learned, what I gained, was so much more than scientific knowledge. It was the foundation of the best part of my life, both professionally and personally. This thesis is expression of this life changing experience, and I am so grateful for it. I am grateful for having found the strength to persevere despite difficulties. And I am so very grateful to the many wonderful persons that made it possible.

First of all, **Sarah**: anything I have accomplished in the Netherlands would not have been possible without your exceptional support. What a fantastic opportunity you gave me. I surely was the least favorable candidate for a possible year internship: zero experience in research and a huge language barrier. Amazingly, you didn't say no, but offered a 3 months deal, accompanied by a very kind letter detailing all the valid reasons why it could not be longer. I kept that email on my desk, read it every morning, and that motivated me earning the remaining 9 months. 12 years have passed now, I made it! During the entire time, I cannot remember one day where you weren't by my side. Always present, always smiling, yet straight to the point, factual, precise. You infuse your work with incredible enthusiasm, intelligence, determination, sharp humor (why not), and generosity. You are such an inspiration and living proof that great professionalism and human qualities may actually coexist in one person. You lead by example Sarah, and it was an absolute privilege to had you as my promoter.

And, how fortunate I was to have you **Bob** as my co-promoter and daily guide throughout this journey. What a fantastic person you are, so kind and caring, so incredibly dedicated to work (and plants!). Your door was always open for me, sorry to disturb you all the time and make you startle on your chair! Although I must admit that was quite funny actually. Thanks for your infinite patience and calm resolution which kept me motivated and relieved my stress. I vividly remember the day you told me "Sara, no worries. I have no doubts you will make it". The power of a supervisor's words to his student

is underestimated. Your encouraging words helped me believing in my abilities and forgiving my failures, I will be forever thankful for that. Our weekly talks were priceless.

Dear Prof. **Braun**, Prof. **Cahn**, Prof. **van Haren** (Neeltje), Prof. **Hulshoff Pol**, and Dr. **Lequin**: thank you for accepting to be part of the Assessment Committee. Dear Maarten, thanks for sharing your knowledge in pediatric neuroradiology, and for the many scans we have reviewed together, I have learned so much from you. And dear Prof. Ecker, dear **Christine**: thank you so much for joining the Examination Committee of my defence, it is such a pleasure, and an honor for me. Also thanks for letting me be part of your team in Frankfurt for two weeks: the professional and relaxed atmosphere that you create in your work environment is so magical that even the quality assessment of hundreds of brain scans turned into an amazing working experience.

Dear **Patrick**, thank you so much for welcoming in the Netherlands and your generous opportunity to help with the ADHD project! You obviously taught me so much more than what I produced in return: statistics, English, neuropsychology, computer programming, brain processing. But most importantly, thanks for listening to me. I admired your profound knowledge and professionalism accompanied with sincere friendship. Thanks for our endless discussions over work and life, I wish you all the best with your work and your beautiful family. How fantastic it was to watch our children playing together!

Marieke, my very first supervisor! Thanks for your help during the first months of my internship: how to say this and that in English, how to run command lines in Linux, what to order at the cantine, where is the Emergency room (yes, that too). Your big smiles and funny jokes made me realize: *I thought this would be a nice place!? And I. was. right.*

And dear Prof. **Blom** (cara Johanna), I certainly haven't forgotten you! I will be forever grateful for having met you at the University of Modena, and for arranging my internship at the NICHE lab in Utrecht: it changed my life forever, and I will never, ever, thank you enough. It will be fantastic to meet again, and please send my greetings to the lab!

Dear **NICHE (ex-)colleagues**, thanks for being THE BEST colleagues! I cannot imagine a cosiest place in the world for scientific research. Every single one of you was so friendly with me, and thanks for having spoken English in my presence: I felt the most welcomed expat ever! **Dienke**, thanks for helping me out in all possible ways: coaching, scripting, analyzing, writing, you name it. Your incredible talent for science and for people will take you very far away. Oh wait, almost forgetting that you already are the DIRECTOR of a mental health institute, you such a rock star! Best of luck with everything! **Lara**,

one of the finest neuroscientists and persons I could possibly work with, your talent is amazing and often prompted me to do more. I loved our talks about linear models, and sometimes about guys ;) both complex topics, aren't they? **Sanne**, my awesome roomy! Thanks for your invaluable help with the Belastingdienst (I haven't forgotten), your warm welcome at your place, and for asking to be your paranymph: what an honor and special experience, thank you! **Chantal**, what a joy to share the room with you! I miss our talks ending in songs: "you know Sara, once I was afraid … *once I was afraid, I was petrified, kept thinking I could never live without you by my side …*" We could not help ourselves haha. And so many thanks **Dori** for our daily chats and your kind self! To all other (new and past)-**NICHErs**: **Branko, Vincent** (my brother)**, Jan, Bram, Caitlyn, Myrte** (my hiking HERO!)**, Iris, Janna, Annemieke, Anneke, Juliette, Sarai, Sara, Yvonne, Miriam, Tabitha, Anna, Maarten, Gisela, Rosanne, Sanne V., Lizanne, Tamar, Devon,** and my interns **Hanne** and **Dominique**: thank you so much for your help and the great time spent together over the years! Undoubtedly, NICHE truly was … a niche.

My PhD project was founded by the largest multi-centre, multi-disciplinary observational study on biomarkers for autism spectrum disorder, the EU-AIMS Longitudinal European Autism Project (LEAP): so proud to be part of such a great international study! Inevitably, it came with an equally great number of challenges. Not a piece of cake. But, we managed. And, I think we can even say we succeeded it! and from all the incredibly hard work I have learned so much, so I am very thankful to LEAP. The best part of which were my amazing international colleagues from all participating sites, my so-called **AIMS family**: thank you guys for sharing all the adventures, and the lessons learnt.

> *"Science, my lad, has been built upon many errors; but they are errors which it was good to fall into, for they led to the truth." (Journey to the Center of the Earth, Jules Verne)*

And now, to my dear **colleagues at the CBG-MEB:** THANK YOU all for being such wonderful colleagues! I am so lucky and honored to be part of FT1. The job is challenging, but you guys make our collaboration smooth, stimulating, and fun! **Lieke, Taina** and **Bart**: so many thanks for your warm welcome at the CBG, for your careful supervision in this new chapter of my professional career (hopefully the last!), and for according some time off to finalize my thesis despite the considerable workload of the team. I am looking forward to dedicate my new free time to learning Dutch, promise! **Loes**: I love our chats! best of luck with your PhD: you will do it great, no doubts! Hi **André**, thanks for your critical thinking and honest feedbacks, we all learn so much from you, I certainly do. Thank you **Jaap** for your dedication to teaching and kind encouragements, and thanks **Rou-Afza** to show me how to work with extreme

accuracy and unmistakable enthusiasm! **Sabine, Hester, Therese, Siona, Pinar, Cristel**, **Taco**: thank you for the kind "*How is life and the PhD going*" talks. How relieving to share personal challenges besides work, happy to answer that *finally it is done!* To all of you and other (ex)-FT1rs -**Elizabeth, Hemme, Gerlienke, Dasha** (miss you!), **Peter, Louise, Karlijn, Inge, Hendrik, Janneke, Hanneke, Derk, Marco, Stefanie, Ninke, Maarten, Parand**-, and **Fabian**: thanks for the smiles, coffees, lunches, chats, and for inspiring me every day to do more and better in my work: I look forward to the next years with you!

A very special thanks to my doctor, **Dr. Ossewaarde**. My start in the Netherlands was not the easiest. All of a sudden, I experienced the Hospital from the other side: examinations, medicines, words as *diagnosis* and *prognosis* had a whole different meaning to me. *Why me?* Oh well, why not. *Why NOW?* Turns out, better here than in my home country. But most importantly, *what is going to happen?* You helped me to see (literally) my future again with great professionalism intertwined with kindness. I could not complete an entire neuroimaging project without the constant care of your team or, as I like to call it, my second family at the UMCU. I am a very grateful patient.

And now I will switch to Italian to thank the dear persons from my home country, starting from my **paranymphs**! Ci tenevo ad avere vicino due persone forti che mi hanno aiutato lungo il percorso, grazie ragazzi per accompagnarmi nel rash finale!

Rosa, carissima. Grazie per la tua amicizia, le tue telefonate, non mi faccio sentire spesso (migliorerò in questo, lo giuro) eppure, e non ti ringrazierò mai abbastanza, quanto ti ho sentita vicina in questi anni. Sei un'amica leale e una delle donne più forti e intelligenti che io abbia mai incontrato. Quando mi sembra che non ce la faccio, mi faccio ispirare da te, et voilà, anything is possible. Ti venissero dubbi al riguardo, hai il bambino più bello del mondo che è la naturale conseguenza di quanto lo è la sua mamma. Ti voglio bene.

Ciao **Vi**, sei bravo, e questo è indubbio, ma soprattutto molto in gamba in tutti i sensi. Grazie per esserci sempre come se ci fossimo sentiti il giorno prima, e per il tuo preziosissimo aiuto con tutte le figure, e la copertina fenomenale: non lo sottovalutare, i complimenti me li hanno fatti TUTTI, but all credits go to the best graphic designer in the world people! which happens to be my brother. Successo meritato nel lavoro e nella vita, you will do it great because you are great! (in inglese rende meglio secondo me)

Al resto della mia famiglia, innanzitutto la mia bellissima **sorellina**: grazie per essermi stata vicina sempre. Sensibile, intelligente, creativa e capace di QUALSIASI cosa, sono sicura che riuscirai in tutto ciò tu desideri. Cari mamma e papà, grazie per avermi fatto studiare e lasciata libera nelle mie scelte. **Papà,** grazie per l'incoraggiamento, l'affetto e l'aiuto che non mi sono mai mancati da parte tua. Grazie per i libri che mi compravi da

piccola e che hanno nutrito la mia passione per la conoscenza. Soprattutto, grazie del tuo esempio di responsabilità e impegno sul lavoro, cosa che non si impara altrimenti e che cerco di seguire. **Mamma,** invece tu non hai esitato a prendere un aereo, anche se ti faceva paura, per venirmi ad aiutare con il mio bimbo neonato per un mese: è stato impagabile e l'ho apprezzato tantissimo, non so come avremmo fatto altrimenti. Per l'aiuto concreto in tutte le cose, grazie mille.

E alla mia dolce famiglia acquisita, in primis **Rosa** (mammina): grazie per avermi subito accolta a casa tua con le tue magliette e i buoni pranzetti. Al caro nonnino **Antonio** che guardandomi dal Cielo spero sia orgoglioso almeno un pochino quanto lo era il giorno che l'ho incontrato. **Rino**, un cuore così buono e generoso che un giorno hanno dovuto ripararlo: come una persona straordinariamente forte e sensibile possano coesistere. Grazie per avermi ospitato a casa tua con premura e discrezione, sono riuscita a scrivere un capitolo intero in tre giorni, il che è un miracolo. Zio **Gianky**, uno zio dolcissimo e presente: grazie per le telefonate tutte le sere che ci fanno sentire un po' meno soli e lontani.

E infine, le due persone più vicine al mio cuore. Caro **Marco**, è da quando mi conosci che sto lavorando al dottorato: alleluia (come canti tu), la tesi è finita. Grazie per avermi sopportato in tutti questi anni, e ricordato, continuamente, che la vita è soprattutto altro, *oltre* al lavoro. Quanto è vero. Mi hai cambiato la vita in tutti i modi possibili, in meglio. A modo tuo, con proposte dolci e piuttosto maldestre, ma che probabilmente erano l'unico modo possibile. Mi sei piaciuto subito e conquistato poco a poco, e ancora adesso non credo alla fortuna dell'averti incrociato sul mio percorso. Unico rimpianto non esserci messi insieme prima. Ora quindi non perdiamo tempo, e giriamo il mondo insieme: *vieni con me?* (sì lo so che dici che decido tutto io ☺)

Nicolas, amore mio, sei il bambino più straordinario che io abbia mai conosciuto. Grazie per le tue risate gioiose e la tua voglia continua di giocare e di conoscere. Grazie per le tue chiacchere e le tue canzoncine, sei un'infusione di allegria quotidiana! Grazie per i tuoi salti alti alti, i disegni colorati, le costruzioni, i libri, le paroline dolci, le tue domande intelligenti, e il tuo generoso affetto. Scusa se la mamma ogni tanto (spesso) andava su a lavorare, o se con tristezza non vi accompagnava in vacanza. Adesso la mamma ha finito il suo libro, e non vede l'ora di godersi ancora di più insieme a papà questa vita meravigliosa che ci hai regalato.

Sara

CURRICULUM VITAE

Sara Ambrosino was born on Oct 2nd, 1978 in Ravenna, Italy. She completed high school at scientific lyceum in 1996. In 1998, she started studying Medicine at the University of Ferrara, Italy, and deepened her interest in Neurology with one year residency at the Bordeaux Segalen University, France. In 2006 she obtained her master degree in Medicine (full marks), with a research thesis on status epilepticus in pediatric population. In Jul 2012, she specialized cum laude in Child and Adolescents Neurology and Psychiatry at the University of Modena and Reggio Emilia, Italy, with a research thesis on cortical morphometry in ADHD performed at the NICHE neuroimaging lab of Prof. dr. Sarah Durston in Utrecht, the Netherlands. From Jan 2013, she worked as Research Assistant at the NICHE lab, and 10 months later she started her PhD program in Clinical and Experimental Neuroscience, while coordinating locally the EU-AIMS Longitudinal European Autism Project, a large international longitudinal study on Autism Spectrum Disorder, under the supervision of Sarah Durston and Bob Oranje. Since Sept 2022 she works as a clinical assessor at the Dutch Medicines Evaluation Board, with focus on medicinal products for Neurology and Psychiatry.

UMC Utrecht

Universiteit Utrecht

ISBN 978-90-393-7584-6